

Reducing the environmental impact of distribution centres

Environmental impact assessment of the load-bearing structures of distribution centre design alternatives

Master thesis of Amarins Kroes



Reducing the environmental impact of distribution centres

Environmental impact assessment of the load-bearing structures of distribution centre design alternatives

by

A. Kroes

to obtain the degree of Master of Science
at the Delft University of Technology,
to be defended publicly on Tuesday May 18, 2021 at 14:45

Student number:	4928946	
Thesis committee:	Prof.dr.ir. J.G. (Jan) Rots	TU Delft
	Dr. H.M. (Henk) Jonkers	TU Delft
	Dr.ir. G.J.P. (Geert) Ravenshorst	TU Delft
	M.A. (Michiel) Visscher MSc	Royal HaskoningDHV

An electronic version of this thesis is available at <http://repository.tudelft.nl/>

Preface

My thesis has been written to finalise the master track Building Engineering. This track is part of the master's programme of Civil Engineering at Delft University of Technology. During this master's programme, I gained interest in the combination between structural design of buildings and sustainability. I am happy that I got the opportunity to dive into these topics for this research and I hope to continue to learn about these subjects in the future.

I would like to thank my graduation committee members Michiel Visscher, Geert Ravenshorst, Henk Jonkers, and Jan Rots. Firstly, I would like to thank Michiel Visscher from Royal HaskoningDHV for his practical approach and to remind me to keep the end goal in mind. The weekly meetings really helped me to set up this research. Secondly, I would like to express my gratitude towards my supervisors from Delft University of Technology. Geert Ravenshorst, I would like to thank you for your knowledge on timber structures and Henk Jonkers, I would like to thank you for your knowledge on sustainability. Finally, I would like to thank Jan Rots for his role as chairman of the graduation committee.

I would also like to thank my colleagues at Royal HaskoningDHV for their time and effort to answer my questions. Furthermore, I would like to thank Bouwen met Staal and Brink Staalbouw for thinking along with me about the steel design alternatives.

The pandemic influenced my graduation process and especially during these times, I am very thankful for the support that I got from my family and friends. I would especially like to thank my boyfriend Thijs. Even though we live far apart, he was always there to support me. I am also very thankful for my roommates, with whom I spent most of my time during the lock down. I would like to thank them for always being there for me and that I was able to express my feeling to them at any time.

Summary

Buildings influence the environment due to the emission of greenhouse gases, energy use, water consumption, and waste generation. The load-bearing structures of buildings also have a significant share in these emissions. Currently, European and national regulations oblige to focus on sustainability in designs as well. In this research, it is therefore investigated how the environmental impact of a specific case study can be reduced (the Base design). This is a distribution centre's load-bearing structure and is a sway steel structure with one mezzanine floor made from concrete and steel.

In the first part of this research, the design choices to reduce the yearly environmental impact of a distribution centre's load-bearing structure are investigated. This is done by following three circular economy strategies to improve the Base design. The first strategy focuses on the building's initial material use, where it is aimed to reduce the current impact of these materials as much as possible. This strategy is applied in a non-sway steel structure and a non-sway timber structure. The second strategy focuses on the afterlife of a building. This led to a steel sway structure where Design for Deconstruction is applied, which means that extra attention is given to the connections to ensure reuse is possible at the end of life. The third strategy focuses on extending the use stage, meaning that the design is optimised for multiple functions. This is implemented in two designs where the principle of Design for Adaptability is applied.

In the second part of the research, several environmental impact calculation methods to measure the environmental impact are investigated. It is decided to consider the current product impact (Stages A1-A3 of a Life Cycle Assessment) and the final stage (Stage D), where benefits and loads beyond the system boundary are calculated. As a result, the yearly environmental impact is calculated for the different design alternatives and is given in a shadow price (in euros) per year. This is done separately for the main load-bearing structure and the mezzanine floor load-bearing structure.

From the environmental impact calculation of the design alternatives, it can be concluded that there are several ways to reduce the environmental impact of a distribution centre. Though, the following design aspects influence this most significantly. Firstly, it is concluded that environmentally friendly material should always be chosen over other materials to reduce the environmental impact of a building. More specifically, it is recommended to design a timber sway structure (Alternative B) if the reference service life of the building is unknown or if a long reference service life is expected. For a short reference service life, it is recommended to focus on the afterlife of a building. This strategy is most effective if this is combined with a reduction in initial material use. For the main load-bearing structure, Alternative A with an end of life scenario with a high chance of reuse results in the lowest yearly environmental impact. For the mezzanine floor, the demountable floor design with a high chance of reuse of Alternative C leads to the lowest yearly environmental impact. Besides, using the building for a longer time is also an effective measure to reduce the yearly environmental impact. The reference service life may extend if a building is designed for multiple functions. This can be assessed by asking the client about their expectations of the use of the building. By assessing this issue in the design phase, it can be decided to include some overcapacity to ensure a longer reference service life.

Contents

Preface	i
Summary	ii
List of figures	v
List of tables	x
Abbreviations	xiii
1 Introduction	1
1.1 Circular economy principles	2
1.2 Circular building strategies	4
1.3 Case study	6
2 Research definition	8
2.1 Problem definition	8
2.2 Research objective	8
2.3 Research questions	9
2.4 Scope	9
2.5 Research outline	10
3 Building material characteristics	11
3.1 Steel	11
3.2 Concrete	11
3.3 Timber	12
3.4 Conclusion	14
4 Principles to extend the functional service life	15
4.1 Design for Deconstruction (DfD)	15
4.2 Design for Adaptability (DfA)	18
5 Setup of design alternatives	20
5.1 Research question 3a: Optimise design for its initial material use	20
5.2 Research question 3b: Optimise design for its residual value	21
5.3 Research question 3c: Optimise design for multiple functions	22
5.4 Overview of comparisons and design alternatives	22
6 Designs	24
6.1 Base design: Sway structure (steel and concrete)	26
6.2 Alternative A: Non-sway structure (steel and concrete)	31
6.3 Alternative B: Non-sway structure (timber and concrete)	35
6.4 Alternative C: Demountable sway structure (steel and concrete)	42
6.5 Alternatives D: Non-sway structure with future function change (steel and concrete)	48
6.6 Overview of design alternatives	50
7 Environmental impact calculation	51
7.1 Life Cycle Assessment	51
7.2 Scope and goal of the analysis	53
7.3 Functional unit and system boundaries	53
7.4 Methodology for the allocation rules	55
7.5 Quantifying the materials in the system	57
7.6 Conclusion	57

8 Environmental impact calculation results	64
8.1 Research question 3a: Optimise design for its initial material use	64
8.2 Research question 3b: Optimise design for residual value	66
8.3 Research question 3c: Optimise design for multiple functions	69
8.4 Main findings	70
9 Discussion	73
9.1 Discussion of results	73
9.2 Comparing the results to literature	74
9.3 Limitations of the research	74
9.4 Implications of the research	75
10 Conclusion	76
11 Recommendations	78
11.1 Recommendations for future research	78
11.2 Recommendations for practice	78
12 References	80
Appendices	87
A Guidelines for the structural calculations	89
B Base design	96
C Alternative A	131
D Alternative B	144
E Alternative C	179
F Alternative D1	191
G Alternative D2	195
H Environmental data	199
I Environmental impact calculation	207
J Environmental impact calculation results	223

List of figures

Figure 1-1: Global final energy use per m ² (UN Environment and International Energy Agency, 2017)	1
Figure 1-2: From a linear to a circular economy (Government of the Netherlands, n.d.)	2
Figure 1-3: Outline of a circular economy (Ellen MacArthur Foundation, 2015).....	3
Figure 1-4: Value creation of a circular economy (Ellen MacArthur Foundation, 2015).....	3
Figure 1-5: 9R strategies to increase the circularity of a product (Potting, Hekkert, Worrell, & Hanemaaijer, 2017)	4
Figure 1-6: Strategy 1: Optimise for one function (Vonck, 2019)	5
Figure 1-7: Strategy 2: Optimise residual value (Vonck, 2019).....	5
Figure 1-8: Strategy 3: Optimise for multiple functions (Vonck, 2019).....	5
Figure 1-9: 3D view of the distribution centre (Royal HaskoningDHV Internal Document, 2020c).....	6
Figure 1-10: Visualisation of the main and mezzanine load-bearing structure	6
Figure 1-11: 3D view of the structure (Royal HaskoningDHV Internal Document, 2020c).....	7
Figure 2-1: Overview of the research	10
Figure 3-1: Manufacturing process of sawn timber, glulam, CLT, and LVL (Van Wijnen, 2020)	13
Figure 4-1: Building layers (Brand, 1995).....	15
Figure 4-2: Elevation of the main floor beam showing openings for ducts and piping	17
Figure 4-3: Left: non-extended end plate on a steel beam. Right: extended end plate on a steel beam	18
Figure 5-1: Non-sway structure (left) and sway structure (right) (Den Hollander, n.d.)	20
Figure 5-2: Explanation of how the sub-research questions will be answered	23
Figure 5-3: Set up of design alternatives	23
Figure 6-1: Necessary internal heights (Royal HaskoningDHV Internal Document, 2020a)	24
Figure 6-2: Example of a robotic floor with openings (O'Brien, 2019)	25
Figure 6-3: Part of the floor grid of the mezzanine floor, where the available areas for structural elements are schematised (own illustration, based upon (Royal HaskoningDHV Internal Document, 2020c))	25
Figure 6-4: Front view of the structure (Royal HaskoningDHV Internal Document, 2020c)	26
Figure 6-5: Top view of the Base design at the dotted blue line shown in Figure 6-4	27
Figure 6-6: Top view of the Base design at the dotted green line shown in Figure 6-4.....	27
Figure 6-7: Top view of the roof beams (at zoom in shown in Figure 6-6).....	28
Figure 6-8: Mechanics scheme of the stabilising portal frame in the y-direction.....	29
Figure 6-9: Mechanics scheme of the stabilising portal frame in the x-direction.....	29
Figure 6-10: Composite flooring system (Bouwen met Staal, 2013).....	30
Figure 6-11: Part of mezzanine floor (own illustration based upon Royal HaskoningDHV Internal Document).....	30
Figure 6-12: Top view of Alternative A at the dotted blue line shown in Figure 6-4.....	31
Figure 6-13: Top view of Alternative A at the dotted green line shown in Figure 6-4.....	32
Figure 6-14: Mechanics scheme of the frame in the y-direction	33
Figure 6-15: Mechanics scheme of the stabilising portal frame in the x-direction.....	33
Figure 6-16: Visualisation of the vertical bracing in the façade.....	34
Figure 6-17: Top view of Alternative B at the dotted blue line shown in Figure 6-4	36
Figure 6-18: Top view of Alternative B at the dotted green line shown in Figure 6-4	37
Figure 6-19: Mechanics scheme of the frame in the y-direction	38
Figure 6-20: Single tapered beam (Blaß & Sandhaas, 2017).....	38
Figure 6-21: Mechanics scheme of the frame in the x-direction	39
Figure 6-22: Visualisation of the vertical bracing in the façade.....	39
Figure 6-23: Mezzanine floor layout.....	40
Figure 6-24: Layout of the CLT floors used in the design (Karacabeyli & Douglas, 2013).....	41
Figure 6-25: Connection between beams and column (own illustration, made with IDEA StatiCa).....	42
Figure 6-26: Top view of Alternative C at the dotted blue line shown in Figure 6-4.....	43
Figure 6-27: Top view of Alternative C at the dotted green line shown in Figure 6-4.....	44
Figure 6-28: Mechanics scheme of the stabilising portal frame in the y-direction.....	44

Figure 6-29: Mechanics scheme of the stabilising portal frame in the x-direction.....	45
Figure 6-30: Removing the cement floor from a hollow core slab (Buunk & Heebing, 2017)	45
Figure 6-31: Hollow core slab and steel beam in the Temporary Courthouse (De Danschutter et al., 2017).	46
Figure 6-32: Chosen mezzanine floor layout for Alternative C.....	47
Figure 6-33: Chosen mezzanine floor layout for Alternative B	48
Figure 6-34: Top view of Alternative D2 at the dotted blue line shown in Figure 6-4	49
Figure 7-1: Life cycle stages (own illustration, based upon NEN (2019))	51
Figure 7-2: Separation of the total load-bearing structure into the main and mezzanine floor load-bearing structure ...	54
Figure 7-3: Life cycle stages that are investigated for this research.....	55
Figure 7-4: Overview of the flow chart to calculate the yearly environmental impact of stages A1-A3 and D	58
Figure 7-5: Step 1 of the environmental impact calculation (Stage A1-A3)	59
Figure 7-6: Step 2 of the environmental impact calculation (Stage A1-A3)	60
Figure 7-7: Step 3 of the environmental impact calculation (Stage D, for timber)	61
Figure 7-8: Step 3 of the environmental impact calculation (Stage D, for steel and concrete)	62
Figure 7-9: Step 4 of the environmental impact calculation (Stage D)	63
Figure 7-10: Step 5 of the environmental impact calculation (Stages A1-A3 and D).....	63
Figure 8-1: Yearly environmental impact of the main load-bearing structures of Alternative A and B (stages A1-A3+D), where the general end of life scenario is used.....	65
Figure 8-2: Yearly environmental impact of the mezzanine structure of Alternative A and B (stages A1-A3+D), where the general end of life scenario is used.....	65
Figure 8-3: Yearly environmental impact of the main load-bearing structure of the Base design and Alternative C for the end of life scenario based upon the Disassembly Index (stages A1-A3+D)	67
Figure 8-4: Yearly environmental impact of the mezzanine load-bearing structure of the Base design and Alternative C for the end of life scenario based upon the Disassembly Index (stages A1-A3+D)	67
Figure 8-5: Yearly environmental impact of the main load-bearing structure of Alternative A if the general end of life scenario or the end of life scenario with a higher chance of reuse (with the Disassembly Index) is used	68
Figure 8-6: Yearly environmental impact of the main load-bearing structures of Alternatives A and D2 (stages A1- A3+D)	69
Figure 8-7: Comparison between the mezzanine structure of Alternatives C, D1, and D2 (stages A1-A3+D).....	69
Figure 8-8: Yearly environmental impact of the main load-bearing structures of Alternative A (or Alternative D1; calculated with an end of life scenario with a higher chance of reuse) and Alternative B	71
Figure 8-9: Yearly environmental impact of the mezzanine load-bearing structures of Alternatives B and C (stages A1- A3+D)	72
Figure 9-1: Calculation of the environmental impact of substituted material, where SP = shadow price.....	73
Figure 9-2: Two options of the warehouse and bump outs (Royal HaskoningDHV Internal document, 2021)	75
Figure A-1: Pressure on surfaces	91
Figure A-2: Distribution of wind load over the height of the facade based on h/b (NEN, 2005a).....	91
Figure A-3: Representative figures for wind load on vertical walls (NEN, 2005a)	92
Figure A-4: Representative figures for wind load on the roof (NEN, 2005a)	93
Figure A-5: Reference area for friction (NEN, 2005a).....	94
Figure A-6: Area distribution of a parapet on a roof (Royal HaskoningDHV Internal Document, 2020a)	95
Figure A-7: Snow load on the roof of building (Royal HaskoningDHV Internal Document, 2020a)	95
Figure B-1: Mechanics scheme of the stabilising portal frame in the y-direction	97
Figure B-2: Mechanics scheme of the stabilising portal frame in the x-direction	97
Figure B-3: Connection between the floor beam (IPE 450) and the secondary beam (HEB 650-CB).....	106
Figure B-4: Connection between the primary mezzanine beam (HEB 450, shown in blue) and the secondary mezzanine beam (HEB 650-CB, shown in orange) (own illustration, made with IDEA StatiCa)	106
Figure B-5: Resulting deformation of the footing.....	107

Figure B-6: Connection of the main column and the end plate with anchors on top of the concrete footing	107
Figure B-7: Connection between the continuous roof beam and the main column.....	108
Figure B-8: Connection between the continuous roof beam and the main column including haunches	109
Figure B-9: Drawings of the connections for the y-direction.....	110
Figure B-10: Details of connections between column and roof beams for another building of the same client	111
Figure B-11: Final design for the connection between the main column and roof beams	112
Figure B-12: Continuous beam with two sizes of beams (left: 3D view, right: 2D view)	113
Figure B-13: Example of a connection between the mezzanine primary beam and a mezzanine column	113
Figure B-14: Determination of buckling curve (NEN, 2016a).....	119
Figure B-15: Horizontal deflection for governing characteristic load situation (SLS 16) for the x-direction.....	120
Figure B-16: Horizontal deflection for governing characteristic load situation (SLS 16) for the y-direction.....	120
Figure B-17: Vertical deflection for governing characteristic load combination (SLS 17) for the x-direction	120
Figure B-18: Vertical deflection for governing characteristic load combination (SLS 17) for the y-direction	120
Figure B-19: Buckling lengths for a sway system (Veljkovic, 2019).....	122
Figure B-20: Buckling lengths for a non-sway system (Veljkovic, 2019).....	122
Figure B-21: Normal forces in the frame in the x-direction (for ULS 6).....	122
Figure B-22: Shear forces in the frame in the x-direction (for ULS 6).....	123
Figure B-23: Bending moments in the frame in the x-direction (for ULS 6).....	123
Figure B-24: Normal forces in the frame in the y-direction (for ULS 6).....	123
Figure B-25: Shear forces in the frame in the y-direction (for ULS 6).....	123
Figure B-26: Bending moments in the frame in the y-direction (for ULS 6).....	123
Figure B-27: Location of governing beam (shown in green) and column (shown in blue) in the x-direction	123
Figure B-28: Equivalent uniform moment factors (NEN, 2016a)	129
Figure C-1: Example of two beam-beam connections	132
Figure C-2: Example of two steel column base connections.....	132
Figure C-3: Schematisation of local façade column check	133
Figure C-4: Overview of the horizontal wind loads in the y-direction	135
Figure C-5: Overview of the horizontal wind loads in the x-direction	136
Figure C-6: Principle showing how the roof bracing is calculated (this is an example for a smaller building)	136
Figure C-7: Screenshot of SCIA model of the bracing carrying the wind coming from the x-direction	137
Figure C-8: Screenshot of SCIA model of the bracing carrying the wind coming from the y-direction	137
Figure C-9: Schematisation of vertical wind bracing with the wind load on the system.....	138
Figure C-10: Horizontal deflection of the bracing systems due to the wind load (from SCIA).....	139
Figure C-11: Deflection of beams in y-direction (from SCIA).....	139
Figure C-12: Deflection of beams in x-direction	139
Figure C-13: Normal forces in the frame in the x-direction (for ULS 7)	142
Figure C-14: Shear forces in the frame in the x-direction (for ULS 7)	142
Figure C-15: Bending moments in the frame in the x-direction (for ULS 7)	142
Figure C-16: Normal forces in the frame in the y-direction (for ULS 6)	142
Figure C-17: Shear forces in the frame in the y-direction (for ULS 6)	142
Figure C-18: Bending moments in the frame in the y-direction (for ULS 6)	142
Figure D-1: Reduced cross section for a fire duration of 60 minutes (from Stora Enso Calculatis tool)	146
Figure D-2: Schematisation of local façade column check.....	146
Figure D-3: Overview of the horizontal wind loads in the y-direction.....	148
Figure D-4: Overview of the horizontal wind loads in the x-direction.....	148
Figure D-5: Screenshot of SCIA model of the timber bracing carrying the wind coming from the x-direction.....	149
Figure D-6: Screenshot of SCIA model of the timber bracing carrying the wind coming from the y-direction.....	149
Figure D-7: 3D-view of a part of the roof beams, bracings, lateral supports, and columns	150

Figure D-8: Top view of the structure at the dotted green line shown in Figure 6-4, including the lateral supported beams that were excluded in Figure 6-18.....	151
Figure D-9: Horizontal deflection of the bracing systems due to the wind load (from SCIA)	152
Figure D-10: Initial deflection of beams in y-direction (from SCIA)	152
Figure D-11: Initial deflection of the smaller beams in x-direction	153
Figure D-12: Initial deflection of a part of the bracing system due to their self-weight (from SCIA)	153
Figure D-13: Shear forces in the frame in the y-direction (for ULS 7)	154
Figure D-14: Bending moments in the frame in the y-direction (for ULS 7)	154
Figure D-15: Normal forces in the frame in the x-direction, for the higher beams (for ULS 7).....	154
Figure D-16: Shear forces in the frame in the x-direction, for the lower beams (for ULS 7)	155
Figure D-17: Bending moments in the frame in the x-direction, for the lower beams (for ULS 7)	155
Figure D-18: Normal forces in the beams in the y-direction (for ULS 6)	155
Figure D-19: Normal forces in the columns in the y-direction (for ULS 6)	155
Figure D-20: Shear forces in the frame in the y-direction (for ULS 6)	155
Figure D-21: Bending moments in the frame in the y-direction (for ULS 6)	155
Figure D-22: Normal forces in the beams in the x-direction (for ULS 6)	156
Figure D-23: Normal forces in the columns in the x-direction (for ULS 6)	156
Figure D-24: Shear forces in the frame in the x-direction (for ULS 6)	156
Figure D-25: Bending moments in the frame in the x-direction (for ULS 6)	156
Figure D-26: Failure modes applicable for a timber beam with steel plates (Sandhaas, Munch-Andersen, & Dietsch, 2018).....	164
Figure D-27: Force-fitting element joint with glued-in reinforcement bars (Loebus, Dietsch, & Winter, 2017)	166
Figure D-28: Column base connection types	175
Figure D-29: Explanation on how to determine the height of the Lignatur floor element (Lignatur AG, 2014).....	176
Figure E-1: Normal forces in the frame in the x-direction (for ULS 6).....	182
Figure E-2: Shear forces in the frame in the x-direction (for ULS 6)	182
Figure E-3: Bending moments in the frame in the x-direction (for ULS 6)	182
Figure E-4: Normal forces in the frame in the y-direction (for ULS 6).....	183
Figure E-5: Shear forces in the frame in the y-direction (for ULS 6)	183
Figure E-6: Bending moments in the frame in the y-direction (for ULS 6)	183
Figure E-7: VBI hollow core slab calculation (2108 mm long) for a robotic load for Alternative C in the SLS state	185
Figure E-8: VBI hollow core slab calculation (2108 mm long) for a robotic load for Alternative C in the ULS state...	186
Figure E-9: VBI hollow core slab calculation (4215 mm long) for a robotic load for Alternative C in the SLS state	186
Figure E-10: VBI hollow core slab calculation (4215 mm long) for a robotic load for Alternative C in the ULS state.	187
Figure F-1: Hollow core slab calculation for SLS state for Alternative D1, calculated with the VBI calculator	191
Figure F-2: Hollow core slab calculation for ULS state for Alternative D1, calculated with the VBI calculator	192
Figure F-3: Live loads on the columns, calculated in SCIA	192
Figure F-4: Dead loads on the columns, calculated in SCIA	192
Figure F-5: Normal forces in the frame in the x-direction (for ULS 7)	192
Figure G-1: Hollow core slab calculation for SLS state for Alternative D2, calculated with the VBI calculator	195
Figure G-2: Hollow core slab calculation for ULS state for Alternative D2, calculated with the VBI calculator	196
Figure G-3: Live loads on the columns, calculated in SCIA	196
Figure G-4: Dead loads on the columns, calculated in SCIA	196
Figure G-5: Normal forces in the frame in the x-direction (for ULS 7)	196
Figure I-1: PEF equation, where A and B are input and C, D, and E are output (Backx, 2020)	209
Figure J-1: Comparison between the Base design and Alternative A, for stages A1-A3 (incl. reuse).....	223
Figure J-2: Comparison between the Base design and Alternative A, for stages A1-A3 and D	223
Figure J-3: Comparison between the main load-bearing structure of Alternative A and B (stages A1-A3)	224
Figure J-4: Comparison between the mezzanine structure of Alternative A and B (stages A1-A3).....	224

Figure J-5: Comparison between mezzanine structure of Alternative A and B, if none of the steel will be reused	225
Figure J-6: Comparison between the mezzanine structure of Alternative A and B, if the bonus for recycling of Alternative A is reduced with 10%	225
Figure J-7: Comparison between the main load-bearing structure of the Base design and Alternative C for stages A1-A3, where the chance of reuse is based upon the Disassembly Index	226
Figure J-8: Comparison between the mezzanine floor of the Base design and Alternative C (stages A1-A3, where the advantage of reusing the elements is not considered)	226
Figure J-9: Comparison between the Base design if the Disassembly Index is used to calculate the chance of reuse (Base design (DI)) and if the general end of life scenarios are used (Base design (no DI))	227

List of tables

Table 6-1: Dutch Building Regulations 2012 (Tabel 2.10.2) for a non-residential function	24
Table 6-2: Total amount of material per design alternative	50
Table 7-1: Environmental prices per EIC for LCA (Stichting Bouwkwiteit, 2019)	52
Table 7-2: Parameters used in the functional unit.....	53
Table 7-3: Technical service life (TSL) for different element types (Straub et al., 2011).....	54
Table 8-1: Total shadow costs for the biogenic carbon storage of Alternative B	66
Table 8-2: Total shadow price of the main load-bearing structure of each design alternative for A1-A3	70
Table 8-3: Total shadow price of the mezzanine load-bearing structure of each design alternative for A1-A3	70
Table A-1: Load factors according to EN-1990 (NEN, 2002).....	90
Table A-2: ψ Factors according to EN-1990 (NEN, 2002).....	90
Table A-3: Basis of wind calculation	91
Table A-4: Calculation of peak velocity pressure	92
Table A-5: Recommended values of external pressure coefficients for walls of rectangular buildings (NEN, 2005a)....	93
Table A-6: External wind load on vertical walls	93
Table A-7: Building shape factors and external loads on the roof (based upon Table 7.2 of EN-1991-1-4).....	94
Table A-8: Wind pressure on parapet	95
Table A-9: Internal wind pressure.....	95
Table B-1: Translation of castellated beam to a regular beam	96
Table B-2: Loads on portal frame (Y-direction)	98
Table B-3: Reference of load cases and the numbering used in the SCIA model.....	101
Table B-4: Governing load cases.....	101
Table B-5: Loads on portal frame (X direction)	103
Table B-6: Explanation of parameters of eq. B-1.....	108
Table B-7: Approximation of the moment arm for different types of connections.....	108
Table B-8: Flexibility factor for connections in Figure B-7 (x-direction) (Staalbouwkundig Genootschap, 1999).....	109
Table B-9: Stiffness calculation of the connection between the roof beam and the columns (x-direction)	109
Table B-10: Updated stiffness calculation of the connection between the roof beam and the columns (x-direction) ..	110
Table B-11: Flexibility factor for connections in Figure B-9 (y-direction) (Staalbouwkundig Genootschap, 1999).....	110
Table B-12: Stiffness calculation of the connection between the roof beam and the columns (y-direction).....	111
Table B-13: Updated stiffness calculation of the connection between the roof beam and the columns (y-direction) ..	112
Table B-14: Translating a castellated beam to a regular beam with the section modulus in the strong direction	113
Table B-15: SLS results of the structural verifications performed in SCIA	120
Table B-16: Buckling lengths of the columns, from SCIA	121
Table B-17: Buckling lengths of the beams, from SCIA	121
Table B-18: Governing unity checks for the members of the base design.....	122
Table B-19: Bending and axial compression check parameters for method 2.....	125
Table B-20: Interaction method 2 parameters	125
Table B-21: Bending and axial compression check parameters for method 2.....	129
Table B-22: Interaction method 2 parameters	129
Table C-1: Calculation of maximum length of a building without/between expansion joints (Fisher, 2005)	131
Table C-2: Design options based upon thermal expansion issues	131
Table C-3: Loads on non-sway frame (Y-direction).....	133
Table C-4: Loads on non-sway frame (X direction).....	134
Table C-5: Largest normal forces in the horizontal roof bracing system	137
Table C-6: SLS results of the structural verifications performed in SCIA	138
Table C-7: Buckling lengths of the columns, from SCIA.....	140
Table C-8: Buckling lengths of the beams, from SCIA.....	140

Table C-9: Translation of a non-standard castellated beam to a regular beam (Grünbauer, n.d.).....	141
Table C-10: Governing unity checks for the members of the Alternative A.....	141
Table D-1: Properties of GL24h (NEN, 2013) and C24 (NEN, 2016b)	144
Table D-2: Parameters in eq. D-2 (NEN, 2005b).....	145
Table D-3: Values for <i>kmod</i> for service class 1 (NEN, 2005b), the load duration class is given in Table D-4.....	145
Table D-4: Examples of load-duration assignment	145
Table D-5: Recommended partial factor <i>γM</i> for different material types (NEN, 2005b)	145
Table D-6: Values for <i>kdef</i> for different material types for service class 1 (NEN, 2005b).....	145
Table D-7: Parameters in eq. D-3	146
Table D-8: Largest normal forces in the horizontal roof bracing system	150
Table D-9: Final deflection results of the structural verifications performed.....	152
Table D-10: Buckling lengths of the beams	153
Table D-11: Governing unity checks for the members of Alternative B	154
Table D-12: Input for the calculation of the splitting failure and block shear failure	163
Table D-13: Calculation of the possible failure modes of the connection.....	164
Table D-14: Comparison between timber floor systems	165
Table E-1: Flexibility factor for connections in Figure B-9 (y-direction) (Staalbouwkundig Genootschap, 1999).....	179
Table E-2: Stiffness calculation of the connection between the roof beam and the columns (y-direction)	179
Table E-3: Flexibility factor for connections in Figure B-7 (x-direction) (Staalbouwkundig Genootschap, 1999).....	180
Table E-4: Stiffness calculation of the connection between the roof beam and the columns (x-direction)	180
Table E-5: SLS results of the structural verifications performed in SCIA	180
Table E-6: Buckling lengths of the columns, from SCIA	181
Table E-7: Buckling lengths of the beams, from SCIA	181
Table E-8: Buckling lengths of the bracing, from SCIA	181
Table E-9: Governing unity checks for the members of alternative C	182
Table E-10: Comparison between concrete (and steel) floor systems	184
Table E-11: Derivation of the width of the hollow core slab members.....	187
Table F-1: Governing unity checks for the members of Alternative D1	192
Table G-1: Governing unity checks for the members of Alternative D2.....	196
Table H-1: Environmental profile of the CO ₂ -equivalent per kg of material, from the One Click LCA tool.....	199
Table H-2: Characteristics of the structural steel EPDs.....	200
Table H-3: Environmental impact of structural steel EPDs (A1-A3) and shadow price conversion	200
Table H-4: Characteristics of the ComFlor steel floor deck EPD	201
Table H-5: Environmental impact of ComFlor steel deck EPDs (A1-A3) and shadow price conversion.....	201
Table H-6: Characteristics of structural concrete (in situ) EPDs	202
Table H-7: Environmental impact of structural concrete (in situ) EPDs (A1-A3) and shadow price conversion	202
Table H-8: Characteristics of structural concrete (in situ) EPDs	203
Table H-9: Environmental impact of stages A1-A3 of generic Dutch values for virgin and recycled concrete, used to calculate the bonus for stage D.....	203
Table H-10: Characteristics of concrete hollow core slab EPDs	204
Table H-11: Environmental impact of concrete hollow core slab EPDs (A1-A3) and shadow price conversion.....	204
Table H-12: Characteristics of structural glulam EPDs.....	205
Table H-13: Environmental impact of structural glulam EPDs (A1-A3) and shadow price conversion	205
Table H-14: Bonus of structural glued laminated timber EPDs (stage D) and shadow price conversion	205
Table H-15: Characteristics of structural CLT EPDs.....	206
Table H-16: Environmental impact of structural CLT EPDs (A1-A3) and shadow price conversion	206
Table H-17: Bonus of structural cross laminated timber EPDs (stage D) and shadow price conversion	206
Table I-1: Evaluation of ten equations against eight analysis criteria (Allacker et al., 2014).....	208
Table I-2: Evaluation of the end of life equations of EN 15804:2012+A2:2019 against eight analysis criteria	208

Table I-3: Parameters in PEF equation block A	209
Table I-4: Parameters in PEF equation block B.....	209
Table I-5: Parameters in PEF equation block C	210
Table I-6: Parameters in PEF equation block D	210
Table I-7: Parameters in PEF equation block E.....	211
Table I-8: Parameters in module D1 in the end of life formula in EN 15804:2012+A2:2019	212
Table I-9: General end of life scenarios for different materials	213
Table I-10: End of life scenarios for different materials after reuse has taken place	213
Table I-11: Technical disassembly factors used in the Disassembly Index (Durmisevic, 2006).....	214
Table I-12: Technical disassembly factor scores for Alternative C, these values are used as the chance of reuse	215
Table I-13: Technical disassembly factor scores for the Base design, these values are used as the chance of reuse	215
Table I-14: End of life scenarios for different materials after reuse has taken place	215
Table I-15: Input for environmental impact calculation of stages A1-A3.....	216
Table I-16: Processing the data for environmental impact calculation of stages A1-A3.....	217
Table I-17: Input for the environmental impact calculation of stage D for concrete and steel elements	218
Table I-18: Processing the data for environmental impact calculation of stage D for concrete and steel elements	219
Table I-19: Result of environmental impact calculation	220
Table I-20: Input for the environmental impact calculation of stage D for timber elements	221
Table I-21: Processing the data for environmental impact calculation of stage D for timber elements.....	222

Abbreviations

AP	Acidification potential	52
ADPe	Abiotic Depletion Non-fuel.....	52
ADPf	Abiotic Depletion Fuel.....	52
CLT	Cross laminated timber.....	13
DfA	Design for Adaptability.....	15
DfD	Design for Deconstruction.....	15
DI	Disassembly Index.....	55
EI	Environmental Impact.....	52
EIC	Environmental Impact Category.....	52
EoL	End of life.....	55
EP	Eutrophication potential.....	52
EPD	Environmental Product Declaration.....	52
FAETP	Freshwater Ecotoxicity.....	52
FSL	Functional service life.....	4
FU	Functional unit.....	53
Glulam	Glued laminated timber.....	13
GWP	Global Warming Potential.....	52
HTP	Human Toxicity Potential.....	52
LCA	Life Cycle Assessment.....	51
LCI	Life Cycle Inventory.....	51
LCIA	Life Cycle Impact Assessment.....	52
LVL	Laminated veneer lumber.....	13
MAETP	Marine Ecotoxicity.....	52
NMD	Nationale MilieuDatabase, in English: National Environmental Database.....	52
ODP	Ozone Layer Depletion.....	52
PEF	Product Environmental Footprint.....	56
POFP	Photochemical Oxidant Formation Potential.....	52
RSL	Reference Service Life.....	53
TAETP	Terrestrial Ecotoxicity.....	52
TSL	Technical service life.....	4

1 Introduction

Buildings have a large influence on the global energy use. It was found that the building sector is responsible for 30% of the global energy use and accounts for 28% of the energy-related CO₂ emissions (UN Environment and International Energy Agency, 2017). This use of energy consists of embodied and operational energy. The embodied energy is attributed to the energy needed to construct a building, from excavation activities and processing of natural resources to manufacturing and transporting elements (Milne & Reardon, 2013). The operational energy is ascribed to the energy consumption for a building to be in use. Several case studies have shown that the operational energy consumption has the highest share (80 to 90%) in the total energy use of buildings throughout their lifecycle (Ramesh, Prakash, & Shukla, 2010). As a response to this high energy use, measures are being taken to reduce the operational energy of buildings. During the Paris Agreement in 2015, it was decided that the energy intensity per square meter of a building needs to be reduced with 30% in 2030 (UN Environment and International Energy Agency, 2017). This aimed reduction is visualised in Figure 1-1 in blue. Also, the European Union requires new buildings to be nearly energy-neutral (European Union, 2020b). This means that for new buildings, the operational energy will be reduced. By also focusing on the embodied energy, the total energy use can be reduced even further.

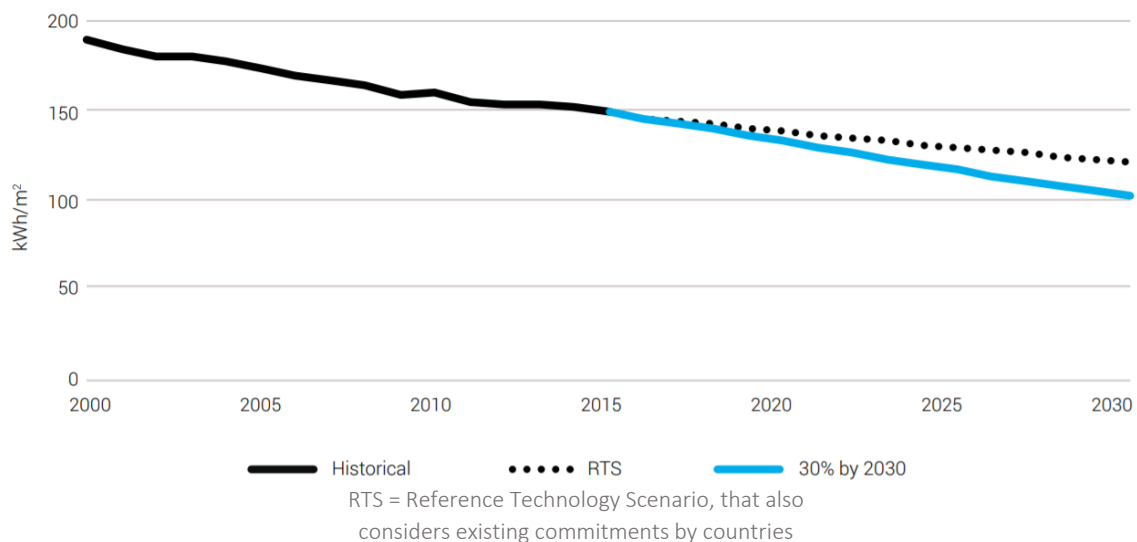


Figure 1-1: Global final energy use per m² (UN Environment and International Energy Agency, 2017)

Besides, the construction sector plays a large role in waste generation and the use of unsustainable materials. The European Union (2020a) reports that the construction sector was responsible for more than 35% of the European Union's total waste generation in 2016. Furthermore, in Europe, the greenhouse gas emissions are estimated to be 5 to 12% of the total greenhouse gas emissions (European Union, 2020a). A reason for these amounts of waste is the setup of our current economy, which is dominantly linear. In a linear economy, products are fabricated from virgin materials, then used, and in the end discarded as waste (Ellen MacArthur Foundation, 2015). If we continue with this linear economy, the World Bank estimates that the annual waste generation will increase with 70% by 2050 (Kaza, Yao, Bhada-Tata, & Van Woerden, 2018). Also, it is predicted that the use of materials such as fossil fuels, biomass, metals, and minerals will double in the upcoming forty years (OECD, 2018).

1.1 Circular economy principles

The European Union wants to transition towards a circular economy. In a circular economy, products can be reused and recycled infinitely, and no waste exists. This transition is visualised in Figure 1-2.

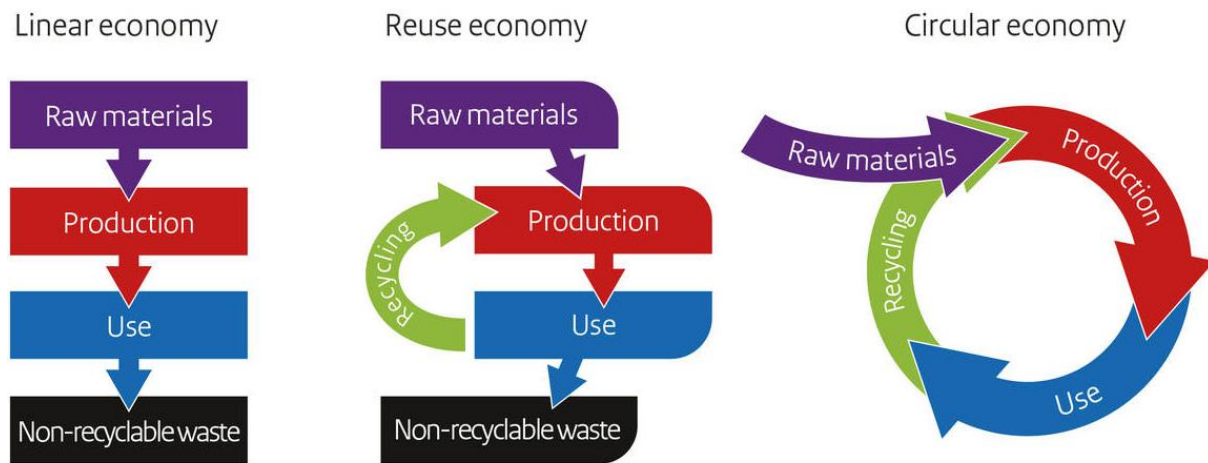


Figure 1-2: From a linear to a circular economy (Government of the Netherlands, n.d.)

Circular economy principles have been researched extensively by the Ellen MacArthur Foundation. Their definition of a circular economy is as follows: *“A circular economy is one that is restorative and regenerative by design and aims to keep products, components, and materials at their highest utility and value at all times, distinguishing between technical and biological cycles”* (Ellen MacArthur Foundation, 2015). To clarify this definition, they have set up the following main principles for the circular economy:

1. Preserve and enhance natural capital by controlling finite stocks and balancing renewable resource flows.
In a circular economy, it is aimed to use materials within the system. If this is not possible, resources should be selected wisely: it is aimed to use technologies and processes that use renewable (or better performing) resources.
2. Optimise resource yields by circulating products, components, and materials in use at the highest utility at all times in both technical and biological cycles.
In a circular economy, waste should be prevented as much as possible. So, it is aimed to use materials as long as possible by maximizing the number of consecutive cycles or by extending the time spent in each cycle. In other words: keep materials and products longer in use by remanufacturing, refurbishing, and recycling.
3. Foster system effectiveness by revealing and designing out of negative externalities.
A circular economy aims to minimize the negative impacts that cause damage to human health and natural systems, for example waste and pollution.

These principles are also depicted in Figure 1-3. In this figure, the second principle is illustrated through biological cycles in green and technical cycles in blue. In the biological cycles, non-toxic materials are restored into the biosphere, whereas in the technical cycles, the materials are released onto the market, with the highest possible quality.

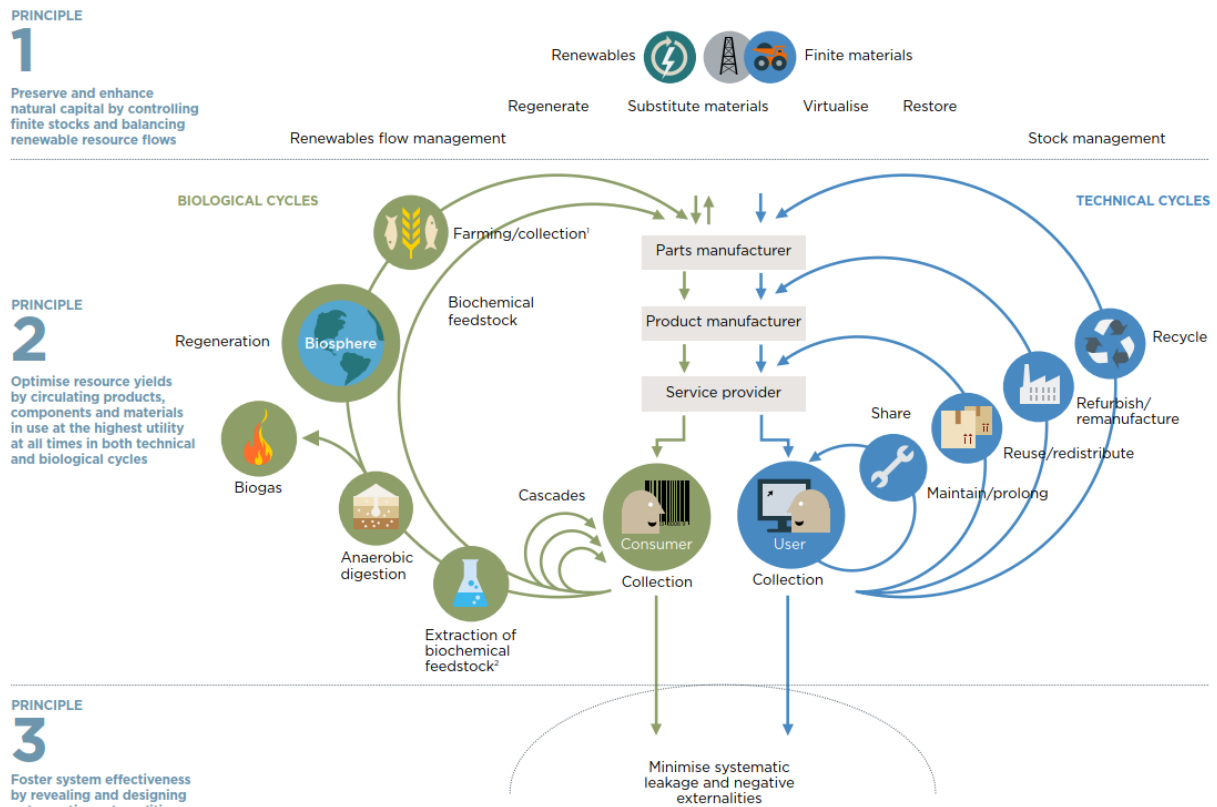


Figure 1-3: Outline of a circular economy (Ellen MacArthur Foundation, 2015)

Left: principles of a circular economy are given. Right: Visual explanation of these principles.

The circular economy aims to create social and environmental value. However, the circular economy also aims for economic value (Van Buren, Demmers, van der Heijden, & Witlox, 2016). Opposed to the linear economy, where money can be earned right away, creating economic value for the circular economy can be more difficult. The Ellen MacArthur Foundation (2015) has set up the following principles on how to create value in a circular economy (visualised in Figure 1-4):

1. Power of the inner circle
The smaller the circle is, the more value can be created. Maintaining and prolonging a product retains most of the value of a product. A second option is reusing or redistributing a product. Thirdly, refurbishing or remanufacturing can be applied and finally recycling.
2. Power of circling longer
Value can be created by prolonging a product's cycle, by maximising the number of successive cycles and/or the length of each cycle, because no new materials and energy are needed to create a new product.
3. Power of cascaded use
Diversifying reuse across the value chain creates value. Materials will then be reused in another product with a different purpose, making sure that the number of virgin materials can be reduced.
4. Power of pure inputs
Using uncontaminated materials in a product increases the possibility to separate, collect, and redistribute these materials at a later stage. This ensures that the number of virgin materials can be reduced.

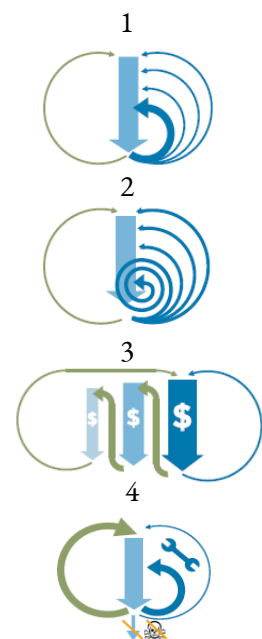


Figure 1-4: Value creation of a circular economy (Ellen MacArthur Foundation, 2015)

These principles show that an important aspect to create value in a circular economy is reducing the virgin materials needed. This can be explained as follows: firstly, a region or company that follows the circular principles will be less dependent upon the import of raw materials from other regions or companies (Van Buren et al., 2016). Secondly, many products use fossil materials that are limitedly available on earth. In a circular economy, the dependence upon these resources will also decrease.

Another way to look at circularity is by means of the 9 R's (Raad voor de leefomgeving en infrastructuur, 2015) This list is shown in the following figure. To create a circular economy, it is aimed to follow the strategies with the lowest numbers.

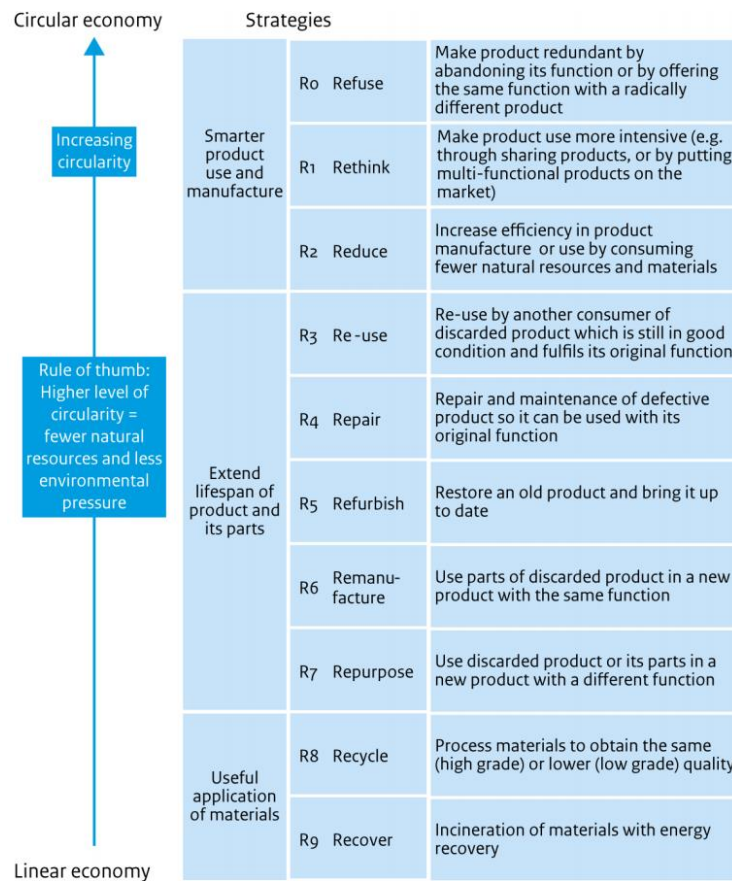


Figure 1-5: 9R strategies increasing circularity (Potting, Hekkert, Worrell, & Hanemaaijer, 2017)

1.2 Circular building strategies

The circular economy principles can also be applied to the building industry. In this sub-chapter, circular building strategies are explained. In general, it can be stated that a building that stands for a longer period is more environmentally friendly than a building that only stands for a shorter period. Therefore, in the design phase of a building, the yearly environmental impact needs to be estimated. This is the total environmental impact divided by the service life. There are different perspectives to estimate the service life (Straub, Van Nunen, Janssen, & Liebrechts, 2011; Tool, 2010):

- Technical service life (TSL): the period in which a building fulfils the technical requirements
- Functional service life (FSL): the period in which the building fulfils the user's functional requirements
- Economic service life (ESL): the period in which it is economically feasible to use the building or to apply maintenance to the building

In a lot of building projects, the technical, functional, and economic service life are not aligned. This means that materials are not used to their full lifespan and that the actual environmental impact is higher than expected. Besides, this does not fit the circular economy principles, where it is aimed to keep materials in use for as long as possible. Therefore, it is necessary to find solutions to use materials for a longer time. In a study by Vonck (2019), three strategies are proposed to align the technical and functional service life better. For each strategy, a figure is made, which is followed by a textual explanation.



Figure 1-6: Strategy 1: Optimise for one function (Vonck, 2019)

In strategy 1, a building is designed for a specific function. Here, the focus lies on matching the technical service life to the functional service life. This can be reached by either selecting a certain material type or optimising the material use for that specific function. Strategy 1 is based upon strategy R2 ‘Reduce’ (as explained in Figure 1-5).

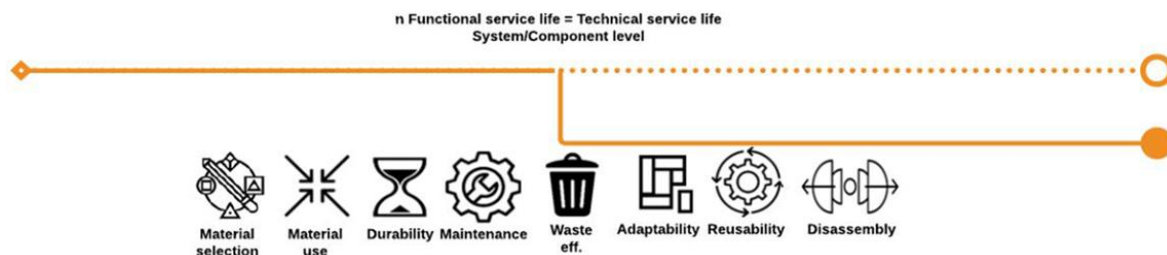


Figure 1-7: Strategy 2: Optimise residual value (Vonck, 2019)

In strategy 2, it is foreseen that the building will not fulfil its function for the whole technical life span. However, the components in the building will have sufficient technical abilities to be used for a longer period. Therefore, this strategy focuses on the afterlife of a building and follows strategy R3 ‘Reuse’ (from Figure 1-5). Reusing elements for other buildings will increase the element’s functional service life and will minimise the need for virgin materials in future buildings. To be able to reuse components, it is vital that the structure is demountable.



Figure 1-8: Strategy 3: Optimise for multiple functions (Vonck, 2019)

Strategy 3 expects that the function of the building might change in the future. These changes are unknown at the time of design and construction and the response to these changes should happen with little time, effort, or costs. To expand the lifespan of the building, strategy R7 ‘Repurpose’ (from Figure 1-5) should be followed. Flexibility and adaptability should be proactive attributes within a system, rather than a reactive action which may cost too much time, effort, or costs (Gosling, Sassi, Naim, & Lark, 2013). The aim of an adaptable building is to deliver the utmost value to the user, leading to an increase of the functional life span (Kissel, Schrieverhoff, & Lindemann, 2012).

1.3 Case study

This research is conducted under the supervision of Royal HaskoningDHV. Royal HaskoningDHV designs distribution centres for a client in Europe. The designs drafted by Royal HaskoningDHV are preliminary designs, made available as a pan-European template. Once a template is finished, a local contractor will work out the design for a specific location. Royal HaskoningDHV sets up a concrete and a steel design, so the contractor can work with their preferred material.

The distribution centre shown in Figure 1-9 is investigated in this research. This is a logistic centre consisting of a warehouse with one mezzanine floor, an office, a welfare area, and two break rooms. In this research, only the warehouse is investigated. This is the main building that is shown in Figure 1-9.

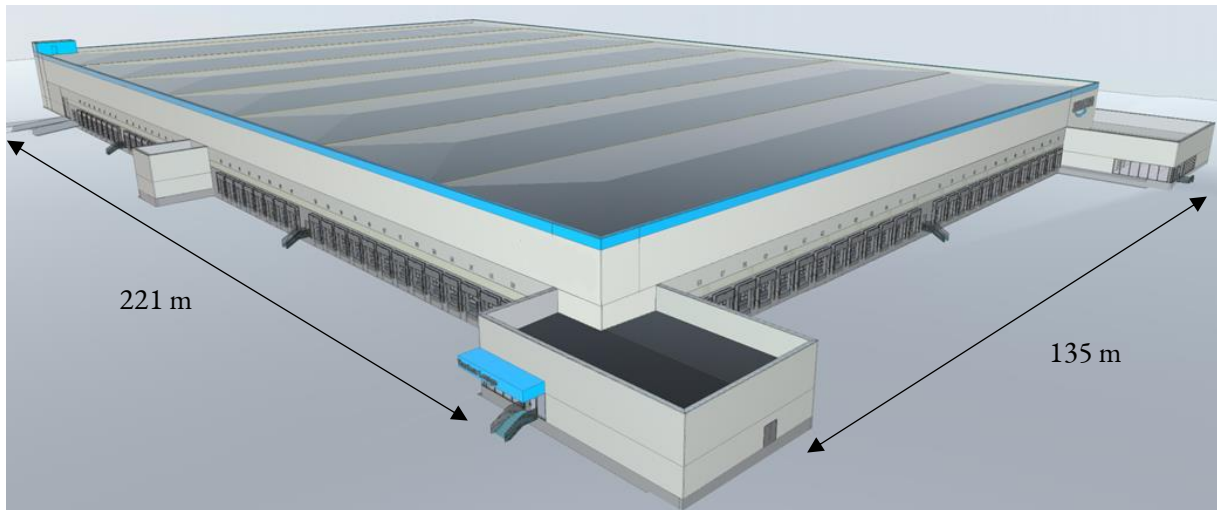


Figure 1-9: 3D view of the distribution centre (Royal HaskoningDHV Internal Document, 2020c)

In Figure 1-11, a 3D view of the structure is shown. This figure shows the steel roof beams, steel columns, steel floor beams, the composite mezzanine floor, the concrete ground floor, and the concrete foundation. To understand this system better, the two main parts of the load-bearing structure will be explained:

- Sway frame made from steel columns and beams
The main load-bearing structure of the building is a steel sway frame. This stability system is chosen because of two reasons. Firstly, because the façade on the ground floor needs to be open for trucks (as can be seen in Figure 1-9). This means that it is not possible to add bracings in the façade. Secondly, because the client requires the building to be erected as fast as possible, which can best be reached with a sway structure.
- Mezzanine floor made from a composite floor with cast in situ concrete on top of a steel deck
The mezzanine floor is used by robots and contains openings for packages to slide down towards the ground floor. This ensures that a very specific floor design is needed. Furthermore, in the design of the warehouse, a possibility for another use in the future is already included. This means that the stability of the building is ensured even without the presence of the mezzanine floor. Thus, the mezzanine floor only needs to carry the vertical loads due to the robotic function.

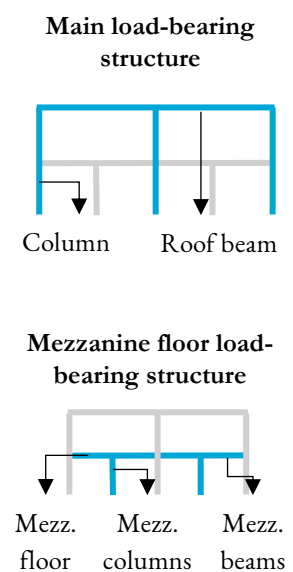


Figure 1-10: Visualisation of the main and mezzanine load-bearing structure

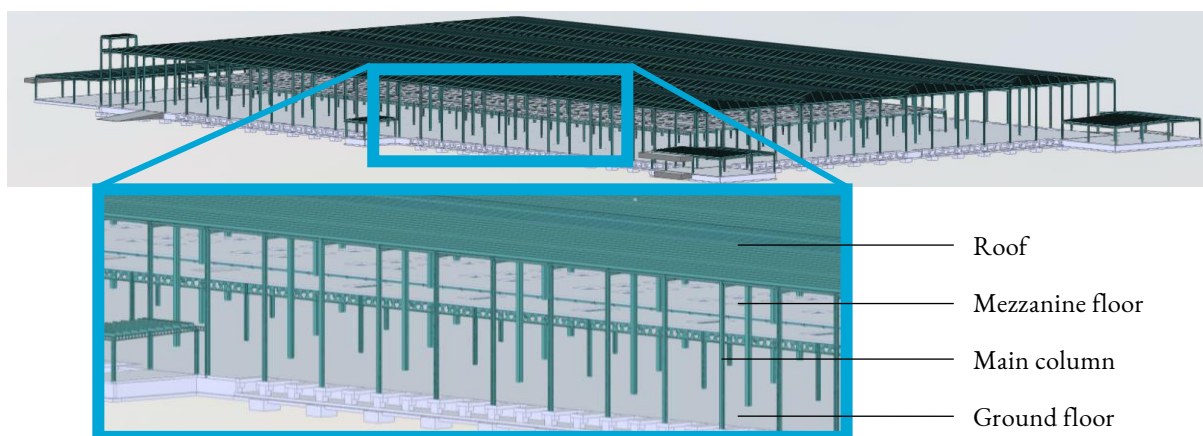


Figure 1-11: 3D view of the structure (Royal HaskoningDHV Internal Document, 2020c)

1.3.1 Sustainability

Sustainability is an important aspect for the client. Their goal is to have 100% net zero carbon buildings by 2040. They want to reach this goal in three steps. First, their focus will mainly lie on reducing all direct emissions. This includes fuel combustion on site, such as diesel generators, gas boilers and refrigerant leaks. Secondly, they will put their focus on indirect emissions from purchased and used energy. Finally, they will focus on all other indirect emissions, such as waste, water use, the building structure, and the building envelope. From internal research of Royal HaskoningDHV, it is found that depending on the type of distribution centre they designed, between 50% and 80% of the CO₂ emissions are caused by the load-bearing structure (Hoeh, 2020). Therefore, it is important to research sustainability improvements in the building structure. To reduce the yearly environmental impact of the case study, the strategies mentioned in the previous sub-chapter can be incorporated into design alternatives for the case study. A link between the strategies and the case study is made:

- Strategy 1 aims to optimise the design for one specific function. This is the case for the current case study design. However, the economic service life of the building is much shorter than the technical service life. This leads to a relatively high yearly environmental impact of the building. Since the economic service life is not expected to change, it is valuable to investigate whether the yearly environmental impact can be reduced if the design is optimised for its initial material use.
- Strategy 2 and 3 aim to find solutions to extend the economic service life of the materials:
 - Strategy 2 focuses on the afterlife of a building, meaning that the design could be optimised for its residual value.
 - Strategy 3 focuses on extending the use stage, meaning that the design could be optimised for multiple functions.

Based upon the 9 Rs it can be stated that Strategy 1 is expected to be most effective, because this strategy follows the R with a low number (R2 'Reduce'). It is expected that the second most effective strategy is Strategy 2 (R3 'Reuse') and the least effective strategy is Strategy 3 (R6 'Remanufacture' and R7 'Repurpose'). It is aimed to find out whether this also holds for the case study.

Notes

To prevent misunderstandings, in this research a point (.) is used as a decimal marker. Furthermore, in this thesis many illustrations are used. If the illustration is made for this thesis, no source is given.

2 Research definition

Based on the introduction, it can be defined where further research is necessary. This chapter first summarises the problem through a problem definition. Based on the problem definition, the objective, research questions and the scope for this research are set up. The chapter continues with the research outline.

2.1 Problem definition

The building sector is responsible for a large portion of the global energy use, water consumption, waste generation, and the emission of greenhouse gases. Also, the load-bearing structures of buildings have a significant share in these emissions. Buildings are often driven by direct economic value and fast erection, but European and national regulations oblige to focus on the sustainability value of designs as well. Therefore, more quantitative in-depth data on sustainable structural design options are needed. Sustainable structural design options can give guidance on what aspects of the structural design have the highest environmental impact. This research will focus on a specific case study: a distribution centre design of Royal HaskoningDHV. For this distribution centre design, it is unknown how the environmental impact can be reduced most effectively.

Assessment methods have been set up to calculate the environmental impact of buildings, but these methods often fail to assess buildings comprehensively. Many of these assessment methods do not consider the end of life of a building, leading to incomplete results (Rios, Chong, & Grau, 2015). Some methods do include the end of life of a building, but it is unknown which of these methods can best be used to quantify the environmental impact of the load-bearing structure of a distribution centre.

2.2 Research objective

This research aims to contribute to science and practice by investigating design choices a structural designer can make to reduce the yearly environmental impact of a distribution centre's load-bearing structure. To reach this goal, different strategies are incorporated in different design alternatives. As explained in sub-chapter 1.2 "Circular building strategies", it is decided to follow strategies 1, 2, and 3. Strategy 1 aims to optimise the design for one specific function, by optimising the material use. Strategy 2 aims to extend the economic service life of the building, by optimising the design for residual value. Finally, strategy 3 aims to extend the economic service life of the building, by optimising the design for multiple functions.

To measure the differences between the design alternatives, it is necessary to perform research on environmental impact calculation methods. Here, it is aimed to find a suitable method to quantify the environmental impact of the load-bearing structure of a distribution centre.

2.3 Research questions

To reach the objective, the following main research question is set up:

Which design choices have most influence on the yearly environmental impact of the load-bearing structure of a distribution centre?

To answer the main research question, the following sub-research questions are set up:

1. What aspects influence the environmental impact of the main building materials (steel, concrete, and timber)?
2. How can the functional service life of building elements be extended?
3. Which material and design choices can be made in the design of a distribution centre to reduce the yearly environmental impact?
 - a. What design choices can be made to reduce the yearly environmental impact of a distribution centre design that is optimised for its initial material use?
 - b. What design choices can be made to reduce the yearly environmental impact of a distribution centre design that is focused on optimising its residual value?
 - c. What design choices can be made to reduce the yearly environmental impact of a distribution centre design that is optimised for multiple functions?
4. How can the environmental impact of a distribution centre's load-bearing structure be quantified in a comprehensive way?
5. Which of the design alternatives that are set up for this research results in the lowest yearly environmental impact?

2.4 Scope

This research is limited to the following scope:

- As it is not possible to investigate the environmental impact of all type of distribution centres, a specific distribution centre layout will be used as input for the design alternatives. This is a distribution centre design with two floor levels. The main load-bearing structure is made from steel and the mezzanine floor is made from steel and concrete.
- The design alternatives must be based upon the same requirements. This will ensure that the comparison of the environmental impact is related to their use, instead of only comparing the impact per kilogram material.
- The location of the design alternatives is unknown. This means that in the calculation of the environmental impact, transportation and specific processes will be kept out of the scope. More specifically, only stages A1-A3 and D of the LCA will be investigated in this research.
- The foundation (including the ground floor) will not be investigated. It is acknowledged that if one design is lighter than another design, the foundation's material use reduces, leading to an overall lower environmental impact.

2.5 Research outline

In the following figure, the overview of the research is shown. For each chapter, the accompanying research question is stated. The research starts with setting up design alternatives, where, based upon the answers to research questions 1, 2, and 3, six design alternatives are drafted. Here, it is aimed to find out how a building's impact on the environment can be reduced. For each design alternative, the necessary mass or area needed for each element is used as input for the second part of the research. In the second part of the research, the environmental impact is investigated and is calculated for each design alternative. Finally, the results are discussed and from this, conclusions and recommendations are given.

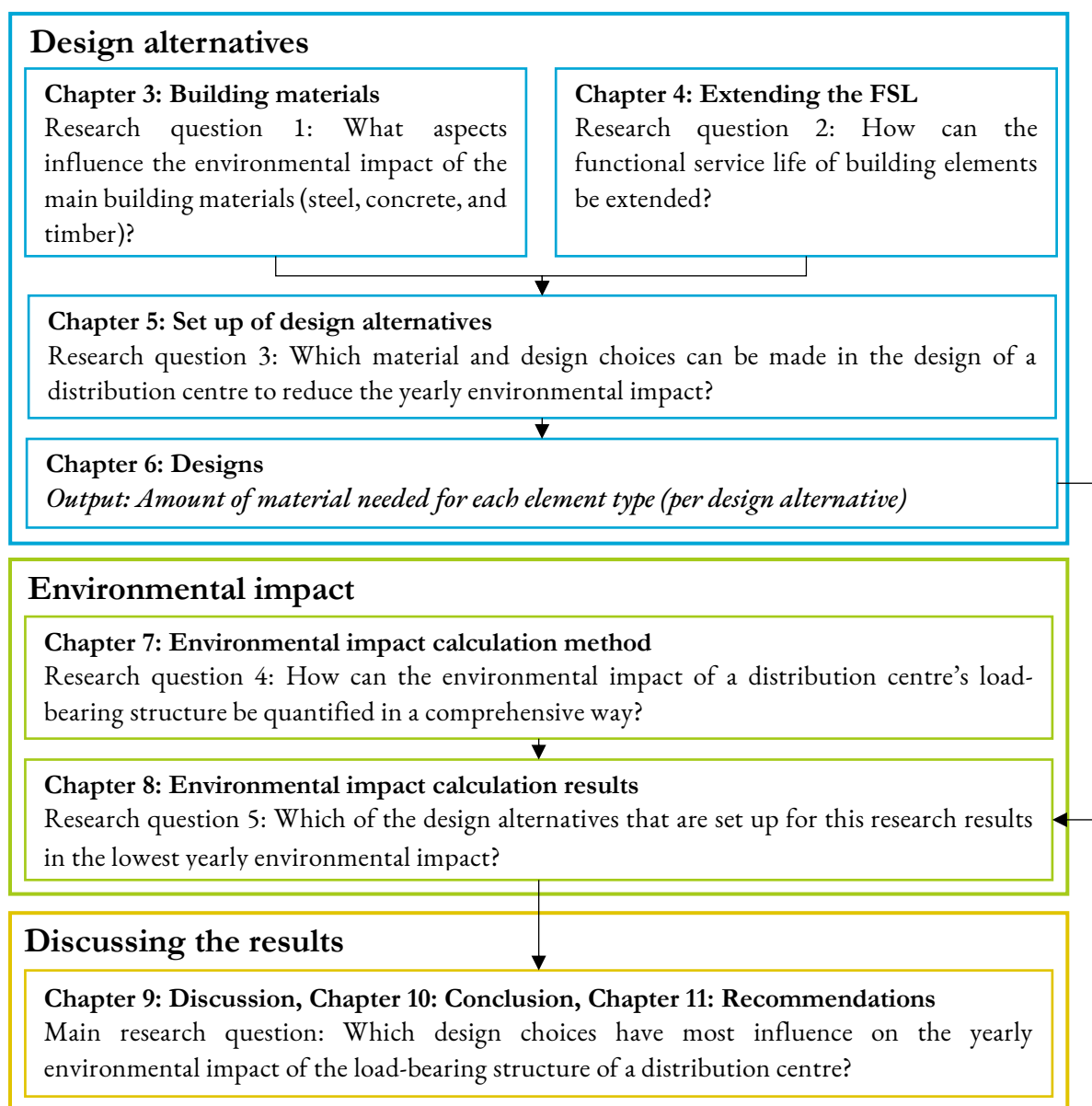


Figure 2-1: Overview of the research

3 Building material characteristics

Buildings are usually constructed out of steel, concrete, and timber. In this subchapter, each material will be assessed on its environmental impact, and its ability to be recycled, adapted, and reused. Recycling, adapting, and reusing are included, because this shows the possibilities to reduce the environmental impact of these materials. Finally, an answer will be given to research question 1 *“What aspects influence the environmental impact of the main building materials (steel, concrete, and timber)?”*

3.1 Steel

The raw materials needed to produce steel are abundantly available on earth. Nonetheless, the production process produces a lot of energy and environmental pollution. Considering specific steel products, some remarks can be given. Sperle et al. (2013) found that the environmental impact of the production of steel is influenced by the steel strength. Per unit of steel weight, an increase of the steel strength also slightly increases the environmental impact. However, when applying higher strength steel, the amount of material can be reduced, which can lead to a lower environmental impact. This shows that it cannot be stated that choosing a certain steel strength will lower the environmental impact as well. In this research, it is therefore decided to use the conventional steel strength S355.

The environmental impact of steel can be reduced by recycling the steel, as steel is 100% recyclable without loss of quality. Virgin steel is produced in a Basic Oxygen Furnace and recycled steel is produced by melting scrap in an Electric Arc Furnace. These processes differ per manufacturer and country, but it can be stated that in general, the production of recycled steel requires much less energy than the virgin steel production process (Burchart-Korol, 2013; IEA, 2020; Yellishetty, Mudd, Ranjith, & Tharumarajah, 2011). Nevertheless, the energy needed for recycled steel is often too high to use renewable energy sources only (Van Maastrigt, 2019).

Steel is vulnerable to corrosion, so it needs to be protected by protective paint. A. Aversch from the steel construction company Brink Staalbouw (personal communication, May 6, 2020), explained that most protective paints have a polluting effect because chemical substances such as ammonia are released into the atmosphere. To reduce pollution, they advise to apply a powder coating instead of a liquid coating. In that case, no coating is lost, because the powder that does not stick to the steel right away can be collected and applied onto the steel again. For a liquid coating, this collection is not possible, which ensures a part of the coating is lost. Nowadays biobased coatings are developed as well, which can be a solution for future designs.

At last, steel has good durability properties, meaning that no major changes occur due to the ageing of the steel (Dunant et al., 2017). This makes steel an effective material to be adapted or reused. The efficiency of the reuse of steel depends on the connection design. If a welded connection is applied, the elements need to be cut, drilled, and welded to be able to reuse it at another location (Fujita & Masuda, 2014). In case a bolted connection is reused, wearing of the bolts is expected. Brink Staalbouw, as a steel construction company that is specialised in circular steel buildings, therefore advises using new bolts for new connections (A. Aversch (Brink Staalbouw), personal communication, August 12, 2020).

3.2 Concrete

Concrete is a composite of water, aggregates, and cement, of which cement has the highest negative influence on the environment. According to NEN-EN 197-1:2018, there are six main cement types. A difference between these cement types is the amount of Portland clinker, which has a negative effect on

the CO₂ emissions. The environmental performance of concrete can be improved by replacing part of the Portland clinker with less harmful binders such as fly ash, blast furnace slag, and limestone flour (Uitvoeringsteam Road Map CO₂-reductie, 2021). However, lowering the amount of clinker in cement reduces the initial strength, reduces the frost resistance, and increases the temperature sensitivity. Therefore, Van Herwijnen (2013) advises using at least 20% clinker in cement. Furthermore, as explained in the paragraph about steel, reinforcement steel also affects the environment.

A designer can choose to use in situ or prefabricated concrete. In case the same type of concrete is used, prefabricated concrete has a higher CO₂ emission than in situ concrete. This difference is caused by the transportation and lifting capacity needed at the construction site (Van Herwijnen, 2013). Also, prefabricated concrete usually needs to have a higher strength with more cement so the concrete can be demoulded earlier, which increases the environmental impact.

Recycling of concrete is possible, but quality is lost in this process. Van Herwijnen (2013) explains the steps that need to occur for recycling. First, the reinforcement steel and concrete need to be separated in the demolition process. Then, the reinforcement steel can be melted into new reinforcement steel. At the same time, the concrete can be transformed into concrete granulate and can be used as a secondary aggregate for new concrete. Ultimately, it is possible to separate the concrete further into cement stones and aggregates. Recycled concrete aggregate has a lower quality than natural aggregates because it contains weak adhered mortar. The weak adhered mortar leads to a lower density, higher porosity, and increased water absorption (Shaban et al., 2019). Besides, recycled concrete aggregate has a lower strength than natural aggregate. Several types of research have investigated the decrease in compressive strength between recycled concrete aggregate and natural aggregate. Debieb & Kenai (2008) found a decrease of 40% for both fine and coarse aggregates. Saravanakumar et al. (2016) found a decrease of 25% and Yang et al. (2020) found a decrease of 42%. Techniques to increase the quality of the recycled concrete aggregate are being developed, but this is not being applied on large scale yet (Shaban et al., 2019). Based upon these quality losses, concrete with recycled material has a maximum of 40% recycled content.

In a design with cast in situ concrete with monolithic joints, reuse is not possible. Therefore, reusability should be considered in the design process, and the focus should lie on using prefabricated elements with demountable connections (Van Herwijnen, 2013).

Adaptability of concrete elements can be reached by applying external reinforcement, which is glued onto the existing structure (Van Herwijnen, 2013). With this solution, it is possible to increase the load-bearing capacity of the concrete, which ensures that the building can be used for another function as well.

3.3 Timber

Timber is considered one of the most environmentally friendly construction materials. Due to photosynthesis, a growing tree sequesters carbon by capturing CO₂ from the atmosphere (Beyer et al., 2010). The amount of CO₂ that is stored in a forest is dictated by the forest growth and tree harvesting rate. The growth rate of a natural forest declines when a forest ages (Salazar & Bergman, 2013). The carbon sequestration rate of forests is proportional to the growth rate, meaning that at some point, mature forests are unable to take up any extra CO₂ (Kyrklund, 1990). This shows that forest preservation is not an efficient method for carbon sequestration. Therefore, timber should be harvested from sustainably managed forests from for example the Forest Stewardship Council (FSC) or Programme for the Endorsement of Forest Certification (PEFC). These organisations guarantee forest growth and keep the harvesting rate up to a sustainable level.

To use a tree for construction, it needs to be felled and manufactured into planks. Felling and manufacturing trees cost energy, but this is only a fraction compared to the energy needed to produce steel or concrete (Van Herwijnen, 2013). Usually, a timber plank on its own is not strong enough to be used as a load-bearing structure. More strength can be gained by using engineered timber elements such as glued laminated timber (glulam), cross laminated timber (CLT), or laminated veneer lumber (LVL). Engineered timber elements have a higher environmental impact than sawn timber. This has to do with the different production process, which can be seen in Figure 3-1. In dark green, the manufacturing process of sawn timber is shown. This process can be extended to create glulam or CLT, which is shown in light green in Figure 3-1. To produce LVL, the timber is peeled instead of sawn and a bonding process at high temperature is necessary. In the research of Van Wijnen (2020), it was found that LVL has the highest environmental impact, which is mainly caused by the extra energy that is needed to reach the high temperature for the bonding process. In second place, glulam and CLT are located and finally, sawn timber has the lowest environmental impact.

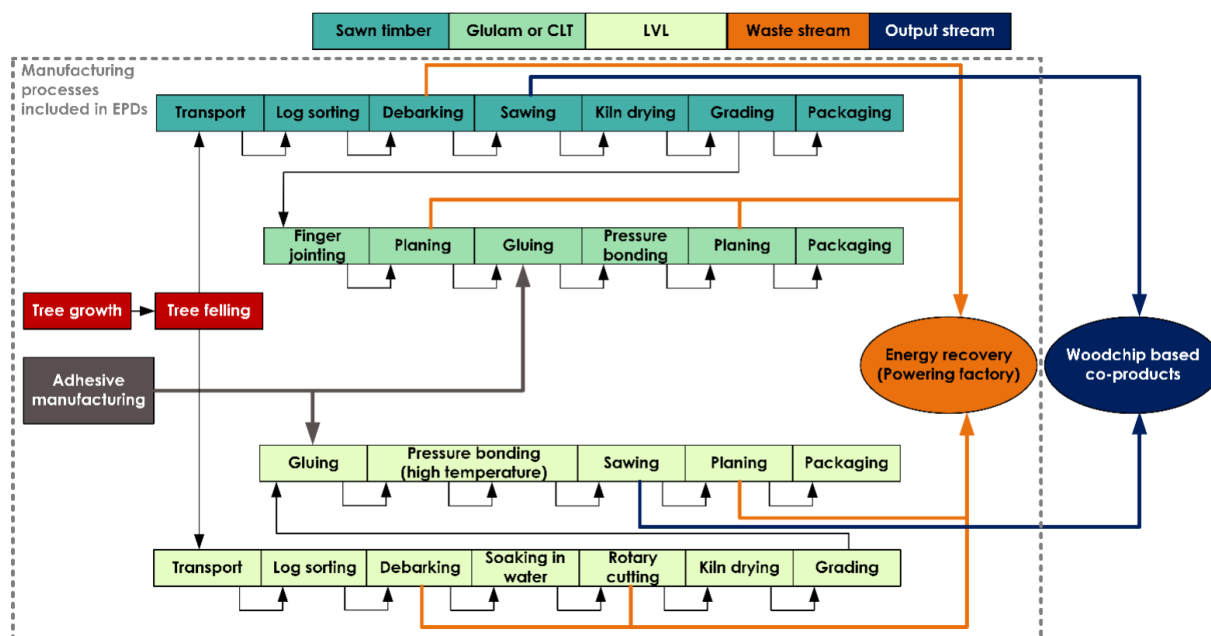


Figure 3-1: Manufacturing process of sawn timber, glulam, CLT, and LVL (Van Wijnen, 2020)

At the end of life, a timber element can be incinerated, recycled, reused, or end up in the landfill. Most often timber elements are incinerated. Then, the carbon dioxide that was stored in the timber is released back into the atmosphere, together with the incineration emissions. As an alternative, there is more and more interest in using the produced energy from incineration as a renewable energy source for other production processes (Beyer et al., 2010).

In case timber is recycled, this can only lead to lower quality products such as chipboards or fibreboards, where sawdust and shavings from the timber are used as input (Beyer et al., 2010).

Different researchers (Crews, Hayward, & MacKenzie, 2008; Crews & MacKenzie, 2008; Falk, Maul, Cramer, Evans, & Herian, 2008; Hradil et al., 2014), discovered the effect of reuse for timber elements by performing physical tests. It was found that reused timber elements have lower strength properties than virgin timber elements. For a known load history, the strength properties can be estimated at 20% to 55%

of the strength properties of the virgin material. Besides, it was discovered that the modulus of elasticity remains the same as the virgin material.

3.3.1 European Product Declaration (EPD) data

In Europe, manufacturers can set up a European Product Declaration (EPD). This is a sheet with data on the environmental impact of the product that is assessed. In the EPDs, there is a lack of data about the structural performance of sawn timber and glued laminated timber (Dias, Dias, Silvestre, & De Brito, 2020). The strength class influences the environmental impact, but only some EPDs specify the strength properties of the assessed product. Often, a range of strength properties is given, which results in high variability of the EPD results.

Dias et al. (2020) also investigated which types of strength classes were most often assessed in EPDs. They found that for sawn timber and CLT, strength class C24 was most often assessed and for glulam, GL24h was considered as conventional. Therefore, it is decided to apply these strength classes in this research as well.

3.4 Conclusion

This chapter answered research question 1 *“What aspects influence the environmental impact of the main building materials (steel, concrete, and timber)?”*

In general, it can be stated that the environmental impact of building materials is dependent upon the product characteristics. A higher steel strength results in a higher environmental impact per kg steel. For concrete, prefabrication results in a higher impact and the environmental impact is influenced by the amount and type of cement. Finally, due to the production process, sawn timber has the lowest environmental impact, followed by glulam and CLT, and lastly LVL.

For steel, the environmental impact can be reduced by applying recycled steel instead of virgin steel. A downside of steel is the necessity of protective paints, which impact the environment negatively. At the end of life, steel can be recycled into high quality products without loss of quality and due to the good durability properties is reuse a feasible solution as well.

Concrete cannot be recycled as well as steel, as its quality reduces significantly. Research is being conducted to increase the quality of recycled concrete, but this is not applied on large scale yet. An option to lower the environmental impact of concrete is using less clinker in the cement, where a minimum of 20% clinker should be followed. At the end of life, it is possible to reuse the concrete if demountable connections are applied, this means that prefab elements should be used, instead of in situ concrete.

Timber has an important advantage compared to steel and concrete: carbon is sequestered in the material. In the production process, energy is needed to produce different engineered timber elements. At the end of life, recycling leads to a reduction in quality and reuse has the disadvantage that the strength properties are reduced, which makes reuse less interesting compared to steel or concrete.

4 Principles to extend the functional service life

In this chapter, research question 2 “*How can the functional service life of building elements be extended?*” will be answered. This was already shortly mentioned in sub-chapter 1.2 “Circular building strategies”. Here, it was stated that the functional service life can be extended by following strategy 2 “Optimise for residual value” or strategy 3 “Optimise for multiple functions”. For strategy 2, Vonck (2019) suggested focusing on reusability and disassembly. This is part of the principle Design for Deconstruction (DfD). For strategy 3, Vonck (2019) suggested incorporating flexibility and adaptability of the structure. Both aspects are considered in the principle Design for Adaptability (DfA).

4.1 Design for Deconstruction (DfD)

Design for Deconstruction aims to reuse components. Design for Deconstruction can be applied on different scales: relocation of a whole building, reuse of components, reprocessing of materials, and recycling of materials. It is aimed to follow the principle of the power of the inner circle of the Ellen MacArthur Foundation, so first investigate the possibilities of the relocation of a whole building, followed by the reuse of components, reprocessing of materials, and finally recycling of materials. Per category, different aspects apply. These aspects are explained in the following paragraphs.

Relocation of a whole building means that at the end of life, the building will be disassembled and reconstructed at another location. To do so, components need to be removed from the building separately. This will be explained in the following paragraph.

Reuse of components means that it is possible to remove a component system or specific element without having to remove other elements (Durmisevic, 2006). The following aspects need to be considered on the reuse of components level:

- Layer building components and make sure objects are not integrated so parallel disassembly is possible (Crowther, 2000; Van Vliet, 2018). The building should be divided into layers that can be maintained and adapted without affecting other layers. This is based on the model of Brand (1995), which can be seen in Figure 4-1. Brand argues that building layers with different life cycles should not be integrated or connected. He defines the life cycle of the site to be eternal, the structure including the foundation and load-bearing elements to last between 30 and 300 years, the skin to last for 20 years, the services such as heating, ventilating, air conditioning, electrical wiring to last 7 to 15 years, the space plan with vertical partitions, doors, ceilings, and floors to be able to change every 3 years, and stuff needs to be able to move on a daily basis.
- Use prefabricated elements instead of elements that are built on site. This reduces the amount of work on the construction site and thus also eases the disassembling process (Crowther, 2005). The amount of work is reduced because standard connections are used (Durmisevic, 2006), connections are easier accessible (Rios et al., 2015), and a complete component system can be disassembled at the same time (Van Vliet, 2018).

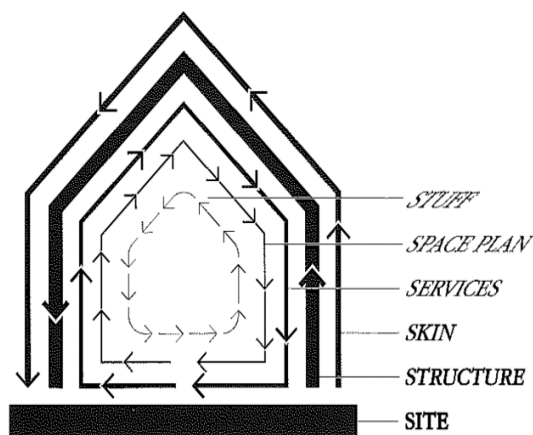


Figure 4-1: Building layers (Brand, 1995)

- Limit the component size such that it can be handled properly (Crowther, 2005; Van Vliet, 2018). During the construction phase, requirements are given to the dimensions of the elements. This is based on transport and handling limitations. For disassembly, handling of components is even more important, as it should be possible to remove only parts of the structure.
- Make connections easily accessible (Crowther, 2005; Rios et al., 2015). Here, it is meant that it is possible to access the connections without having to demolish elements (Durmisevic, 2006).
- Use dry connections to be able to separate elements (Rios et al., 2015; Van Vliet, 2018).
- Minimise the number of different connection types, so disassembly speed increases and fewer types of tools are necessary (Crowther, 2000; Guy, Shell, & Esherick, 2006).
- Minimise the number of connections, so disassembly speed increases (Crowther, 2005; Van Vliet, 2018). The more connections are used in a building, the more time demounting takes. Also, it increases the possibility of damaging elements.

Reprocessing of materials aims to use the materials to manufacture new building elements (Crowther, 2005). Component remanufacturing requires the following aspects to be considered:

- Use dry connections so materials can be separated from each other (Crowther, 2000).

Besides, the following features belong to the reprocessing of materials and material recycling:

- Apply a simple composition of materials to simplify the sorting process (Crowther, 2000; Rios et al., 2015).
- Avoid toxic and hazardous materials, because these materials cannot be reused or recycled (Akinade et al., 2016; Crowther, 2005; Guy et al., 2006; Rios et al., 2015).
- Avoid finishes to materials that contaminate the base material, because this also ensures that the materials cannot be reused or recycled anymore (Crowther, 2000).

In addition to the design aspects, Design for Deconstruction can only be successful if the following steps are also considered:

- Disassembly guide (Morgan & Stevenson, 2005; Rios et al., 2015; Van Vliet, 2018)
Without a disassembly guide, it is very likely that building elements that are designed to be reused will be destroyed, because disassembly is more complicated and takes more time than mechanical demolition. According to research from the US Army Corps of Engineers in 2002, disassembly time increases with three to eight times compared to mechanical demolition. During the design process, the way the building should be disassembled should be investigated. This contains information on the order of disassembly, which specific knowledge is necessary to demount a product, and how elements should be handled after disassembly.
- Create a material inventory (Morgan & Stevenson, 2005; Platform CB'23, 2019)
Information about the elements used should be written down in a material inventory. This includes material specifications, warranties, and manufacturers details. For the load-bearing structure, it is at least necessary to know which design principles are used, the load-bearing capacity of elements, and which loads elements are carrying. This ensures that it is possible to determine in the future which materials can be reused. In the Netherlands, Madaster has been set up as a material inventory and the European Union has set up BAMB, which stands for Building As Material Banks.

4.1.1 Implementing DfD in the case study

The case study covers the design of a load-bearing structure and excludes the specific design of components, so Design for Deconstruction is implemented on the reuse of components level. For the case study, the following additions should be followed:

- Layering of building components

In the case study, ducts and piping pass through the castellated beams. For the main floor beam, this can be seen in Figure 4-2 in green. In the roof, also some pipes are integrated into the straight castellated beams. In case the structure will be demounted, the services will be removed as well. The services are not fixed in the castellated beams, ensuring that the castellated beams are not affected by this change.

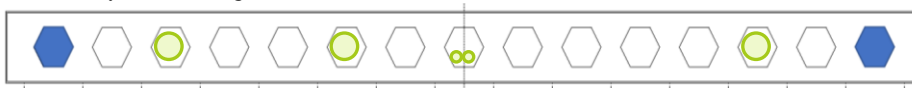


Figure 4-2: Elevation of the main floor beam showing openings for ducts and piping (Royal HaskoningDHV Internal Document, 2020a)

- Use of prefabricated elements

In the case study, prefabricated steel elements are used, but the mezzanine floor and ground floor in the design are made from in situ concrete. The ground floor is kept outside the scope, but the mezzanine floor should be altered into a prefab concrete floor.

- Limit the component size

The beams and columns used in the case study design have significant lengths. However, due to the large grid and the limited dimensions of the steel elements in the other directions, it is expected that it is possible to remove these elements from the building.

Based upon the Design for Deconstruction principles, the following aspects for the connections in between components are guiding:

- Accessibility of connections

Connections should be easily accessible to prevent damage to the elements. The connections between the beams and columns in the case study design are accessible, so it is expected that this can be reached in this alternative as well. For the mezzanine floor, it is possible to access the connection between the steel beams and the steel deck. However, the connection between the concrete and steel cannot be accessed.

- Use dry connections

An important aspect of Design for Deconstruction is the use of dry connections that can be demounted relatively easily. In a steel design, dry connections can be created with plates that are connected by bolts. For the concrete floor, no monolithic joints should be used.

- In case welded connections between steel elements are used, it should be aimed to use connecting elements which do not extend beyond the element. This is based upon the fact that in a steel connection, end plates are often used. An example of an end plate connection is shown in Figure 4-3 on the next page. Here, the end plate is welded onto the beam and bolted onto the column. Following the Design for Deconstruction principle, the use of welds should be prevented. However, for the figure on the left, where the end plate does not extend from the beam, the beam can be reused in another layout as well. If the beam in the figure on the right will be reused, the welded end plate can be in the way, resulting in lower reusability. Therefore, it should be aimed that welded connecting elements do not extend beyond the elements.

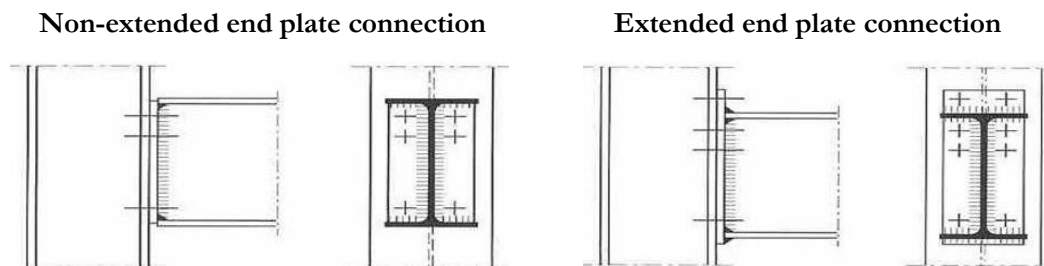


Figure 4-3: Left: non-extended end plate on a steel beam. Right: extended end plate on a steel beam (“Flexibele Momentverbindingen Tussen Liggers En Kolommen,” n.d.)

Specifically, for the case study design, it is advised to use straight beams instead of angled beams. The angle of this beam (as shown in Figure 6-8) is specifically designed for the case study building. According to Brink Staalbouw, a steel construction firm that is specialised in circular steel buildings, the reusability of these beams is lower compared to straight beams. In case these beams need to be reused in a building with another angle, the beams need to be cut at the sides, which reduces the chances of reuse (A. Aversch (Brink Staalbouw), personal communication, August 12, 2020).

4.2 Design for Adaptability (DfA)

The principle Design for Adaptability is characterised by a building’s ability to respond to change. A product may reach its functional service life due to many reasons, but this all comes down to the fact that the product was unable to meet or adapt to the changing needs of the user (Kasarda et al., 2007).

Design for Adaptability can be applied on different levels. Taking the whole building into consideration (which Vonck (2019) entitles as flexibility), the application of Design for Adaptability means that the function of the building will be altered, but the main load-bearing structure can remain the same. Thus, the load-bearing structure should not hinder possible alterations. This can be reached by:

- Apply an open building plan for flexible space management (Akinade et al., 2016)
- Choosing a multi-purpose grid (Crowther, 2000; Gosling et al., 2013)
- Minimizing the number of columns (Van Herwijnen, 2013)
- Minimizing the number of load-bearing walls (Van Herwijnen, 2013)
- Overcapacity in storey height: The storey height is higher than necessary (Van Herwijnen, 2013)
- Overcapacity in the number of storeys: Possibility to add more storeys to a building (Tool, 2010)
- Overcapacity in floor area: Have excess floor area available (Tool, 2010)
- Layer building elements (Gosling et al., 2013), which is based upon the idea from Brand (1995) and is shown in Figure 4-1.

When looking at the separate components (which Vonck (2019) entitles as adaptability), Design for Adaptability means the following:

- A component should have overcapacity and should thus be able to carry more loads than before (Landman, 2016; Van Herwijnen, 2013). Here, it should be kept in mind that increasing the loads on the floors also influences the dimensions of the beams, columns, and foundation.
- Layering of building components (Crowther, 2000)
The components within the building layers of Brand (1995) should also be layered to allow for the possibility of adjusting the building layout through the relocation of components without significant construction work.

4.2.1 Implementing DfA in the case study

Design for Adaptability can also be applied to the case study. Applying this to the whole building, alteration of the function should be possible without having to change the load-bearing structure. This means that the load-bearing structure should not hinder possible function alterations. This does not change the load-bearing structure directly, and therefore it is decided to only consider the component level of Design for Adaptability for the case study. On the component level, Design for Adaptability means the following:

- Overcapacity of components

The robotic mezzanine floor can be altered such that another use is possible. This ensures that not only the floor should be able to carry the overcapacity, but also the beams and columns carrying this floor. Due to the openings located in the robotic mezzanine floor, the current mezzanine floor does not have any potential to be used for another function. Making the mezzanine floor adaptable means that it is possible to replace the floor as well. The current floor design is a cast in situ composite floor which is difficult to replace. So, this floor should be changed into a floor that fits in the Design for Deconstruction concept. In addition, the ground floor can be used as an industrial storage area for large and heavy products. As the ground floor lies outside the scope, only the possibility of removing the mezzanine floor could be considered. Though, this is part of the Design for Deconstruction concept.

- Layering of building components

As explained in paragraph 4.1.1 “Implementing DfD in the case study”, the structure and services cross each other at certain locations. However, if a change in services is needed to accommodate for another function in the building, the castellated beams are not affected by this change. As the adaptivity of the services is not part of this research, it is decided to keep layering of the structural components and the services out of the scope of this research.

5 Setup of design alternatives

In this chapter, design alternatives are set up to answer research question 3 “*Which material and design choices can be made in the design of a distribution centre to reduce the yearly environmental impact?*”. This is divided into three sub-questions that follow the three strategies mentioned in paragraph 1.2 “Circular building strategies”. These questions leave room for many structural design decisions. In this chapter, it is aimed to narrow these general design concepts down. Therefore, in the following paragraphs, for each sub-research question, a more specific problem statement, research question, and scope are set up. At the end of this chapter, an overview of the alternatives is given.

5.1 Research question 3a: Optimise design for its initial material use

In this paragraph, it will be explained how research question 3a can be answered: “*What design choices can be made to reduce the yearly environmental impact of a distribution centre design that is optimised for its initial material use?*”. To answer this question, two different comparisons are made.

5.1.1 Comparison 1: Determining the effect of the amount of material on the environmental impact

Firstly, it is aimed to find out how the amount of material can be reduced for the base design, because less material is inherent to a lower environmental impact. For a framed steel structure, this can be reduced by changing a sway frame (shown on the right in Figure 5-1) into a non-sway structure (shown on the left). In a non-sway frame structure, the beams and columns only need to carry the vertical loads, because the bracing elements carry the lateral loads more efficiently. However, it is unknown to what extent the material use can be reduced in case a non-sway structure is applied, instead of a sway structure. Therefore, it is aimed to compare the differences between a sway and a non-sway structure. In chapter 6.1 “Base design: Sway structure (steel and concrete)” and chapter 6.2 “Alternative A: Non-sway structure”, both designs are explained. Finally, in chapter 6.6 “Overview of design alternatives”, these designs are compared based on their material use.

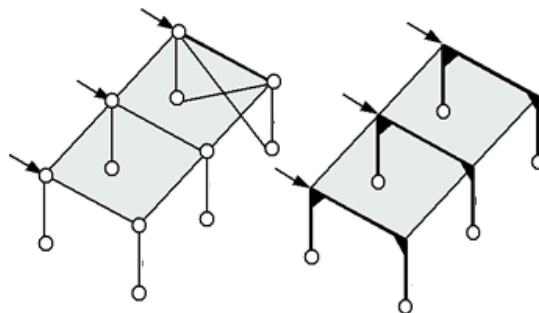


Figure 5-1: Non-sway structure (left) and sway structure (right) (Den Hollander, n.d.)

The non-sway structure is made with pinned connections and a brace to carry the wind load. The sway structure is made with moment resisting connections, which provide stiffness to carry the wind load.

It must be noted that it is also possible to investigate these differences for other materials as well. Though, it is aimed to find out what the differences are between a non-sway and a sway frame to conclude whether this alteration is significant. This goal can be reached by investigating one material type and therefore, it is decided to investigate a steel structure only. Furthermore, to make a fair comparison between the designs, the same mezzanine floor load is used. This means that influence of the mezzanine floor design is kept out of the scope of this comparison.

5.1.2 Comparison 2: Determining the effect of the type of material on the environmental impact

Secondly, it is aimed to find out what the effect is of changing the type of material to reduce the environmental impact, as this is an important design step for structural engineers. It is unknown whether this is also the case for a distribution centre which is usually made from steel and concrete. Hence, a comparison is made between a steel non-sway structure with a concrete and steel mezzanine floor (explained in chapter 6.2 “Alternative A: Non-sway structure”) and a timber alternative (explained in chapter 6.3 “Alternative B: Non-sway structure”). Also, these designs are compared upon their material use in chapter 6.6 “Overview of design alternatives”.

It is expected that a non-sway frame will reduce the amount of material needed in a design significantly. Therefore, it is proposed to only compare a steel non-sway frame with a timber non-sway frame, meaning that a sway frame is excluded from the scope.

5.2 Research question 3b: Optimise design for its residual value

In this paragraph, it will be explained how research question 3b can be answered: “*What design choices can be made to reduce the yearly environmental impact of a distribution centre design that is focused on optimising its residual value?*”. Here, it is foreseen that the building will not fulfil its function for the whole technical life span. Reusing elements for other buildings will increase the element’s functional service life and will minimise virgin material need in future buildings. Consequently, the Design for Deconstruction concept should be followed.

5.2.1 Comparison 3: Determining the relationship between the reuse of a traditional design and a demountable design

In the Base design, reuse is not considered. This can be seen in the connection design, where welded connections are applied. It is possible to reuse elements that have a welded connection, but then the elements need to be cut, drilled, and welded to be able to use it at another location (Fujita & Masuda, 2014). This reduces the residual value of the elements.

The principles mentioned in chapter 4.1.1 “Implementing DfD in the case study” can be followed to create a demountable design that maximises the residual value of the elements. However, it is unknown whether this will lead to a lower environmental impact than if a regular design will be reused in the future. More specifically, it is unknown what the effect is on the total material use between these cases. Therefore, a comparison is made between the material use of a steel sway structure with a composite concrete-steel mezzanine floor (explained in chapter 6.1 “Base design: Sway structure (steel and concrete)”) and a demountable steel sway structure with a demountable mezzanine floor (explained in chapter 6.4 “Alternative C: Demountable sway structure”).

To make a comparison between the main load-bearing structure of a non-demountable design and a demountable design, it is decided to focus on a sway structure only. In a sway structure, bending moments need to be transferred. The stiffer the connection, the higher the bending moment in the connection can be. In case of a demountable design, it is aimed to use dry connections, for which it is more difficult to provide a stiff connection. As it is aimed to find out how much material is needed in a demountable design, it is important to investigate the effect of a less stiff connection on the main load-bearing structure.

5.3 Research question 3c: Optimise design for multiple functions

In this paragraph, it will be explained how research question 3c can be answered: “*What design choices can be made to reduce the yearly environmental impact of a distribution centre design that is optimised for multiple functions?*”. As explained under paragraph 4.2.1 “Implementing DfA in the case study”, the mezzanine floor in the base design is designed to be used by robots and can be altered such that it can be used for another function.

5.3.1 Comparison 4+5: Determining the relationship between the environmental impact of service life extension and extra material use due to another function

It is aimed to find out how much extra material is needed to change the robotic mezzanine floor into a floor with another function. Here, not only the extra materials needed for the floors is included, but also the extra materials needed for the floor beams and columns. Suitable functions with a higher live load are an office or retail function and an industrial function. This leads to the following comparisons:

- Comparison 4: Non-sway steel structure with a robotic mezzanine floor (live load of 3 kN/m², explained in chapter 6.2 “Alternative A: Non-sway structure”) and one with an office or retail function (live load of 4 kN/m², explained in chapter 6.5.1 “Alternative D1: Non-sway structure with office/retail on the mezzanine floor”)
- Comparison 5: Non-sway steel structure with a robotic mezzanine floor (Alternative A) and one with an industrial function (live load of 7.5 kN/m², explained in chapter 6.5.2 “Alternative D2: Non-sway structure with industrial storage on the mezzanine floor”)

It is decided to consider a non-sway frame because this will provide more insight in the material use than for a sway frame. In a non-sway frame, the dimensions of the columns are dependent upon the vertical forces. This is different than for a sway frame, for which the dimensions of the columns are based upon their capability to carry horizontal wind loads.

It is also acknowledged that it is possible to investigate the differences per material type. However, insight into the extra material needed for another function can already be gained when investigating one type of material. Therefore, it is decided to only investigate a steel main load-bearing structure.

5.4 Overview of comparisons and design alternatives

To summarize how the sub-research questions are answered, Figure 5-2 (on the next page) is made. From this figure, the comparisons between alternative designs are explained. These designs are further explained in Figure 5-3. From this figure, it becomes clear that the Base design is optimised for the current situation and is focused on functionality and fast erection. As an improvement, less material can be used (Alternative A) or a more sustainable material as timber can be used (Alternative B). Alternative C is optimised for the future situation by being demountable and thus reusable. Alternatives D1 and D2 are optimised for the future situation by being adaptive.

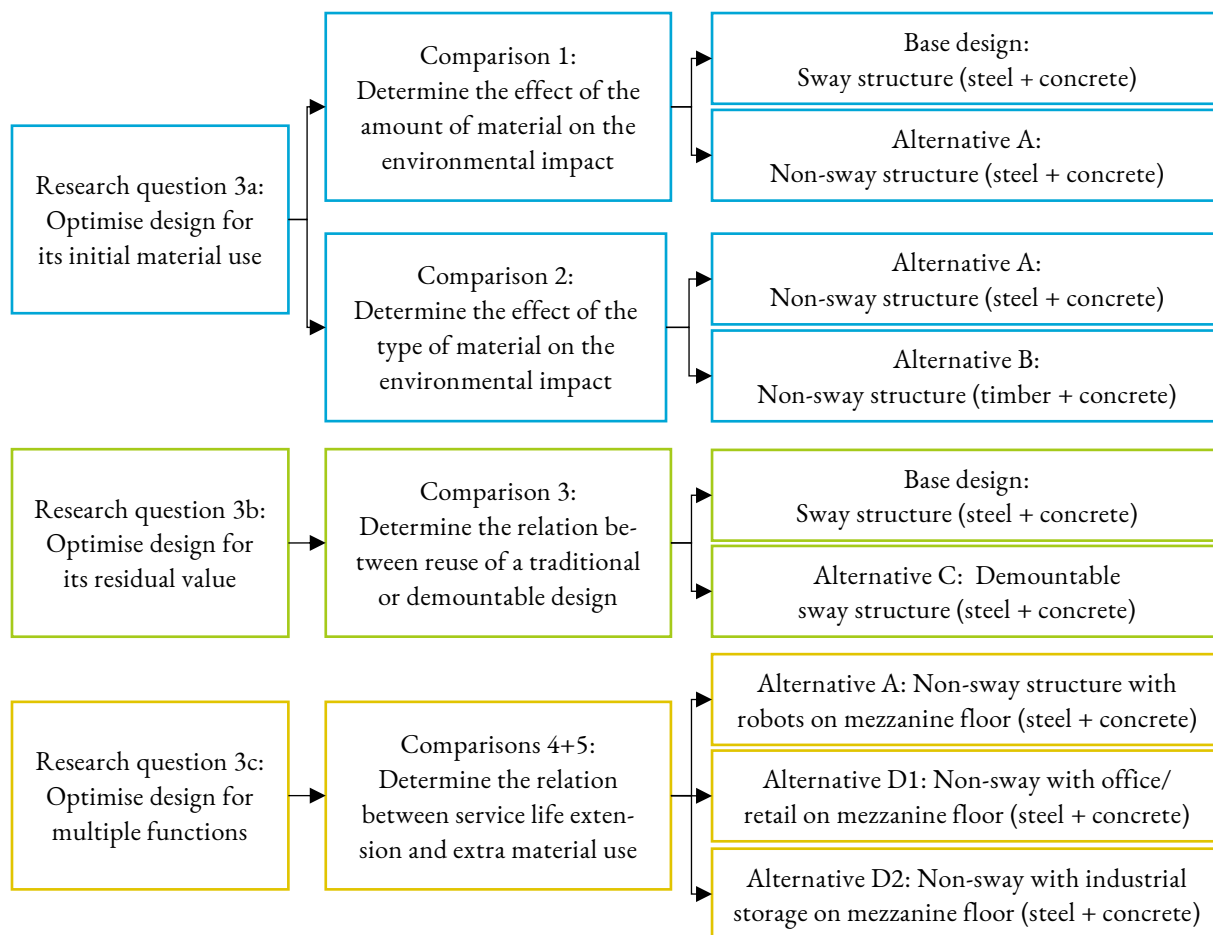


Figure 5-2: Explanation of how the sub-research questions will be answered

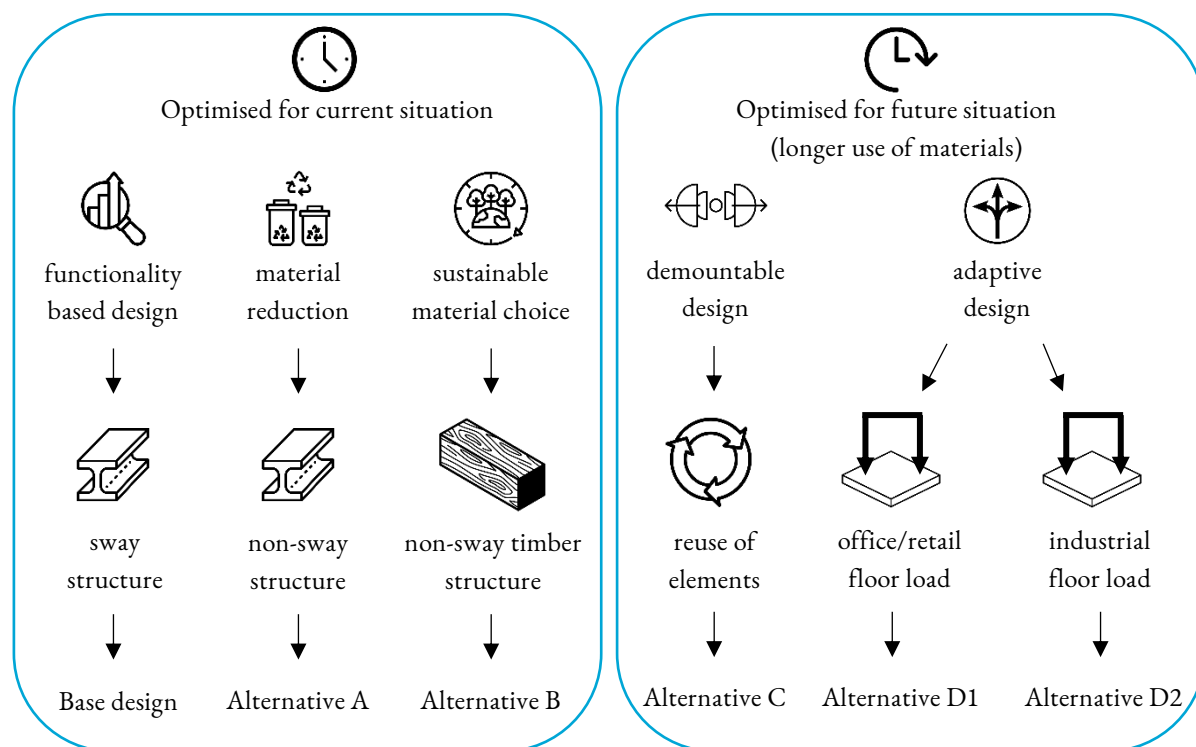


Figure 5-3: Set up of design alternatives

6 Designs

In this chapter, the design alternatives of Figure 5-3 are worked out. This includes the structural design of the main load-bearing structure and of the mezzanine floor. At the end of this chapter, an overview is given on the amount of material needed per design alternative. To ensure that these alternatives are comparable, the following guiding principles are set up:

- Each design must be based upon the same structural verifications. These are given in Appendix A “Guidelines for the structural calculations”. Here, also the deflection requirements for the serviceability limit state are given (in Appendix A.1 “Deflection requirements (SLS)”).
- The distribution centre will be built somewhere in Europe, so the general Eurocode regulations apply. In a later stage, a local contractor will specify this according to the local regulations. For the loads, this means general values are used. This is explained in Appendix A.2 “Loads”. This appendix includes the following sections: “Load factors”, “Wind load”, and “Snow load”.
- Rainwater must be able to runoff from the roof. A minimum of 5% has been set for an envelope-shaped roof.
- For the specific use of the building, requirements regarding the free height are provided by the client. This can be found in Figure 6-1.

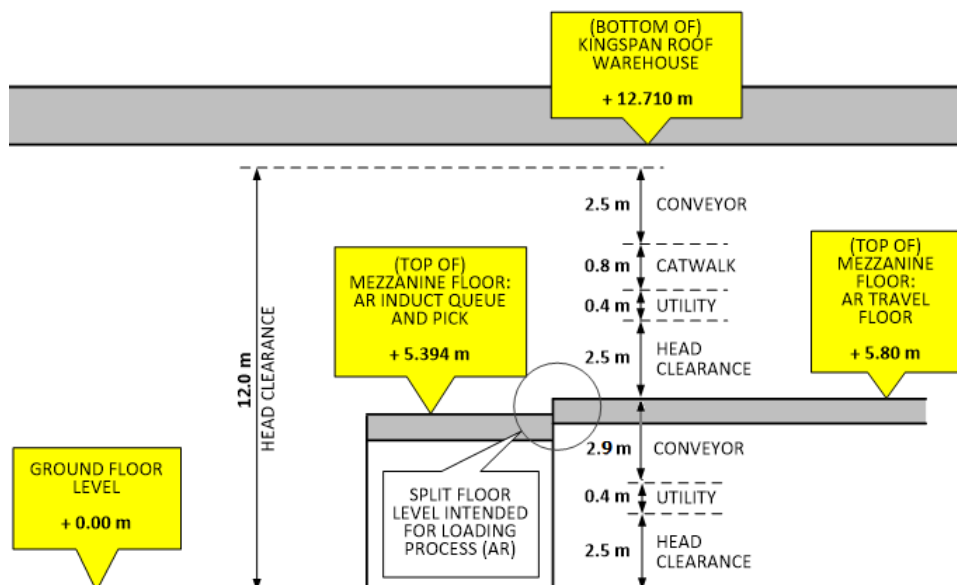


Figure 6-1: Necessary internal heights (Royal HaskoningDHV Internal Document, 2020a)

- Fire safety must be regarded according to the building regulations and the client.
 - Building regulations regarding fire vary throughout Europe. For the design, the Dutch building regulations (Bouwbesluit in Dutch) are followed (see Table 6-2). These requirements are safe for the other possible locations as well (Royal HaskoningDHV Internal Document, 2020a). The case study has a floor at 5.8 meters above the ground floor. So, the warehouse must be protected from fire for at least 90 minutes.

Table 6-1: Dutch Building Regulations 2012 (Tabel 2.10.2) for a non-residential function

Highest floor level	Fire resistance (until collapse of the structure) [minutes]
≤ 5 meters	60
Between 5 and 13 meters	90
> 13 meters	120

- Fire safety is also an important aspect for the client. The client aims to minimise the chance of a fire, because no money can be earned if the building needs to be evacuated. Also, the chance of damage due to a fire should be minimised as much as possible because this makes sure that the building cannot be used for even a longer period.
- How the building is kept safe from fire is explained in chapters 6.1 and 6.3.

- Robots drive on the mezzanine floor. This can be seen in Figure 6-2. In this figure, also openings with slides are shown. The robots bring the packages to these slides, so they end up on the ground floor. The robots navigate through robotic tiles on the mezzanine floor: on each robotic tile, a barcode is placed that the robots can scan. Each robotic tile has a dimension of 1054 by 1054 mm. The column grid needs to be a multitude of these dimensions, ensuring that the main grid of the warehouse is based upon robotic tiles.

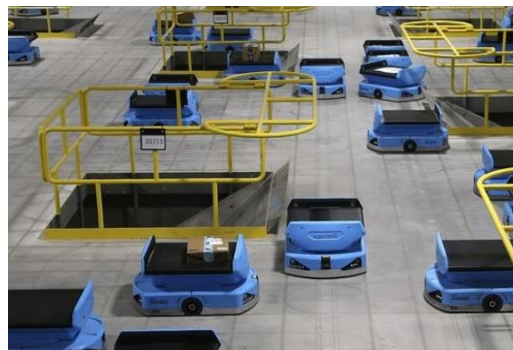


Figure 6-2: Example of a robotic floor with openings (O'Brien, 2019)

This can be seen in Figure 6-3. In this figure, the robotic areas are shown in red. The robots drive next to the openings, which ensures that next to an opening, at least one robotic tile should be available. The yellow areas represent the areas where the package slides are located. This means that in case a column is placed in this area, the functionality of the ground floor reduces. The columns should be placed outside the red area and preferably outside the yellow area. Thus, it is aimed to place the columns in the areas which are depicted in green.

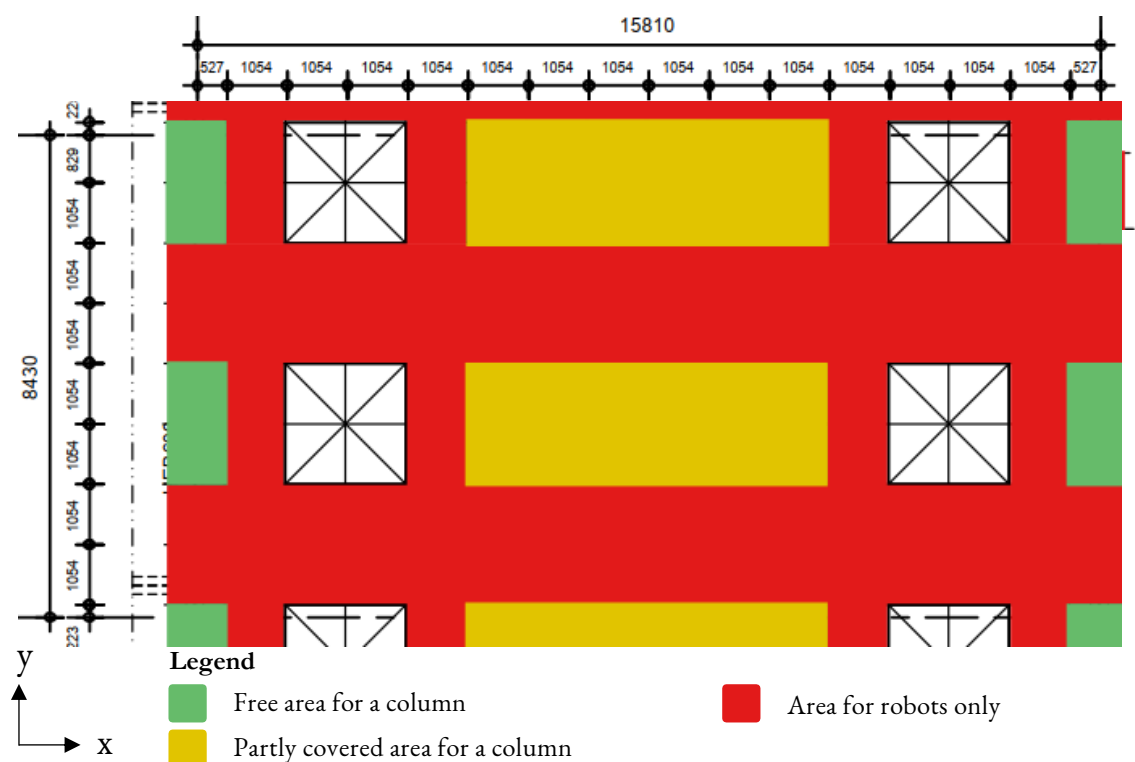


Figure 6-3: Part of the floor grid of the mezzanine floor, where the available areas for structural elements are schematised (own illustration, based upon (Royal HaskoningDHV Internal Document, 2020c))

This figure has been set up based upon the main grid of 15.81 by 8.43 m. In green, the areas where structural elements can be placed are shown, the colour yellow represents the locations where structural elements could better not be placed, and in the red areas, no structural elements can be placed.

6.1 Base design: Sway structure (steel and concrete)

In chapter 1.3 “Case study”, the distribution centre design as designed by Royal HaskoningDHV was introduced. To ensure this design is comparable to the design alternatives of this research, a new design is made. This new design will be discussed in this chapter. In this chapter, specific profiles are given for the beams and columns based upon the calculations performed in Appendix B “Base design”.

6.1.1 Fire safety

The client requires fire spreading to be prevented as much as possible. Therefore, a dense sprinkler system is laid out. This sprinkler system has a very low failure probability. In practice this means that there are two water pumps: a diesel and an electric pump. This guarantees that if one of the systems fails, the other system can take over this process. In addition, there must be two independent water supplies. Depending on the location this could be pumped from two water tanks or from a water tank and from surface water. These water supplies must be large enough to sprinkle the building for at least 90 minutes, this is the period in which the Building Decree requires the building to be fire safe. The sprinkler system is modelled. It is found out that this system can control the fire and keeps the temperatures of the structure well below the critical temperature. Moreover, a smoke extraction system and a heat extraction system are incorporated in the designs. Together, these measures result in a design that is safe for a 90-minute fire. It is therefore decided that the structural elements can be unprotected. This also holds for the other steel and concrete design alternatives (Alternatives, A, C, D1, and D2).

6.1.2 Structural system

To understand the building, two plans are made (Figure 6-5 and Figure 6-6). The locations of these plans are shown in Figure 6-4.



Figure 6-4: Front view of the structure (Royal HaskoningDHV Internal Document, 2020c)

In this figure, two lines are drawn that represent a top view. The dotted blue line represents the view shown in Figure 6-5 and the dotted green line represents the view shown in Figure 6-6.

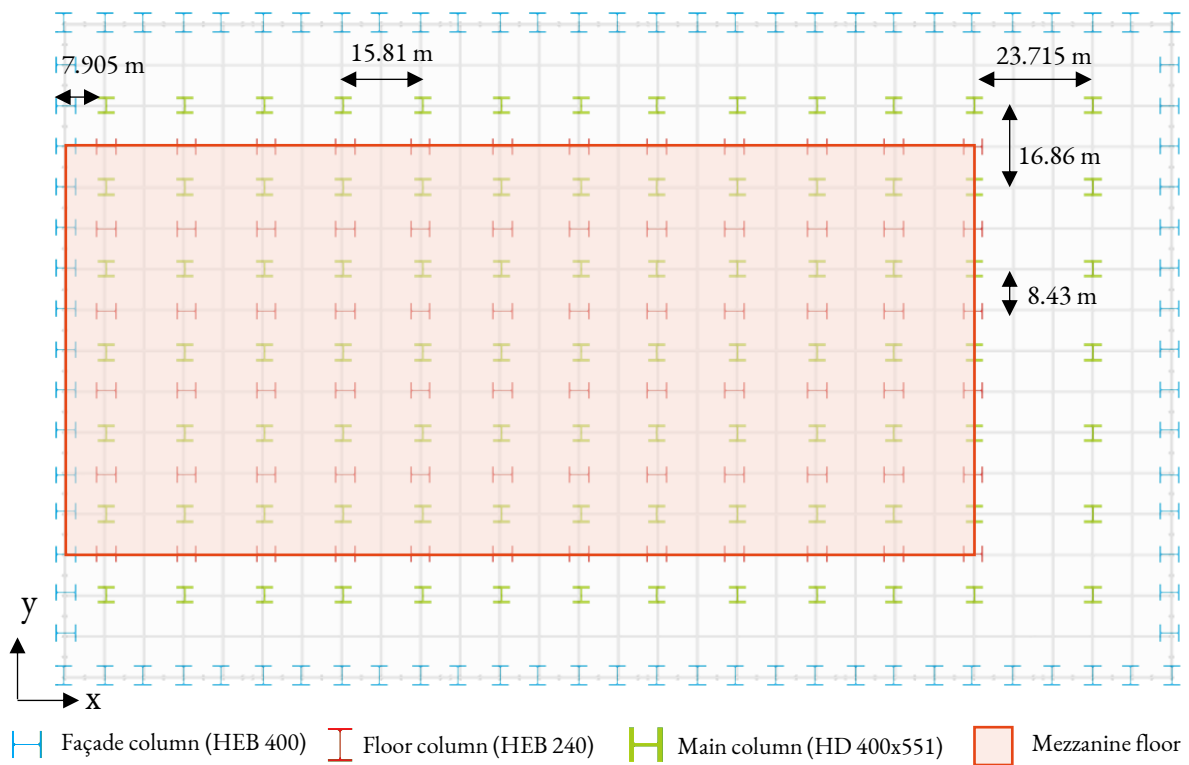


Figure 6-5: Top view of the Base design at the dotted blue line shown in Figure 6-4

In this figure, the façade columns, main columns, and mezzanine floor columns are shown. To be able to see where these elements are located, they are enlarged.

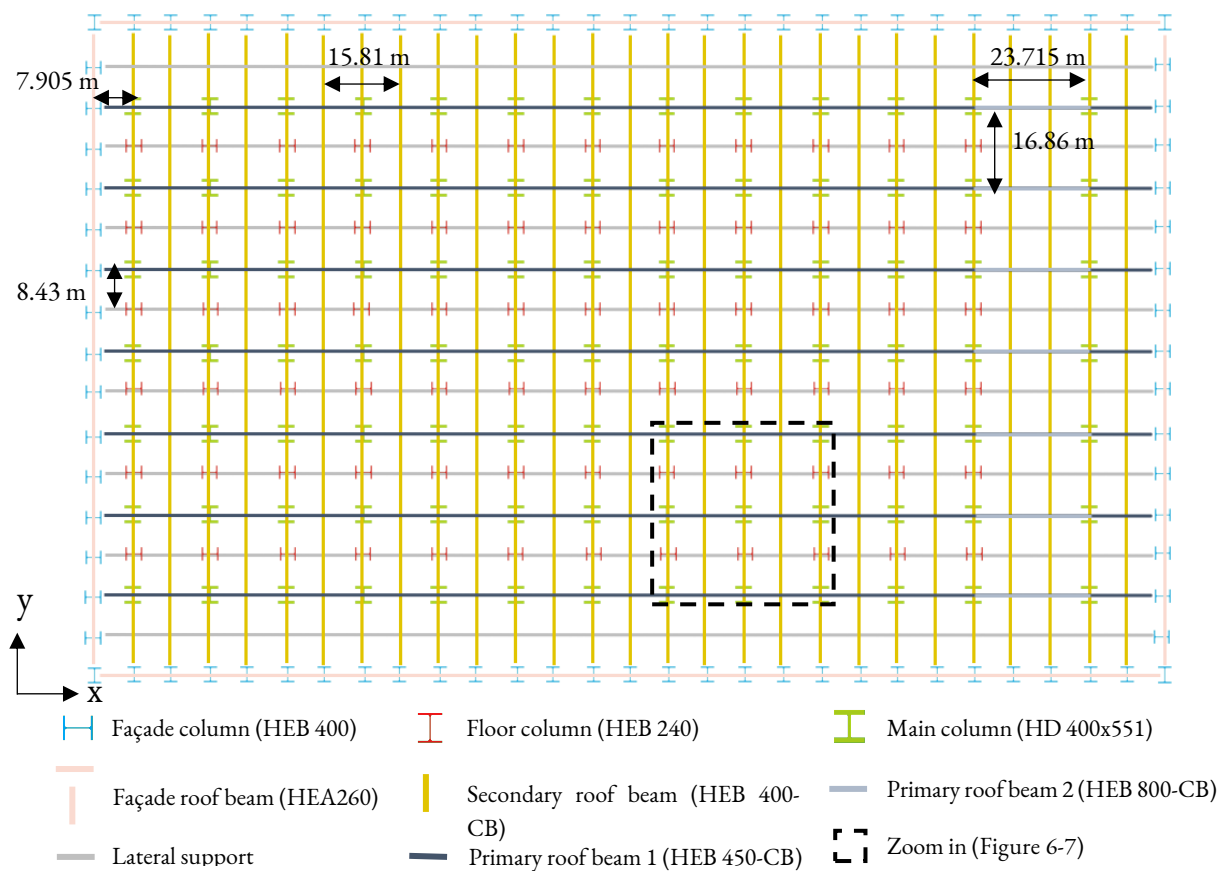


Figure 6-6: Top view of the Base design at the dotted green line shown in Figure 6-4

This figure shows the same layout as Figure 6-5, but now includes the roof beams as well.

6.1.2.1 Load distribution on the roof

The load distribution on the roof beams is visualised in Figure 6-7. On top of the secondary roof beams, purlins are placed. These purlins carry the loads coming from the roof plates. In Figure 6-7, the load transfer of the purlins to the secondary roof beams is shown in red. This load is simplified as a distributed load on the secondary roof beams, instead of separate point loads coming from the purlins.

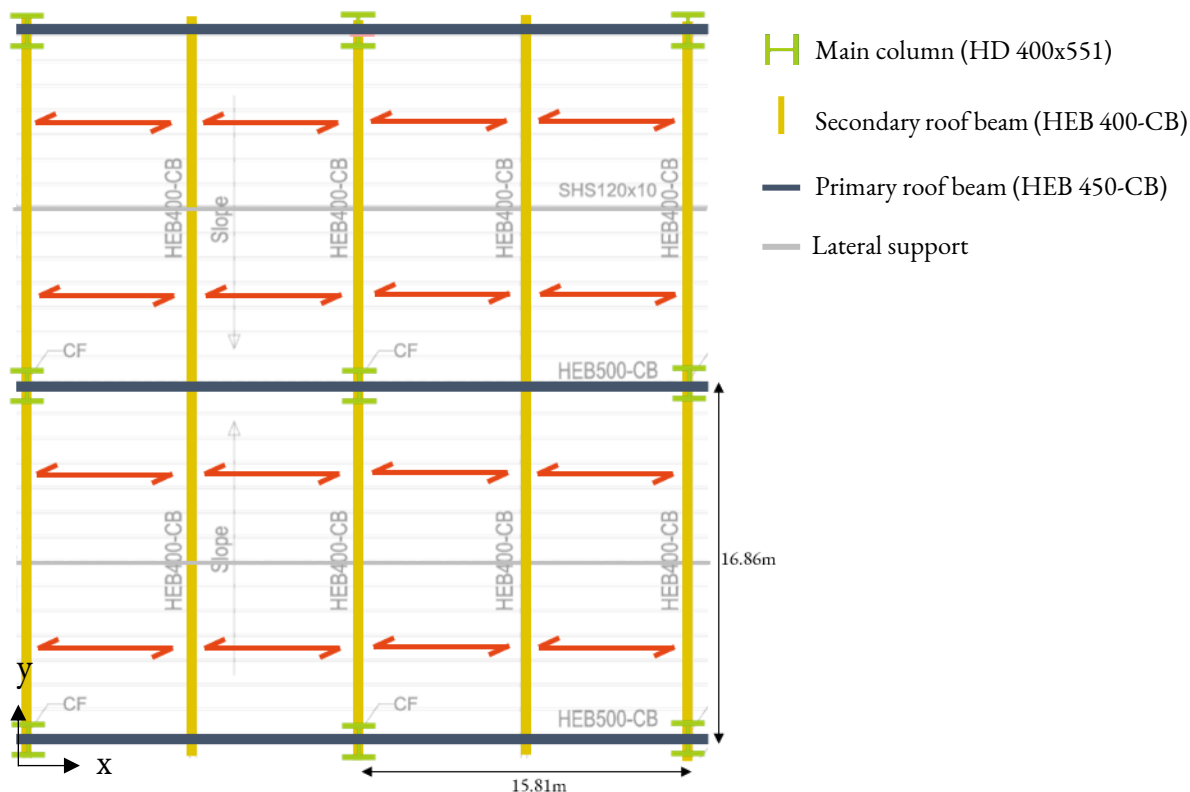


Figure 6-7: Top view of the roof beams (at zoom in shown in Figure 6-6)

The profiles are enlarged in this picture to be able to see where they are located. The red arrows represent the transfer of the loads from the purlins to the secondary roof beams.

6.1.2.2 Schematisation of two sections

On the next page, two sections are shown. To clarify these figures, the following remarks are made:

- The possibility for another use in the future is already included in the design. This means that the stability of the building is ensured even without the presence of the mezzanine floor. Therefore, the connection between the mezzanine floor beams and the columns are hinged connections.
- To guarantee safety for the maintenance workers on the roof, a one-meter high parapet is placed along the perimeter of the roof. The parapet is shown in purple, on top of the façade columns.
- The two sections are designed with help of the software package SCIA. The schematisation of the stabilisation system in SCIA is given in Appendix B.1 “Schematisation of stabilisation system (as modelled)”. The loads on these sections are further explained in Appendix B.2 “Loads”. The results of these calculations are found in Appendix B.5 “Results of structural calculations”.
- The connections between the mezzanine floor beams, the connections between the column and foundation, and the connections between the columns and beams are designed and calculated in Appendix B.3. The rotational stiffness of each connection is calculated with help of the simplifications by M. Steenhuis (Jaspart & Weynand, 2016).

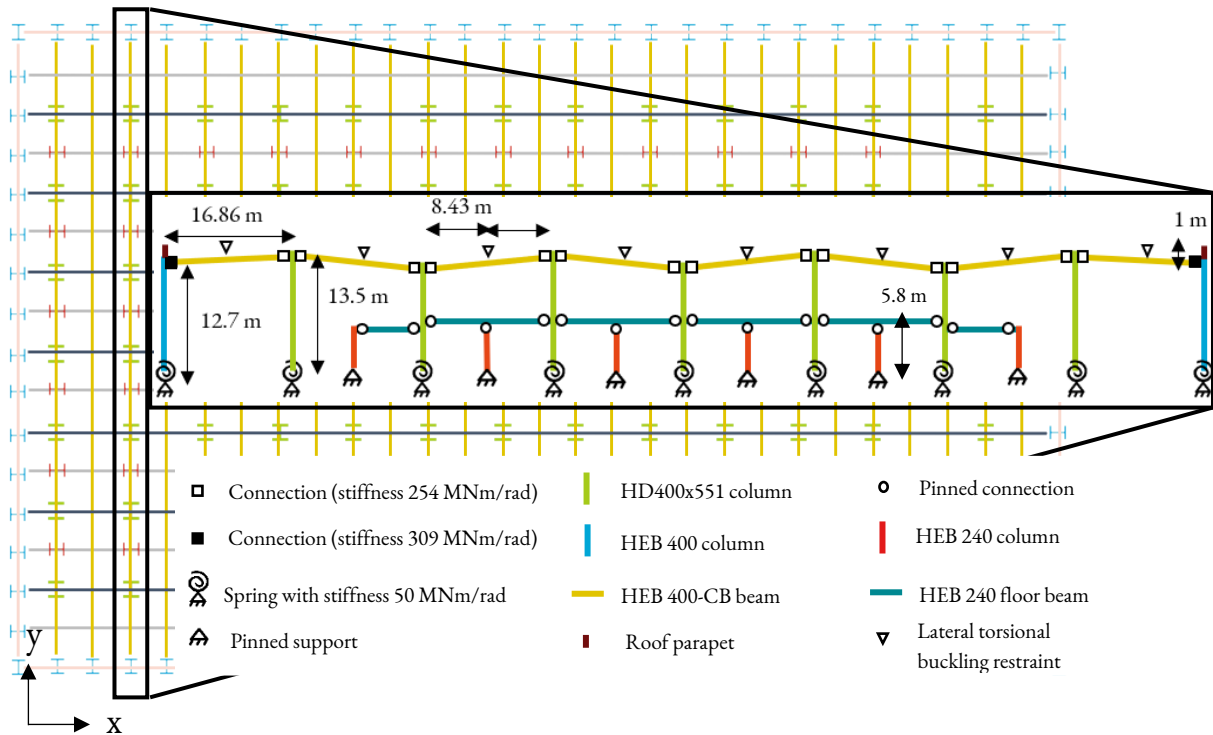


Figure 6-8: Mechanics scheme of the stabilising portal frame in the y-direction

In this figure, the portal frame structure is shown with the mezzanine floor beams located halfway the columns. The mezzanine floor beams are connected by hinges. This ensures that only the roof beams and roof columns carry the lateral loads. As can be seen in the figure, the castellated beams are placed at an angle, for the rainwater runoff. Furthermore, a parapet is placed to guarantee safety for workers on the roof.

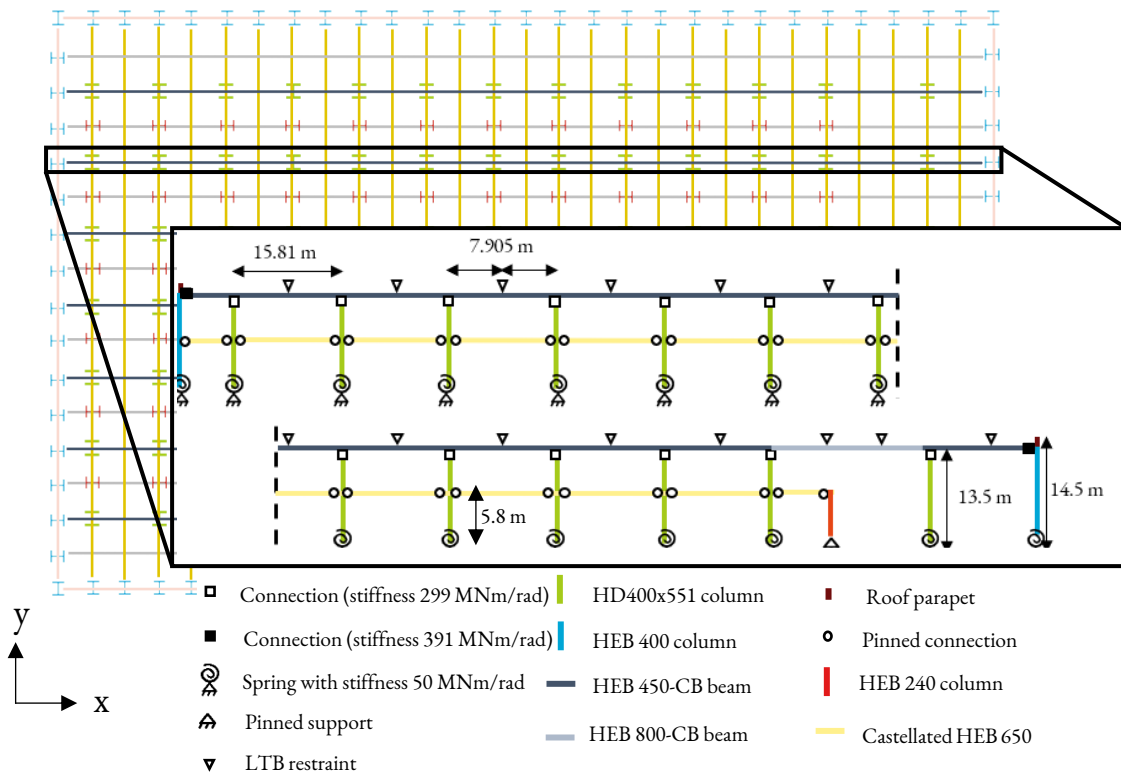


Figure 6-9: Mechanics scheme of the stabilising portal frame in the x-direction

6.1.3 Mezzanine floor design

The mezzanine floor is a ComFlor75 floor. This is a thin steel deck with an in situ concrete layer on top. The floor spans in one direction. An example of such a floor can be seen in Figure 6-10. Compared to other floor systems, a ComFlor75 floor has a limited height. Furthermore, the steel decking is easy to handle and no heavy cranes are necessary, making the system easy to assemble. In this research, the design made by the manufacturer is used.

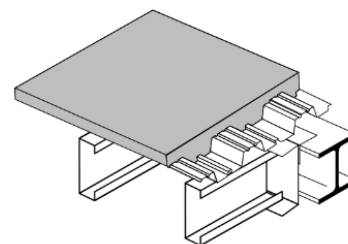


Figure 6-10: Composite flooring system (Bouwen met Staal, 2013)

The layout of the floor is seen in Figure 6-11. In this figure, the openings in the floor are shown by means of blue crosses. In this figure, also the loads on the floor are written down in the legend, and are based upon the loads given in Appendix B.4.1 “Mezzanine floor beam check”. From the floors, the loads are transferred to the floor beams (shown in red). Then, the loads are transferred onto the secondary beams (shown in blue), which then transfers the load to the main beams (shown in green). Finally, the loads are transferred to the columns (shown in black). The structural calculations can be found in Appendix B.4 “Mezzanine floor design”. Based on these calculations, the profiles are chosen.

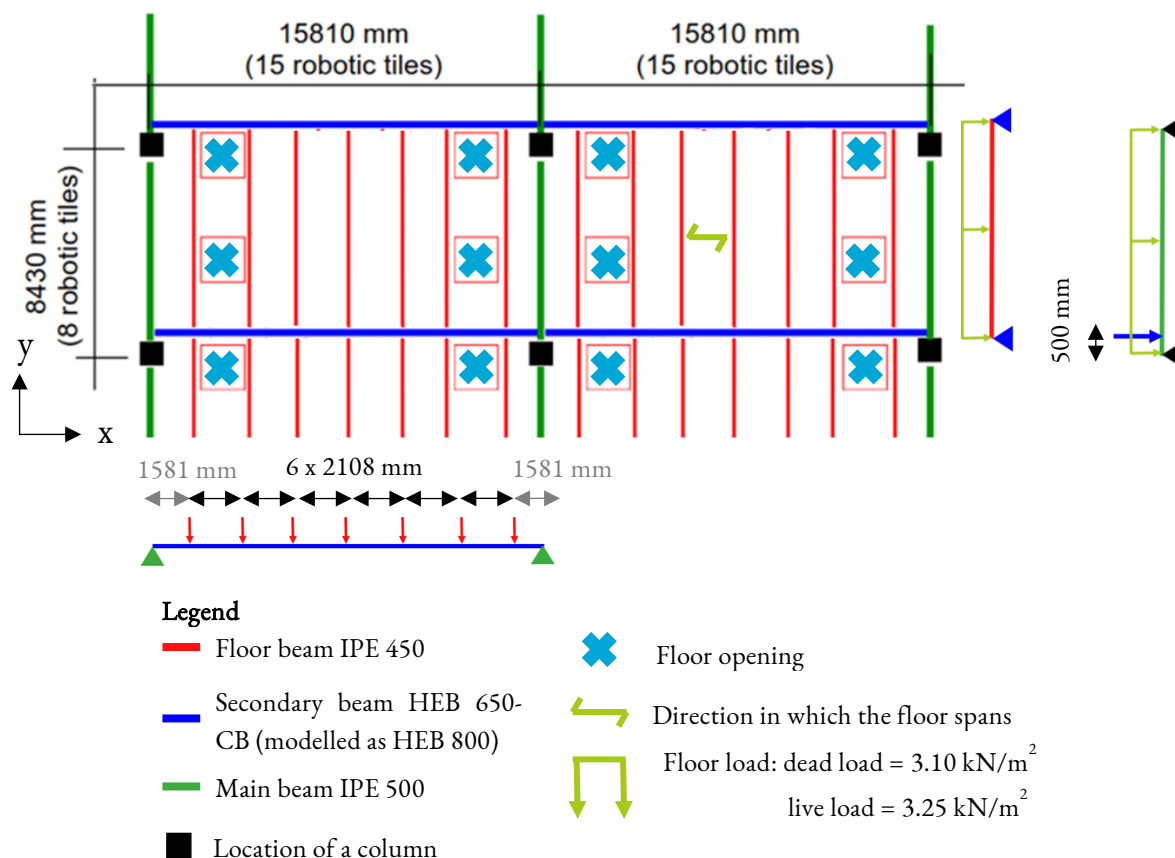


Figure 6-11: Part of mezzanine floor (own illustration based upon Royal HaskoningDHV Internal Document)

6.2 Alternative A: Non-sway structure (steel and concrete)

Alternative A is a non-sway steel structure, where a truss structure carries the wind loads. This truss structure is located in the roof and transfers the loads onto the bracings in the façade. This assures that the beams and columns outside the non-sway structure do not have to carry the wind loads, ensuring less material needed compared to the base design. In this chapter, the non-sway steel structure that is designed in this research is explained.

6.2.1 Thermal expansion

Thermal expansion can become an issue for larger steel buildings. This issue can be solved by including expansion joints in the building or by placing the braces more to the inside of the building, such that the exterior parts can expand. The maximum length of a steel non-sway building without expansion joints or between expansion joints has been investigated with the findings from Fisher (2005). This calculation can be found in Appendix C.1.1 “Thermal expansion” and has resulted in a maximum length of 140.2 meters.

Based upon the thermal expansion issue, two structural designs are set up (see Appendix C.1.1 “Thermal expansion”). Here, a dilatation system with bracing is compared to a system with braces only. It is found that the dilatation system requires more material, so the system with bracing is chosen.

6.2.2 Structural system

The two plans as shown in Figure 6-4 for the base design are also made for this alternative. This can be seen in the following figures.

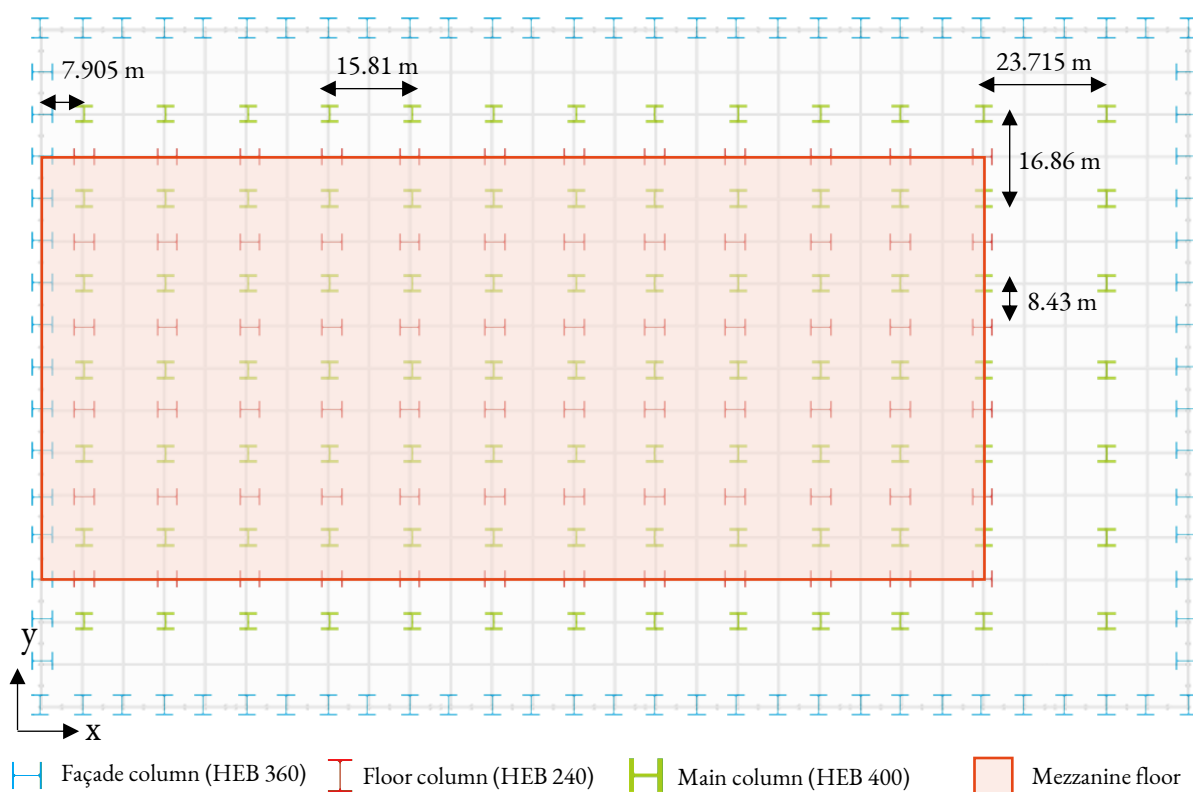


Figure 6-12: Top view of Alternative A at the dotted blue line shown in Figure 6-4

In this figure, the façade columns, main columns, and mezzanine floor columns are shown. To be able to see where these elements are located, they are enlarged.

In Figure 6-13, the plan shown in green in Figure 6-4 is shown. In this figure, the roof beams on top of the main columns are depicted as well. The bracing in the roof is designed as elements that only carry tension forces. This is explained in Appendix C.3.1 “Horizontal bracing”.

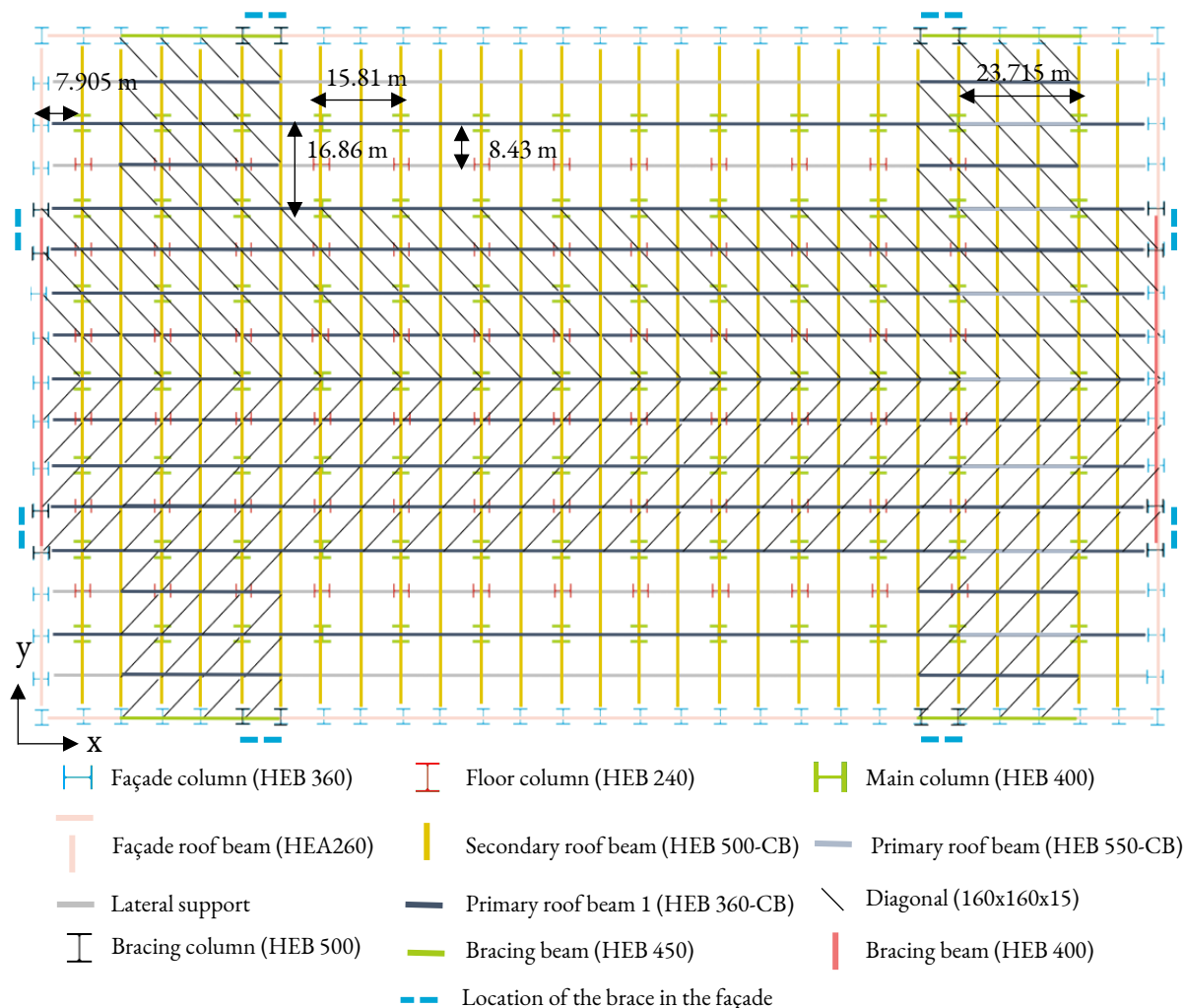


Figure 6-13: Top view of Alternative A at the dotted green line shown in Figure 6-4

6.2.2.1 Load distribution on the roof

The load distribution on the roof is the same as shown in Figure 6-7 of the Base design. The diagonals do not carry the vertical loads, the primary and secondary beam do.

6.2.2.2 Schematisation of two sections

In the following figures, two sections (in the y-direction and x-direction) are shown. The two sections are schematised as if they are carried by a support at the end of the section. This support acts as the bracing in the roof. In this figure, hinged connections between the beams and columns are drawn and a stiff connection is used for the column base connections. Details of these connections can be found in Appendix C.1.2 “Connection design”.

The two sections are designed with help of the software package SCIA. The loads on these sections are further explained in Appendix C.2 “Loads”. The results of these calculations are found in Appendix C.4 “Results of structural calculations”.

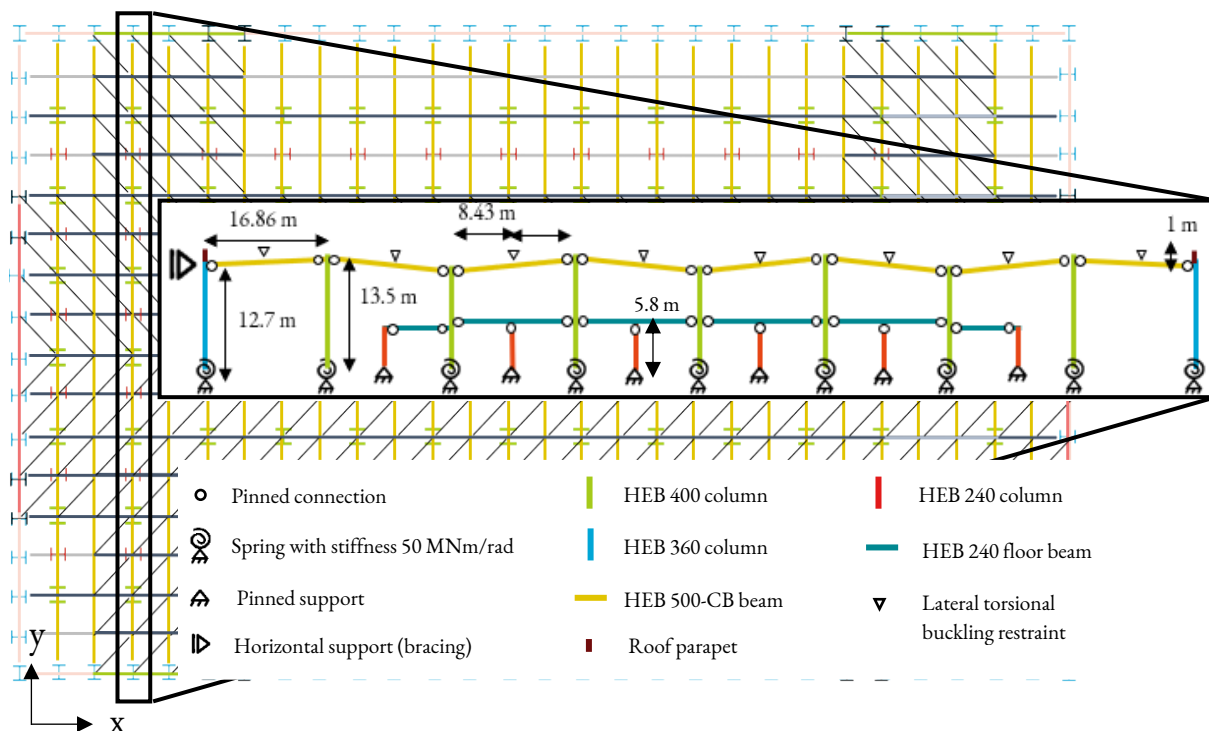


Figure 6-14: Mechanics scheme of the frame in the y-direction

In this figure, the portal frame structure is shown with the mezzanine floor beams located halfway the columns. The mezzanine floor beams are connected by hinges. The frame is stabilised by bracing in the roof and façade. This is modelled as horizontal support at the end of the frame. Castellated beams are placed at an angle, for the rainwater runoff. In addition, a parapet is placed to guarantee safety for workers on the roof.

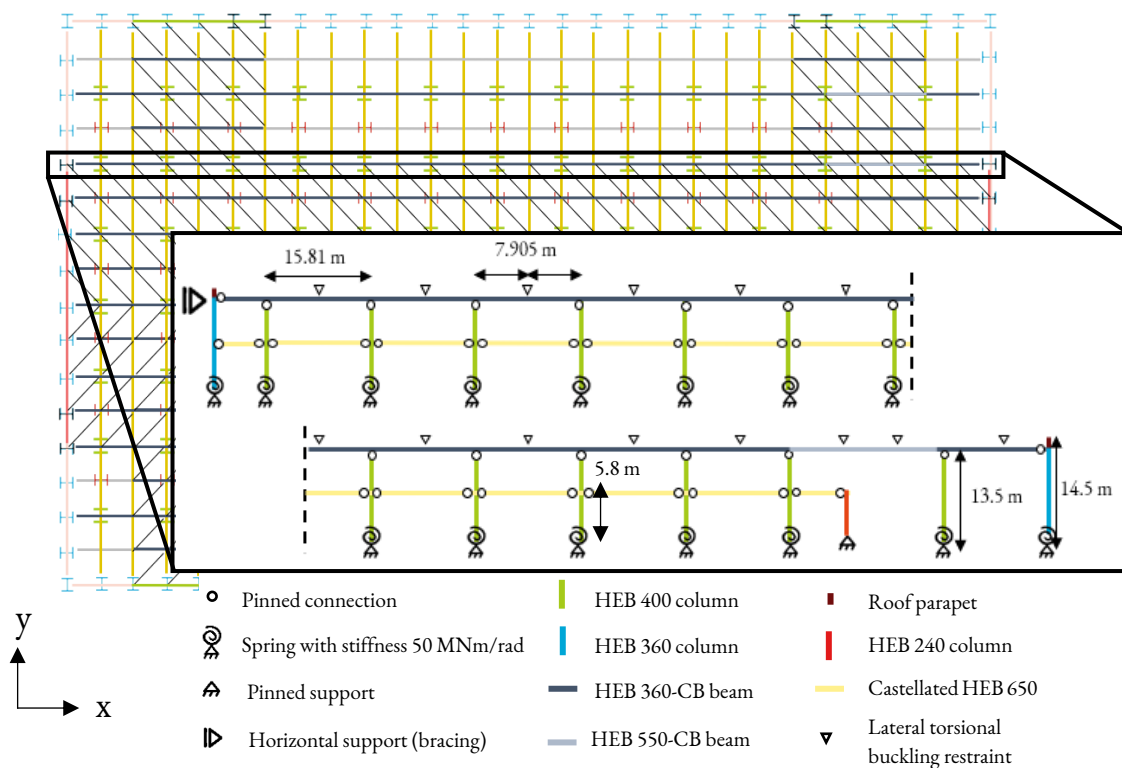


Figure 6-15: Mechanics scheme of the stabilising portal frame in the x-direction

6.2.2.3 Vertical bracing elements

The vertical bracing elements are shown in the following figure. Here, it is visualised that the bracing element is as wide as two grid lines. This is considered the maximum width of the vertical brace. This does mean that the normal force in the diagonals becomes too large for an angled profile that only carries tension forces. Therefore, the diagonals are made from circular hollow sections that also take up compression forces. The calculation of the vertical bracing elements is further explained in Appendix C.3.2 “Vertical bracing”.

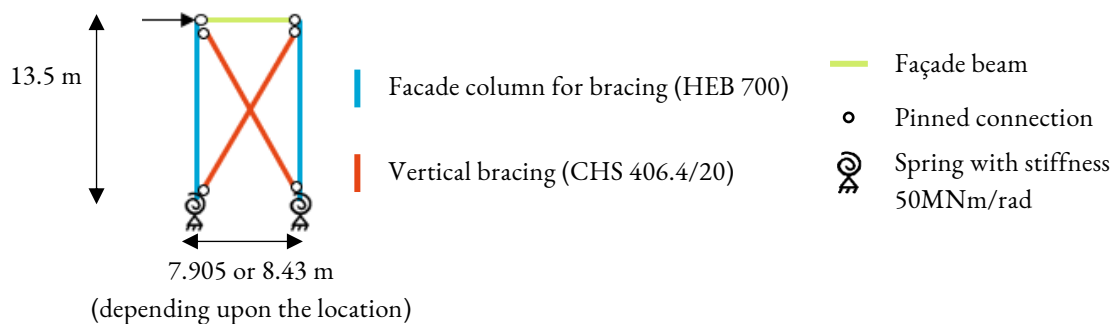


Figure 6-16: Visualisation of the vertical bracing in the façade

6.2.3 Mezzanine floor design

For this design alternative, the main load-bearing structure is investigated. This means that the mezzanine floor design is kept out of the scope. Thus, the same load as was used in the Base design is used for this alternative as well.

6.3 Alternative B: Non-sway structure (timber and concrete)

In this chapter, a timber non-sway structure is designed. In this alternative, it is aimed to keep the same grid as used in the base design. This ensures that the roof beams need to have a span of 15.81 and 16.86 meters. The beams need to be made from engineered timber to be able to carry this span (De Groot, 2018). Based upon the explanation given in paragraph 3.3.1 “European Product Declaration (EPD) data”, the beams and columns are made from GL24h. Furthermore, it is aimed to apply strength class C24 if possible, because this will lead to the lowest environmental impact. For the materials used, the properties are given in Appendix D.1 “Material and product properties”. These details are used for the calculations of the elements.

6.3.1 Shrinkage and swelling

As explained in the previous chapter, thermal expansion can become an issue for a steel building. Timber is not as sensitive to temperature changes as steel. For a timber building, thermal expansion has barely any effect, but swelling and shrinkage due to moisture changes can have a significant impact on a structure. Wood namely swells when the wood moisture content increases and shrinks when the wood moisture content reduces (Blaß & Sandhaas, 2017). To prevent issues with shrinkage and swelling, EN 1995-1-1 (article 10.2 (3)) requires the producer to dry the timber to the moisture content of the completed structure. This means that shrinkage and swelling lie outside the scope of the structural design of this alternative.

6.3.2 Fire safety

As explained in the introduction of chapter 6 “Designs”, the building should be safe from fire for 90 minutes. From a fire model, it is found that the Base design is safe with a sprinkler installation, a smoke extraction system, and a heat extraction system, without having to protect the steel structure. For a timber structure, no fire model has been made. However, the fire safety consultant of this project did conclude that with these fire safety measures taken, the chance of fire propagation in a timber structure is also very low. Besides, the client requires the building to be damage free in case of fire. By modelling the fire for a timber building, more insight can be gained. If the fire safety systems seem unsafe for a timber structure, it is possible to include extra measures as well (for example, spraying water on critical elements such that they will not fail).

To gain insight in how safe the timber is for fire without any fire safety measures, the fire resistance of the structure is investigated. If the timber is exposed to fire, this results in a reduced cross-section. The timber structure is considered safe if this reduced cross-section can carry the loads during a fire. For each element in the timber design, the reduced cross-section method is applied to determine whether the element is indeed strong enough in case of fire. This method is explained in Appendix D.1.3 “Fire safety”. From this calculation, it is found that all elements contain enough mass to withstand a fire of 30 minutes, meaning that even without fire safety measures, the structure is relatively safe for fire.

6.3.3 Structural system

The plan as shown in blue in Figure 6-4 is also made for this alternative (Figure 6-17). From this figure, it can be noted that the columns are squared. This is chosen because this results in an element that is strong in both directions. This is an advantage for columns where buckling is not allowed to occur.

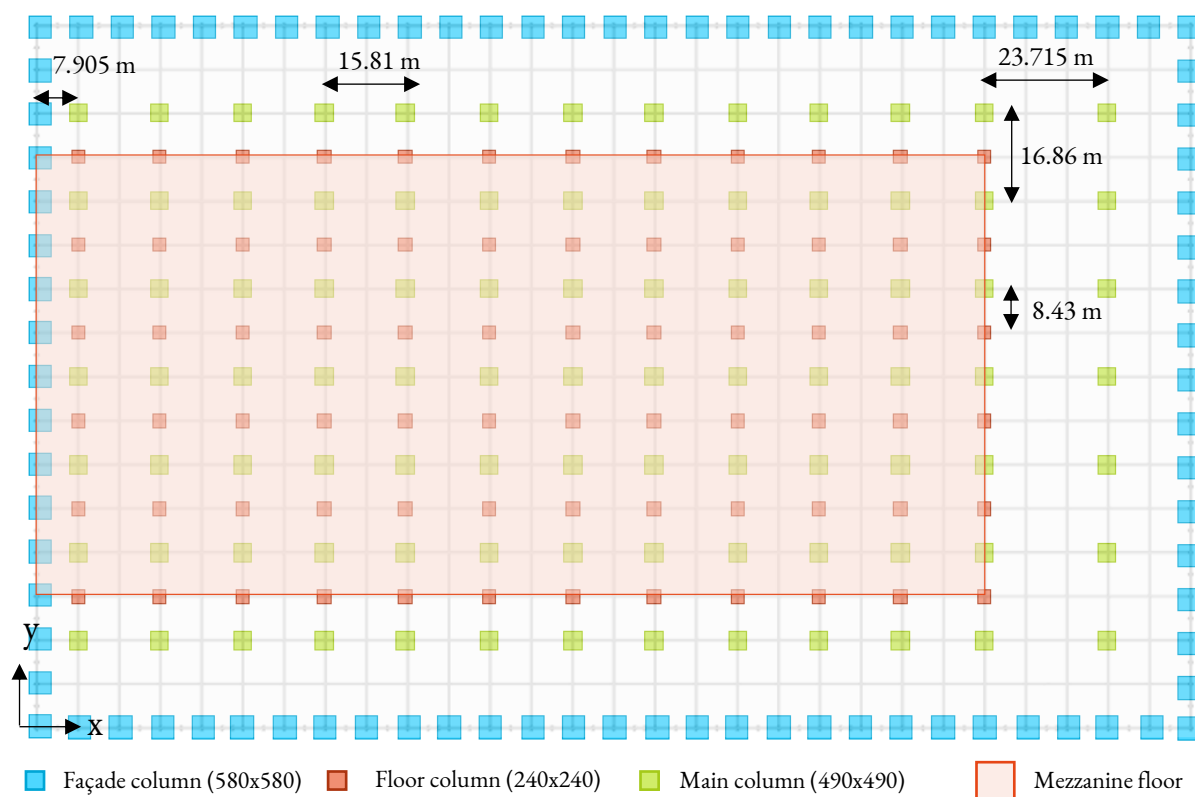


Figure 6-17: Top view of Alternative B at the dotted blue line shown in Figure 6-4

In this figure, the façade columns, main columns, and mezzanine floor columns are shown. To be able to see where these elements are located, they are enlarged.

The plan as shown in green in Figure 6-4 is shown in Figure 6-18 on the next page. In this figure, the beams are shown. These beams are made from high narrow cross sections (between 1:6 to 1:8 of the height), because this is more economical than low wide cross sections. Furthermore, the horizontal bracing is shown (this is based upon the calculation of Appendix C.3.1 “Horizontal bracing”). Additional lateral supports are excluded to keep the figure clear. These beams are included in an enlargement of this figure in Appendix D.4 “Roof plan of the structure”. Finally, it must be explained that the beams in the roof bracing are wider than shown in this figure, the actual widths of these beams are given in Table D-11.

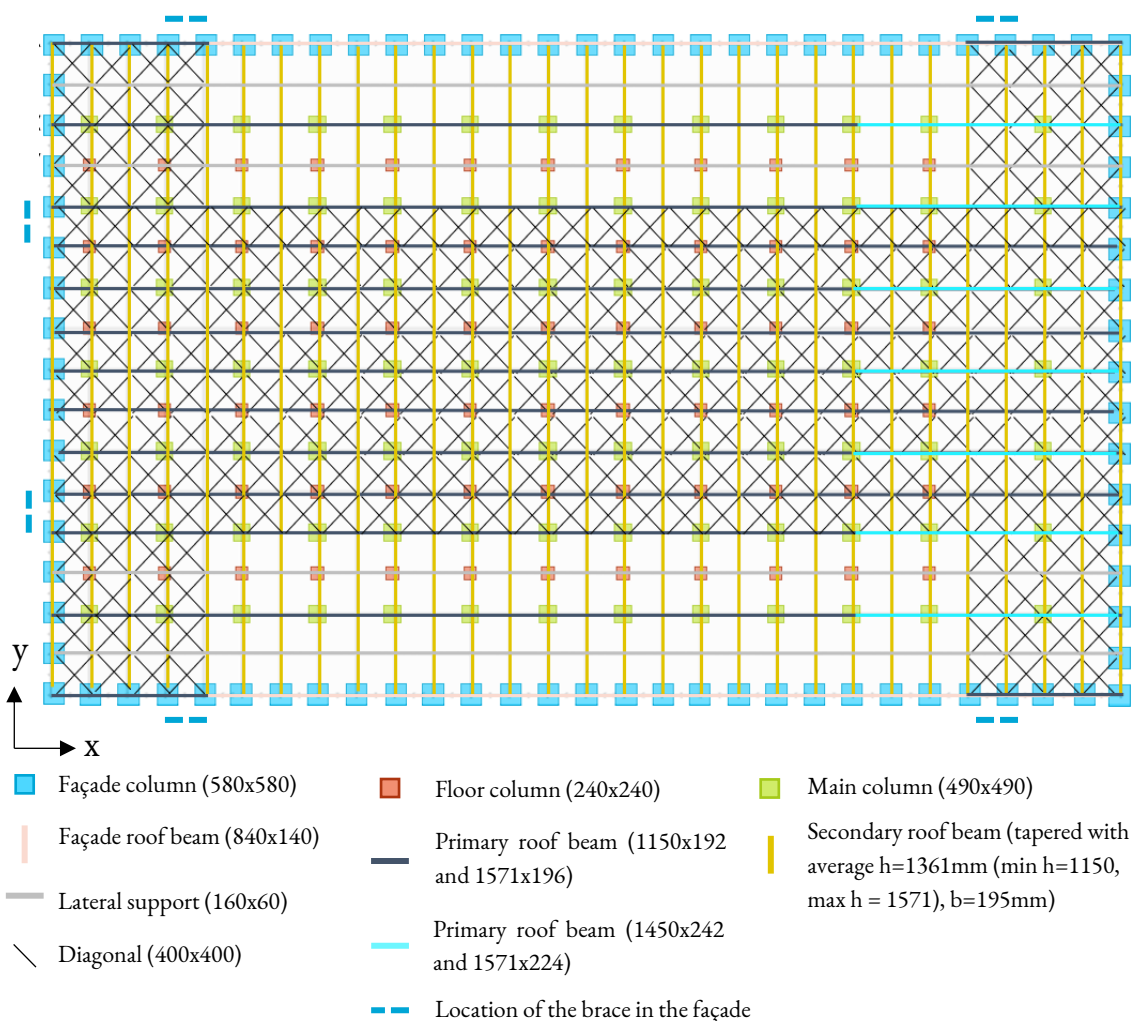


Figure 6-18: Top view of Alternative B at the dotted green line shown in Figure 6-4

Important: additional lateral supports are added between all beams in the roof and the beams in the roof bracing are wider than shown. This is left out to keep the figure clear.

6.3.3.1 Load distribution on the roof

The load distribution on the roof is the same as shown in Figure 6-7 of the Base design. The diagonals do not carry the vertical loads, the primary and secondary beam do. In addition, some extra lateral supports are added to reduce the buckling lengths of the beam. This is done as the ideal centre-to-centre distance between beams in a timber system is around 5 meters. As it is not possible to add extra columns, lateral braces are placed. In the x-direction, these braces are placed every 3.95 meters and in the y-direction, the braces are placed every 4.22 meter. This ensures that smaller beams can be applied in the design. The lateral supporting beams are included in an enlargement of this figure in Appendix D.4 “Roof plan of the structure”. In this Appendix, also a 3D-view of the roof beams, bracings, lateral supports, and columns is given.

6.3.3.2 Schematisation of two sections

In Figure 6-19 and Figure 6-21, two sections (in the y-direction and x-direction) are shown. The profiles shown here are based upon the calculations given in Appendix C.4 “Results of structural calculations”. Just like in Alternative A, the frame stabilised by the wind bracing in the façade. The wind load needs to be transferred from the frame to these wind bracings by means of bracings in the roof. For the sections shown in the following figures, this is modelled with a horizontal support. The support reaction of this

horizontal support is calculated in Appendix D.2 “Loads”. These loads are used to calculate which profiles should be used for the bracing elements. For the bracing elements, large normal forces need to be transferred, which means that the connection between the brace and the beams can be governing. Therefore, the connection is calculated in Appendix D.5.4 “Connection in the bracing system”.

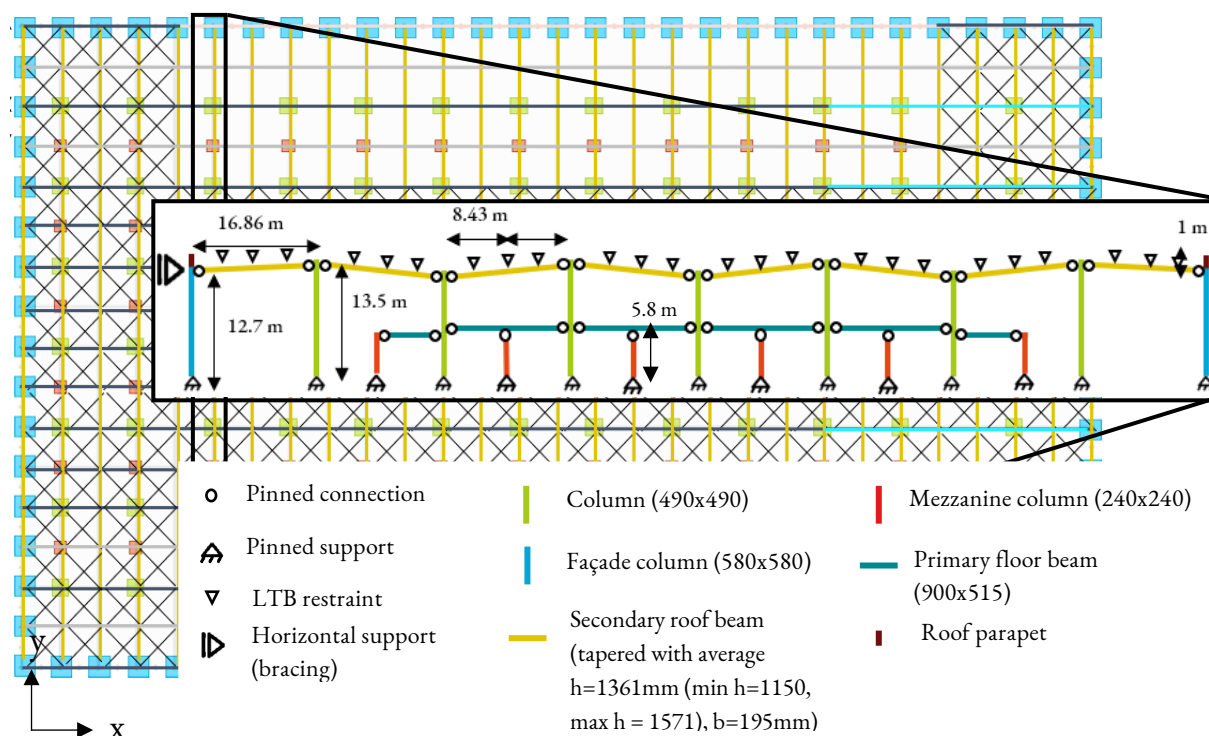


Figure 6-19: Mechanics scheme of the frame in the y-direction

In this figure, the frame structure is shown with the mezzanine floor beams located halfway the columns. The mezzanine floor beams are connected by hinges. The frame is stabilised by bracing in the roof and façade. This is modelled as horizontal support at the end of the frame. As can be seen in the figure, tapered beams are used to make sure rainwater will runoff. Furthermore, a parapet is placed to guarantee safety for workers on the roof.

From Figure 6-19, it can be seen that the beams are placed at an angle. To ensure this angle, it is possible to use a single tapered beam, which already includes this angle in the design of the beam. The tapered beam design is found in Figure 6-20.

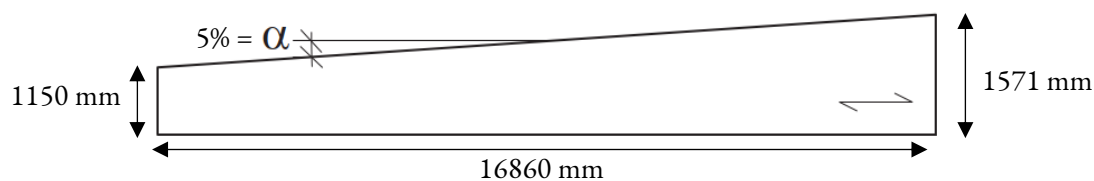


Figure 6-20: Single tapered beam (Blaß & Sandhaas, 2017)

To connect the tapered beams with the primary beams in the x-direction, two sections are checked. First, the section where the tapered beam has the lowest height. This is shown in Figure 6-21. At the locations where the tapered beam has the highest height, the primary beams must also have extra height.

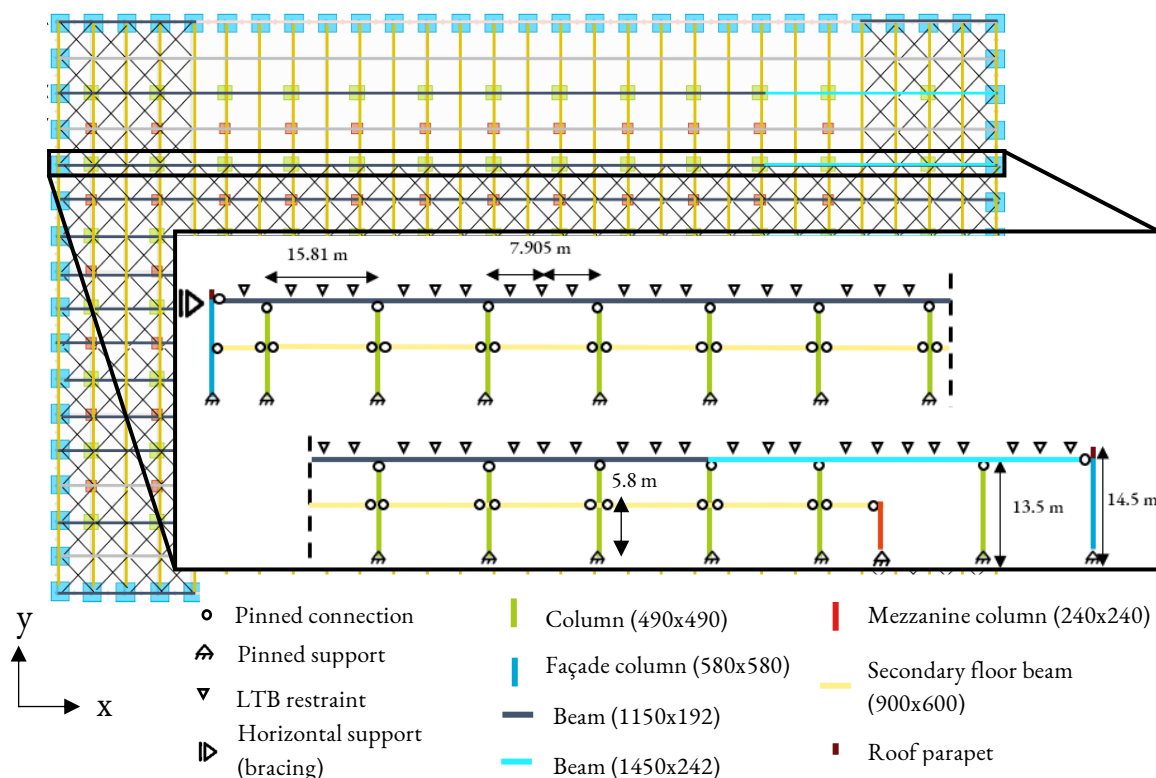


Figure 6-21: Mechanics scheme of the frame in the x-direction

Important: At the location where the tapered beam is higher, the beams also have more height. For the beam shown in dark blue, the following dimensions are used: 1571x196 and for the beam shown in bright blue, the following dimensions are used: 1571x242

6.3.3.3 Vertical bracing elements

The vertical bracing elements are shown in the following figure. The wind braces in the façade are made from steel. This choice is made because the normal forces in the diagonals are very high. A steel brace made from a circular hollow section is therefore used. The calculation of the vertical bracing elements is further explained in Appendix D.3.2 “Vertical bracing”.

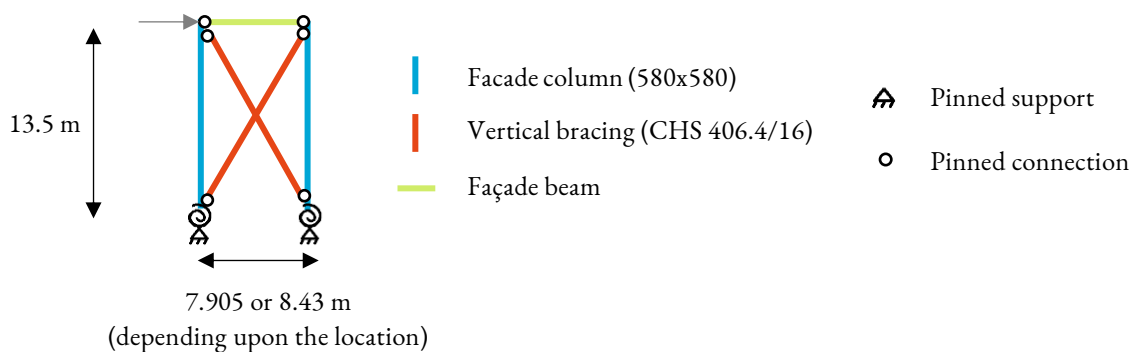


Figure 6-22: Visualisation of the vertical bracing in the façade

6.3.4 Mezzanine floor design

Timber storey floors are usually made from CLT or LVL. In Table D-14 in Appendix D.6 “Mezzanine floor design”, a comparison between four timber floor systems is made. The conclusions are as follows:

- An LVL floor such as the Kielsteg floor should not be applied in the design, because this has a relatively high environmental impact.
- No direct EPD data is available for the Lignatur floor. Therefore, it was initially decided not to consider this floor type. In hindsight, it would have been possible to analyse the Lignatur floor with other EPD data, for example for glulam. However, this does mean that in this research, the Lignatur floor has not been analysed.
- A downside of the CLT rib panel compared to the CLT panel is the necessary thickness.
- The production process of a CLT panel and a CLT rib panel differs. According to Stora Enso (2018), it is economically more interesting to apply CLT rib panels for a longer span and CLT panels for a shorter span.

In the design, the floors will only have to span a short distance, so it is decided to use a CLT panel with limited height. In Appendix D.6.1 “Two-way spanning CLT panel”, it is investigated whether the CLT panel could span in two directions. However, this means that additional concrete and steel needs to be connected to the timber. However, in chapter 4.1 “Design for Deconstruction (DfD)”, it is explained that for reprocessing of materials and material recycling it is best to have a simple composition of materials and secondary finishes to the base material should be avoided as much as possible. Therefore, it is decided to let the CLT panel only span in one direction. The floor layout is shown in Figure 6-23.

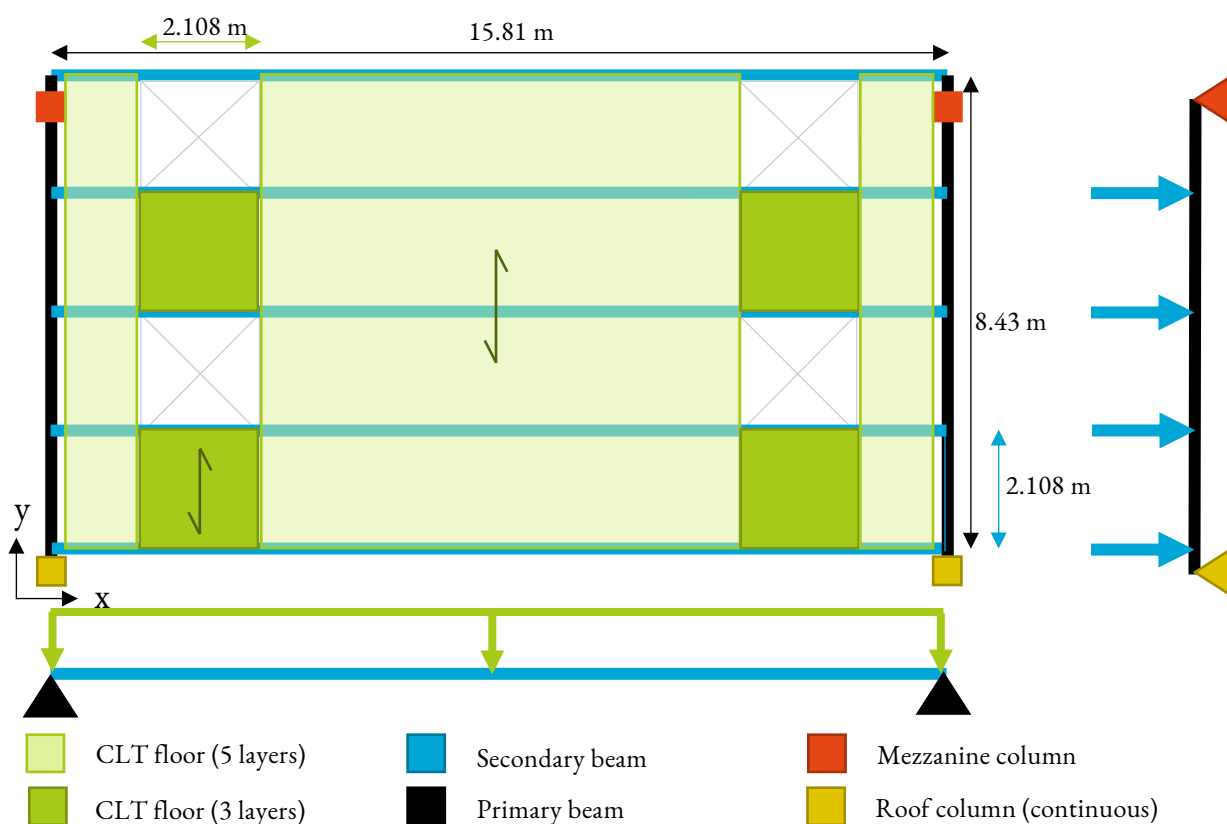


Figure 6-23: Mezzanine floor layout

The green displays where the floor panels lie. The loads from the floors are transferred to the secondary beams, which then transfers the load to the primary beams, onto the columns.

Based upon the calculations shown in Appendix D.6.3 “CLT 3-layer floor panel check”, the CLT floor with the length of 2.108 meters is designed, this floor is shown in Figure 6-24 on the left. Based upon this calculation, the CLT floor is designed with five layers, from which the top layers span in the same direction as the floor. The CLT floor that spans 8.430 meters is also calculated, this calculation is found in Appendix D.6.3 “CLT 3-layer floor panel check”. As this floor lies on multiple beams, only three timber layers are necessary for this design. This design can be found in Figure 6-24 on the right. Both designs have a thickness of 175 mm, to ensure that the floors have the same thickness.

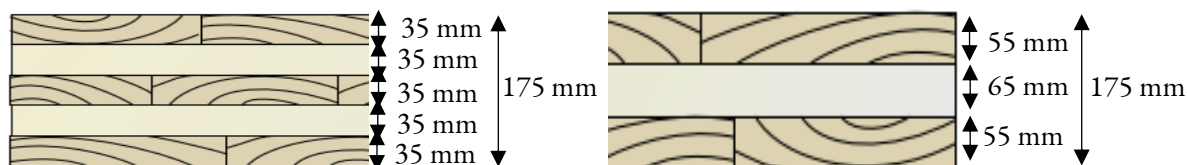


Figure 6-24: Layout of the CLT floors used in the design (Karacabeyli & Douglas, 2013)

Left: A CLT element made from five layers. The fibres in the top layer have the same direction as the floor spans. Right: A CLT element made from three layers. The fibres in the top layer have the same direction as the floor spans.

6.3.4.1 Top layer

To ensure a smooth and even floor, the CLT floor will be covered with a concrete top layer of 50 mm thick. As the mezzanine floor of the Base design also has a concrete top, this is expected to fulfil the client’s floor requirements. For this design alternative, it is intended to use simple material compositions and to avoid secondary finished to the base material, so the concrete top layer should not be connected to the timber floor directly. The thickness of the top layer is assumed based upon two projects with a demountable concrete floor, namely the Temporary Courthouse in Amsterdam and a research project under the supervision of the concrete floor design company VBI (Buunk & Heebing, 2017; De Danschutter, Noomen, & Oostdam, 2017). The demountable concrete floor of the Temporary Courthouse can be seen in Figure 6-31.

6.3.4.2 Mezzanine floor beams and columns

The location of the mezzanine floor beams is shown in Figure 6-23. For a glulam beam, the economic width ranges between 1:6 to 1:8 of the height. However, if this is followed for this specific design, the mezzanine floor must be raised due to the space needed below the floors (as shown in Figure 6-1). From the dimensions given in this figure, it is decided to design beams with a maximum height of 900 mm (which is equal to the maximum beam height of the base design). The dimensions of the beams are based upon the calculations found in Appendix D.6.4 “Timber secondary mezzanine floor beam checks” and Appendix D.6.5 “Timber primary mezzanine floor beam”.

The columns below the mezzanine floor are made from a rectangular profile, to prevent buckling. The calculation of the columns can be found in Appendix D.6.6 “Mezzanine floor column check”.

6.3.5 Possible improvements of the design

The total weight of the structure is based upon the explanations given in this chapter. However, some improvements are still possible. The most important improvements are explained in Appendix D.7 “Possible improvements of the design”.

6.4 Alternative C: Demountable sway structure (steel and concrete)

Alternative C is a specifically designed demountable structure, because it is expected that the distribution centre will not fulfil its function for the whole technical life span. This ensures that elements can be used for another function. This design is based upon the guiding principles given in chapter 5.2 “Research question 3b: Optimise design for its residual value”.

6.4.1 Connection designs

The connections are an important aspect of this design alternative, so the Design for Deconstruction aspects should be followed. Based upon the explanation given in chapter 4.1.1 “Implementing DfD in the case study”, the beam-column connection shown in the following figure is set up.

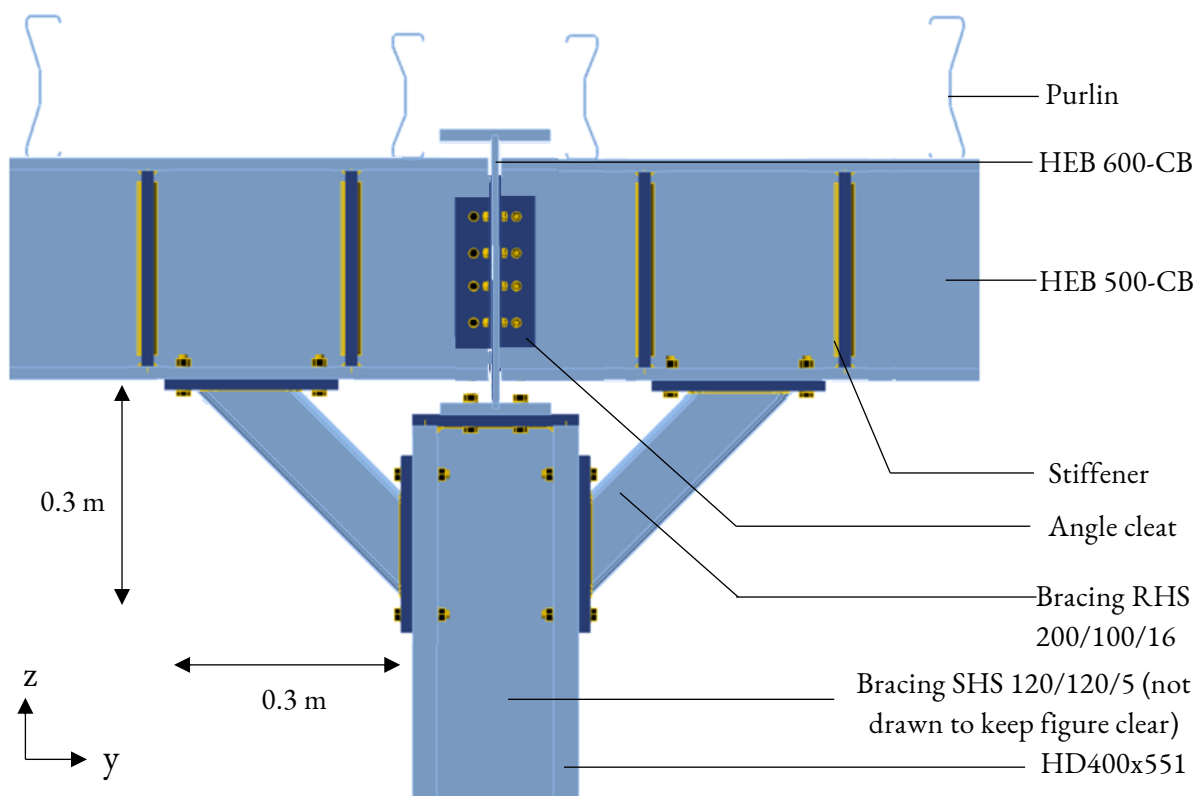


Figure 6-25: Connection between beams and column (own illustration, made with IDEA StatiCa)

For the beam-column connection, some important changes compared to the base design are incorporated based upon chapter 4.1.1 “Implementing DfD in the case study”. Firstly, the roof beams are placed at an angle. However, the rainwater must be able to run off. Therefore, it is decided that this is provided by the purlins on top of the roof beams. Furthermore, the roof beams should be easily demountable from the columns. Secondly, in the design, the main roof beam (HEB 600-CB) is connected to the column with a non-extending end plate. Thirdly, for the connection between the secondary roof beam and the primary roof beam, only dry connections should be applied. This is realised with a cleat angled profile. To provide enough stiffness, bracing is added. Due to the use of bolts, the bracing can be removed from the main load-bearing elements. Together the stiffness of the connection between the column and primary roof beam and the stiffness between the primary roof beam and the secondary roof beam is determined. This is explained and calculated in Appendix E.2 “Beam-column connections”.

Also, the column base connection is assessed based upon the ability to be demounted. By considering the column base connection of the Base design (shown in Appendix B.3.2 “Column base connection”), it is

decided that this connection does not need to be altered. Firstly, because in this design, the column base is connected to the foundation with anchors that can be unbolted, making it possible to remove the column and end plate. Secondly, the extending end plate is not considered a problem in this design. This is due to the fact that the column is made from an HD profile. This type of profile is only used as a column and will never be used in another form. Therefore, the reusability of the column is not reduced with protruding elements at the column base.

6.4.2 Schematisation of two sections

With the determination of the connections, two sections are designed. The following figures visualise the design as calculated in Appendix E.3 “Results of structural calculations”.

Compared to the base design, larger roof beams are necessary. This is ensured by the lower stiffness between the main columns and roof beams, because a lower moment can be carried at this connection. This results in a higher bending moment in the middle of the beam and thus a larger beam. The larger roof beams ensure more stability of the system. Therefore, it is possible to reduce the size of most of the columns (‘Main column 1’ in Figure 6-26). However, one column had to be enlarged, as larger forces were exerted on this part of the structure.

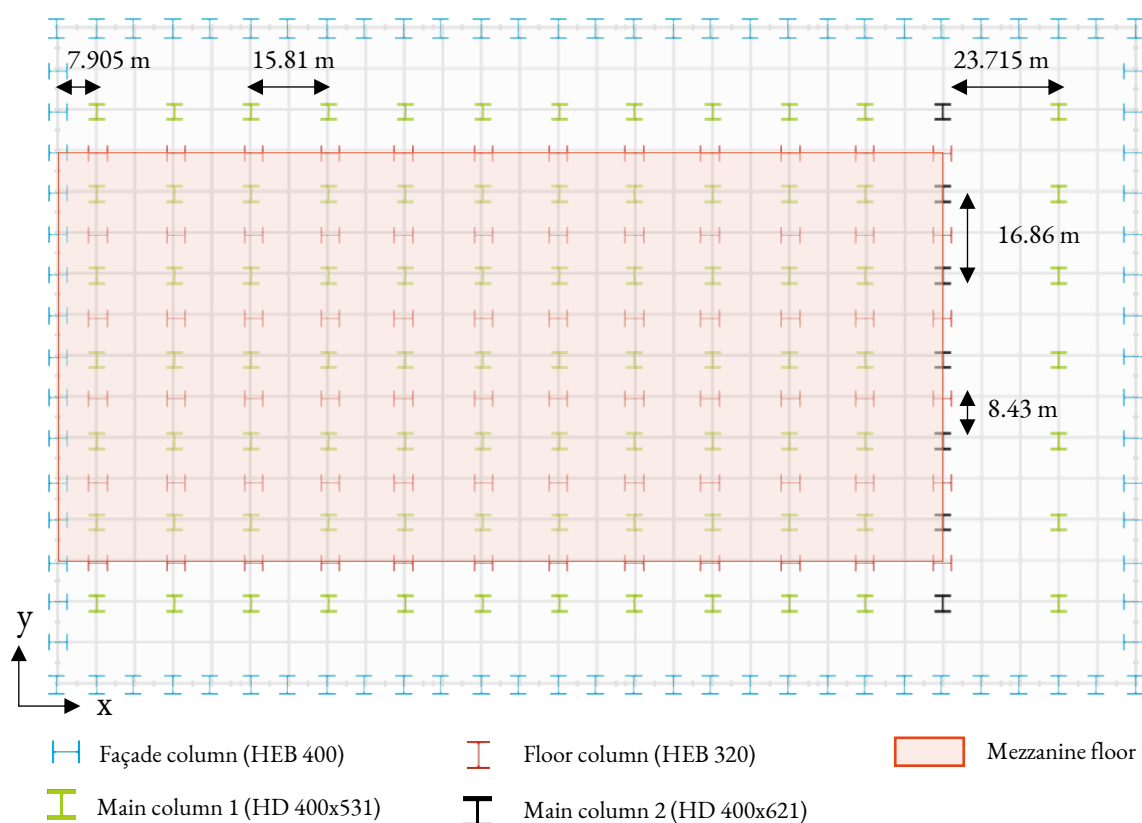


Figure 6-26: Top view of Alternative C at the dotted blue line shown in Figure 6-4

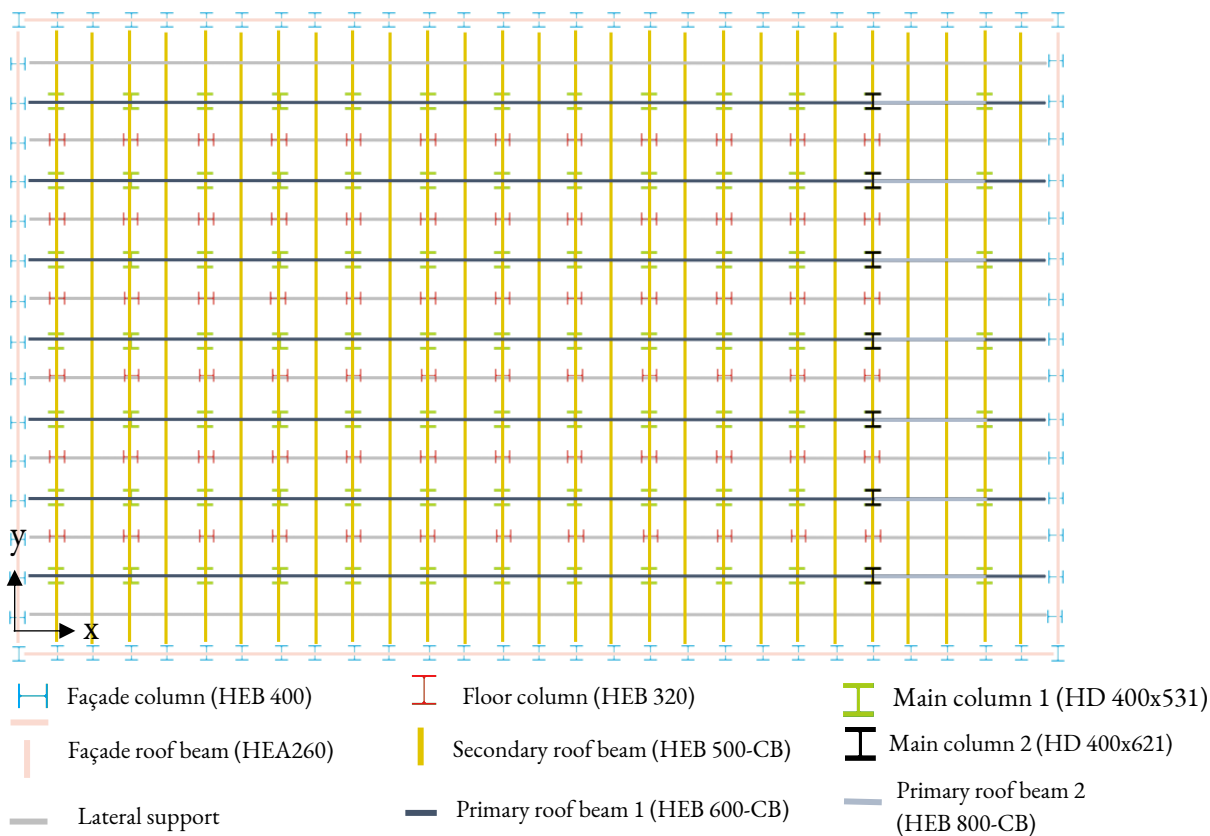


Figure 6-27: Top view of Alternative C at the dotted green line shown in Figure 6-4

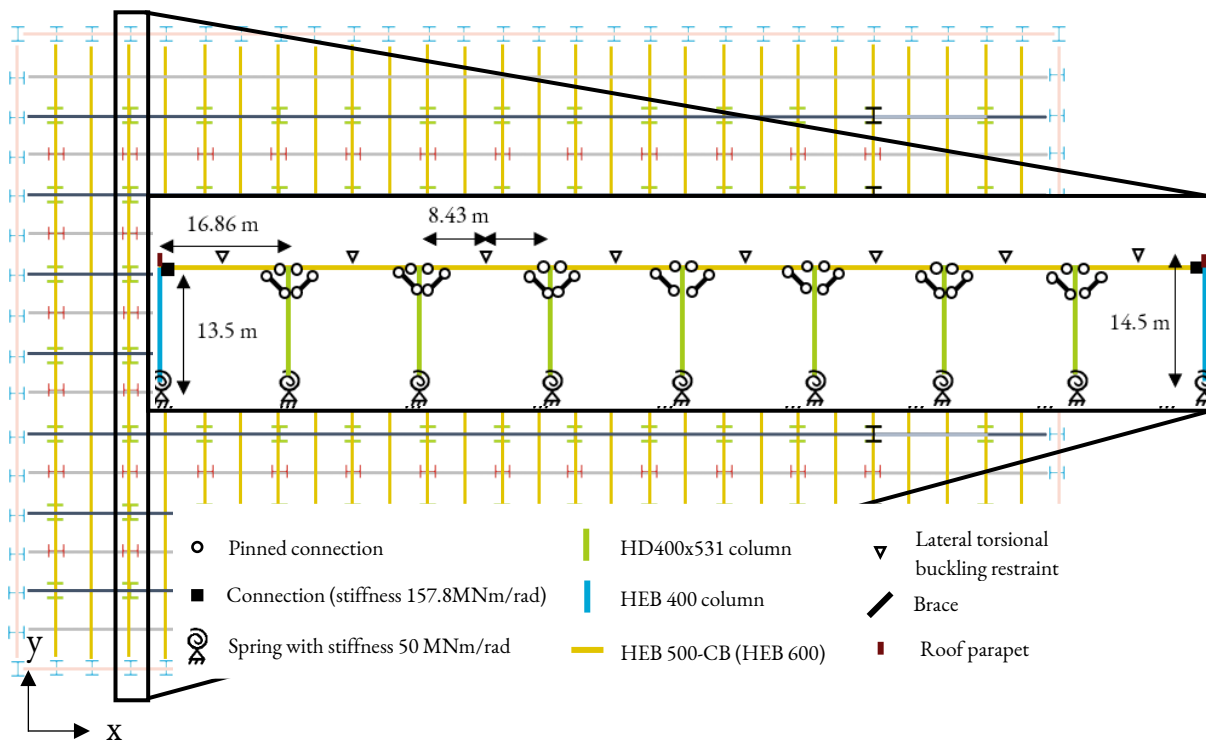


Figure 6-28: Mechanics scheme of the stabilising portal frame in the y-direction
 The portal frame is established through the small braces and the stiff connection between the exterior columns and beams (for which the stiffness is calculated in Appendix E.2 “Beam-column connections”).

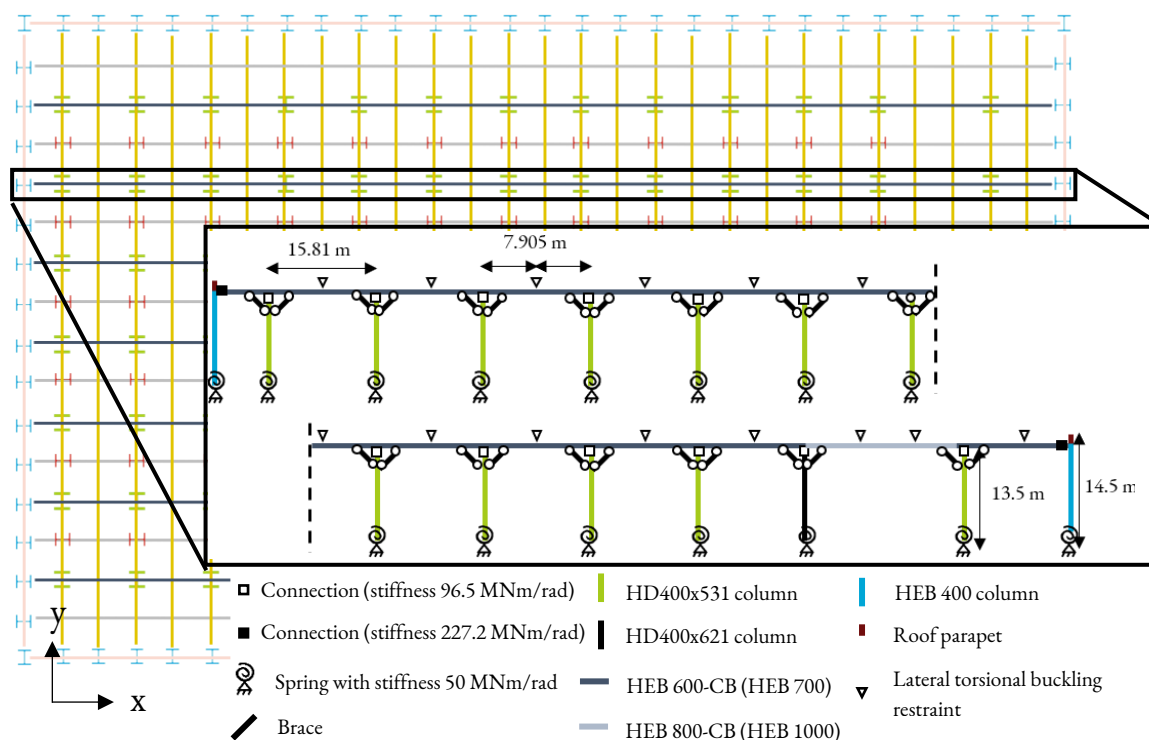


Figure 6-29: Mechanics scheme of the stabilising portal frame in the x-direction

In this figure, the portal frame structure is shown. The beams and columns are connected by relatively stiff connections (calculated in Appendix E.2 “Beam-column connections”).

6.4.3 Mezzanine floor design

For a demountable mezzanine floor, paragraph 4.1.1 “Implementing DfD in the case study” is also followed. Based on this knowledge, a comparison between different floor systems is made in Table E-10 in Appendix E.4 “Mezzanine floor design”. For the design, a floor that has limited height and weight is advantageous. From the table in the Appendix, it becomes clear that this can be reached by applying a quantum deck floor or a hollow core slab. In this research, a hollow core slab will be applied, as this is more widely used, resulting in multiple available EPDs. This does mean that prefab concrete is used, which has a higher environmental impact than cast in situ concrete (as explained in chapter 3.2 “Concrete”).

An issue with a hollow core slab is the necessity of applying a top layer. Usually, this top layer is casted on site. However, for this alternative, it is necessary to make the top floor demountable. Multiple top floor designs are investigated:

- Cement top floor (wet)
A cement floor can be casted on top of the hollow core slab. VBI and Nijhuis Bouw have conducted research in 2005 on the ability of such a floor to be demounted. In this research, it was found that it is relatively easy to remove such a floor (Buunk & Heebing, 2017). This process can be seen in Figure 6-30. Even though it is relatively easy to remove this floor, it does increase the demounting time.



Figure 6-30: Removing the cement floor from a hollow core slab (Buunk & Heebing, 2017)

- Raised top floor (wet)

It is also possible to apply a raised top floor made from casted concrete. This can be ensured by placing elements in between the hollow core slab and the top floor. An example can be found in Figure 6-31, but it is also possible to place insulation material in between the hollow core slab and the top floor (Buunk & Heebing, 2017). Compared to the wet cement top floor, demounting of this floor is considered easier and is therefore suitable to use in this design alternative.

- Raised top floor (dry)

The top floor can also be made from cement-bonded fibreboard (Buunk & Heebing, 2017). However, this is unsuitable for this design, as the robots need a perfectly smooth surface.

From this comparison, it is decided to apply a raised wet cement top floor. The same top floor as for the timber alternative is applied. This is C30/37 concrete of 50 mm thick, leading to a load of 1.2 kN/m².

An example of a demountable raised top floor is shown in Figure 6-31. Usually, the top floor ensures the diaphragm action of the floor, but a demountable top floor is unable to ensure this. Therefore, additional measures need to be taken. In De Danschutter et al. (2017), it was explained that for the Temporary Courthouse in Amsterdam, the diaphragm action in the floor was ensured by enclosing the hollow core slabs with steel beams. The horizontal forces in the slabs are transmitted to the steel beams through the newly developed beam-slab connection.

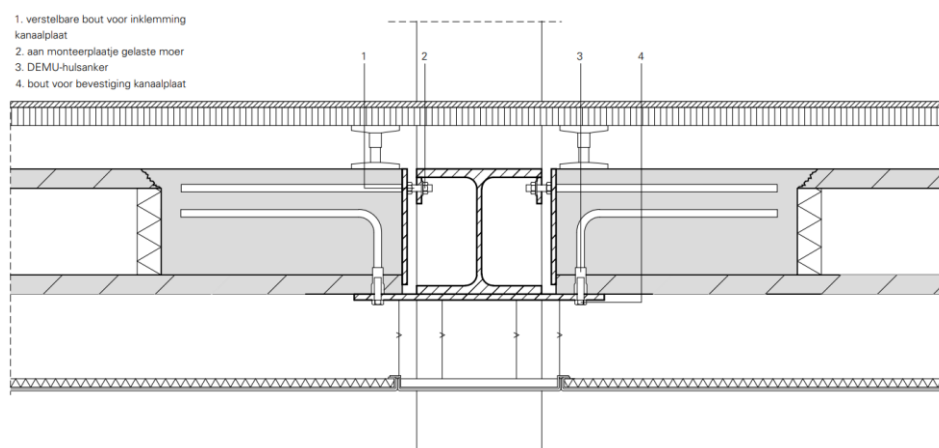


Figure 6-31: Hollow core slab and steel beam in the Temporary Courthouse (De Danschutter et al., 2017). This is a demountable connection as the top floor can be demounted from the hollow core slab.

6.4.3.1 Schematisation of mezzanine floor

The demountable floor design is shown in Figure 6-32. In this design, the mezzanine floor will be made from a hollow core slab of 150 mm thick. This has been checked with the hollow core slab calculator from VBI. The export of this calculation is found in Appendix E.4.1 “Floor calculations (robotic function)”.

The floor beams are also designed. First, it is calculated whether it is possible to integrate the floor beams in the hollow core slabs, which reduces the total height of the floor system. An example of an integrated beam is shown in Figure 6-31. From the technical report of Hamerlinck & Potjes (2007), this calculation has been made for the floor design shown in Figure 6-32. However, from this calculation, it is found that the integrated beam is insufficiently strong to span 15.81 meters with the given loadings. Therefore, it is decided to design the floor with non-integrated beams instead.

The secondary beam, shown in light blue in Figure 6-32, has the same design as the base design: a castellated HEB 650. The calculation behind this design choice can be found in Appendix E.4.2 “Steel

secondary mezzanine floor beam checks for the floor with robotic function”. The primary beam, shown in black in Figure 6-32, is a HEB500. The column is made from an HEB 320 profile. The calculations for the primary beam and column are not included, as the calculation steps are the same as given as in Appendices B.4.3 and B.4.4 of the Base design.

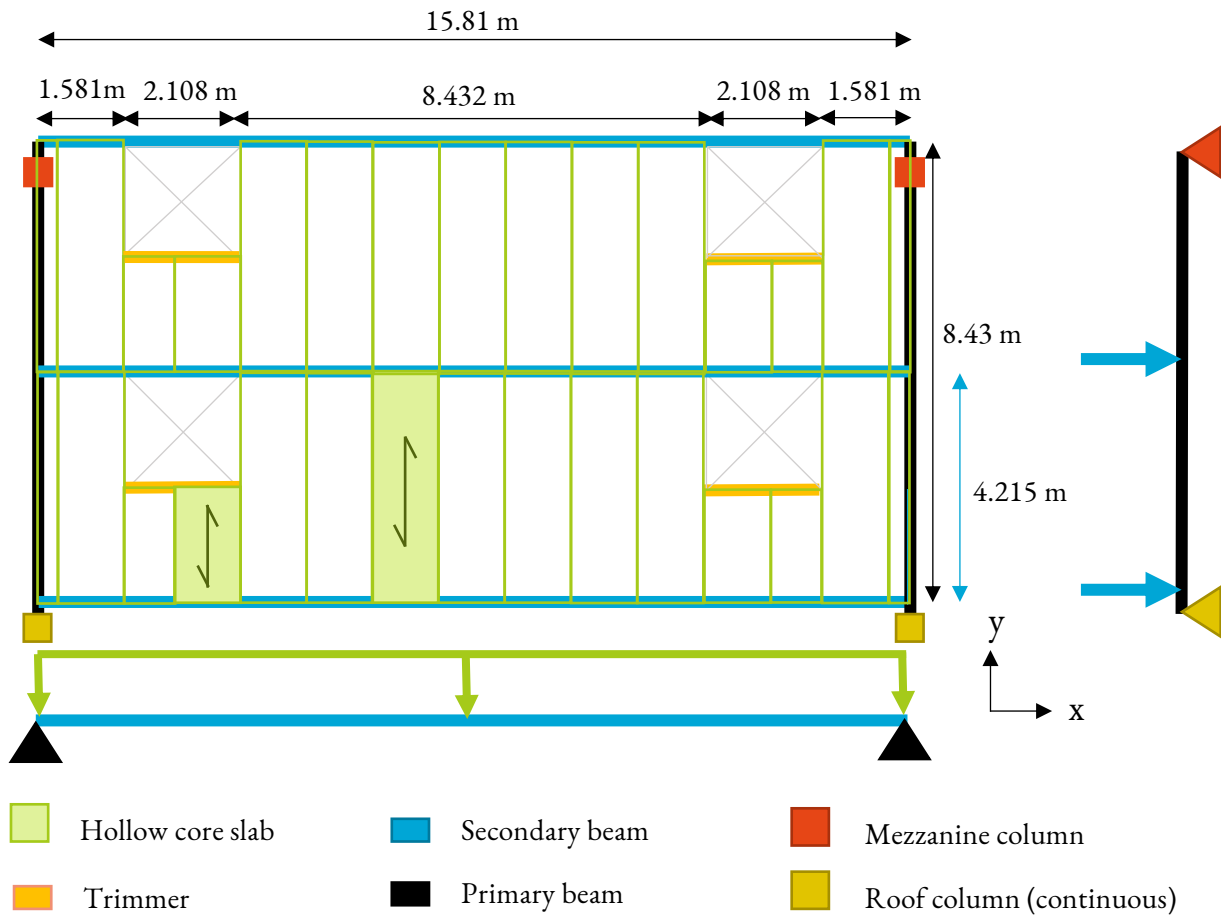


Figure 6-32: Chosen mezzanine floor layout for Alternative C

In green, the hollow core slabs are shown. In between the openings, the hollow core slabs are 2107 mm; the other hollow core slabs span 4215 mm. They transfer their load onto the primary floor beams, then to the secondary floor beams, and finally to the columns.

6.5 Alternatives D: Non-sway structure with future function change (steel and concrete)

Alternative D1 and D2 both incorporate a future function change. In this chapter, both the mezzanine floor design and the main load-bearing structure are designed and calculated.

6.5.1 Alternative D1: Non-sway structure with office/retail on the mezzanine floor

For this alternative, it is expected that the mezzanine floor will be used for an office or retail function instead of robots. To prevent the placement of a new floor, a demountable floor is aimed for. In that case, the openings in the robotic floor can also be closed relatively easily. So, the mezzanine floor of Alternative C is used as a starting point for this design (as explained in chapter 6.4.3 “Mezzanine floor design”).

The floor layout of Figure 6-33 is designed for the office or retail function. The higher floor load for these functions, an imposed floor load of 4 kN/m^2 , is included in the design of the hollow core slabs. This is calculated with help of the hollow core slab calculator from VBI, which can be found in Appendix F.1.1 “Floor calculations (office or retail function)”. From this calculation it becomes clear that no changes need to be incorporated: the floor and floor beams remain the same as for Alternative C.

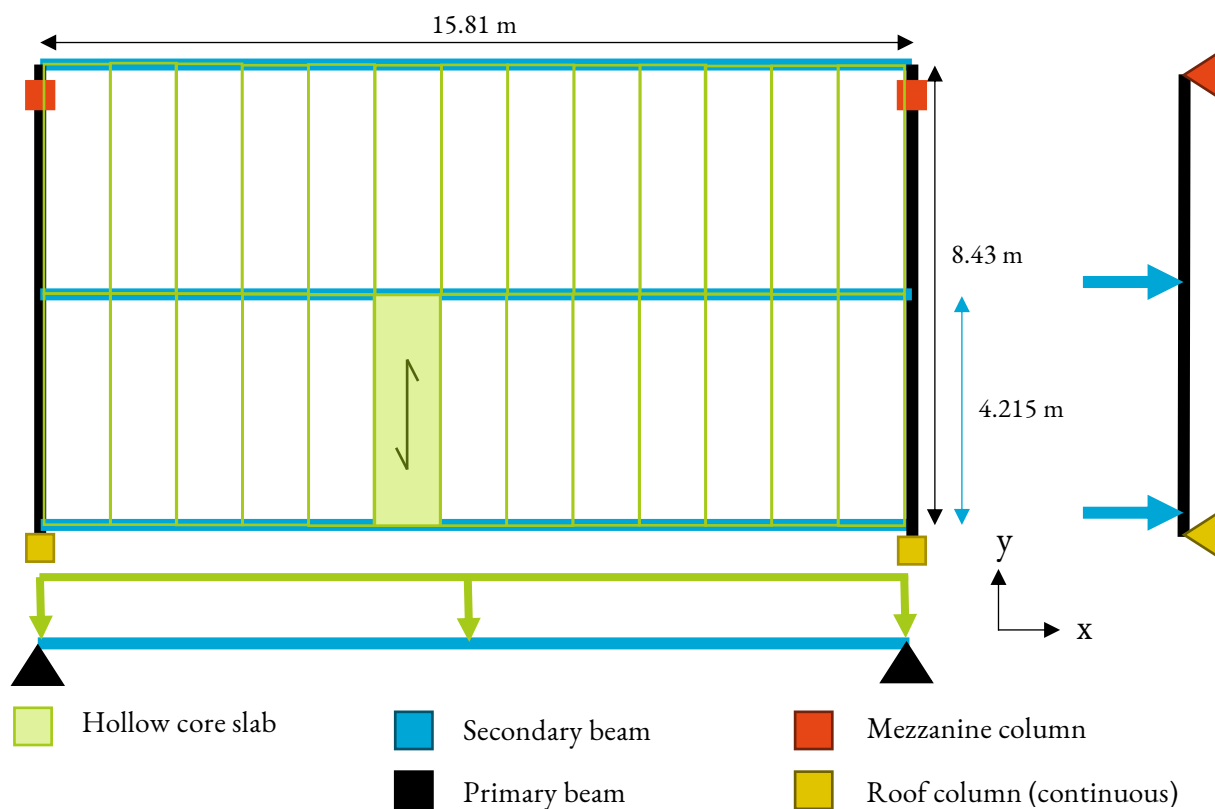


Figure 6-33: Chosen mezzanine floor layout for Alternative B

In green, the hollow core slabs are shown. They transfer their load onto the main floor beams, onto the secondary floor beams, onto the columns.

The main load-bearing structure must be able to carry a heavier floor load. The main load-bearing structure of Alternative A is used as a starting point and it is verified in Appendix F.2 “Results of structural calculations” whether the columns can carry this new load. It is found that the structural system of Alternative A is strong enough to carry the mezzanine floor loads. Therefore, the structural system given in chapter 6.2.2 “Structural system” also holds for this design.

6.5.2 Alternative D2: Non-sway structure with industrial storage on the mezzanine floor

For this alternative, an industrial storage floor load is expected in the future. The same floor layout as shown in Figure 6-32 can be applied for this design alternative as well. For the industrial function, an imposed floor load of 7.5 kN/m^2 is included in the design of the hollow core slabs. This calculation has been performed with the VBI calculator and can be found in Appendix G.1 “Floor calculations (industrial function)”.

Due to this increase, the secondary floor beams need to be enlarged. Instead of an HEB 650-CB, an HEB 700-CB will be used in the design. The primary floor beams are made from HEB 650 beams. To be able to make a connection between the primary floor beams and the mezzanine floor columns, HEB 320 profiles will be applied in the design. The calculations steps are the same as given in Appendices B.4.2, B.4.3, B.4.4 and E.4.2 and are therefore not included in this report.

Also the main load-bearing structure is verified. From the calculation given in Appendix G.2 “Results of structural calculations”, it is found that the structural system of Alternative A is not strong enough to carry the additional mezzanine floor loads. Therefore, the main columns of Alternative A (made from HEB 400 profiles) are changed into columns made from HEB 600 profiles. This can be seen in the following figure. Other than that, the structural system given in chapter 6.2.2 “Structural system” also holds for this design.

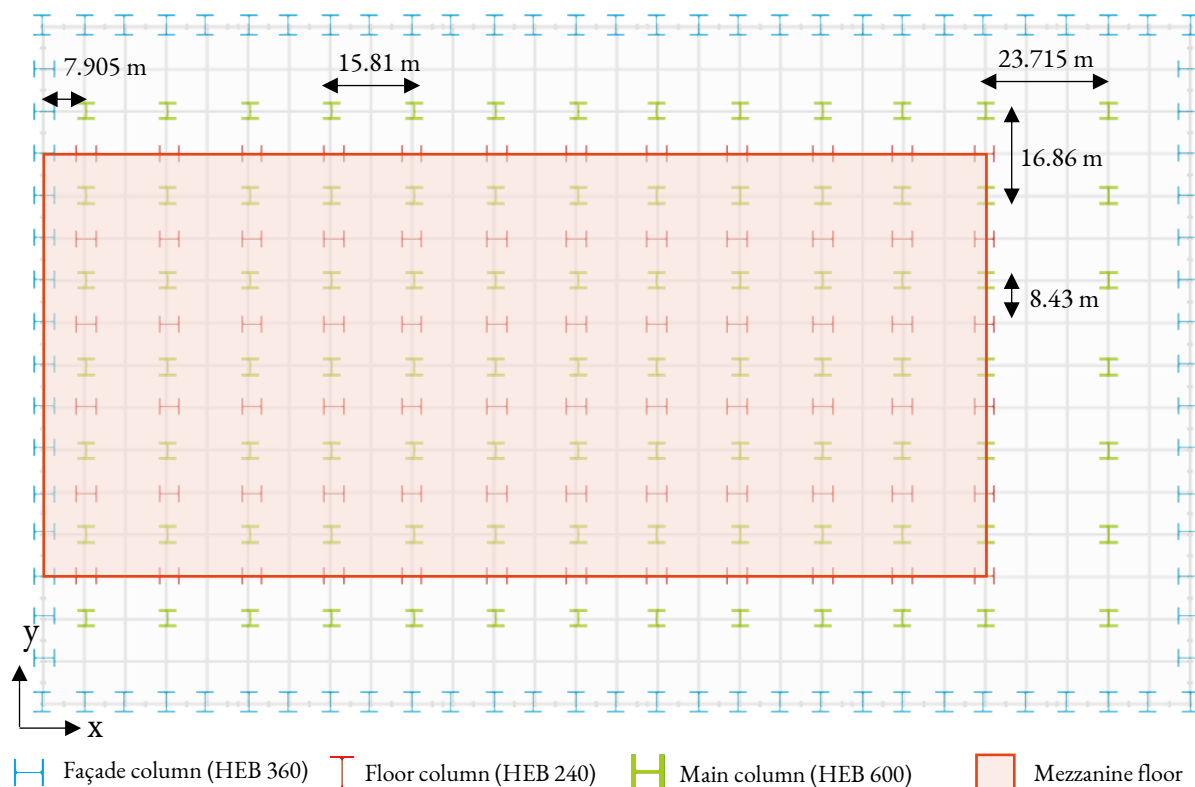


Figure 6-34: Top view of Alternative D2 at the dotted blue line shown in Figure 6-4

6.6 Overview of design alternatives

For each design, an overview of the used elements and their weight or area is given in the Appendix. For the Base design, Alternative A, B, C, D1, and D2 this is respectively Appendix B.6, C.5, D.8, E.5, F.3, and G.3 “Element overview”. This data is combined in the following table and is used as input for the environmental impact calculation (in the table, the data is rounded to provide a better overview).

Table 6-2: Total amount of material per design alternative

Element	Total weight [kg]	Total area [m ²]
<i>Base design: Sway structure (steel + concrete)</i>		
Steel main load-bearing structure	1 777 000	
Steel mezzanine floor	1 029 000	
ComFlor steel		13 000
ComFlor concrete	3 697 000	
<i>Alternative A: Non-sway structure (steel + concrete)</i>		
Steel main load-bearing structure	1 693 000	
Steel mezzanine floor	1 029 000	
ComFlor steel		13 000
ComFlor concrete	3 697 000	
<i>Alternative B: Non-sway structure (timber + concrete)</i>		
Glulam main load-bearing structure	1 863 000	
Steel bracing	10 000	
Glulam mezzanine floor elements	2 138 000	
CLT mezzanine floor	1 067 000	
Concrete top floor	1 525 000	
<i>Alternative C: Demountable sway structure (steel + concrete)</i>		
Steel main load-bearing structure	2 108 000	
Steel mezzanine floor	732 000	
Hollow core	3 405 000	
Concrete top layer	1 525 000	
<i>Alternative D1: Non-sway structure with office/retail on mezzanine floor (steel + concrete)</i>		
Steel main load-bearing structure	1 693 000	
Steel mezzanine floor	732 000	
Hollow core	3 929 000	
Concrete top layer	1 759 000	
<i>Alternative D2: Non-sway structure with industrial storage on mezzanine floor (steel + concrete)</i>		
Steel main load-bearing structure	1 763 000	
Steel mezzanine floor	808 000	
Hollow core	3 929 000	
Concrete top layer	1 759 000	

7 Environmental impact calculation

In this chapter, the Life Cycle Assessment method is first explained. This is followed by the scope and goal of the Life Cycle Assessment for this research. Then, the functional unit and system boundaries are given. With this knowledge, the methodology of the Life Cycle Assessment is set up. At the end of this chapter, an answer is given to research question 4 *“How can the environmental impact of a distribution centre’s load-bearing structure be quantified in a comprehensive way?”*. Here, also a flow chart of the calculation steps is given. With this flow chart, other engineers will be able to calculate the yearly environmental impact of a design.

7.1 Life Cycle Assessment

The environmental impact of structures can be quantified with a Life Cycle Assessment (LCA), being part of the Eurocode (ISO 14040). In a classical LCA, the focus lies on an in-depth material assessment, which can take up to two or three months to conduct (Vogtländer, 2015). A classical LCA consists of four phases: the goal and scope definition phase, Life Cycle Inventory phase, Life Cycle Impact Assessment phase, and the interpretation phase (NEN, 2019).

During the first phase, the goal of the LCA is determined. Based on this goal, the scope including the system’s boundary and level of detail is defined.

The second phase is called the Life Cycle Inventory (LCI) phase. During this phase, the inputs and outputs of a product throughout its lifecycle are compiled and quantified. This leads to a table with the emissions of materials during the different stages shown in Figure 7-1: the product stage (A1-A3), construction process stage (A4, A5), use stage (B1-B7), end-of-life stage (C1-C4), and the beyond end of life stage (D). The beyond end of life stage contains benefits and loads outside the system's boundary. This includes reuse, recycling, and energy recovery options such as incineration and landfilling.

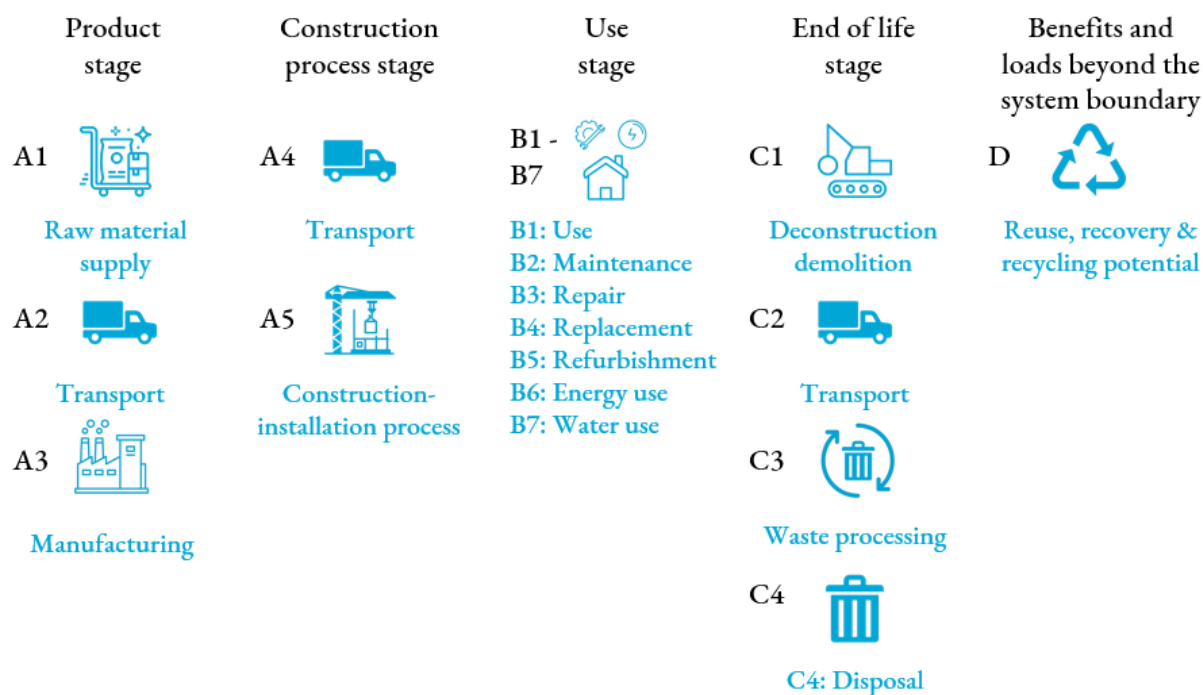


Figure 7-1: Life cycle stages (own illustration, based upon NEN (2019))

During the third phase, the Life Cycle Impact Assessment (LCIA) phase, an Environmental Product Declaration (EPD) sheet is created. This sheet contains data on the environmental impact of a product per stage, calculated per Environmental Impact Category (EIC). In Europe, seven Environmental Impact Categories must be assessed in an EPD. These categories can be found in Table 7-1 under EPD data. Companies that set up an EPD must follow EN 15804 and show their underlying assumptions and background information, such that it can be verified. The Dutch Building regulations prescribe an assessment of eleven Environmental Impact Categories instead of seven (Stichting Bouwkwaliiteit, 2019). This data is gathered in a national database, the Nationale MilieuDatabase (NMD). The categories that must be included can be found in Table 7-1 under NMD data. Also, in the Netherlands, a shadow price calculation has been set up to make it easier to understand the environmental impact. The shadow price represents the costs that need to be made to eliminate one kilogram of its corresponding equivalent unit from the environment. This is a single value, making it easier to compare different designs. The environmental price as external costs can be found in Table 7-1. In this table, the unit for ADPf is kg antimony (Sb) equivalent. However, in EPD datasets this unit is megajoules (MJ). To use the shadow price calculation, a conversion of $4.81E-4$ kg Sb eq./MJ is performed.

Table 7-1: Environmental prices per EIC for LCA (Stichting Bouwkwaliiteit, 2019)

Data	EIC	EIC unit	Shadow price [€/kg equivalent]	Shadow price unit	
EPD	NMD	Global Warming Potential (GWP)	kg CO ₂ eq.	€ 0.05	€/kg EIC eq.
		Ozone Layer Depletion (ODP)	kg CFC-11 eq.	€ 30.00	€/kg EIC eq.
		Acidification potential (AP)	kg SO ₂ eq.	€ 4.00	€/kg EIC eq.
		Eutrophication potential (EP)	kg PO ₄ 3- eq.	€ 9.00	€/kg EIC eq.
		Photochemical Oxidant Formation Potential (POCP)	kg C ₂ H ₄ eq.	€ 2.00	€/kg EIC eq.
		Abiotic Depletion Non-fuel (ADPe)	kg Sb eq.	€ 0.16	€/kg EIC eq.
		Abiotic Depletion Fuel (ADPf)	kg Sb eq.	€ 0.16	€/kg EIC eq.
	Human Toxicity Potential (HTP)	kg 1,4-DCB eq.	€ 0.09	€/kg EIC eq.	
	Freshwater Ecotoxicity (FAETP)	kg 1,4-DCB eq.	€ 0.03	€/kg EIC eq.	
	Marine Ecotoxicity (MAETP)	kg 1,4-DCB eq.	€ 0.0001	€/kg EIC eq.	
	Terrestrial Ecotoxicity (TAETP)	kg 1,4-DCB eq.	€ 0.06	€/kg EIC eq.	

The final phase of the classical LCA interprets the results of the LCI and LCIA. The results are summarized, discussed, and concluded to write recommendations based on the goal and scope definition.

In this research, a Fast Track LCA is performed. A Fast Track LCA compares design alternatives by using the EPD-output from classical LCAs performed by third parties as input (Vogtländer, 2015). The advantage of a Fast Track LCA is that it only takes a couple of hours to conduct, as opposed to the months it takes to perform a classical LCA.

In a Fast Track LCA, the following procedure will be followed (Vogtländer, 2015):

1. Establish the scope and goal of the analysis
2. Establish the functional unit and system boundaries
3. Set up a methodology for the allocation rules
4. Quantify materials in the system
5. Calculate the environmental impact of each alternative

7.2 Scope and goal of the analysis

The first goal of the Fast Track LCA is to determine the yearly environmental impact of the design alternatives, as explained in chapter 6 “Designs”.

The second goal of the Fast Track LCA is to compare these alternatives. This is explained in chapter 5 “Setup of design alternatives”. It is aimed to answer the following goals:

1. Determine the effect of the amount of material
2. Determine the effect of the type of material
3. Determine the relationship between service life extension and extra material use
4. Determine the relation between reusing a traditional design and a demountable design

7.3 Functional unit and system boundaries

7.3.1 Functional unit

The yearly environmental impact (EI/RSL) will be calculated with the functional unit (FU) as given in the following formula. This is based upon the Dutch Milieuprestatie Gebouw (MPG) calculation.

$$FU = \frac{m_i * \text{shadow price}}{RSL} \text{ in } \left[\frac{\text{€}}{\text{year}} \right] \quad \text{eq. 7-1}$$

Table 7-2: Parameters used in the functional unit

Parameter	Unit	Definition
m_i	kg	Mass of the element type i. This mass differs per design alternative.
Shadow price	€/kg	This is determined with the conversion given in Table 7-1
RSL	years	Reference service life of the building. This is the expected service life of a building for specific in-use conditions (Hovde, 2005). The RSL is based upon the design alternative and the TSL of the materials used. The RSL-value can be equal to the TSL, ESL, or FSL and will be altered to provide insight into the different design alternatives.

In Table 7-2, the RSL is explained. Here, it is stated that the RSL is based upon the TSL of the materials used. In this research, the TSL is estimated based upon a research by the Dutch knowledge centre SBR (Straub et al., 2011). They aimed to collect TSL data by investigating standardised verifiable procedures in different countries. However, they could not find robust international data that also meet the ISO standard criteria, so they decided to use the data from the Dutch NMD as a starting point. From this, the experts assessed construction products based on their properties and inherent performance, their conditions, and in which stage certain decisions are made. The data has been compiled into a list, where the TSL of each product is given as an average number. This average number is based on the Dutch construction practices and is now also recorded in the NMD. In this research, the necessary data is found in Table 7-3.

Table 7-3: Technical service life (TSL) for different element types (Straub et al., 2011)

Type	Element type	Material	Product name	TSL
Main load-bearing structure	Column, beam, console	Concrete	Concrete, prefab	100
		Concrete	Concrete, in situ	100
		Timber	Timber, not preserved	100
		Metal	Steel profile	100
Floor	Load-bearing floor	Concrete	Hollow core slab	100
		Concrete	Steel plate and in situ concrete floor	100
		Timber	Timber	75

7.3.2 System boundaries

For the calculation of the yearly environmental impact, the load-bearing structure of each design alternative is considered separately. However, the total load-bearing structure is not the main interest of this research. As the mezzanine floor and the main load-bearing structure are very different, it is important to consider these aspects separately from each other. This is visualised in the following figure. It shows that for each design alternative, the main load-bearing structure (including the main columns and roof beams, and for the non-sway structures also bracing elements in the roof and in the façade) is considered separately from the mezzanine floor load-bearing structure (including the floor, the floor beams, and the floor columns).

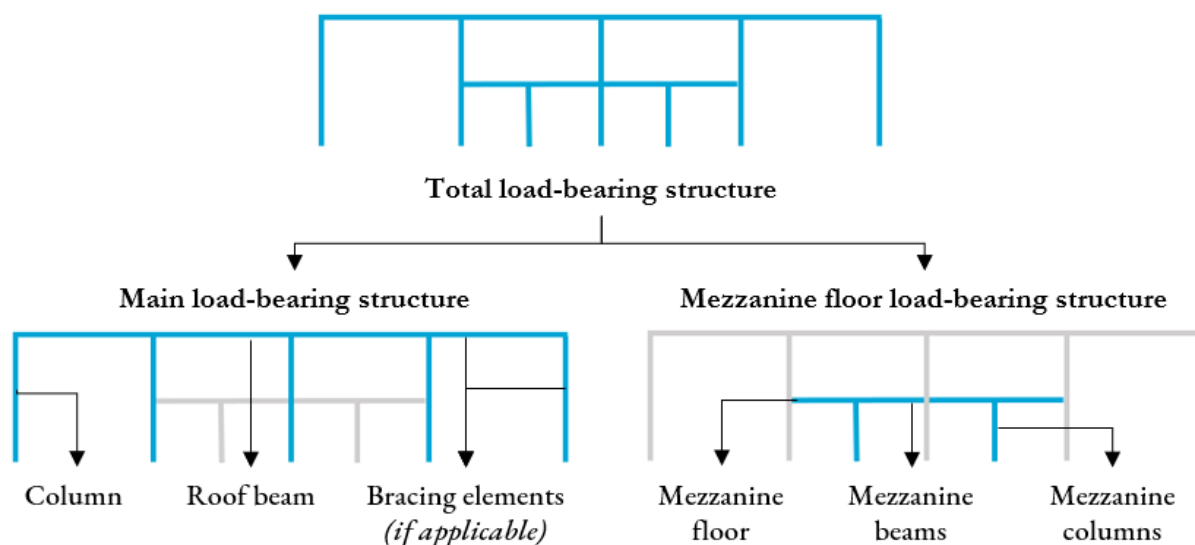


Figure 7-2: Separation of the total load-bearing structure into the main and mezzanine floor load-bearing structure

The rules to set up an EPD (EN 15804:2012), prescribe that it is obligatory to include stages A1-A3 in an EPD. In this research, it is aimed to quantify the environmental impact in a comprehensive way. By only considering stages A1-A3, this aim cannot be reached. Therefore, the benefits that can be gained at the end of life (stage D) are also included. This is also visualised in Figure 7-3, where the stages that are included in this research are shown in blue and the stages that are excluded are shown in grey. In this research, stages A1-A3 are also assessed without stage D, because stage D contains data for an uncertain future scenario.

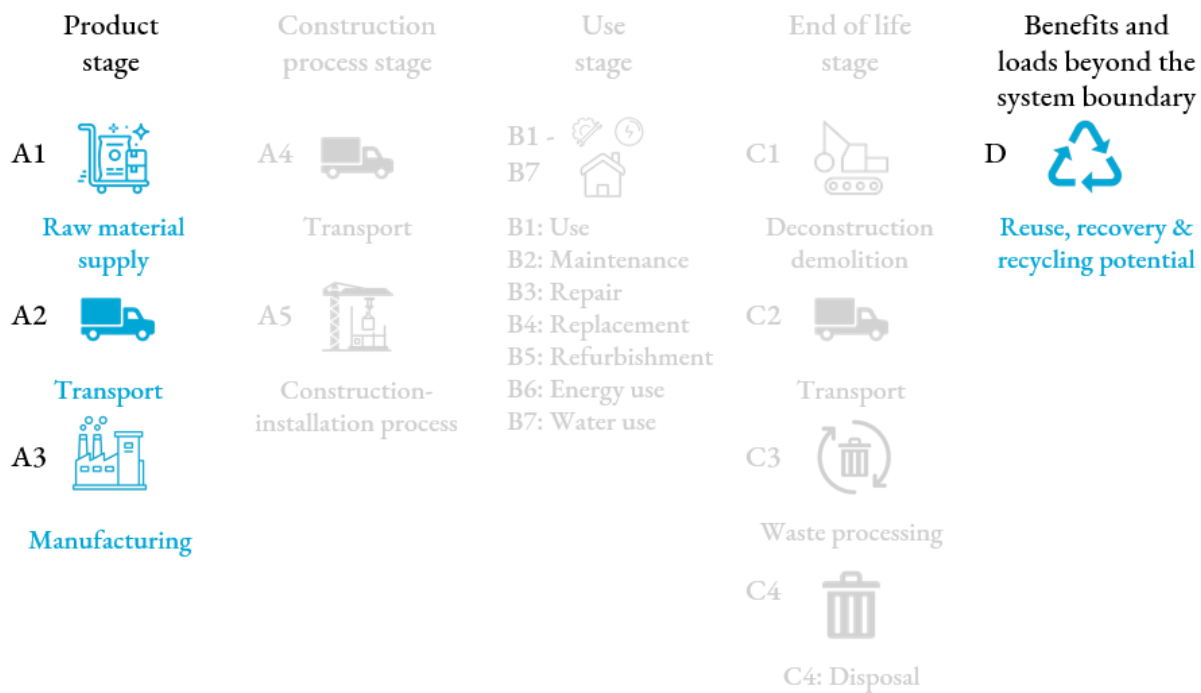


Figure 7-3: Life cycle stages that are investigated for this research

The stages that are included in this research are shown in blue and the stages that are excluded in this research are shown in grey

The exclusion of stages A4-A5, B, and C can be explained. The construction process stage (A4-A5) is not included, because the location of the building is unknown. For the use stage (B1-B7), specific data on the expected maintenance is needed. This is unknown and therefore excluded. Stages C and D contain data on the end of life (EoL). Due to the rules of EN 15804:2019, both stages are based upon a general framework, without a widely accepted approach to model the end of life. In the following sub-chapter, it is explained how this is solved for stage D. But due to the limited time available, stages C1-C4 are left out of the scope of this research.

7.4 Methodology for the allocation rules

The first step to calculate the yearly environmental impact of stages A1-A3 and D, is determining the end of life scenario. The end of life scenarios explain which percentage of the materials will be reused, recycled, incinerated, or ends up at the landfill. In this research, two end of life scenarios are considered:

- A general end of life scenario is followed for most comparisons. For each material, a general end of life scenario is given in Appendix I.1.3 “General end of life scenarios”.
- In this research, it is investigated in what way the chance of reuse at the end of life can be enlarged. Specifically, this is performed for Alternative C where Design for Deconstruction is included. In Appendix I.1.4 “End of life scenarios with higher chance of reuse”, a new end of life scenario is drafted. This is based upon the Disassembly Index (DI) and calculated for the Base design, Alternative A, and Alternative C. For a DI equal to 1, the whole building can be demounted, and for a DI equal to 0, none of the building elements can be demounted.

The total environmental impact of stages A1-A3 can be derived from the EPD datasets directly. These EPDs are gathered via the One Click LCA tool from Bionova. From an investigation of several EPDs, it was found that EPD data can vary significantly. Due to time limitations, it is decided to investigate the most extreme EPD datasets. This means that for every construction material, the most environmentally

friendly and least environmentally friendly material is analysed. From the total environmental impact, the yearly environmental impact can be calculated. This is based upon the chance an element will be reused at the end of life. If an element will be reused, it is assumed that it can be used for the whole technical service life (TSL). This means that the environmental impact of these elements (EPD data from stages A1-A3) is divided by the TSL and the elements that will not be reused at the end of life are divided by the RSL. Together, the yearly environmental impact for stages A1-A3 is calculated. This procedure is further explained in Appendix Table I-15 and Table I-16. Here, the calculation steps and an example are given.

Next to reuse, materials can be recycled, incinerated, or end up as landfill at the end of life (stage D). In an EPD, often a combination of these options is considered in stage D. This is different for the glulam and CLT EPDs, where only incineration is expected as end of life scenario. This ensures that the environmental impact of stage D can be obtained from these EPDs directly. The calculation steps and an example of this stage are shown in Appendix Table I-20 and Table I-21.

For concrete and steel, the EPDs do consider a fixed combination of reuse, recycling, and landfilling as end of life scenario. In this research, these EPDs cannot be used for stage D, because a demountable design (Alternative C) is created to investigate the effects if the chance of reuse increases. Therefore, other end of life methods are investigated. From Appendix I.1 “Comparison between end of life methods”, it is concluded that the Product Environmental Footprint (PEF) method is a comprehensive end of life method. This method is explained in Appendix I.1.1 “Product Environmental Footprint (PEF) methodology”. Based upon the PEF methodology, the rules to set up EPDs were updated (EN 15804:2012+A2:2019), which resulted in specific end of life formulas as well (Seyed Shahabaldin, 2020). In this research, these end of life formulas are compared to the other methods as well, from which the results are given in Table I-2 in Appendix I.1. It can be concluded that the updated EPD rules provide a suitable method to allocate end of life processes. As EPDs following the updated rules EN 15804:2012+A2:2019 are barely found, this method is used as follows:

- Recycling

The total bonus for material recycling is calculated with the end of life formula of EN 15804:2012+A2:2019 (eq. I-7 given in Appendix I.1.2 “End of life formulas in EN 15804:2012+A2:2019”). Also for stage D, the yearly bonus is calculated. For the elements that will be reused at the end of life, recycling is still possible and thus considered in the calculation by dividing the recycling bonus by the TSL. Some elements will be recycled directly. Then, the recycling bonus is divided by the RSL.

- Landfilling

In case an element ends up in the landfill, no bonus is assigned to these materials.

The procedure for the calculation of stage D for the steel and concrete elements is given in Appendix Table I-17 and Table I-18. Here, also an example calculation is given. This is followed by Appendix Table I-19, where the yearly environmental impact calculation for stages A1-A3 and D are combined.

7.5 Quantifying the materials in the system

To quantify the materials in the system, two steps must be performed. First, for each design alternative, the total amount of materials must be calculated. This is already done in chapter 6.6 “Overview of design alternatives”. Second, the environmental impact data is gathered. In Appendix H “Environmental data”, each EPD is first explained. This is followed by the calculation of the total shadow price for stages A1-A3 and stage D for the timber EPDs. The calculation steps and an example calculation for stages A1-A3 and D are given in Appendix I.2 “Procedure and example calculation of the environmental impact”.

In the timber EPDs, a distinction is made between biogenic carbon and fossil carbon in the production stage (Stages A1-A3). The biogenic carbon amount refers to the CO₂ that is sequestered in the timber and the fossil carbon refers to the CO₂ that is released into the atmosphere in the production process. At the end of life stage (Stage C), the biogenic carbon is also released back into the atmosphere. Stage C is excluded in this research, so to make a fair comparison with the other materials, only the fossil carbon is considered. The advantage of the carbon being stored in the timber building is an extra advantage, yet not considered in this research.

7.6 Conclusion

In this chapter, research question 4 “*How can the environmental impact of a distribution centre’s load-bearing structure be quantified in a comprehensive way?*” is answered. In the following paragraphs, the answer to this research question is given.

To determine the environmental impact, it is decided to follow the Life Cycle Assessment (LCA) method. With this method, European Product Declarations (EPDs) are created. From these EPDs, data for the product stage (A1-A3) is gathered. To quantify the environmental impact in a comprehensive way, also the benefits and loads due to the end of life scenario are included (stage D). In this way, the current and future impact is included in the environmental impact calculation. Data of stage D in EPDs is based upon a general framework, so therefore other methods are examined. From this examination, the method from the updated EN 15804:2012+A2:2019 is applied. This leads to the calculation of the yearly environmental impact for different design alternatives (given in a shadow price (in euros) per year). This is done separately for the main load-bearing structure and the mezzanine floor load-bearing structure.

Comparing the LCA calculation for this research to the common way to perform an LCA, some remarks must be made. As acknowledged in chapter 2.1 “Problem definition”, normal assessment methods do not assess the environmental impact comprehensively, as they do not consider the end of life of a building. In a regular LCA, only one general end of life scenario is considered. Furthermore, the yearly environmental impact of elements to be reused is divided over the RSL, instead of the TSL. This shows that, based upon the regular LCA method, a designer does not become aware of the advantages of reusing elements. This is a pity, because buildings are usually not used for their total technical service life and it is possible for a designer to optimise the residual value of elements. By making the end of life scenario an important part of the LCA calculation, a designer can assess whether reusing elements is indeed a feasible end of life scenario and how these end of life scenarios can become true.

7.6.1 Flow chart of the calculation steps

In the previous paragraphs, the calculation steps were explained and for specific calculations, a reference was made to the Appendices. These explanations are combined in a flow chart. This flow chart is made for structural engineers that want to calculate the yearly environmental impact of a design. First, an overview of all the steps that are performed is given in Figure 7-4. On the following pages, the specific calculation steps for Stages A1-A3 (the burdens) and Stage D (the bonus) are given.

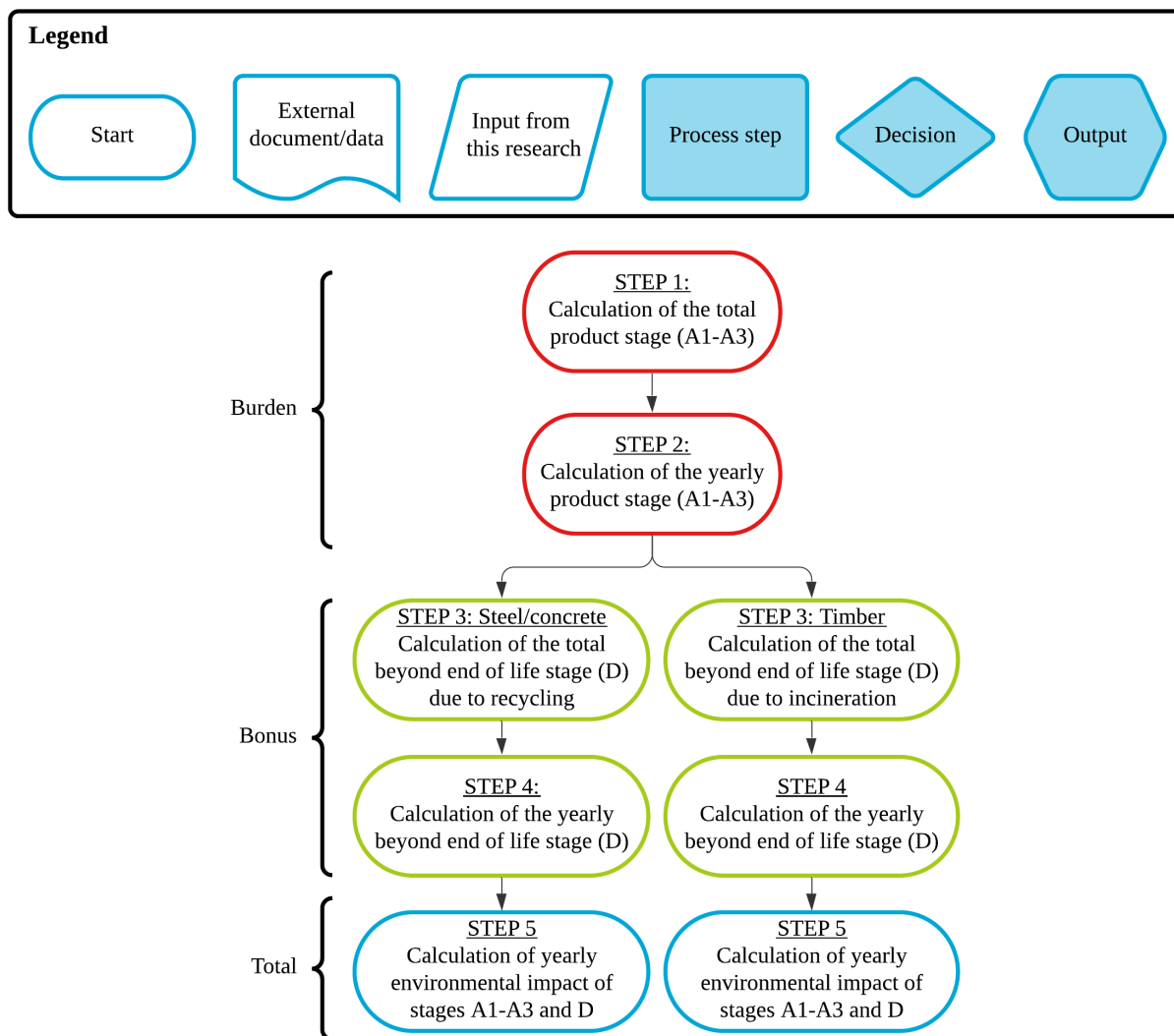


Figure 7-4: Overview of the flow chart to calculate the yearly environmental impact of stages A1-A3 and D

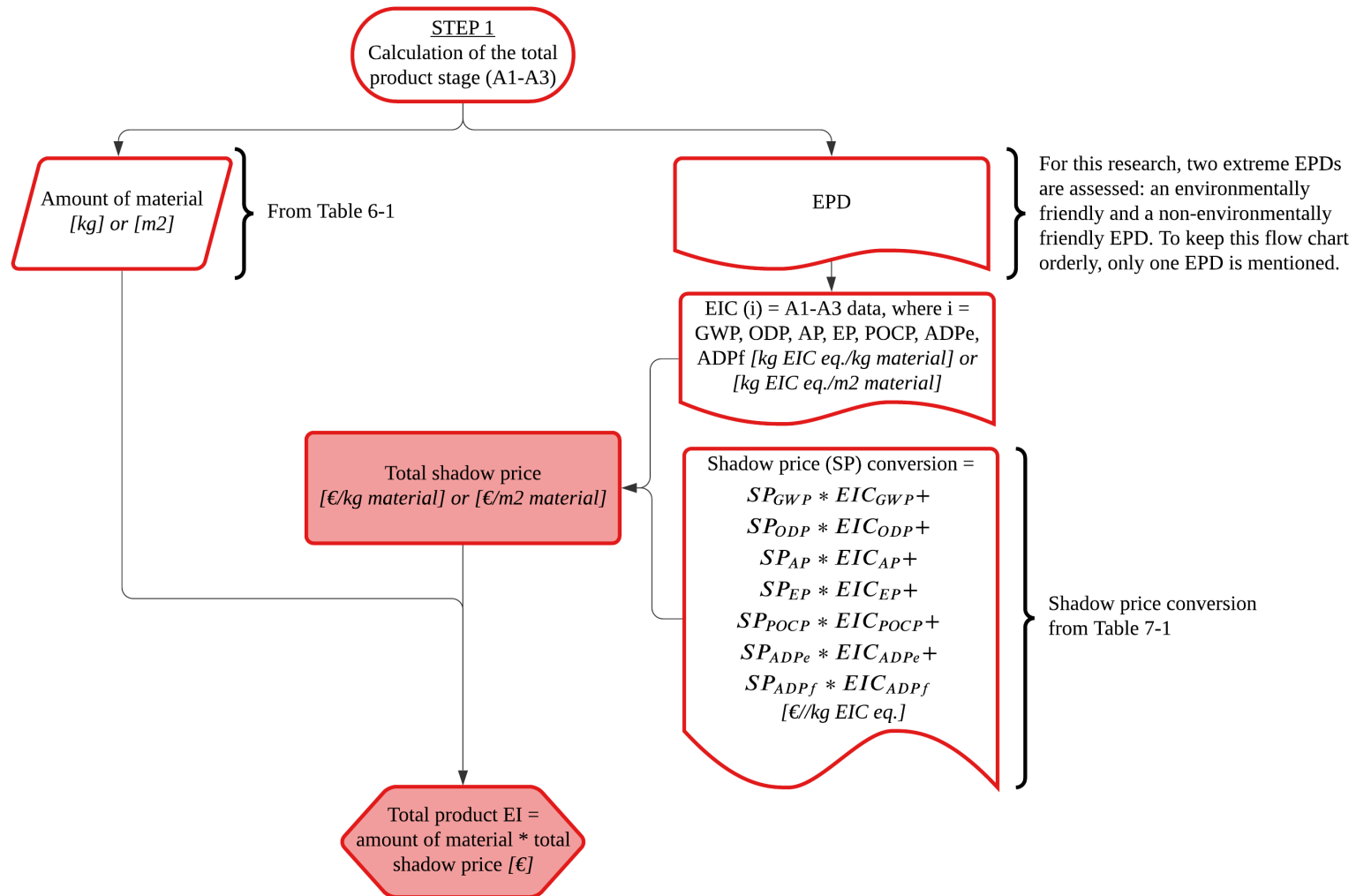


Figure 7-5: Step 1 of the environmental impact calculation (Stage A1-A3)

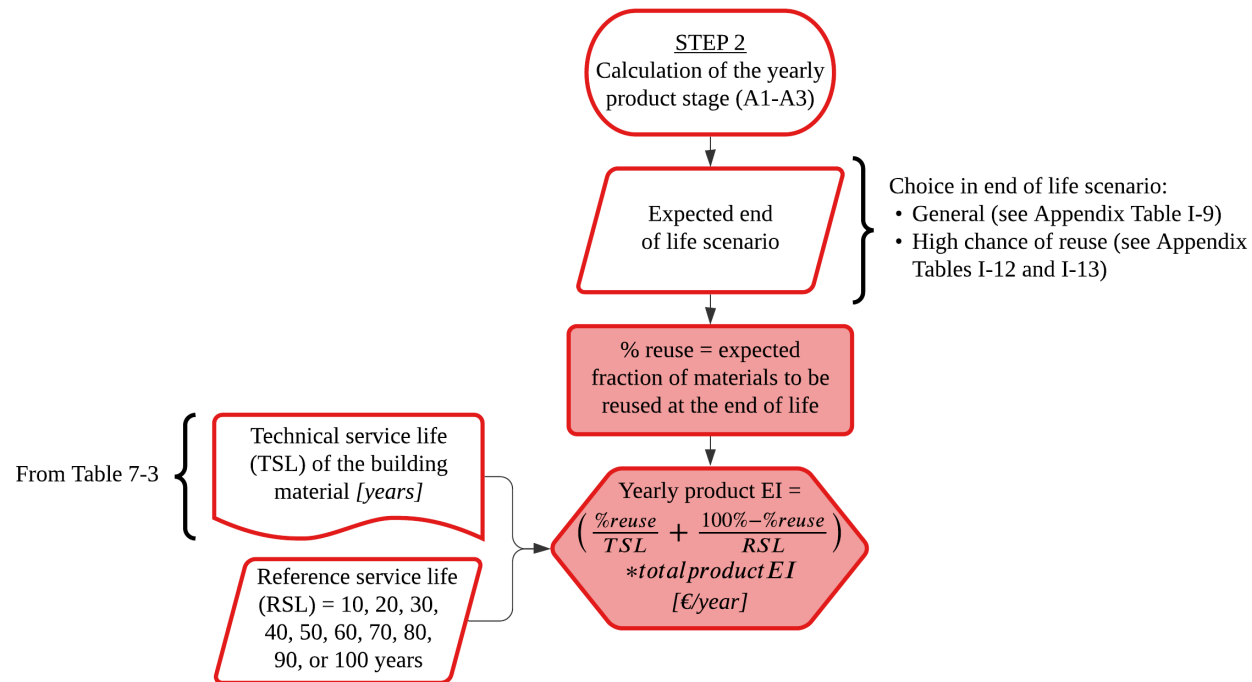


Figure 7-6: Step 2 of the environmental impact calculation (Stage A1-A3)

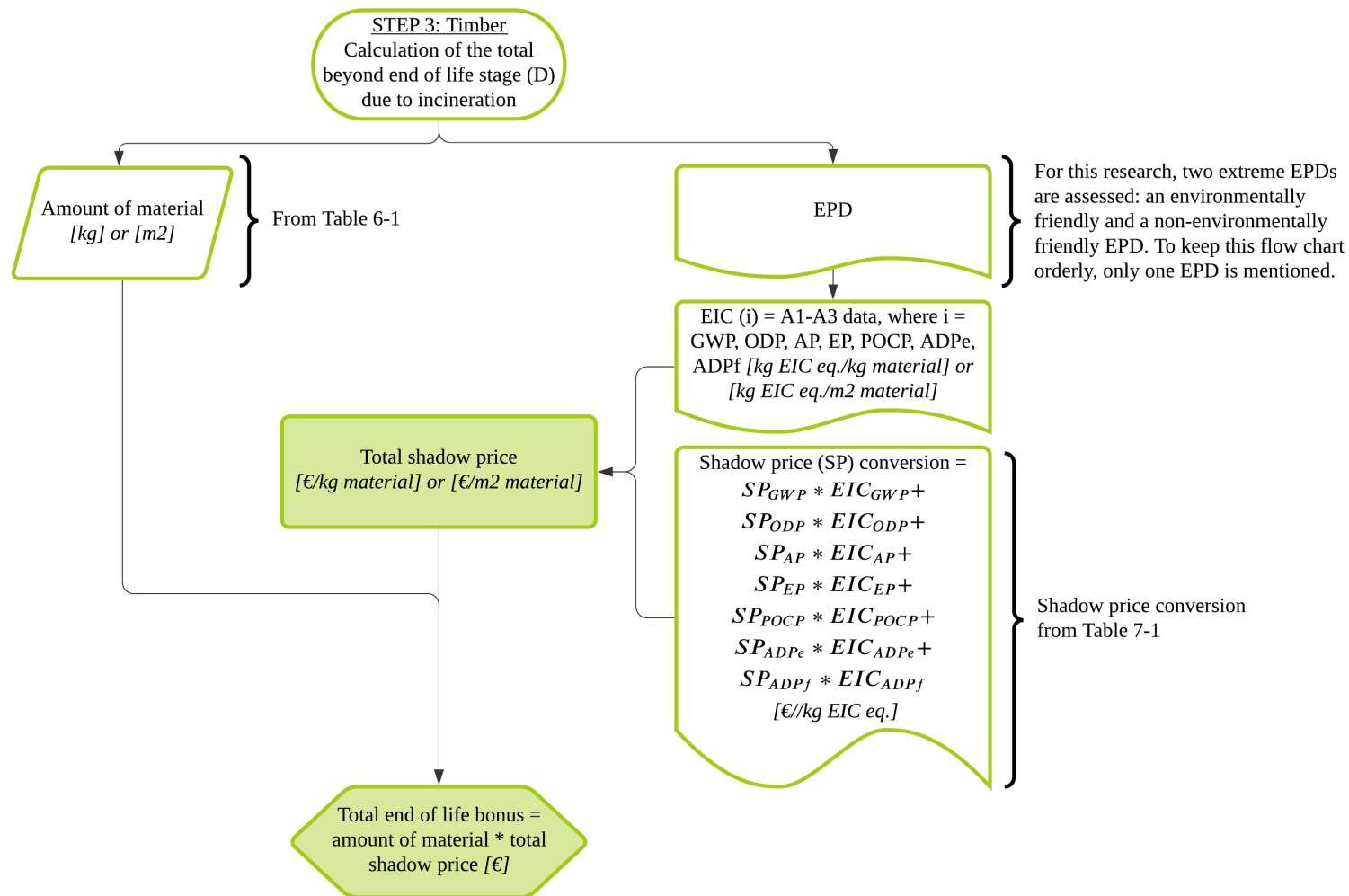


Figure 7-7: Step 3 of the environmental impact calculation (Stage D, for timber)

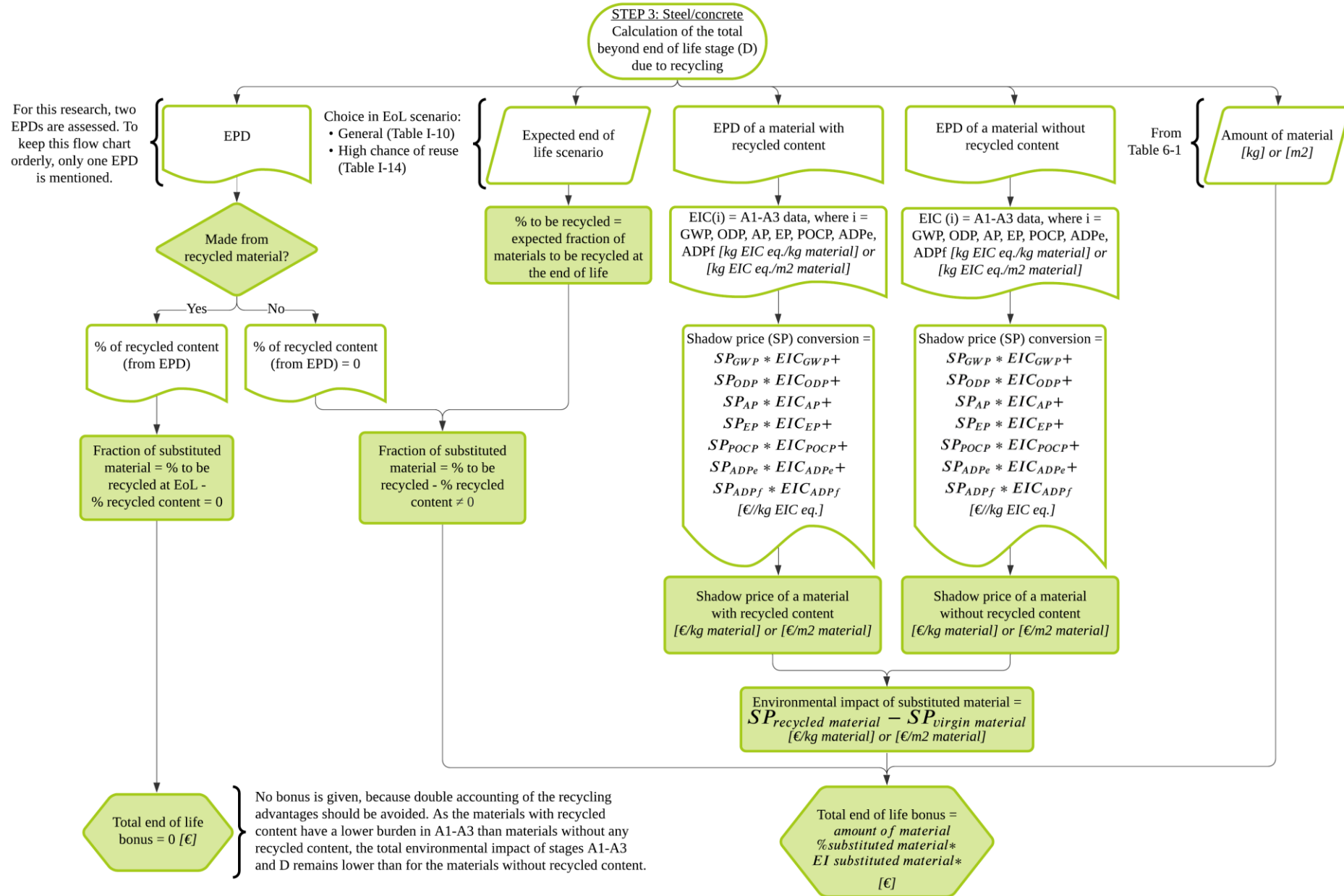


Figure 7-8: Step 3 of the environmental impact calculation (Stage D, for steel and concrete)

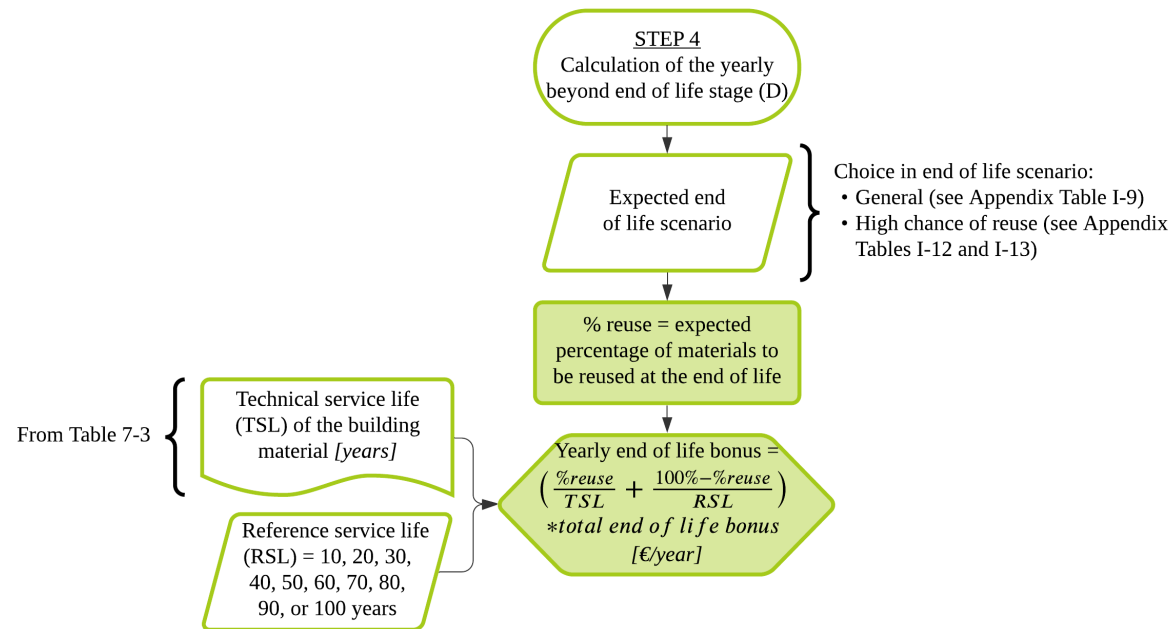


Figure 7-9: Step 4 of the environmental impact calculation (Stage D)

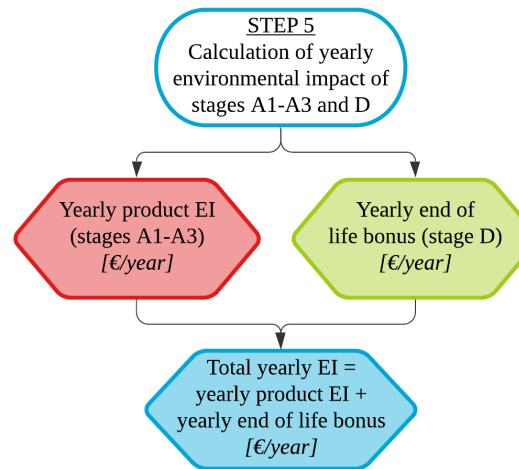


Figure 7-10: Step 5 of the environmental impact calculation (Stages A1-A3 and D)

8 Environmental impact calculation results

In this chapter, research question 5 “*Which of the design alternatives that are set up for this research results in the lowest yearly environmental impact?*” is answered. To answer this question in a useful way, the comparisons as explained in chapter 5 “Setup of design alternatives” are analysed. For each comparison, an explanation is given for stages A1-A3 and D and some insights are given if stage D is kept outside the scope.

The yearly environmental impact is calculated for each design alternative. For the case study, the yearly environmental impact is calculated for an RSL of 10 or 20 years. However, it is aimed to reduce the environmental impact of the case study, and if materials are used longer, the yearly environmental impact also reduces. Therefore, in this research also longer periods are investigated with a maximum ESL equal to the TSL.

In this research, different end of life scenarios are considered. It must be noted that this influences the results significantly. This means that if an alternative is based upon the end of life scenario including the Disassembly Index (DI) (Appendix I.1.4 “End of life scenarios with higher chance of reuse”), instead of the general end of life scenario (Appendix I.1.3 “General end of life scenarios”), this is explained by mentioning EoL with DI behind the alternative’s name.

8.1 Research question 3a: Optimise design for its initial material use

8.1.1 Comparison 1: Determining the effect of the amount of material on the environmental impact

For this comparison, the main load-bearing structures of the Base design (a sway structure) and Alternative A (a non-sway structure) are compared based on the amount of material needed. From 6.6 “Overview of design alternatives”, it is calculated that Alternative A requires 4.7% less material. Both load-bearing structure designs are made from steel only, so this conclusion also holds for the environmental impact of stages A1-A3. It is assumed that the end of life scenario for both designs is the same, so the same conclusion holds for the environmental impact of stages A1-A3 and D as well. The results of the total environmental impact are given in Appendix J.1.2.1 “Sensitivity of the mezzanine floor”.

8.1.2 Comparison 2: Determining the effect of the type of material on the environmental impact

For the comparison between Alternative A (steel non-sway structure) and Alternative B (timber non-sway structure), the main load-bearing structure and the mezzanine load-bearing structure are both analysed.

For the main load-bearing structure, it can be concluded that for the same RSL, the timber alternative has a lower impact than the steel alternative for stages A1-A3 and stage D. This can be seen in Figure 8-1 on the next page.

Furthermore, from Figure 8-1, it is noted that the difference between the lowest environmental impact and the highest environmental impact of Alternative A is a lot smaller than for Alternative B. This is due to the fact that only the least environmentally friendly steel receives a bonus for recycling in stage D. The most environmentally friendly steel is already made from 100% recycled steel and double accounting of the advantages of recycling is thus avoided.

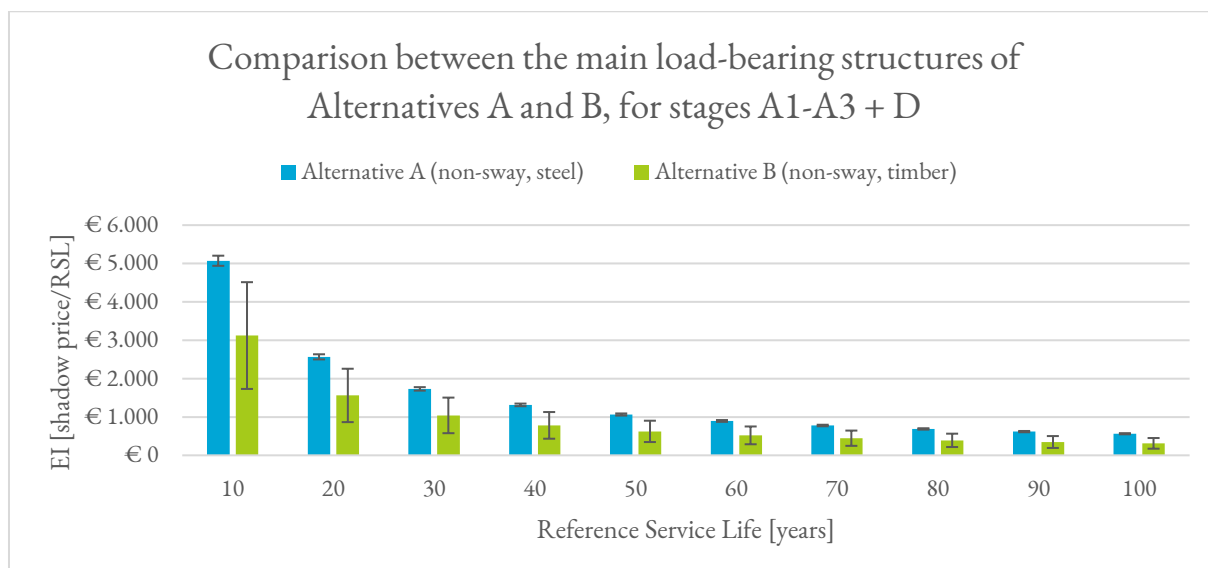


Figure 8-1: Yearly environmental impact of the main load-bearing structures of Alternative A and B (stages A1-A3+D), where the general end of life scenario is used

To investigate the sensitivity of the results, the main load-bearing structure is also considered for stages A1-A3 only. This can be seen in Appendix Figure J-3. It is found that if stage D is excluded, the least environmentally friendly timber has a slightly higher impact than the most environmentally friendly steel (made from 100% recycled steel). If this chance appears to be lower, the timber alternative has a lower impact, resulting in the same conclusion as for stages A1-A3 and D.

In Figure 8-2, the comparison for the mezzanine load-bearing structure is made. For the mezzanine floor, it can be concluded that until 75 years, the most environmentally friendly steel has a higher impact than the most environmentally friendly timber, but a lower impact than the least environmentally friendly timber. After 75 years, it is expected that a new mezzanine floor is needed, because the TSL of the timber floor will be reached (as explained in Table 7-3). This results in a higher environmental impact than for the steel alternative.

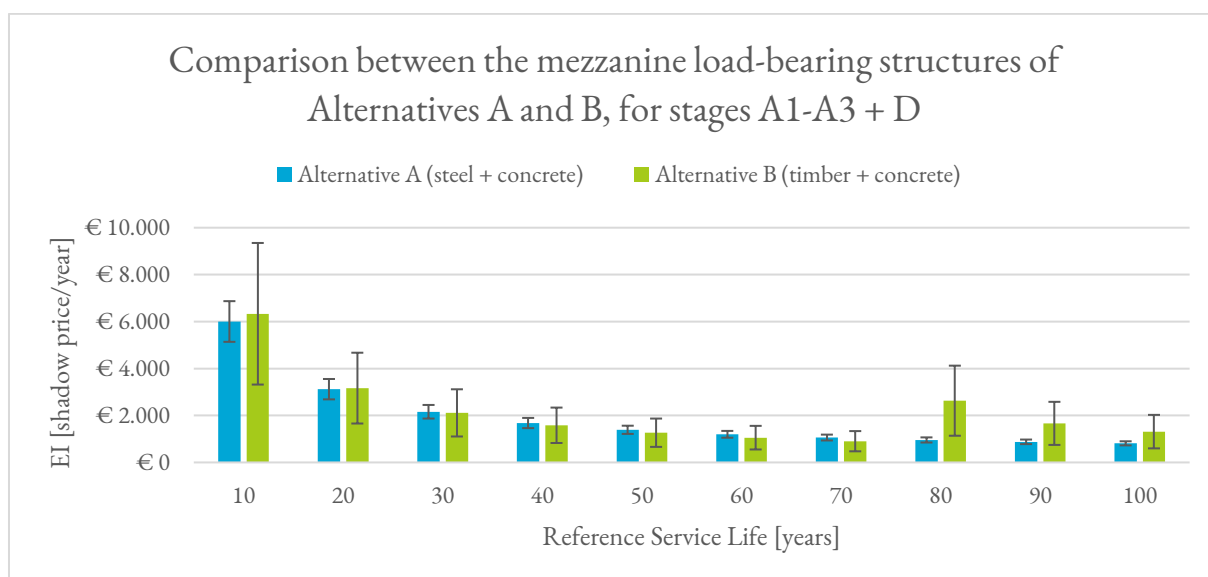


Figure 8-2: Yearly environmental impact of the mezzanine structure of Alternative A and B (stages A1-A3+D), where the general end of life scenario is used

In addition, the sensitivity of stage D for the mezzanine floor is considered. In Figure 8-2, it can be seen that for every RSL, the least environmentally friendly materials of Alternative B have a higher impact than the materials of Alternative A, this is caused by two factors. Firstly, because the timber beams in the mezzanine floor structure are not designed in an effective way. Due to the height limitations, the timber is relatively thick and low, resulting in more materials needed compared to a timber beam without height limitations. Secondly, it is found that for a short RSL, the steel-concrete floor has the advantage of reuse, which is more effective than incinerating the timber after a short RSL. This comparison is also considered for stages A1-A3 only (shown in Appendix Figure J-4), which results in a bit different conclusion: until 75 years, the least environmentally friendly timber has a lower impact than the least environmentally friendly steel. Also, a change in stage D is considered in the Appendix. From Appendix Figure J-5, it is found that even if the steel is not being reused, the same conclusion holds. And the recycling bonus, which is set up for this research, is also investigated: if this bonus is reduced with 10%, a slight change is found: for an RSL of 50 or 60 years, the least environmentally friendly timber has a lower impact than the least environmentally friendly steel and concrete.

To conclude, EN 15804:2012+A2:2019 states that the effect of temporary carbon storage shall not be included in the calculation of the Global Warming Potential. Therefore, this is not considered in the analysis. However, if materials are used for a long period of time, the carbon storage in the timber is considered an additional advantage compared to steel and concrete elements. The following table gives insight in the biogenic carbon influence by showing the total biogenic carbon content of Alternative B. This is based upon the total mass of Alternative B and the EPD data given in Table H-13 and Table H-16. This shows that if timber is used for a long time, this sequestration ensures that timber is more advantageous than expected.

Table 8-1: Total shadow costs for the biogenic carbon storage of Alternative B

Element	Average of two EPDs (the results are rounded)
Glulam main load-bearing structure	– € 151 000
Glulam mezzanine floor elements	– € 173 000
CLT mezzanine floor	– € 85 000

8.2 Research question 3b: Optimise design for residual value

8.2.1 Comparison 3: Determining the relationship between the reuse of a traditional design and a demountable design

For the comparison to determine the relation between reusing a traditional design ('Base design') and a demountable design ('Alternative C'). If these main load-bearing structures are compared based on material use, the Base design has a lower impact, because it requires 18.6% less material than for Alternative C. For this comparison, it is more interesting to investigate the impact of reuse at the end of life. To do so, the end of life scenarios with a higher chance of reuse are considered. This is explained in Appendix I.1.4 "End of life scenarios with higher chance of reuse". From this explanation, it becomes clear that the chance of reuse for the Base design is lower than for Alternative C.

The yearly environmental impact of stages A1-A3 and D is shown in the following figure. From this figure, it can be concluded that up to an RSL of 60 years, the demountable design (Alternative C) has a lower environmental impact. This conclusion also holds for a scenario where stage D is kept outside the scope (shown in Appendix Figure J-7).

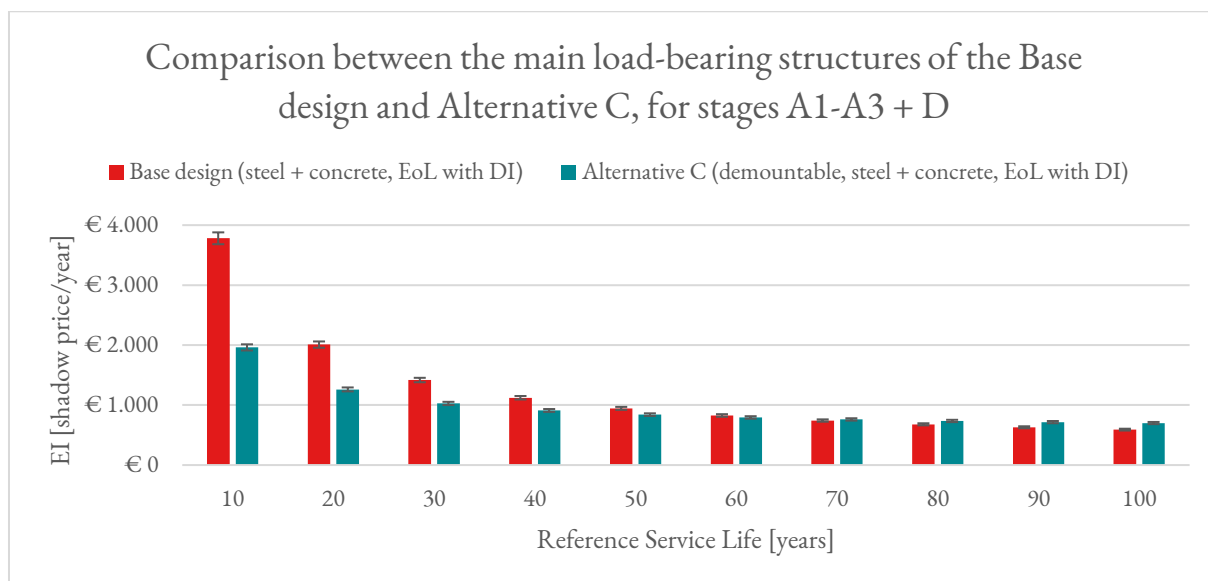


Figure 8-3: Yearly environmental impact of the main load-bearing structure of the Base design and Alternative C for the end of life scenario based upon the Disassembly Index (stages A1-A3+D)

The mezzanine floor structure is analysed as well, where a distinction is made between the total mezzanine floor structure (including the floor, floor beams, and floor columns) and the mezzanine floor on its own.

The yearly impact of the total mezzanine floor structure is shown in the following figure. It is concluded that the yearly environmental impact of Alternative C is lower than the Base design if the most environmentally friendly materials are chosen. This is mainly because fewer floor beams are necessary for the design of Alternative C. It can also be noted that after an RSL of 50 years, the impact for the least environmentally friendly material of the Base design reduces. This reduction is caused by the recycling potential of the steel beams. This advantage is not found if stage D is excluded from the scope. Then, the least environmentally friendly materials of Alternative C remain below the impact of the least environmentally friendly materials of the Base design.

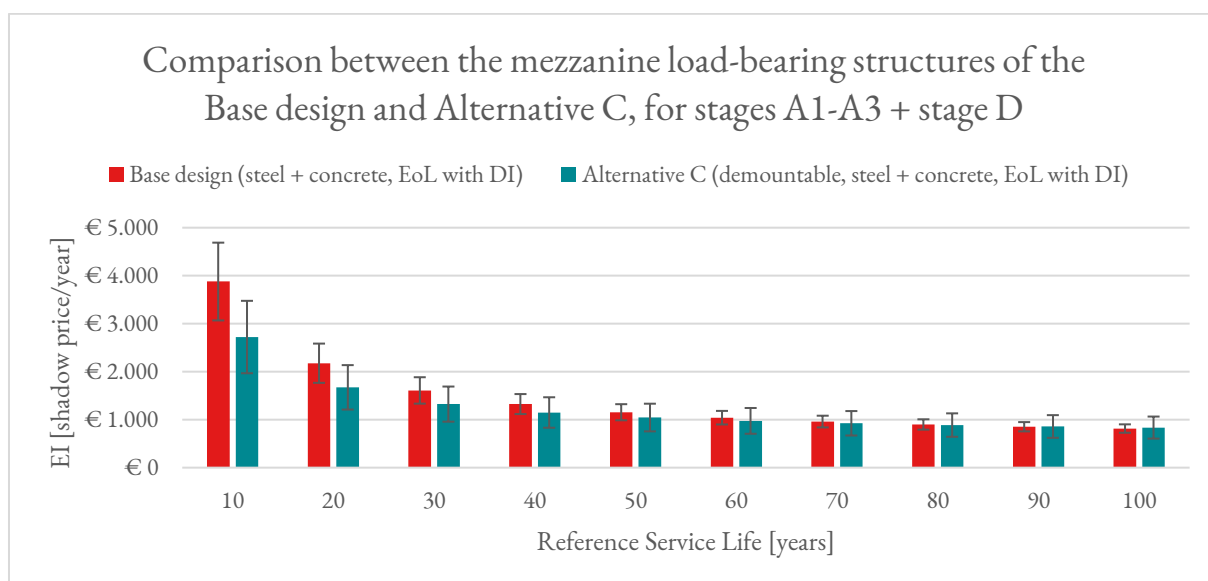


Figure 8-4: Yearly environmental impact of the mezzanine load-bearing structure of the Base design and Alternative C for the end of life scenario based upon the Disassembly Index (stages A1-A3+D)

Considering the mezzanine floor on its own, it can be concluded that the manufacturer choice is very important. The least environmentally friendly materials of Alternative C have a higher impact than the Base design, but looking at the most environmentally friendly EPDs, Alternative C has a lower impact. To visualise this conclusion, Appendix Figure J-8 is made. It is important to mention that there was only one EPD available for the steel deck, which explains the less extreme values. Considering reuse as well, a similar result is found as displayed in Figure 8-4. However, two differences must be explained. For the mezzanine floor, only up to an RSL of 30 years, the least environmentally friendly materials of Alternative C have a lower impact than the materials of the Base design. Another difference is found: if stage D is excluded from the scope, this conclusion also holds up to an RSL of 40 years. This shows that for Alternative C, the higher chance of reuse does not weigh up against the higher environmental impact of the materials themselves. This is a different conclusion than for the total mezzanine load-bearing structure.

To find out what the effect is of the higher chance of reuse (based upon the Disassembly Index), the difference between the general end of life scenario and the end of life scenario with higher chance of reuse (with DI) are compared in Appendix Figure J-9. It is found that for a short RSL, the difference between the two scenarios is very large (40.8% for an RSL of 10 years). The longer the materials are used, the less influence the two scenarios have: at an RSL of 90 years, the difference is only 3%. For the mezzanine floor, a maximum reduction of 35.4% is found. Considering both end of life scenarios for Alternative A as well, even a larger reduction is found and is visualised in the following figure. As this is a significant reduction without a lot of effort in the design process, this is an important insight. This reduction is larger, because for Alternative A, simple connections are used that are easy to disassemble at the end of life. These examples show that aiming to reuse as many elements as possible will have a large influence on reducing the environmental impact.

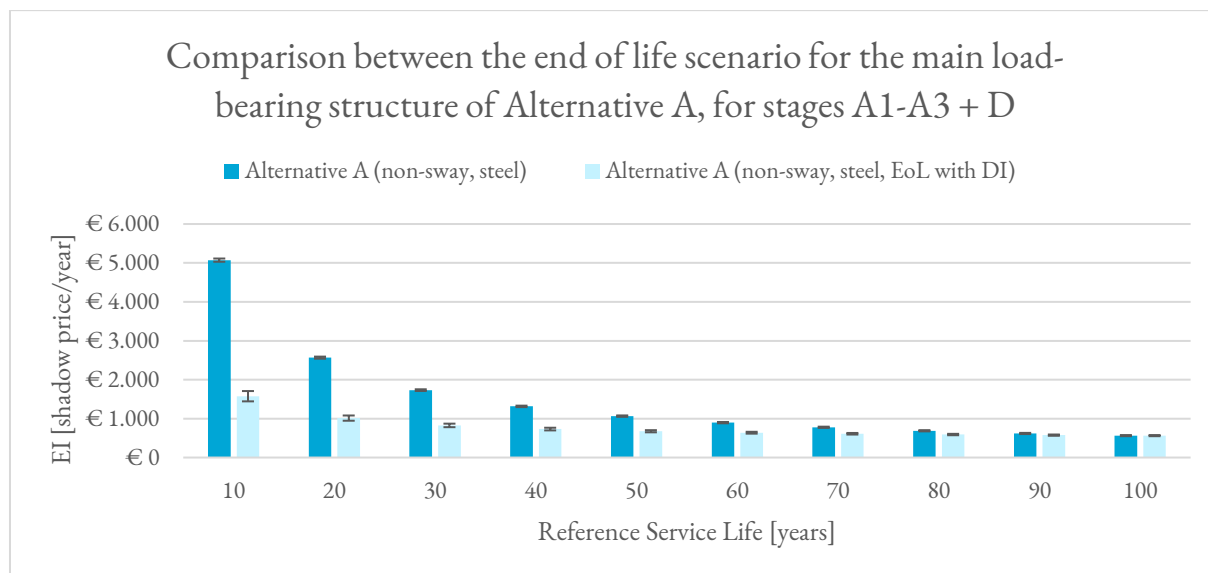


Figure 8-5: Yearly environmental impact of the main load-bearing structure of Alternative A if the general end of life scenario or the end of life scenario with a higher chance of reuse (with the Disassembly Index) is used

8.3 Research question 3c: Optimise design for multiple functions

8.3.1 Comparison 4 and 5: Determining the relationship between the environmental impact of service life extension and extra material use for another function

The main load-bearing structure of Alternative A is compared to Alternatives D1 and D2. No additional material is needed to change Alternative A into Alternative D1, but for Alternative D2, 4.1% extra steel is needed. As the same materials are used, this leads to an environmental impact increase of 4.1%. This is visualised in the following figure.

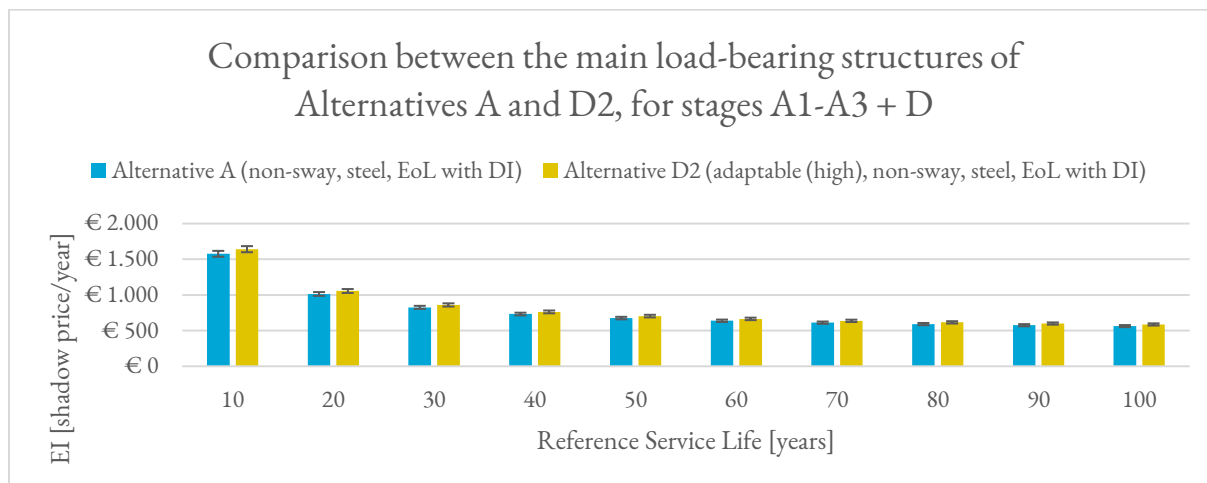


Figure 8-6: Yearly environmental impact of the main load-bearing structures of Alternatives A and D2 (stages A1-A3+D)

For the mezzanine floor, the same structure as for Alternative C is used, namely a demountable hollow core floor. To make a fair comparison, the mezzanine floors are also compared to that of Alternative C instead of Alternative A. This comparison is shown in the following figure, which shows that more material is needed if the function changes. If the same RSL is expected, Alternative C will have the lowest environmental impact. Based on this comparison, the owner of the building can estimate whether this overcapacity should be incorporated in the design.

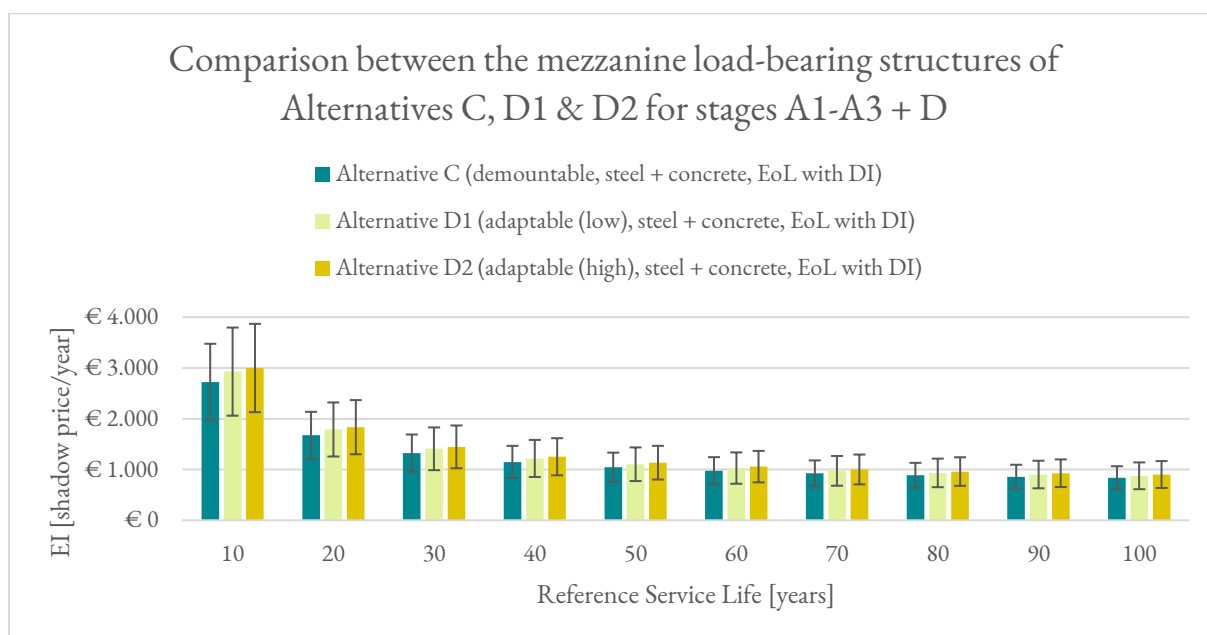


Figure 8-7: Comparison between the mezzanine structure of Alternatives C, D1, and D2 (stages A1-A3+D)

To quantify the differences as well, the following remarks are made. For stages A1-A3 and D, the environmental impact for the least environmentally friendly materials of Alternative D1 is between 7.1% and 9.2% higher than for Alternative C. For the most environmentally friendly materials, this lies between 1.2% and 4.7%. For the comparison between Alternative D2 and Alternative C, the least environmentally friendly materials have between 8.7% and 10.1% extra, and for the most environmentally friendly materials between 5.0% and 7.6% extra.

8.4 Main findings

To provide insight in the current shadow costs per alternative, the total environmental impact is calculated for stages A1-A3. For the main load-bearing structure, the results are found in Table 8-2, and for the mezzanine load-bearing structure in Table 8-3. From these tables, it can be concluded that if only the product environmental impact is considered, the timber alternative (Alternative B) has the lowest environmental impact.

Table 8-2: Total shadow price of the main load-bearing structure of each design alternative for A1-A3

	Base design	Alternative A	Alternative B	Alternative C	Alternative D1	Alternative D2
Average	€ 195.000	€ 186.000	€ 40.000	€ 231.000	€ 186.000	€ 193.000
Low	€ 58.000	€ 55.000	€ 28.000	€ 68.000	€ 55.000	€ 57.000
High	€ 332.000	€ 316.000	€ 51.000	€ 394.000	€ 316.000	€ 329.000

Table 8-3: Total shadow price of the mezzanine load-bearing structure of each design alternative for A1-A3

	Base design	Alternative A	Alternative B	Alternative C	Alternative D1	Alternative D2
Average	€ 166.000	€ 166.000	€ 83.000	€ 141.000	€ 151.000	€ 159.000
Low	€ 79.000	€ 79.000	€ 57.000	€ 62.000	€ 68.000	€ 71.000
High	€ 253.000	€ 253.000	€ 109.000	€ 220.000	€ 233.000	€ 247.000

The tables show that the environmental impact depends highly upon how the materials are manufactured. Mainly for the material steel, large differences in EPD datasets are found. Considering stages A1-A3, the environmental impact can increase with 5.8 times per kilogram steel. This is followed by the hollow core slab (2.4x), CLT (2.3x), in situ concrete (1.8x), and glulam (1.8x). Less significant increases are found if stage D is included in the analysis.

In addition, from the comparisons, the following can be said:

- In this research, changing the steel sway structure (Base design) into a steel non-sway structure (Alternative A) leads to an environmental impact reduction of 4.7%.
- The choice of timber in the main load-bearing structure (Alternative B) results in a significantly lower environmental impact than the steel alternative (Alternative A) with a general end of life scenario. For stages A1-A3 and D, a reduction between 65% and 68% is possible for environmentally friendly materials and for less environmentally friendly materials, a reduction between 13% and 22% is expected (depending upon the RSL). T
- Changing the mezzanine floor structure from a steel-concrete floor (Alternative A) into a timber and concrete alternative (Alternative B) results in a reduction or increase of the environmental impact in stages A1-A3 and D, depending upon the materials chosen. For the most environmentally friendly materials, the impact reduces significantly until 75 years (reduction

between 35% and 50%, depending upon the RSL). Considering these stages for the materials with a high impact, the steel-concrete floor has the lowest environmental impact (reduction between 13% and 37%).

- The main load-bearing structure of the demountable design (Alternative C) has a lower environmental impact than the Base design for an RSL up to 60 years (for stages A1-A3 and D, with the end of life scenario based upon the DI).
- Changing the mezzanine floor structure from a composite steel deck floor (Base design) to a hollow core floor (Alternative C), changes the floor beam layout as well, resulting in a lower environmental impact if the most environmentally friendly materials are chosen. Considering the floors on their own, the choice in EPD is very important.
- By comparing the Base design for the different end of life scenarios (general and based upon the DI), it is concluded that if reuse is an important aspect at the end of life, the environmental impact can be reduced significantly. An even higher reduction is found for the comparison between Alternative A for a general end of life scenario and an end of life scenario based upon the DI.
- Investigating overcapacity of the mezzanine floor for an office or retail function (Alternative D1) leads to an additional environmental impact for the mezzanine floor structure only. Only if the RSL is expected to increase due to this overcapacity, this leads to a lower impact. This conclusion also holds for the design alternative with overcapacity for an industrial storage function on the mezzanine floor (Alternative D2). Here, not only an increase in environmental impact is found for the mezzanine floor, but also for the main load-bearing structure.

8.4.1 Conclusion

To answer research question 5 “Which of the design alternatives that are set up for this research results in the lowest yearly environmental impact?”, the results of the comparisons are combined. This is done for the main load-bearing structure and for the mezzanine load-bearing structure.

For the main load-bearing structure, the lowest environmental impact results are found for the steel non-sway structure with a high chance of reuse at the end of life (Alternative A (with DI), shown in Figure 8-5) and the timber alternative (Alternative B, shown in Figure 8-1). These results are combined in the following figure.

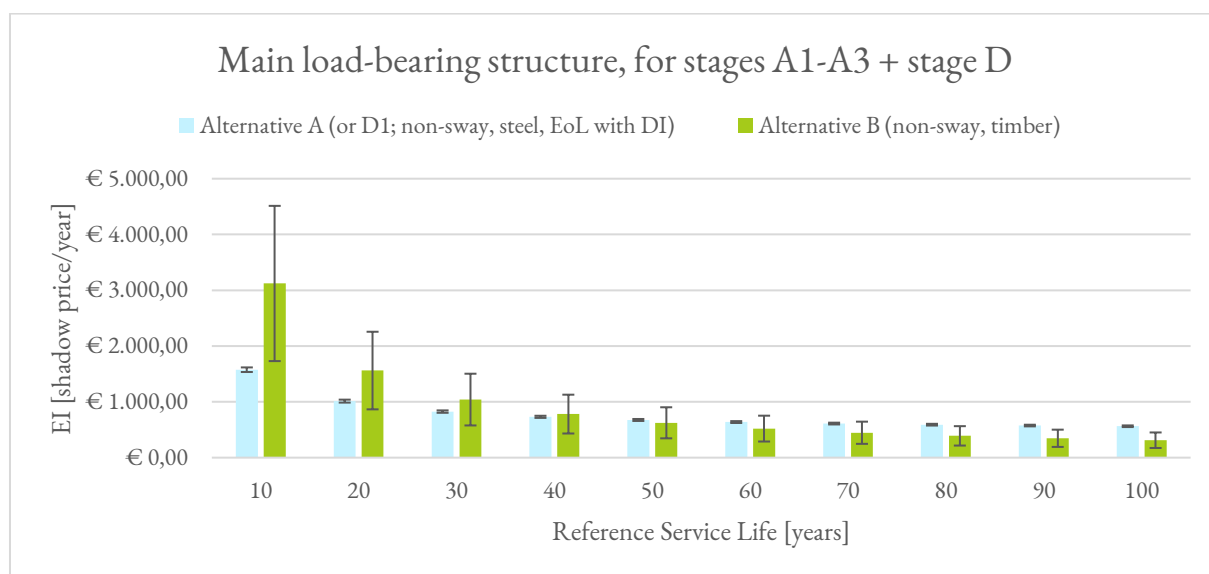


Figure 8-8: Yearly environmental impact of the main load-bearing structures of Alternative A (or Alternative D1; calculated with an end of life scenario with a higher chance of reuse) and Alternative B

From Figure 8-8, it can be concluded that for a reference service life of 10 years, Alternative A has the lowest yearly environmental impact. For a longer reference service life, the most environmentally friendly timber should be chosen. For an RSL of 80 years or longer, also the least environmentally friendly timber has a lower yearly impact than the steel alternative. From the comparisons, it becomes clear that using materials for a longer RSL, the yearly environmental impact reduces quite significantly. This shows the potential of the adaptable design Alternatives D1 and D2. For both alternatives, it is found that if the RSL becomes longer due to its adaptivity, it can become interesting to choose for these designs instead of Alternative A or B. Though, if the timber design (Alternative B) is used for an RSL of 30 years or longer, the yearly environmental impact remains lower than the yearly environmental impact of the steel Alternatives D1 and D2 (Alternative D1). The same conclusion is found for Alternative D1 as for Alternative D2, because only a slight increase of materials is needed for Alternative D2.

For the mezzanine load-bearing structure, the lowest yearly environmental impact results are found for the timber and concrete floor (Alternative B, shown in Figure 8-2) and the demountable concrete floor with steel beams, with a high chance of reuse at the end of life (Alternative C (with DI), shown in Figure 8-4). These results are combined in the following figure. This figure shows that if the most environmentally friendly materials are used, the demountable mezzanine structure (Alternative C) has the lowest yearly environmental impact up to an RSL of 30 years. For a longer RSL, the environmentally friendly timber and concrete of Alternative B result in the lowest yearly impact. At an RSL of 75 years, it is expected that a new timber floor must be installed, so the yearly environmental impact increases significantly at this point. This conclusion changes a bit if an adaptable mezzanine floor structure results in a longer RSL. If the RSL becomes 10 years longer compared to the timber alternative (Alternative B), the yearly environmental impact of Alternative D1 is lowest up to an RSL of 50 years and up to an RSL of 40 years for the timber alternative. Implementing the overcapacity of Alternative D2 does not result in a reduction in yearly environmental impact.

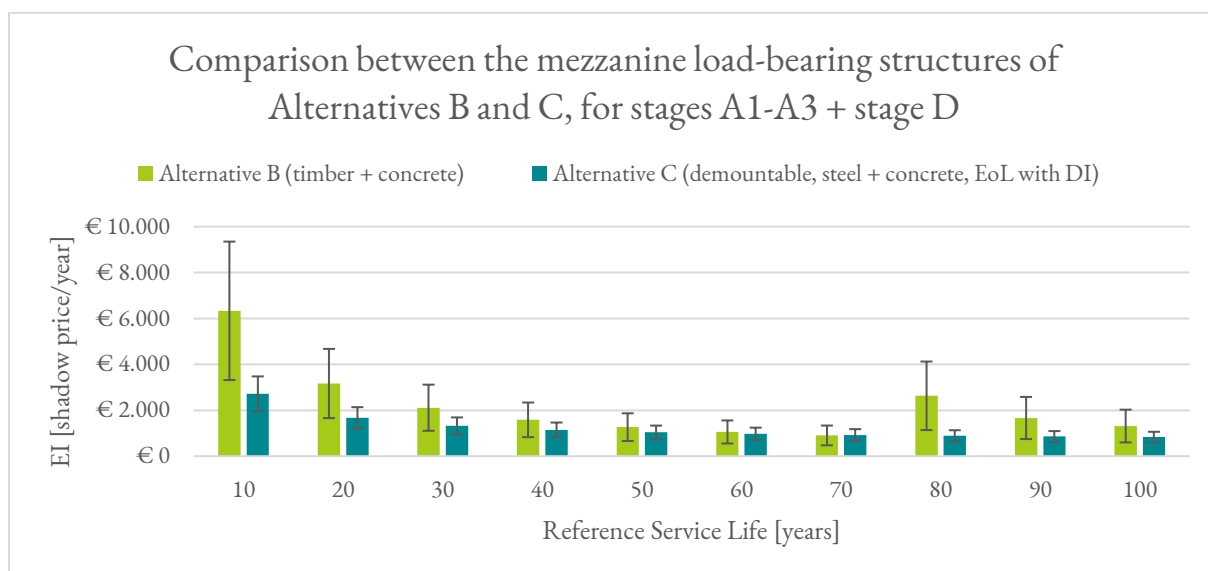


Figure 8-9: Yearly environmental impact of the mezzanine load-bearing structures of Alternatives B and C (stages A1-A3+D)

9 Discussion

In chapter 8, the results of the environmental impact calculation are given and discussed. These results are further elaborated on in this chapter. First, the results are discussed by explaining the results if assumptions change. The results are then compared to literature, followed by clarifying the limitations of the research, and by explaining the implications of the research. This chapter ends with recommendations for future research and for practice.

9.1 Discussion of results

Two end of life scenarios are investigated in this research: the general end of life scenario (explained in Appendix I.1.3) and the end of life scenario with a higher chance of reuse (explained in Appendix I.1.4). For both end of life scenarios, a bonus is given to virgin materials that are expected to be recycled at the end of life. This is called the environmental impact of substituted material. In Figure 9-1, it is shown how this impact is calculated. This impact is used as a bonus for stage D for steel and concrete (as explained in step 3 of the LCA flow chart, given in Figure 7-8). In this calculation, it is assumed that the shadow price of the recycled material ($SP_{recycled\ material}$) is made from the highest possible percentage of recycled content. This means that for steel, it is assumed that 100% recycled steel will be made in the recycling process and for concrete, it is assumed that concrete with 40% recycled content will be made in the recycling process. It is possible that at the end of life, the materials are not recycled or recycled into a material with lower recycled content. This shows that choosing a material based upon the advantage of stage D is risky, as the bonus of stage D can turn out lower than expected. Therefore, it should be aimed to choose the most environmentally friendly materials based upon the product stage. These materials will always have a lower environmental impact than less environmentally friendly variants.

$$\text{Environmental impact of substituted material} = SP_{recycled\ material} - SP_{virgin\ material}$$

[€/kg material] or [€/m² material]

Figure 9-1: Calculation of the environmental impact of substituted material, where SP = shadow price
This is part of the calculation of Step 3 given in Figure 7-8

For the end of life scenario with a higher chance of reuse, the Disassembly Index is used to calculate the chance of reuse. This is a theoretical method that is based upon the design phase only. Practical issues are thus not regarded. If the chance of reuse turns out to be lower than expected, the yearly environmental impact of Alternatives A, C, D1, and D2 with a high chance of reuse at the end of life increases. This means that it is possible that the yearly environmental impact of the timber design (Alternative B) is lower than the steel and concrete alternative (Alternative A) for any RSL.

In the environmental impact calculation method, it is assumed that if elements are reused at the end of life, they will be used for the total technical service life. If this assumption does not hold, the yearly environmental impact will increase significantly for the Alternatives A, C, D1, and D2 with an end of life scenario with a high chance of reuse. This means that the advantage of using timber (Alternative B) to reduce the environmental impact becomes even more clear.

In this research, it is assumed that steel and concrete can be reused, recycled, or disposed at the end of life, whereas timber is assumed to only be incinerated or disposed. This is based upon the general end of life scenarios given in Table I-9. Though, it is possible to reuse or recycle timber. If timber is reused or recycled, the yearly environmental impact can reduce, which may lead to the conclusion that also for a short RSL, the timber alternative leads to the lowest yearly environmental impact.

In the rules to set up an EPD is stated that the effect of temporary carbon storage in timber should not be included in the environmental impact calculation. This rule is included, because at the end of life, it is expected that the carbon is released back into the atmosphere. Though, if the timber is used for a long time, carbon sequestration is considered an additional measure to reduce the yearly environmental impact.

Together, this shows that most assumptions are made for the steel and concrete designs. It is possible that these assumptions become true, but to be sure this is the case at the end of life, it is important to include these expectations in a disassembly guide (as explained in chapter 4.1 “Design for Deconstruction (DfD)”).

9.2 Comparing the results to literature

The three strategies that are followed in this research are based upon three principles of the circular economy. The theory prioritizes which strategy is most effective in transitioning from a linear to a circular economy (see Figure 1-5): first manufacture and use products in a smarter way, then extend the lifespan of products and their parts, and finally minimise waste at the end of life. If this theory is followed, it should be found that Alternative A and B are most environmentally friendly (‘reduce’), then Alternative C (‘reuse’), and finally Alternatives D1 and D2 (‘repurpose’). This conclusion is not directly found in this research. Reducing the materials will reduce the direct environmental impact, but if materials are only used for a short period, the yearly environmental impact remains very high. So, it should be aimed to combine the strategies as much as possible.

From literature, it is found that timber has a low environmental impact compared to other materials. This conclusion is also found in this research for stages A1-A3. Considering stages A1-A3, the yearly environmental impact of a demountable steel and concrete structure with a high chance of reuse is lower for a short RSL. For a longer RSL, the timber alternative has the lowest yearly environmental impact. Furthermore, the timber industry points out that timber beams are most effective for high narrow cross sections (between 1:6 to 1:8 of the height). This conclusion is also found in this research by comparing the beam design of the mezzanine floor to the roof beams. For the mezzanine floor, there were height restrictions, which resulted in thicker cross sections compared to the timber roof beams, where slender cross sections were used. As a result, the timber main load-bearing structure has the lowest yearly environmental impact for an RSL of 20 years or longer, whereas for the mezzanine floor structure, this is true for an RSL of 30 years. From this comparison, it is concluded that if less efficient cross sections are used, the material amounts increase, resulting in a higher environmental impact as well. If height restrictions apply, the advantage of timber compared to steel beams reduce.

9.3 Limitations of the research

The foundation is excluded from this research. If the foundation is considered, this may lead to different results because of two main reasons. Firstly, for a lighter structure, less material is needed in the foundation, resulting in a lower environmental impact. Secondly, for the steel design alternatives, where some stiffness is designed for the column base connection, the foundation needs to be heavier than if a pinned connection is designed (as done for the timber structure (Alternative B)). The stiffness of the column base is defined as 50 MNm/rad. This is considered a lower boundary for a stiff connection and therefore used for an initial design phase. Increasing this stiffness will result in a reduction of materials above the ground, but also increases the materials needed for the foundation.

For the investigated case study, a dense sprinkler system with a low failure probability is incorporated in the design. This ensures that no additional fire safety measures have to be included in the structural designs. For another case study, it is likely that a less safe sprinkler system will be used. Then, other

measures are needed to protect the structure from fire. In Breunese & Maljaars (2015), several fire protection systems per material are discussed. Here, it is explained that for the steel elements, foams, blankets, intumescent paints, or coatings can be used to protect the steel from the heat. Furthermore, they state that concrete can be protected with boards or spray mortars, and timber can be protected with panels (such as mineral wool or plasterboard), intumescent coating or by impregnation. For timber, it is also possible to increase the cross sections to be safe for fire. With help of a fire model, it can be predicted which measures are needed to create a fire safe structure. Fire protection measures as sprinklers and protection both influence the environmental impact of a building. This shows that only considering the structural design of a building provides a limited view on the total building environmental impact.

In the environmental impact calculation of this research, the transportation between the manufacturing plants and the building site, the installation processes, and the demolishing processes are not investigated. These processes do influence the environmental impact, so the results of this research should be assessed critically. An example where these differences are found is the comparison between a cast in situ floor and a prefabricated floor. Prefabricated elements require other, often heavier, equipment than if in situ elements are used. This can increase the environmental impact of the hollow core slabs used for Alternatives C, D1, and D2.

Another issue in this research is the lack of available EPD data. Many EPDs are available via the One Click LCA tool, but many manufacturers do not draft an EPD. This means that the use of EPDs is only able to provide a narrow view on the environmental impact of different type of products.

9.4 Implications of the research

Functionality is an important aspect for the client. Therefore, some remarks must be made on the reduced functionality of a non-sway frame compared to a sway frame. The first advantage of a sway frame is the rapid deployment of the building. This is possible with a sway frame because the frame is stiff enough to carry the lateral loads. Consequently, the use of temporary supports can be minimised, resulting in faster erection than for a non-sway frame. Secondly, in a sway frame, the whole façade can be used for docking doors, whereas for a non-sway frame, bracing is needed at some locations. This means that the design freedom in the layout is reduced. Though, it is aimed to consider the non-sway building as well, so a solution is sought. This is visualised in Figure 9-2. Option 1 in Figure 9-2 shows the current distribution centre design, with the warehouse and several bump outs. If the bump outs are stacked (shown as Option 2 in Figure 9-2), a larger façade area is available that can be used for the bracing elements. This reduces the need to design a sway frame.

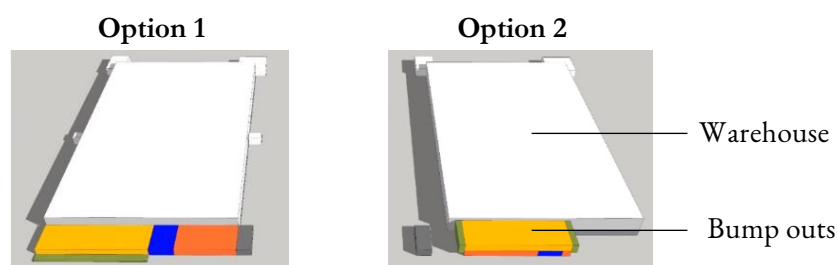


Figure 9-2: Two options of the warehouse and bump outs (Royal HaskoningDHV Internal document, 2021) Option 1 means that more area is needed for the bump outs, whereas option 2 shows a reduction of ground floor area needed for the bump outs, which means that there is room to change the location of the docking doors, such that bracing can be placed in the façade.

10 Conclusion

This research consists of two main aspects. First, design choices to reduce the environmental impact of a distribution centre's load-bearing structure are investigated. Second, an environmental impact calculation method is sought and performed. In this chapter, first the sub-research questions are answered, which is followed by answering the main research question.

What aspects influence the environmental impact of the main building materials (steel, concrete, and timber)?

The production process of building materials influences the environmental impact greatly. The impact of steel can be reduced significantly by using recycled steel instead of virgin steel. In concrete, the type of cement influences the environment. This can be reduced by choosing another type of cement or by reducing the amount of clinker in the cement. As timber is naturally grown, this has a low environmental impact compared to steel and concrete. Due to the production process, sawn timber has the lowest environmental impact, followed by glulam and CLT, and lastly LVL.

How can the functional service life of building elements be extended?

The service life can be extended by following the principles Design for Deconstruction or Design for Adaptability. Design for Deconstruction aims to extend the service life by reusing the elements at the end of life. Looking at components, the following should be considered: building components should be layered (so parallel disassembly is possible), made from prefabricated elements, connected with dry and accessible connections, connected with a minimal number of connector types and connectors, and the building components should have a limited size. On a material level, the functional service life can be extended by recycling and material reprocessing. To make sure recycling and reprocessing are always possible, it is advised to use a simple composition of materials, to avoid toxic and hazardous materials, and to avoid finishes that contaminate the base material. Design for Adaptability aims to overcome the situation where the building cannot meet the future needs of the user. Components should therefore have some redundancy and the components should be layered, making it possible to remove certain parts without having to remove the entire component.

Which material and design choices can be made in the design of a distribution centre to reduce the yearly environmental impact?

The yearly environmental impact of buildings can be reduced either by focusing on the initial material use or by aiming to extend the service life of the elements. This is considered for a specific case study, a distribution centre design that was initially designed by Royal HaskoningDHV. This is a sway steel structure with one mezzanine floor made from concrete and steel. Two alternative designs are set up that aim to reduce the environmental impact of the initial material use: a non-sway steel structure and a non-sway timber structure. Three alternative designs are created to extend the service life. The first extends the service life by focusing on the residual value of a design. For this alternative, the Design for Deconstruction guidelines are implemented. This led to a steel sway structure where extra attention is given to the connections to ensure reuse is possible at the end of life. The second and third alternatives extend the service life by focusing on optimising the design for multiple functions. In these alternatives, Design for Adaptability is applied. This led to a non-sway steel structure with an office or retail function on the mezzanine floor and one with an industrial function on the mezzanine floor.

How can the environmental impact of a distribution centre's load-bearing structure be quantified in a comprehensive way?

The environmental impact is calculated with European Product Declarations (EPDs). From these EPDs, data for the product stage (A1-A3) is gathered. To quantify the environmental impact in a comprehensive way, also the benefits and loads due to the end of life scenario are included (stage D). In this way, the current and future impact is included in the environmental impact calculation. Stage D is calculated with the updated rules of EN 15804:2012+A2:2019. As a result, the yearly environmental impact is calculated for different design alternatives and is given in a shadow price (in euros) per year. This is done separately for the main load-bearing structure and the mezzanine floor load-bearing structure.

Which of the design alternatives that are set up for this research results in the lowest yearly environmental impact?

Considering the main load-bearing structure for LCA stages A1-A3 and D, it can be concluded that the yearly environmental impact is lowest for the timber sway structure (Alternative B) for a reference service life of 20 years or longer. For an RSL of 10 years, the lowest yearly environmental impact is reached with the steel sway structure (Alternative A) with a high chance of reuse at the end of life. The yearly environmental impact of the main load-bearing structure of Alternative A is reduced even more if the design results in a longer RSL. This can be reached by changing Alternative A into an adaptable design (Alternative D1 or D2). Then, it can be concluded that the timber alternative has the lowest yearly environmental impact if it is used for 30 years or longer.

For the mezzanine load-bearing structure (stages A1-A3 and D), it is concluded that up to an RSL of 30 years, the demountable mezzanine floor design with a high chance of reuse (Alternative C) has the lowest yearly environmental impact. For an RSL of 40 years and longer (until the technical service life of the floor is reached), the timber and concrete floor (Alternative B) has the lowest yearly impact. Furthermore, it can be concluded that if an adaptable design results in a longer RSL, the yearly environmental impact reduces. This can be reached by changing Alternative C into a design with overcapacity (Alternative D1). Then, the timber alternative has the lowest environmental impact if it is used for 40 years or longer. Implementing more overcapacity (as done in Alternative D2) should be prevented, because even for a longer RSL, the other alternatives still lead to a lower yearly environmental impact.

With the answers on the sub-questions, the main research question is answered:

Which design choices have most influence on the yearly environmental impact of the load-bearing structure of a distribution centre?

The yearly environmental impact of the structural design of a distribution centre can be reduced in four ways. Firstly, it can be reduced significantly by choosing the most environmentally friendly material. Secondly, in the design phase, it can be concluded that if it is possible, the reference service life should be extended, because this reduces the yearly environmental impact significantly. Thirdly, a high percentage of elements should be reused and recycled at the end of life to result in a low yearly environmental impact. This is most effective if the building is used for a short time, because the advantage of reusing the materials is most valuable. Due to this finding, it can also be concluded that the material choice should be based upon the RSL. For a short RSL, a sway steel and concrete design (Alternative A) with a high chance of reuse results in the lowest yearly environmental impact. For a longer RSL, the use of a timber sway structure (Alternative B) leads to the lowest yearly environmental impact. If the RSL is unknown in the design phase, it is advised to use timber, because this results in the lowest total environmental impact.

11 Recommendations

11.1 Recommendations for future research

At the start of this research, the strength class of the materials were chosen. However, it is interesting to investigate the environmental impact if another strength class is used in the design, because this can influence the amount of material needed. In this research, EPDs were used to determine the environmental impact. A downside of EPDs is that they do not focus on strength classes. Only in some EPDs, data is given for a specific strength class, whereas other EPDs state that the data holds for multiple strength classes. It is therefore recommended to research other tools that can determine the relationship between the strength class and environmental impact.

All Design for Deconstruction aspects are incorporated in Alternative C. This ensures that it is not possible to investigate the effect of the separate aspects and it cannot be concluded which aspect is most important in a design. It is advised to set up design alternatives that contain only specific aspects as well, to gain insight in which aspects are most important to extend the service life of a building.

For the environmental impact calculation, the technical service life (TSL) is based upon an initial estimation by Straub et al. (2011). However, in future research, it is advised to investigate this issue further, for example by investigating the elements upon the factor categories of ISO 15686-8:2008. Here, the inherent performance, design, work execution, indoor environment, outdoor environment, usage conditions, and maintenance level need to be assessed to estimate the service life.

11.2 Recommendations for practice

If engineering firms want to reach the climate goals, action should be taken. It is therefore advised to follow the conclusion of this research. This means that environmentally friendly material should always be chosen over other materials. More specifically, it is recommended to use timber if the reference service life of the building is unknown or if a long reference service life is expected (Alternative B). For a short reference service life, it is advised to design a non-sway steel and concrete design (Alternative A) if it is expected that many of these elements will be reused and recycled at the end of life. Furthermore, it is recommended to aim to extend the reference service life of the building itself as much as possible, because this is very effective in reducing the yearly environmental impact. Engineering firms should ask the client about their expectations of the use of the building. By assessing this issue in the design phase, it can be decided to include some overcapacity to ensure a longer reference service life. It is also possible to assess the possibilities to use second-hand elements in a new building as well.

At the end of life, the residual value can always be maximised by means of recycling or reprocessing materials. Therefore, it is recommended to always apply a simple composition of materials to simplify the sorting process. Furthermore, the use of hazardous materials and finishes should be prevented to make sure recycling is possible. To make sure the materials do not end up at the landfill after demolition, it is advised to also draft a disassembly guide and a material inventory. Then, if the building is taken down, the demolition workers are able to retrieve most value from the elements.

When the contractor chooses which building materials are used, it is important to verify which materials are chosen. In other words, a control mechanism for a maximum environmental impact of a material should be included in the design requirements. Then, the expected environmental impact will never be exceeded in a later design stage.

For the case study, three specific remarks are made as well. Firstly, the designers are advised to re-assess the necessity to design a sway frame over a non-sway frame. From this research, it is concluded that a non-sway frame results in a reduction in environmental impact. Furthermore, the non-sway frame has more simple connections, making it easier to demount the elements at the end of life. Secondly, the designers should know whether it is necessary to remove the mezzanine floor from the building. In the case study design, the mezzanine floor is not part of the main structural system such that it can always be removed. However, if the mezzanine floor is included in the main structural system, the floors will provide additional stiffness to the building. Especially for the sway structure, this can lead to a reduction in materials. Thirdly, more research is needed on the performance of a more environmentally friendly mezzanine floor design. The Base design contains a composite steel-concrete floor system from which it is known that the client's requirements are fulfilled. For the demountable concrete alternative and the timber alternative with a concrete top floor, these requirements are not fully assessed. If it is aimed to reduce the environmental impact of the mezzanine floor structure as well, the requirements of the client should also be included in this comparison.

12 References

- Akinade, O. O., Oyedele, L. O., Ajayi, S. O., Bilal, M., Alaka, H. A., Owolabi, H. A., ... Kadiri, K. O. (2016). Design for Deconstruction (DfD): Critical success factors for diverting end-of-life waste from landfills. *Waste Management*. <https://doi.org/10.1016/j.wasman.2016.08.017>
- Allacker, K., Mathieux, F., Manfredi, S., Pelletier, N., De Camillis, C., Ardente, F., & Pant, R. (2014). Allocation solutions for secondary material production and end of life recovery: Proposals for product policy initiatives. *Resources, Conservation and Recycling*, 88, 1–12. <https://doi.org/10.1016/j.resconrec.2014.03.016>
- Allacker, K., Mathieux, F., Pennington, D., & Pant, R. (2017). The search for an appropriate end-of-life formula for the purpose of the European Commission Environmental Footprint initiative. *International Journal of Life Cycle Assessment*, 22(9), 1441–1458. <https://doi.org/10.1007/s11367-016-1244-0>
- Backx, S. (2020). *Structural sustainability in the early design phase* (Master Thesis Report (TU Delft)). Master Thesis Report (TU Delft). Retrieved from <http://resolver.tudelft.nl/uuid:f7ca351f-2136-491d-aa09-d515a325ca19>
- Barendsz, M. A., Eldik, C. H. Van, Hamerlinck, A. F., Hollander, J. P. Den, & Snijder, H. H. (2019). *Hallen: Kenmerken en constructiesystemen van stalen hallen en het ontwerp van een éénbeukige geschoorde hal volgens Eurocode 3*. Bouwen met Staal.
- Beyer, G., Defays, M., Fischer, M., Fletcher, J., De Munck, E., De Jaeger, F., ... Wijnendaele, K. (2010). *Timmer aan minder klimaatverandering: Gebruik hout!* Retrieved from https://www.vvnh.nl/system/files/tackle_climate_change_use_wood_0.pdf
- BIMobject. (n.d.). Picture of CPAC Hollow core slab HC 60x300 mm. Retrieved July 1, 2020, from https://www.bimobject.com/nl/scg/product/hc_60x300_mm
- Bionova Ltd. (2019). Getting ready for EN 15804+A2: what's changed and how to prepare for it. Retrieved January 25, 2021, from <https://www.oneclicklca.com/getting-ready-for-en-15804-a2-whats-changed-and-how-to-prepare-for-it/>
- Blaß, H. J., & Sandhaas, C. (2017). Timber Engineering: Principles for Design. In *KIT Scientific Publishing*. [https://doi.org/10.1016/s1474-6670\(17\)54538-3](https://doi.org/10.1016/s1474-6670(17)54538-3)
- Bouwen met Staal. (2013). Duurzame stalen vloersystemen. *Bouwen Met Staal*. Retrieved from https://gratis-publicaties.bouwenmetstaal.nl/pdf_serve.lasso?p=pdf&n=Duurzame+stalen+vloersystemen-1.pdf&pub=158-1.pdf
- Brand, S. (1995). *How buildings learn: What happens after they're built*. Penguin.
- Breneman, S. (2014, November). *CLT Floor Design: Strength, Deflection and Vibrations*. Toward Taller Wood Buildings. Retrieved from <https://www.woodworks.org/wp-content/uploads/TTWB-2014-Breneman-CLT-Floor-Design.pdf>
- Breunese, A. J., & Maljaars, J. (2015). *Course reader CIE5131: Fire Safety Design*. TU Delft.
- Burchart-Korol, D. (2013). Life cycle assessment of steel production in Poland: A case study. *Journal of Cleaner Production*, 54, 235–243. <https://doi.org/10.1016/j.jclepro.2013.04.031>
- Buunk, R., & Heebing, E. (2017). *Remontabel ontwerpen met kanaalplaten - Design for Disassembly*. Bachelor Thesis Report (HAN University of Applied Sciences).

- Crews, K., Hayward, D., & MacKenzie, C. (2008). *Interim industry standard recycled timber - Visually stress graded recycled timber for structural purposes*. Melbourne: Forest&Wood Products Australia.
- Crews, K., & MacKenzie, C. (2008). Development of grading rules for re-cycled timber used in structural applications. *10th World Conference on Timber Engineering 2008, 1*, 231–238.
- Crowther, P. (2000). Developing guidelines for designing for deconstruction. *Deconstruction - Closing the Loop*. <https://doi.org/10.3168/jds.2010-3516>
- Crowther, P. (2005). Design for Disassembly - Themes and principles. *RAIA/BDP Environment Design Guide*. Retrieved from <https://eprints.qut.edu.au/2888/1/Crowther-RAIA-2005.PDF>
- Danielsson, H. (n.d.). *Lecture "CLT: Design and use."* Retrieved from http://www.kstr.lth.se/fileadmin/kstr/pdf_files/Timber_Engineering_2017/CLT_-_design_and_use_new.pdf
- De Danschutter, M., Noomen, P. A., & Oostdam, B. (2017). Tijdelijke rechtbank met permanent karakter. *Bouwen Met Staal, June*(257), 14–19.
- De Groot, W. H. (2018). Lecture Notes for the Course Introduction to Timber Structures (TU Eindhoven). TU Eindhoven, Eindhoven. Retrieved from https://canvas.tue.nl/courses/7506/files/1094446/download?download_frd=1
- Debieb, F., & Kenai, S. (2008). The use of coarse and fine crushed bricks as aggregate in concrete. *Construction and Building Materials*, *22*(5), 886–893. <https://doi.org/10.1016/j.conbuildmat.2006.12.013>
- Den Hollander, J. P. (n.d.). Drawing: Vergelijking geschoord en ongeschoord. Retrieved September 10, 2020, from http://www.jpdh.info/tu_stabiliteit.htm
- Dias, A. M. A., Dias, A. M. P. G., Silvestre, J. D., & De Brito, J. (2020). Comparison of the environmental and structural performance of solid and glued laminated timber products based on EPDs. *Structures*, *26*(April), 128–138. <https://doi.org/10.1016/j.istruc.2020.04.015>
- Dunant, C. F., Drewniok, M. P., Sansom, M., Corbey, S., Allwood, J. M., & Cullen, J. M. (2017). Real and perceived barriers to steel reuse across the UK construction value chain. *Resources, Conservation and Recycling*, *126*(August), 118–131. <https://doi.org/10.1016/j.resconrec.2017.07.036>
- Durmisevic, E. (2006). *Transformable Building Structures* (Doctoral Thesis (TU Delft)). Doctoral Thesis (TU Delft). Retrieved from <https://repository.tudelft.nl/islandora/object/uuid%3A9d2406e5-0cce-4788-8ee0-c19cbf38ea9a>
- Dutch Engineering BV. (2020). Productenoverzicht ComFlor. Retrieved September 17, 2020, from <https://www.dutchengineering.nl/Nederlands/products/e/pm/112/pm/112/>
- Ellen MacArthur Foundation. (2015). Towards a Circular Economy: Business Rationale for an Accelerated Transition. In *Ellen MacArthur Foundation*. Retrieved from https://www.ellenmacarthurfoundation.org/assets/downloads/publications/TCE_Ellen-MacArthur-Foundation_26-Nov-2015.pdf
- European Union. (2020a). *Circular Economy Action Plan: For a cleaner and more competitive Europe*.
- European Union. (2020b). Nearly zero-energy buildings. Retrieved June 8, 2020, from https://ec.europa.eu/energy/topics/energy-efficiency/energy-efficient-buildings/nearly-zero-energy-buildings_en#information-from-individual-countries

- Falk, R. H., Maul, D. G., Cramer, S. M., Evans, J., & Herian, V. (2008). Engineering Properties of Douglas-fir Lumber Reclaimed from Deconstructed Buildings. *Research Paper FPL-RP-650*, 1–47. Retrieved from https://www.fpl.fs.fed.us/documnts/fplrp/fpl_rp650.pdf
- Fisher, J. M. (2005). Expansion Joints: Where, When and How. *Modern Steel Construction*. Retrieved from https://www.aisc.org/globalassets/modern-steel/archives/2005/04/2005v04_expansion_joints.pdf
- Flexibele momentverbindingen tussen liggers en kolommen. (n.d.). Retrieved November 20, 2020, from Joost de Vree website: https://www.joostdevree.nl/bouwkunde2/jpgs/staalverbinding_ligger_kolom_flexibele_momentverbinding_hogeschool_rotterdam.jpg
- Fujita, M., & Masuda, T. (2014). Application of Various NDT Methods for the Evaluation of Building Steel Structures for Reuse. *Materials*, 7(10), 7130–7144. <https://doi.org/10.3390/ma7107130>
- Gosling, J., Sassi, P., Naim, M., & Lark, R. (2013). Adaptable buildings: A systems approach. *Sustainable Cities and Society*, 7, 44–51. <https://doi.org/10.1016/j.scs.2012.11.002>
- Government of the Netherlands. (n.d.). From a linear to a circular economy. Retrieved June 4, 2020, from <https://www.government.nl/topics/circular-economy/from-a-linear-to-a-circular-economy>
- Gross, H. (2013). *Glulam Handbook Volume 1* (Vol. 1). Stockholm: Skogsindustrierna – The Swedish Forest Industries Federation. Retrieved from https://www.woodcampus.co.uk/wp-content/uploads/2019/05/GLU_HAND_VOLUME-1.pdf
- Grünbauer, J. (n.d.). Raatliggertabellen. Retrieved January 27, 2021, from <http://www.grunbauer.nl/ned/lijt2.htm#ipe>
- Guy, B., Shell, S., & Esherick, H. (2006). Design for Deconstruction and Materials Reuse. *Proceedings of the CIB Task Group*, 39(April), 189–209. Retrieved from www.cce.ufl.edu/affiliations/cib
- Hamerlinck, A. F., & Potjes, B. (2007). Technisch Dossier 2: Vloeren van kanaalplaten met geïntegreerde stalen liggers. *Bouwen Met Staal*.
- Hoeh, C. (2020). *Presentation about Net Zero Carbon ARS Facilities*. Royal HaskoningDHV Internal Document.
- Hovde, P. J. (2005, April). The Factor Method – a Simple Tool to Service Life Estimation. *10DBMC International Conference on Durability of Building Materials and Components*. Lyon (France).
- Hradil, P., Talja, A., Wahlström, M., Huuhka, S., Lahdensivu, J., & Pikkuvirta, J. (2014). *Re-use of structural elements: Environmentally efficient recovery of building components*. Espoo: VTT Technology 200. Retrieved from <https://cris.vtt.fi/en/publications/re-use-of-structural-elements-environmentally-efficient-recovery->
- IEA. (2020). *Iron and Steel Technology Roadmap: Towards more sustainable steelmaking*. Retrieved from <https://www.iea.org/reports/iron-and-steel-technology-roadmap>
- Jaspart, J.-P., & Weynand, K. (2016). *Design of Joints in Steel and Composite Structures*. Brussels: ECCS and Ernst & Sohn.
- Karacabeyli, E., & Douglas, B. (2013). *CLT handbook (U.S. Edition)*. Point-Claire, Quebec: FPIInnovations and Binational Softwood Lumber Council.
- Kasarda, M. E., Terpenney, J. P., Inman, D., Precoda, K. R., Jelesko, J., Sahin, A., & Park, J. (2007). Design

- for adaptability (DFAD) - a new concept for achieving sustainable design. *Robotics and Computer-Integrated Manufacturing*, 23(6), 727–734. <https://doi.org/10.1016/j.rcim.2007.02.004>
- Kaza, S., Yao, L. C., Bhada-Tata, P., & Van Woerden, F. (2018). *What a Waste 2.0: A Global Snapshot of Solid Waste Management to 2050*. Washington D.C.: World Bank. Retrieved from <https://openknowledge.worldbank.org/handle/10986/30317>
- KIELSTEG Deutschland GmbH. (2015). *Workbook for Architects and Planners*.
- Kissel, M., Schrieverhoff, P., & Lindemann, U. (2012). Design for adaptability - Identifying potential for improvement on an architecture basis. *NordDesign 2012 - Proceedings of the 9th NordDesign Conference*.
- Kyrklund, B. (1990). The potential of forests and forest industry in reducing excess atmospheric carbon dioxide. Retrieved September 14, 2020, from An international journal of forest and forest industries website: <http://www.fao.org/3/u0700e/u0700e04.htm>
- Landman, M. (2016). *Technical Building Properties with the Probability of Elongating the Functional Service Life*. Master Thesis Report (TU Eindhoven).
- Lignatur AG. (2014). *Workbook*. Waldstatt / CH.
- Loebus, S., Dietsch, P., & Winter, S. (2017). Two-way spanning CLT-concrete-composite-slabs. *New Zealand Timber Design Journal*, 26(3).
- Manfredi, S., Allacker, K., Chomkham Sri, K., Pelletier, N., & de Souza, D. M. (2012). Product Environmental Footprint (PEF) Guide. In *European Commission Joint Research Centre*. [https://doi.org/Ares\(2012\)873782-17/07/2012](https://doi.org/Ares(2012)873782-17/07/2012)
- Milne, G., & Reardon, C. (2013). Embodied energy. Retrieved September 10, 2020, from Your Home website: <https://www.yourhome.gov.au/materials/embodied-energy>
- Morgan, C., & Stevenson, F. (2005). Design for deconstruction - SEDA Design Guide for Scotland. In *SEDA*.
- NEN. (2002). *NEN-EN 1990 Basis of structural design*. Nederlands Normalisatie-instituut.
- NEN. (2005a). *NEN-EN 1991-1-4 Eurocode 1: Actions on structures - Part 1-4: General actions - Wind actions*. Nederlands Normalisatie-instituut.
- NEN. (2005b). *NEN-EN 1995-1-1 Eurocode 5 - Design of timber structures - Part 1-1: General - Common rules and rules for buildings*. Nederlands Normalisatie-instituut.
- NEN. (2011). *NEN-EN 1995-1-2 + C2 Design of timber structures - Part 1-2: General - Structural fire design*. Nederlands Normalisatie-instituut.
- NEN. (2013). *NEN-EN 14080:2013 Timber structures - Glued laminated timber and glued solid timber - Requirements*. Nederlands Normalisatie-instituut.
- NEN. (2016a). *NEN-EN 1993-1-1+C2+A1 Design of steel structures - Part 1-1: General rules and rules for buildings*. Nederlands Normalisatie-instituut.
- NEN. (2016b). *NEN-EN 338 Structural timber - Strength classes*. Nederlands Normalisatie-instituut.
- NEN. (2018). *NEN-EN 197-1 Cement - Part 1: Composition, specifications and conformity criteria for common cements*. Nederlands Normalisatie-instituut.

- NEN. (2019). *NEN-EN 15804:2012+A2:2019 Sustainability of construction works - Environmental product declarations - Core rules for the product category of construction products*. Delft: Nederlands Normalisatie-instituut.
- NIBE. (2021). NIBE EPD Application. Retrieved from <https://app.epdnibe.com/>
- Nicholson, A. L., Olivetti, E. A., Gregory, J. R., Field, F. R., & Kirchain, R. E. (2009). End-of-life LCA allocation methods: Open loop recycling impacts on robustness of material selection decisions. *2009 IEEE International Symposium on Sustainable Systems and Technology*, 1–6. <https://doi.org/10.1109/ISSST.2009.5156769>
- O'Brien, M. (2019, December 30). As robots take over warehousing, workers pushed to adapt. Retrieved March 24, 2021, from WHAM website: <https://13wham.com/news/nation-world/as-robots-take-over-warehousing-workers-pushed-to-adapt-12-30-2019>
- OECD. (2018). Global Material Resources Outlook to 2060. In *Global Material Resources Outlook to 2060*. <https://doi.org/10.1787/9789264307452-en>
- Platform CB'23. (2019). *Framework Circulair Bouwen*.
- Potting, J., Hekkert, M., Worrell, E., & Hanemaaijer, A. (2017). *Circular economy: Measuring innovation in the product chain*. Retrieved from <https://www.pbl.nl/sites/default/files/downloads/pbl-2016-circular-economy-measuring-innovation-in-product-chains-2544.pdf>
- Raad voor de leefomgeving en infrastructuur. (2015). *Circular economy: From wish to practice*. Rli. Retrieved from https://en.rli.nl/sites/default/files/advice_rli_circular_economy_interactive_def.pdf
- Ramesh, T., Prakash, R., & Shukla, K. K. (2010). Life cycle energy analysis of buildings: An overview. *Energy and Buildings*, *42*(10), 1592–1600. <https://doi.org/10.1016/j.enbuild.2010.05.007>
- Rios, F. C., Chong, W. K., & Grau, D. (2015). Design for Disassembly and Deconstruction - Challenges and Opportunities. *Procedia Engineering*, *118*, 1296–1304. <https://doi.org/10.1016/j.proeng.2015.08.485>
- Royal HaskoningDHV Internal document. (2021). *Amazon Net Zero Carbon*.
- Royal HaskoningDHV Internal Document. (2019). *Calculation Report SCT 2021*.
- Royal HaskoningDHV Internal Document. (2020a). *Basis of Design SCT2021*.
- Royal HaskoningDHV Internal Document. (2020b). *Documents IXD*.
- Royal HaskoningDHV Internal Document. (2020c). *Drawings for distribution centre designs*.
- Salazar, J., & Bergman, R. (2013). Temporal Considerations of Carbon Sequestration in LCA. *Proceedings from the LCA XIII International Conference*.
- Sandhaas, C., Munch-Andersen, J., & Dietsch, P. (2018). *Design of Connections in Timber Structures, a state-of-the-art report by COST Action FP1402 / WG 3*.
- Saravanakumar, P., Abhiram, K., & Manoj, B. (2016). Properties of treated recycled aggregates and its influence on concrete strength characteristics. *Construction and Building Materials*, *111*, 611–617. <https://doi.org/10.1016/j.conbuildmat.2016.02.064>
- Seyed Shahabaldin, S. S. (2020). *A comparative study of Product Environmental Footprint (PEF) and EN*

- 15804 in the construction sector concentrating on the End-of-Life stage and reducing subjectivity in the formulas.* Master Thesis Report (KTH Royal Institute of Technology).
- Shaban, W. M., Yang, J., Su, H., Mo, K. H., Li, L., & Xie, J. (2019). Quality Improvement Techniques for Recycled Concrete Aggregate: A review. *Journal of Advanced Concrete Technology*, 17, 151–167. <https://doi.org/10.3151/jact.17.4.151>
- Slimline Buildings. (2020). Slimline. Retrieved September 17, 2020, from https://www.slimlinebuildings.com/slimline-advantages.php#tab_tab3
- Staalbouwkundig Genootschap. (1999). *Momentverbindingen*. Rotterdam.
- Star-Frame Solutions. (2011). Lichtgewicht prefab vloeren. Retrieved September 17, 2020, from [https://www.tatasteelconstruction.com/static_files/Tata Steel/content/products/Building Systems/Comflor/Dutch/Quantum/Downloads/Quantum® Deck infoblad.pdf](https://www.tatasteelconstruction.com/static_files/Tata%20Steel/content/products/Building%20Systems/Comflor/Dutch/Quantum/Downloads/Quantum%20Deck%20infoblad.pdf)
- Stichting Bouwkwiteit. (2019). *Bepalingsmethod Milieuprestatie Gebouw en GWW-werken*. Retrieved from <https://milieudatabase.nl/wp-content/uploads/2019/05/SBK-Bepalingsmethode-versie-3.0-1-januari-2019.pdf>
- Stora Enso. (2017, October). CLT by Stora Enso: Technical brochure. Retrieved October 2, 2020, from <https://www.storaenso.com/-/media/documents/download-center/documents/product-brochures/wood-products/clt-by-stora-enso-technical-brochure-en.pdf?mode=brochure#page=24>
- Stora Enso. (2018). *CLT rib panel by Stora Enso*. Retrieved from www.storaenso.com/clt
- Stora Enso Wood Products GmbH. (2017). *CLT by Stora Enso Technical brochure*.
- Straub, A., Van Nunen, H., Janssen, R., & Liebrechts, M. A. A. M. (2011). *Levensduur van bouwproducten: Methode voor referentiewaarden*. Zwijndrecht: SBR.
- Tool, F. (2010). *Ontwerptool voor de beoordeling van constructieve alternatieven op duurzaamheid* (Master Thesis Report (TU Delft)). Master Thesis Report (TU Delft). Retrieved from <http://resolver.tudelft.nl/uuid:56de9008-8b50-4303-8136-47ac13cd4eda>
- U.S. Army Corps of Engineers, Naval Facilities Engineering Command, & Air Force Civil Engineer Support Agency. (2002). *Unified Facilities Criteria (UFC): Selection of methods for the reduction, reuse, and recycling of demolition waste*. Retrieved from <http://dod.wbdg.org/>.
- Uitvoeringsteam Road Map CO2-reductie. (2021). Road Map CO2 - Presentatie Stuurgroep. Retrieved April 15, 2021, from Betonakkoord website: https://www.betonakkoord.nl/publish/pages/166796/road_map_co2_januari_2021_versie_1_2.pdf
- UN Environment and International Energy Agency. (2017). *Towards a zero-emission, efficient, and resilient buildings and construction sector. Global Status Report*. Retrieved from www.globalabc.org
- Van Buren, N., Demmers, M., van der Heijden, R., & Witlox, F. (2016). Towards a circular economy: The role of Dutch logistics industries and governments. *Sustainability*, 8(7), 1–17. <https://doi.org/10.3390/su8070647>
- Van Herwijnen, F. (2013). Duurzaam construeren met materialen. *Commissie Vakmanschap VNconstructeurs*, 4.
- Van Maastrigt, J. J. (2019). *Quantifying Life Cycle Environmental Benefits of Circular Steel Building Designs* (Master Thesis Report (TU Delft)). Master Thesis Report (TU Delft). Retrieved from

<http://resolver.tudelft.nl/uuid:cf8f1434-ce13-41cd-a1c6-25270c46af68>

- Van Vliet, M. (2018). *Disassembling the steps towards Building Circularity* (Master Thesis Report (TU Eindhoven)). Master Thesis Report (TU Eindhoven). Retrieved from <https://research.tue.nl/en/studentTheses/disassembling-the-steps-towards-building-circularity>
- Van Wijnen, W. W. (2020). *Sustainable timber structures* (Master Thesis Report (TU Delft)). Master Thesis Report (TU Delft). Retrieved from <http://resolver.tudelft.nl/uuid:13919f29-caae-4ae2-ba1b-02aea6e56f35>
- VBI. (n.d.). Uw basis: de kanaalplaatvloer. Retrieved September 17, 2020, from <https://vbi.nl/product/uw-basis-de-kanaalplaatvloer>
- Veljkovic, M. (2019). *Lecture slides Steel Structures II*.
- Vogtländer, J. (2015). *A Practical Guide to LCA for Students, Designers and Business Managers: Cradle-to-grave and Cradle-to-cradle*. Delft: Delft Academic Press (VSSD Publishers).
- Vonck, T. (2019). *An Eco-Effective Structure: A qualitative approach into eco-effective structural design perspectives, criteria, and strategies in both theory and practice* (Master Thesis Report (TU Delft)). Master Thesis Report (TU Delft). Retrieved from <http://resolver.tudelft.nl/uuid:42e532da-e578-4cd0-8288-b40867b8366e>
- Wastiels, L. (2015). *Workshop: EPD, the current debate and challenges*. Brussels. Retrieved from https://www.construction-products.eu/application/files/3015/2481/8429/20151215151002-workshop_epd_slides_1.pdf
- Yang, J., Shaban, W. M., Elbaz, K., Thomas, B. S., Xie, J., & Li, L. (2020). Properties of concrete containing strengthened crushed brick aggregate by pozzolan slurry. *Construction and Building Materials*, *247*, 118612. <https://doi.org/10.1016/j.conbuildmat.2020.118612>
- Yellishetty, M., Mudd, G. M., Ranjith, P. G., & Tharumarajah, A. (2011). Environmental life-cycle comparisons of steel production and recycling: Sustainability issues, problems and prospects. *Environmental Science and Policy*, *14*(6), 650–663. <https://doi.org/10.1016/j.envsci.2011.04.008>

Appendices

A Guidelines for the structural calculations	89
A.1 Deflection requirements (SLS)	89
A.2 Loads	90
B Base design	96
B.1 Schematisation of stabilisation system (as modelled)	96
B.2 Loads	98
B.3 Connection design	106
B.4 Mezzanine floor design	113
B.5 Results of structural calculations	120
B.6 Element overview	130
C Alternative A	131
C.1 Design considerations.....	131
C.2 Loads	133
C.3 Bracing design	136
C.4 Results of structural calculations.....	138
C.5 Element overview.....	143
D Alternative B	144
D.1 Material and product properties	144
D.2 Loads	146
D.3 Roof bracing design.....	149
D.4 Roof plan of the structure	150
D.5 Results of structural calculations.....	152
D.6 Mezzanine floor design.....	165
D.7 Possible improvements of the design	175
D.8 Element overview	177
E Alternative C	179
E.1 Loads on the 2D model.....	179
E.2 Beam-column connections	179
E.3 Results of structural calculations	180
E.4 Mezzanine floor design	184
E.5 Element overview	190
F Alternative D1	191
F.1 Mezzanine floor	191
F.2 Results of structural calculations.....	192
F.3 Element overview	193
G Alternative D2	195
G.1 Floor calculations (industrial function)	195
G.2 Results of structural calculations.....	196
G.3 Element overview.....	197
H Environmental data	199
I Environmental impact calculation	207
I.1 Comparison between end of life methods.....	207

I.2 Procedure and example calculation of the environmental impact	216
J Environmental impact calculation results	223
J.1 Research question 3a: Optimise design for its initial material use	223
J.2 Research question 3b: Optimise design for residual value.....	226

A Guidelines for the structural calculations

The designs are structurally verified for an initial design level. This ensures the following:

- The base design is a repetitive design. This means that only two cross-sections are designed: one in the x-direction and one in the y-direction. Furthermore, repetition can be seen in the chosen profiles: it is aimed to use the same profiles for the elements with the same function (e.g. façade columns will all be made from HEB 400 profiles).
- The structural system needs to be checked for the serviceability limit state (SLS) for the following:
 - Horizontal displacement of the structural system
 - Displacement of elements
- The beams and columns are structurally verified in the ultimate limit state (ULS) as well. To determine the cross-sections that can carry the loads, the following structural verifications are performed on these sections:
 - Cross-sectional checks (columns and beams)
 - Compression resistance
 - Bending resistance
 - Shear resistance
 - Resistance for the combination of bending, axial force, and shear force
 - Stability checks
 - Flexural buckling resistance
 - Lateral torsional buckling resistance
 - Beam-column buckling resistance

For the connections, the following can be said:

- The type of connection (shear or moment connection) must be determined;
- In case a moment connection is applied, the rotational stiffness of this connection is determined with rules of thumb (Staalbouwkundig Genootschap, 1999).

The foundation is outside of the scope, but the stiffness of the supports does influence the design of the main structure. Therefore, the following steps are necessary for the supports:

- In case the support needs to provide some stiffness, this stiffness is calculated with help of the computer software Technosoft.

The design is set up as an initial design, where changes in the design must be anticipated on, so the elements should be designed accordingly:

- Cross-sectional checks should have a unity check ≤ 0.85 .
- Stability checks should have a unity check ≤ 0.80 .

A.1 Deflection requirements (SLS)

The deflection requirements are determined by Royal HaskoningDHV and are based upon the Eurocode rules and rules as provided by the client.

- Horizontal deflection limit:
 - Maximum horizontal deflection per storey = $h / 150$
 - In the design process, a requirement of an UC of 0.80 is provided (see Appendix A “Guidelines for the structural calculations”).

- Maximum horizontal deflection for the whole building = $h / 150$
 - In the design process, a requirement of an UC of 0.80 is provided (see Appendix A “Guidelines for the structural calculations”).
- Ground floor:
 - Maximum deflection = $L / 500$
- Roof:
 - Maximum deflection = $L / 250$
- During construction of the ComFlor75 floor:
 - Maximum deflection = $L / 850$ due to dead loads
 - Maximum deflection = $L / 700$ due to dead loads and construction stage live loads
- During the use stage of the ComFlor75 floor (robotic floors):
 - Maximum deflection = $L / 360$ due to dead loads and robotic live loads
 - Maximum deflection = $L / 650$ due to robotic live loads only
- During the use stage of the ComFlor75 floor (non-robotic floors):
 - Maximum deflection = $3/1000 * L$

A large part of the mezzanine floor is used by robots. The client has set specific design requirements for these floors, as the robots are very sensitive to inaccuracies. These requirements are related to the roughness of the top floor, the allowance of crack widths, and the angles of the floor in case height differences are present. However, these requirements are confidential and cannot be shared in this report. In addition, these requirements are very specific and should be tested on other floor designs. In this research, this cannot be investigated.

A.2 Loads

A.2.1 Load factors

The load factors that are applied can be found in Table A-1. The ψ factors are found in Table A-2. For the mezzanine floor, category E is applied.

Table A-1: Load factors according to EN-1990 (NEN, 2002)

Load Combinations	Permanent loading		Leading variable action	Accompanying variable actions
	Unfavourable	Favourable		
Ultimate limit states (ULS)	1.35	1.00	1.50	$1.50 * \psi_{0,i} (i>1)$
Accidental (ULS)	1.00	1.00	1.00	$1.00 * \psi_{1 \text{ or } 2,i} (i>1)$
Serviceability limit states (SLS)	1.00	1.00	1.00	$1.00 * \psi_{0,i} (i>1)$

Table A-2: ψ Factors according to EN-1990 (NEN, 2002)

Variable loading		ψ_0	ψ_1	ψ_2
Category E	Storage areas	1.0	0.9	0.8
Category H	Roofs	0.0	0.0	0.0
Snow		0.5	0.2	0.0
Wind		0.6	0.2	0.0

A.2.2 Wind loads

The wind loading on the warehouse is based on the rules of EN 1991-1-4. The precise location of the building is unknown, so assumptions had to be made. In the base design, this is based on two factors that are considered to have most influence on the wind loading in Europe: the basic wind velocity in a certain area and the terrain category in relation to the openness of the area. The basic wind velocity ranges between 21 to 36 m/s. It has been decided to set the reference wind velocity to 30 m/s, to cover a significant area in Europe. For the distribution centres, terrain categories II, III and IV are most realistic. Terrain category II refers to an area with low vegetation. Terrain category III refers to an area with regular cover of vegetation or buildings (such as villages, suburban terrain, permanent forest). Terrain category IV refers to an area in which at least 15 % of the surface is covered with buildings and their average height exceeds 15 m. The highest wind loads are found in terrain category II, so this is used as a reference for the design.

Table A-3: Basis of wind calculation

Description		
Building dimensions	Length (L)	221.34 m
	Width (b)	134.88 m
	Height (h), including parapet	14.5 m
	h/d	0.10
Basic wind velocity	v_b	30 m/s
Terrain category		II

The wind loads are positive or negative. This is based upon the drawing shown in Figure A-1, where it can be seen that in case the pressure is towards the surface, a positive sign needs to be used and in case the pressure is moving away from the surface, a negative sign needs to be used.

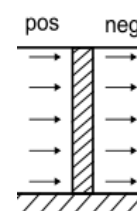


Figure A-1: Pressure on surfaces

A.2.2.1 External wind loads (horizontal)

Based on the dimensions of the building, shown in Table A-3, it is found that the height of the building is smaller than the width of the building. According to EN-1991-1-4, in that case, the wind can be equally distributed over the height of the building (see Figure A-2).

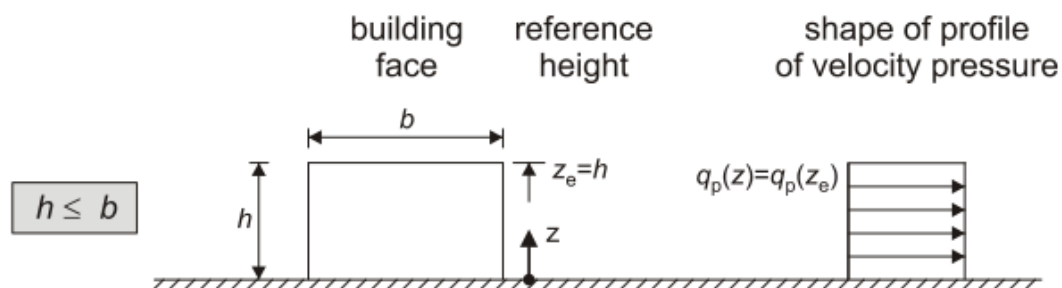


Figure A-2: Distribution of wind load over the height of the facade based on h/b (NEN, 2005a)

The peak velocity pressure is calculated according to the steps shown in Table A-4, where the peak velocity pressure of the load bearing structure is distributed over an area of 10 m² (chapter 7.2.1 of EC 1991-1-4).

Table A-4: Calculation of peak velocity pressure

Description	Parameter	Number	Unit
Air density	ρ_0	1.25	kg/m ³
Air density	ρ_a	0.012	kN/m ³
Basic wind velocity	v_b	30	m/s
Reference mean (basic) velocity pressure	$q_b = \frac{1}{2} * \rho_a * v_b^2 :$	5.52	kN/m ²
Exposure factor (from Figure 4.2 EN-1991-1-4)	$c_s(z)$	2.6	
Peak velocity pressure	q_{p1}	14.34	kN/m ²
Wind area for load bearing structure	A	10	m ²
Peak velocity pressure for load bearing structure	q_{p10}	1.43	kN/10 m ²

For the different wind directions, the figures from EN 1991-1-4 are used. The representative figures for the wind load on the vertical walls can be found in Figure A-3. Due to the large dimensions of the building, there is lack of correlation between the wind on the windward and on the leeward side (zones D and E), when applied simultaneously on the building. This lack of correlation can be applied as follows:

- For buildings with $\frac{h}{d} \geq 5$, the resulting force needs to be multiplied with 1.0
- For buildings with $\frac{h}{d} \leq 1$, the resulting force needs to be multiplied with 0.85
- For intermediate values of $\frac{h}{d}$, the resulting force needs to be multiplied with a factor in between 1.0 and 0.85 (linearly interpolated)

For the warehouse, $\frac{h}{d} = 0.10$, so the resulting force will be multiplied with 0.85.

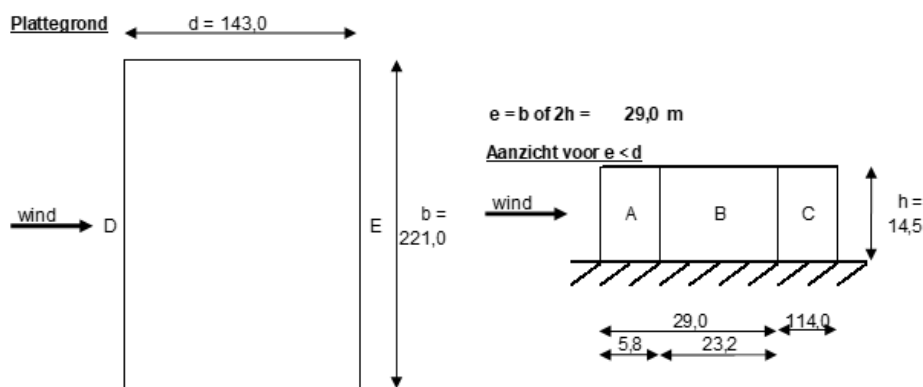


Figure A-3: Representative figures for wind load on vertical walls (NEN, 2005a)

The building shape factors are based on EN 1991-1-4 and can be seen in Table A-5. The applied building shape factors for this building are shown in blue in this table. In addition to these numbers, also $c_s c_d = 1.0$ is applied in the calculation. The wind on the facades is not considered in the verification of the elements, as only two sections as a two-dimensional system is checked. In further design calculations, this should be included.

Table A-5: Recommended values of external pressure coefficients for walls of rectangular buildings (NEN, 2005a)

Zone	A		B		C		D		E	
	$c_{pe,10}$	$c_{pe,1}$	$c_{pe,10}$	$c_{pe,1}$	$c_{pe,10}$	$c_{pe,1}$	$c_{pe,10}$	$c_{pe,1}$	$c_{pe,10}$	$c_{pe,1}$
5	-1,2	-1,4	-0,8	-1,1	-0,5		+0,8	+1,0	-0,7	
1	-1,2	-1,4	-0,8	-1,1	-0,5		+0,8	+1,0	-0,5	
≤ 0,25	-1,2	-1,4	-0,8	-1,1	-0,5		+0,7	+1,0	-0,3	

Table A-6: External wind load on vertical walls

Parameter description	Parameter	Number	Unit
External load A (x and y direction)	$F_{w,e,A} = q_{p10} * c_s c_d * c_{pe,10,A}$	-1.72	kN/m ²
External load B (x and y direction)	$F_{w,e,B} = q_{p10} * c_s c_d * c_{pe,10,B}$	-1.15	kN/m ²
External load C (x and y direction)	$F_{w,e,C} = q_{p10} * c_s c_d * c_{pe,10,C}$	-0.72	kN/m ²
External load D (x and y direction)	$F_{w,e,D} = q_{p10} * c_s c_d * c_{pe,10,D}$	1.00	kN/m ²
External load E (x and y direction)	$F_{w,e,E} = q_{p10} * c_s c_d * c_{pe,10,E}$	-0.43	kN/m ²
Corrected external load D (x and y direction)	$F_{w,e,D,corrected} = F_{w,e,D} * 0.85$	0.89	kN/m²
Corrected external load E (x and y direction)	$F_{w,e,E,corrected} = F_{w,e,E} * 0.85$	-0.61	kN/m²

A.2.2.2 External wind on the roof (vertical)

External wind on the roof should also be considered. The representative figures for the wind load on the roof can be found in Figure A-4, where it can be seen that a roof with a parapet. The calculation for the wind load is given in Table A-7. As a simplification, it is decided that only area I is considered as external wind load on the roof, as this area covers the largest part of the roof.

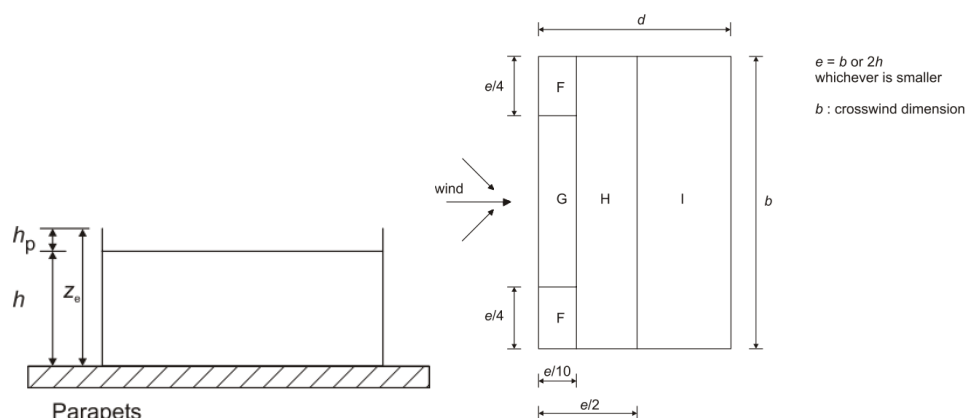


Figure A-4: Representative figures for wind load on the roof (NEN, 2005a)

Table A-7: Building shape factors and external loads on the roof (based upon Table 7.2 of EN-1991-1-4)

Description	Parameter	Number	Unit
Ratio Parapet - Column height	$\frac{h_p}{h} = \frac{1}{13.5}$	0.074	
Building shape factor zone F	$c_{p,e,F}$	-1.32	
Building shape factor zone G	$c_{p,e,G}$	-0.86	
Building shape factor zone H	$c_{p,e,H}$	-0.7	
Building shape factor zone I-	$c_{p,e,I-}$	-0.2	
Building shape factor zone I+	$c_{p,e,I+}$	+0.2	
External load F (x and y direction)	$F_{w,e,F} = q_{p10} * c_s c_d * c_{pe,10,F}$	-1.89	kN/m ²
External load G (x and y direction)	$F_{w,e,G} = q_{p10} * c_s c_d * c_{pe,10,G}$	-1.23	kN/m ²
External load H (x and y direction)	$F_{w,e,H} = q_{p10} * c_s c_d * c_{pe,10,H}$	-1.00	kN/m ²
External load I (x and y direction)	$F_{w,e,I} = q_{p10} * c_s c_d * c_{pe,10,I-}$	-0.29	kN/m ²
External load I (x and y direction)	$F_{w,e,I} = q_{p10} * c_s c_d * c_{pe,10,I+}$	+0.29	kN/m ²

A.2.2.3 Friction forces

Frictional forces result from the friction of the wind parallel to the external surfaces and can be calculated with the following formula: $F_{fr} = c_{fr} * q_{p10} * A_{fr}$

- Friction coefficient = $c_{fr} = 0.04$
- Area of the external surface parallel to the wind = $A_{fr} = 2 * d * b$, which applies to the system shown in Figure A-5 on the left. In the design, the friction force will be divided over two points on the roof beam, which can be seen in Figure A-5 on the right: one point load at the location where the roof beam meets the column and one point load halfway the roof beam. This means that for each point load, the following areas are used as reference:

$$\text{For the x-direction: } A_{fr} = d * b = \frac{15.81}{2} * 16.81 = 132.9 \text{ m}^2$$

$$\text{For the y-direction: } A_{fr} = = \frac{16.86}{2} * 15.81 = 132.9 \text{ m}^2$$

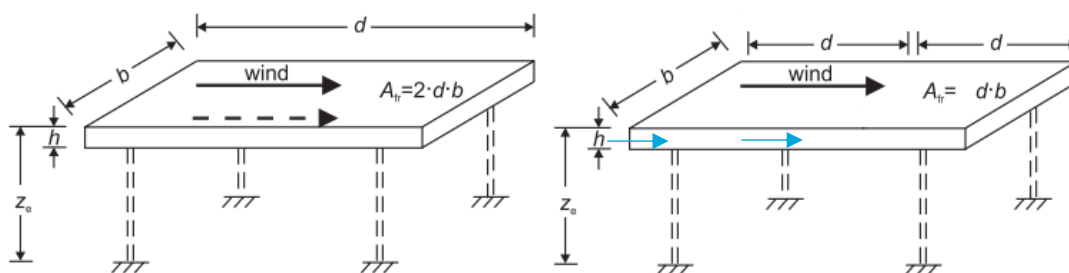


Figure A-5: Reference area for friction (NEN, 2005a)

This leads to the following friction force: $F_{fr} = 0.04 * 1.43 * 132.9 = 7.6 \text{ kN}$

A.2.2.4 Wind on the parapet

On the parapet itself, also a wind load needs to be considered. This is calculated in the following table. The largest part of the parapet is in area D, as shown in Figure A-6.

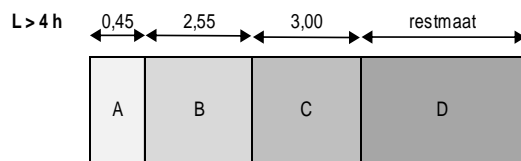


Figure A-6: Area distribution of a parapet on a roof (Royal HaskoningDHV Internal Document, 2020a)

Table A-8: Wind pressure on parapet

Parameter description	Parameter	Number	Unit
Nett pressure coefficient	$c_{net,D}$	1.20	-
External load D (x and y direction)	$F_{w,e,D} = q_{p10} * c_s c_d * c_{net,D}$	1.75	kN/m ²

A.2.2.5 Internal wind pressure

Finally, also the internal wind pressure needs to be investigated. This is shown in Table A-9.

Table A-9: Internal wind pressure

Description	Parameter	Number	Unit
General internal overpressure coefficient	$c_{p,i-}$	0.2	
General internal under pressure coefficient	$c_{p,i+}$	-0.3	
Internal load F (x and y direction)	$F_{w,i-} = q_{p10} * c_s c_d * c_{p,i-}$	0.29	kN/m ²
Internal load G (x and y direction)	$F_{w,i+} = q_{p10} * c_s c_d * c_{p,i+}$	-0.43	kN/m ²

A.2.3 Snow load

The snow load on the building is determined with EN 1991-1-3. The snow load is dependent upon the exact location of the building. This is currently unknown. Considering the range of snow loads throughout the search area in Europe, the characteristic snow load is set at 1.2 kN/m². This is the most prevalent value for seven countries where the altitude height is lower than 500 meters (above sea level).

Snow accumulation for the warehouse is not considered, as the warehouse is the highest building of the total distribution centre. This means that the characteristic snow load of 1.2 kN/m² is governing. This is visualised in Figure A-7.

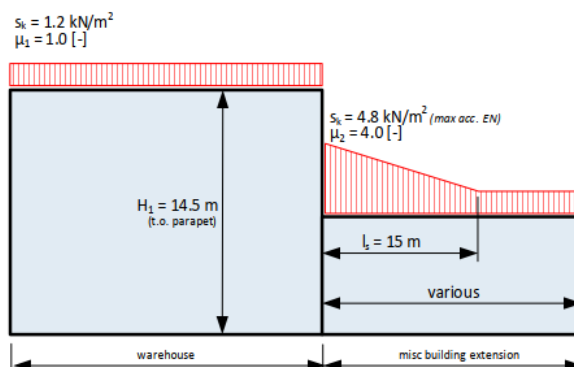


Figure A-7: Snow load on the roof of building (Royal HaskoningDHV Internal Document, 2020a)

B Base design

B.1 Schematisation of stabilisation system (as modelled)

Based upon the two sections shown in Figure 6-8 and Figure 6-9, the following schematisations are made. Some changes are incorporated in this schematisation:

- The mezzanine floor does not provide any lateral stiffness, so this is not modelled in the stability system. In the SCIA model, at the location of the mezzanine floor beams, a point load is modelled.
- The roof beams that are placed in an angle are modelled as straight roof beams. This is done because the angle of the roof beam is only 5%. This is small enough to be neglected in the design calculations. This also means that each column will have the same height. The least favourable situation, with a column height of 13.5 meters is modelled.
- In the design, traditional castellated HEB beams are used. Castellated beams have more height to provide enough strength, while at the same time they are light due to the openings in the beams. A traditional castellated beam is 1.5 times higher than the regular beam (Grünbauer, n.d.). It is not possible to model castellated beams in SCIA. Therefore, the castellated beams are translated into regular HEB beams by considering the elastic section modulus in the strong direction (W_y). This translation is provided in the following table. The original beam type is given in the castellated beam name; this means that an HEB 400-CB is made from a regular HEB 400 element.

Table B-1: Translation of castellated beam to a regular beam

Castellated beam	$W_{y,elastic}$ [$\times 10^3$ mm ³]	Regular beam	$W_{y,elastic}$ [$\times 10^3$ mm ³]
HEB 400-CB	4526	HEB 500	4287
HEB 450-CB	5564	HEB 550	4971
HEB 800-CB	13943	HEB 1000	12895

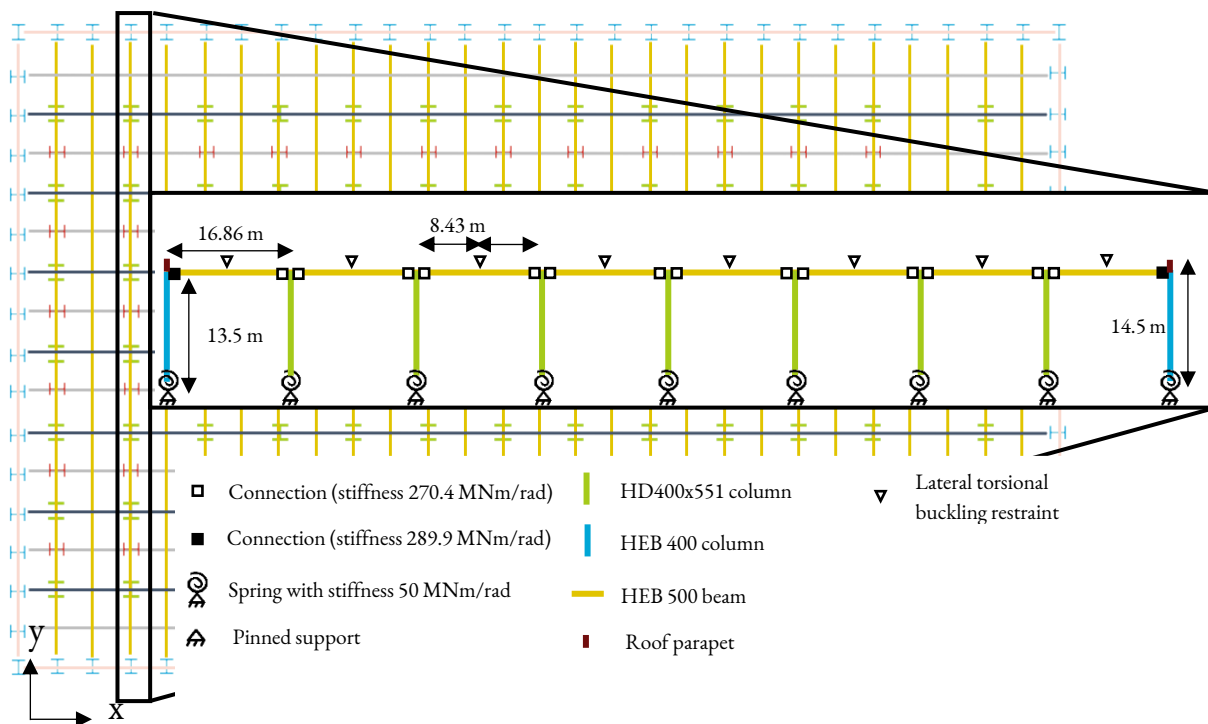


Figure B-1: Mechanics scheme of the stabilising portal frame in the y-direction
 In this figure, the portal frame structure is shown. The beams and columns are connected by relatively stiff connections. This stiffness is calculated in Appendix B.3.

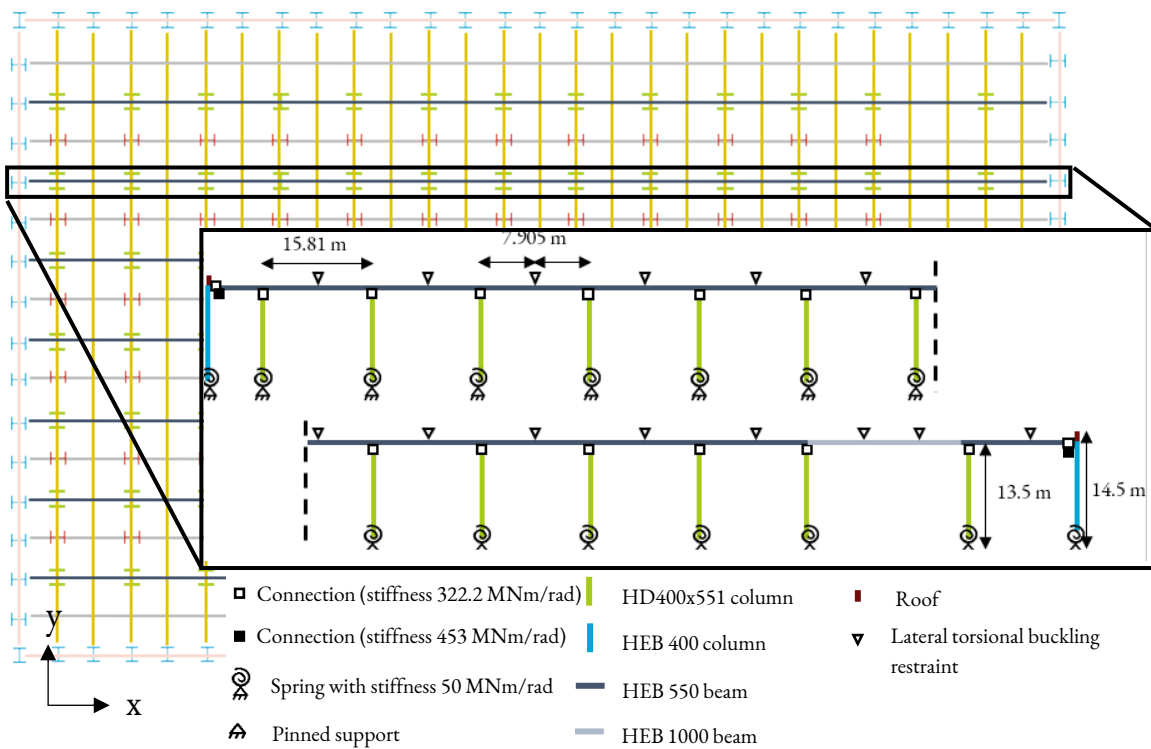


Figure B-2: Mechanics scheme of the stabilising portal frame in the x-direction

B.2 Loads

The explanations given in Appendix A.2 “Loads” also hold for this design alternative. In this Appendix, these loads are further calculated to be used in the SCIA model of this design.

B.2.1 Loads on the 2D model (y-direction)

The base design is investigated as a 3D model. However, in this research, the design will only be checked as a 2D model. Therefore, the loads per square meter need to be translated to loads per meter. This can be seen in Table B-2. In this table, the centre-to-centre distance is written down. This is based upon the lengths given in Figure 6-6. From this figure, it becomes clear that the centre-to-centre distance between the beams in y-direction is 7.905 m. However, the distance between columns is 15.81 meters. As the external wind load is only carried by the stability system, this centre-to-centre distance is set to 15.81 meters.

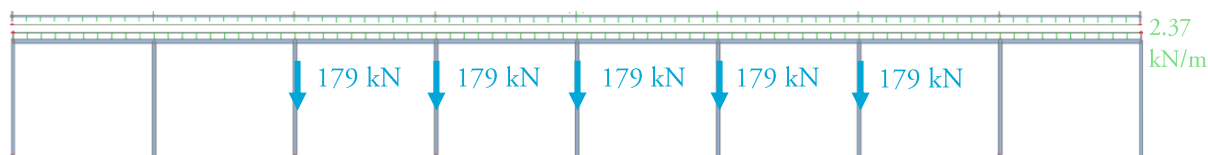
For clarity reasons, the loads have also been visualised in the figures below Table B-2.

Table B-2: Loads on portal frame (Y-direction)

Loads	Load	CTC	Line load
<i>Dead loads (vertical)</i>			
Self-weight	<i>Automatically calculated by SCIA</i>		
Purlins and panels	0,30 kN/m ²	7.905	2.37 kN/m
Mezzanine floor (on every column at 5.4 m)	179 kN	From Appendix B.4.4	
<i>Live loads 1 (vertical)</i>			
Maintenance load	0.4 kN/m ²	7.905	3.16 kN/m
Air unit (on top of every column)	30 kN		
Solar panels	0.25 kN/m ²	7.905	1.98 kN/m
Services	0.10 kN/m ²	7.905	0.79 kN/m
Mezzanine floor (on every column; at 5.4 m)	219 kN	From Appendix B.4.4	
<i>Live loads 2 (snow, vertical)</i>			
Snow load	1.2 kN/m ²	7.905	9.49 kN/m
<i>Live loads 3 (external wind, vertical)</i>			
Wind I (upwards)	0.29 kN/m ²	7.905	2.29 kN/m
Wind I (downwards)	0.29 kN/m ²	7.905	2.29 kN/m
<i>Live loads 4 (external wind, horizontal)</i>			
Friction due to wind	7.6 kN		
Wind D	0.98 kN/m ²	15.81	15.49 kN/m
Wind E	0.61 kN/m ²	15.81	9.64 kN/m
Wind D on parapet	1.75 kN/m ²	15.81	27.67 kN/m
<i>Live loads 5 (internal wind vertical+horizontal)</i>			
Wind F (internal, upwards (over pressure))	0.29 kN/m ²	7.905	2.29 kN/m
Wind G (internal, downwards (under pressure))	0.43 kN/m ²	7.905	3.40 kN/m

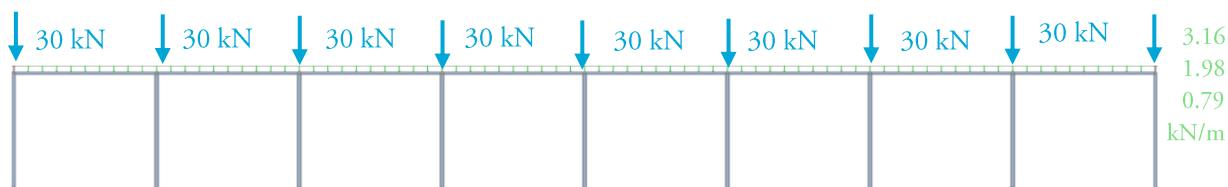
Dead loads

- Self-weight purlins and panels = 2.37 kN/m
- Self-weight beams and columns (automatically calculated by SCIA)
- Mezzanine dead load = 179 kN (see Appendix B.4.4)



Live loads 1

- Maintenance = 3.16 kN/m (short-term)
- Air unit = 30 kN (long-term)
- Solar panels = 1.98 kN/m (long-term)
- Services = 0.79 kN/m (long-term)
- Mezzanine live load = 219 kN (long-term, see Appendix B.4.4)



Live loads 2: Snow

- Snow = 9.49 kN/m



Live loads 3: External wind (vertical)

- Wind I - = 2.29 kN/m

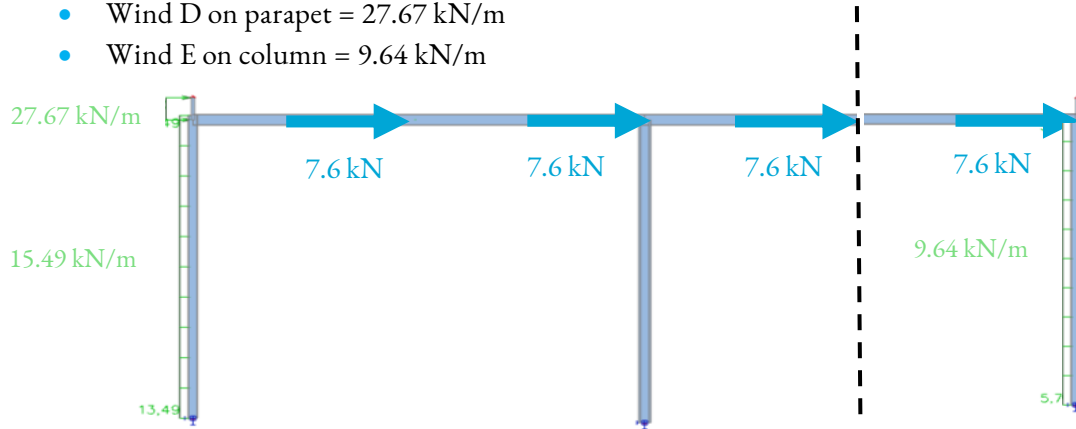


- Wind I + = 2.29 kN/m



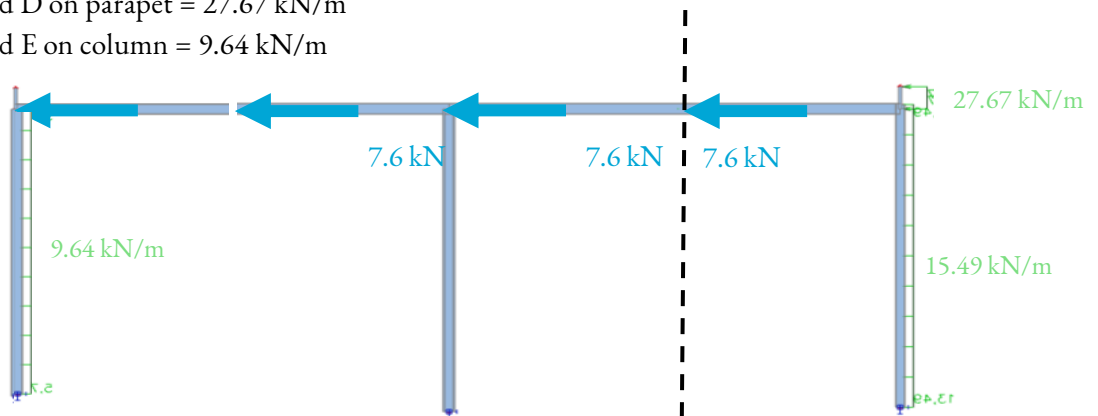
Live loads 4: Wind D+E

- Friction force on beam = 7.6 kN, halfway every beam
- Wind D on column = 15.49 kN/m
- Wind D on parapet = 27.67 kN/m
- Wind E on column = 9.64 kN/m



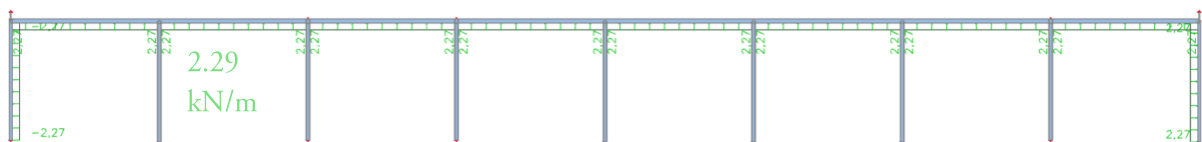
Live loads 4: Wind E+D

- Friction force on beam = 7.6 kN, halfway every beam
- Wind D on column = 15.49 kN/m
- Wind D on parapet = 27.67 kN/m
- Wind E on column = 9.64 kN/m

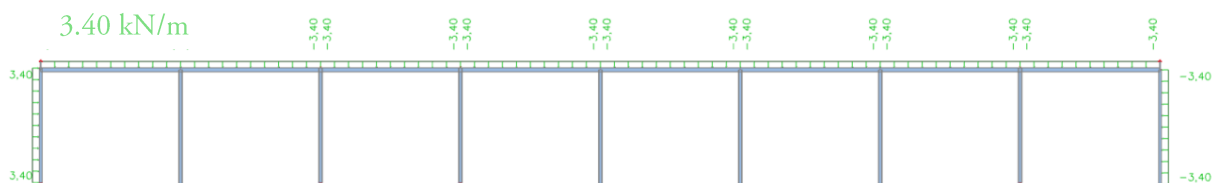


Live loads 5: Internal wind (vertical and horizontal)

- Wind F (over pressure) = 2.29 kN/m



- Wind G (under pressure) = 3.40 kN/m



B.2.1.1 Load combinations

To check the design, the load combinations given in Table B-3 are checked. In case a load case is referred to, the number shown in this table is used. For the permanent loads, a factor of 1.35 is applied and for the variable loads a factor of 1.5 is applied, this is shown in Table B-4 for the governing load cases. From this table, it can be found that the ψ -factors from Table A-2 are not applied in this case. This means that the most unfavourable load combinations are applied.

Table B-3: Reference of load cases and the numbering used in the SCIA model

Load case	Number (ULS)	Number (SLS)
Dead loads, live loads 1, live loads 3 (wind I-), live loads 4 (wind D+E)	ULS 1	SLS 11
Dead loads, live loads 1, live loads 3 (wind I+), live loads 4 (wind E+D)	ULS 2	SLS 12
Dead loads, live loads 1, live loads 3 (wind I-), live loads 4 (wind D+E), live loads 5 (wind G)	ULS 3	SLS 13
Dead loads, live loads 1, live loads 3 (wind I+), live loads 4 (wind E+D), live loads 5 (wind G)	ULS 4	SLS 14
Dead loads, live loads 1, live loads 3 (wind I-), live loads 4 (wind D+E), live loads 5 (wind F)	ULS 5	SLS 15
Dead loads, live loads 1, live loads 3 (wind I+), live loads 4 (wind E+D), live loads 5 (wind F)	ULS 6	SLS 16
Dead loads, live loads 1, live loads 2 (snow)	ULS 7	SLS 17

Table B-4: Governing load cases

Load case nr	Dead loads (ULS = 1.35; SLS = 1.0)	Live loads (ULS = 1.5; SLS = 1.0)
ULS 5	Dead loads (self-weight beams and columns, self-weight purlins and panels, mezzanine dead load)	Live loads 1 (maintenance, air unit, solar panels, services, mezzanine live loads) Live loads 3 (wind I-) Live loads 3 (wind D+E: friction, wind D on column, wind D on parapet, wind E) Wind F
ULS 6	Dead loads (self-weight beams and columns, self-weight purlins and panels, mezzanine dead load)	Live loads 1 (maintenance, air unit, solar panels, services, mezzanine live loads) Live loads 3 (wind I+) Live loads 4 (wind E+D: friction, wind D on column, wind D on parapet, wind E) Live loads 5 (wind F)
ULS 7	Dead loads (self-weight beams and columns, self-weight purlins and panels, mezzanine dead load)	Live loads 1 (maintenance, air unit, solar panels, services, mezzanine live loads) Snow load

B.2.2 Loads on the 2D model (x-direction)

Loads coming from the secondary roof beam are calculated as follows (where $L = 16.86$, which is the length of the secondary roof beam):

*Self-weight from secondary roof beam
(HEB 400-CB):*

$$q_{\text{own.secondarybeam}} := \frac{158 \text{ kN}}{100 \text{ m}} = 1.58 \cdot \frac{\text{kN}}{\text{m}}$$

$$q_{\text{purlins}} := 2.37 \frac{\text{kN}}{\text{m}}$$

$$q_{\text{dead}} := q_{\text{own.secondarybeam}} + q_{\text{purlins}} = 3.95 \cdot \frac{\text{kN}}{\text{m}}$$

$$V_{\text{Ed.dead}} := \frac{1}{2} \cdot q_{\text{dead}} \cdot L = 33.298 \cdot \text{kN}$$

Live loads from secondary roof beam:

$$q_{\text{maintenance}} := 3.16 \frac{\text{kN}}{\text{m}}$$

$$q_{\text{solar}} := 1.98 \frac{\text{kN}}{\text{m}}$$

$$q_{\text{services}} := 0.79 \frac{\text{kN}}{\text{m}}$$

$$q_{\text{live}} := q_{\text{maintenance}} + q_{\text{solar}} + q_{\text{services}} = 5.93 \frac{\text{kN}}{\text{m}}$$

$$V_{\text{Ed.live}} := \frac{1}{2} \cdot q_{\text{live}} \cdot L = 49.99 \text{ kN}$$

Also, the wind load on the secondary roof beam is transferred onto the primary roof beam. This is calculated as follows:

$$q_{\text{windG}} := 3.40 \frac{\text{kN}}{\text{m}} \quad \text{Downward wind force}$$

$$q_{\text{windF}} := -2.29 \frac{\text{kN}}{\text{m}} \quad \text{Upwards wind force}$$

$$q_{\text{windI}} := -2.29 \frac{\text{kN}}{\text{m}} \quad \text{External wind force}$$

$$V_{\text{Ed.wind.G}} := \frac{1}{2} \cdot q_{\text{windG}} \cdot L = 28.662 \cdot \text{kN}$$

$$V_{\text{Ed.wind.F}} := \frac{1}{2} \cdot q_{\text{windF}} \cdot L = -19.305 \cdot \text{kN}$$

$$V_{\text{Ed.wind.I}} := \frac{1}{2} \cdot q_{\text{windI}} \cdot L = -19.305 \cdot \text{kN}$$

Snow load on the secondary roof beam is transferred onto the primary roof beam as follows:

$$q_{\text{snow}} := 9.49 \frac{\text{kN}}{\text{m}}$$

$$V_{\text{Ed.snow}} := \frac{1}{2} \cdot q_{\text{snow}} \cdot L = 80.001 \text{ kN}$$

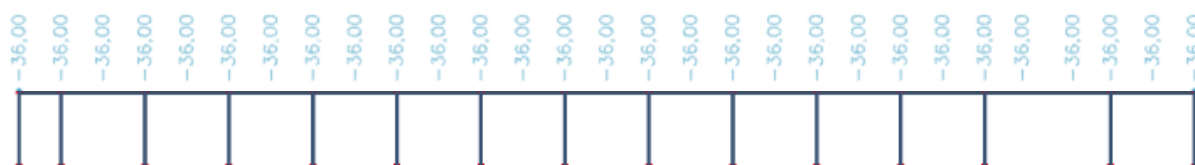
These calculations are included in Table B-5.

Table B-5: Loads on portal frame (X direction)

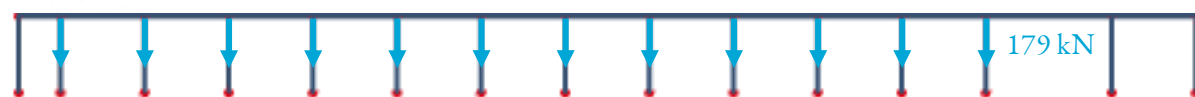
Loads	Surface load	CTC	Line load
<i>Dead loads (vertical)</i>			
Self-weight	<i>Automatically calculated by SCIA</i>		
Self-weight secondary roof beam	36 kN		
Mezzanine floor (on every column; at 5.4 m)	179 kN		
<i>Live loads 1 (vertical)</i>			
Air unit (on top of every column)	30 kN		
Live loads from secondary roof beam	50 kN		
Mezzanine floor (on every column; at 5.4 m)	219 kN		
<i>Live loads 2 (snow, vertical)</i>			
Snow load	80 kN		
<i>Live loads 3 (external wind, vertical)</i>			
Wind I- (upwards)	19 kN		
Wind I+ (downwards)	19 kN		
<i>Live loads 4 (external wind, horizontal)</i>			
Friction due to wind	7.6 kN		
Wind D	0.98 kN/m ²	16.86	16.52 kN/m
Wind E	0.61 kN/m ²	16.86	10.28 kN/m
Wind on parapet	1.75 kN/m ²	16.86	29.51 kN/m
<i>Live loads 5 (internal wind, vertical)</i>			
Wind F (internal, upwards (over pressure))	19 kN		
Wind G (internal, downwards (under pressure))	29 kN		
<i>Live loads 5 (internal wind, horizontal)</i>			
Wind F (internal, upwards (over pressure))	0.29 kN/m ²	8.43	2.45 kN/m
Wind G (internal, downwards (under pressure))	0.43 kN/m ²	8.43	3.62 kN/m

Dead loads

- Self-weight from secondary roof beams = 36 kN (derivation is found above Table B-5)
- Self-weight beams and columns (automatically calculated by SCIA)

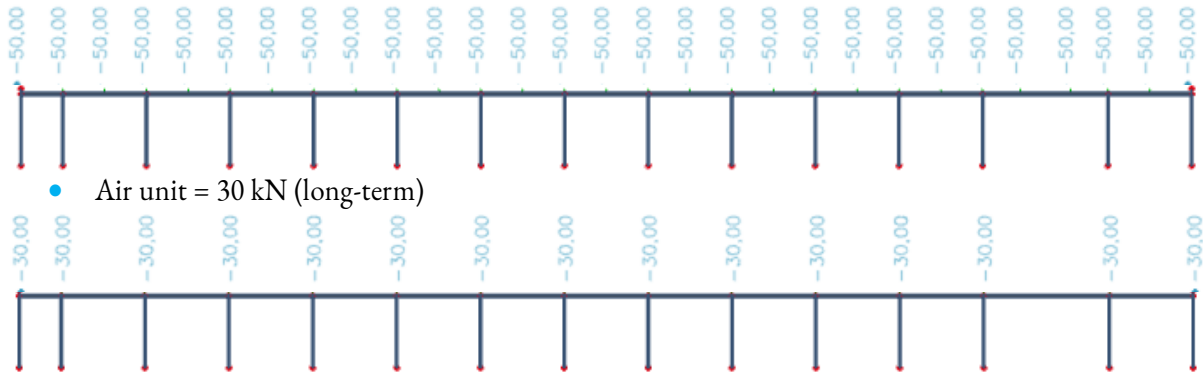


- Mezzanine dead load = 179 kN (see Appendix B.3.4)



Live loads 1

- Live load coming from secondary roof beams = 50 kN (derivation is found above Table B-5)
 - Live loads that are considered are: maintenance, solar panels, and services



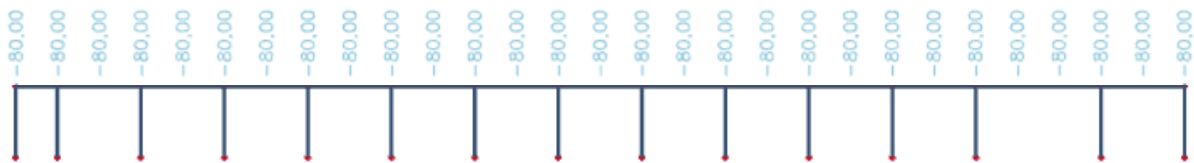
- Air unit = 30 kN (long-term)

- Mezzanine live load = 219 kN (long-term, see Appendix B.4.4)



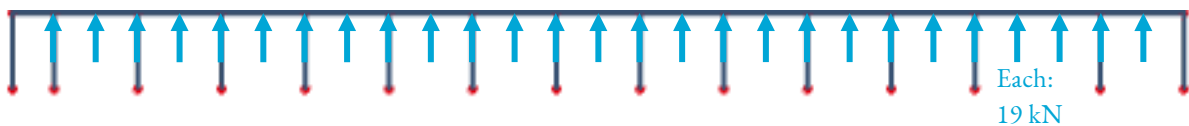
Live loads 2

Snow = 80 kN (derivation is found above Table B-5)



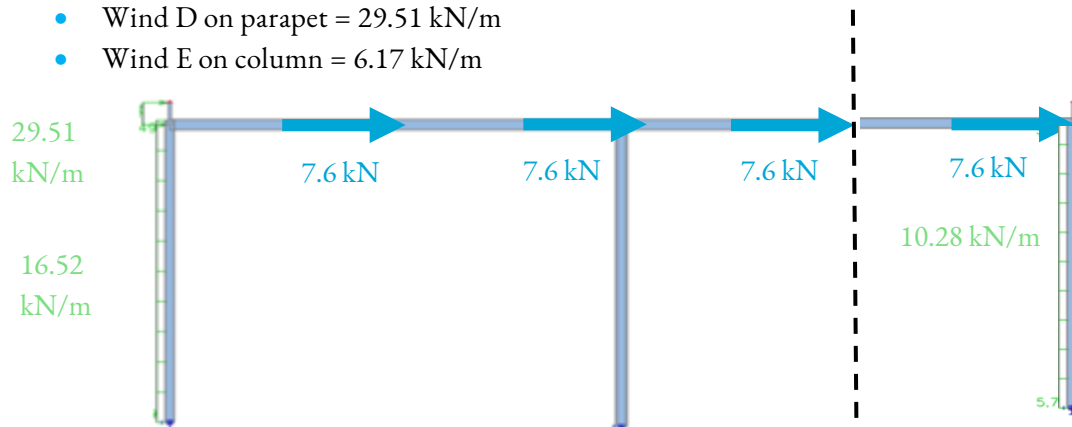
Wind loads 3: External wind (vertical)

- Wind on the roof: vertical upward load of 19 kN (derivation is found above Table B-5)



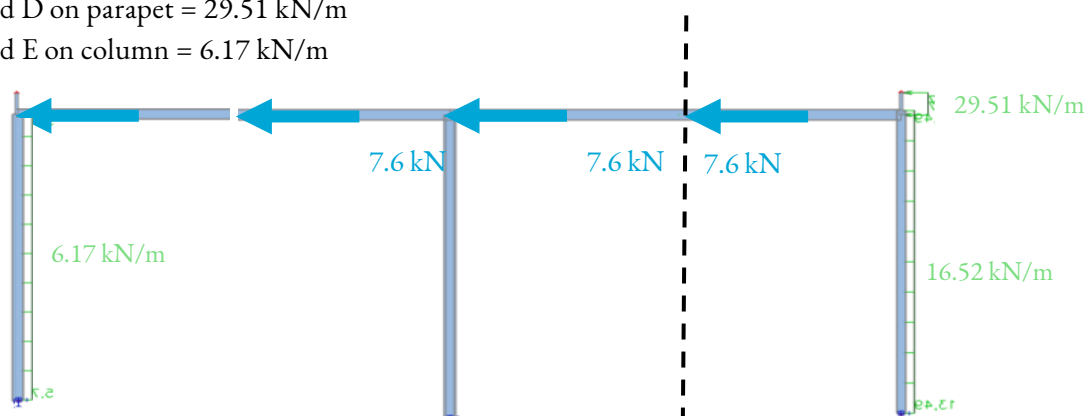
Wind loads 4: Wind D+E

- Friction force on beam = 7.6 kN, halfway every beam
- Wind D on column = 16.52 kN/m
- Wind D on parapet = 29.51 kN/m
- Wind E on column = 6.17 kN/m



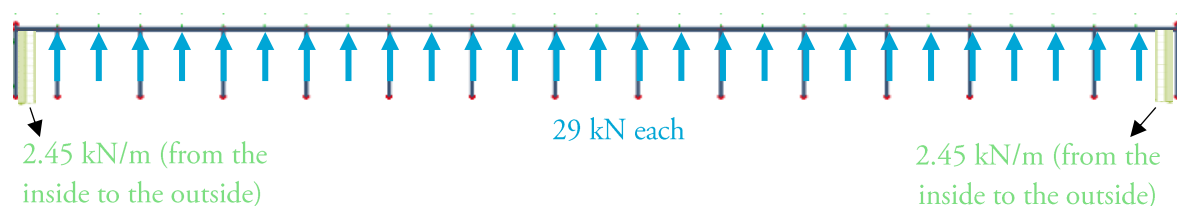
Wind loads 4: Wind E+D

- Friction force on beam = 7.6 kN, halfway every beam
- Wind D on column = 16.52 kN/m
- Wind D on parapet = 29.51 kN/m
- Wind E on column = 6.17 kN/m

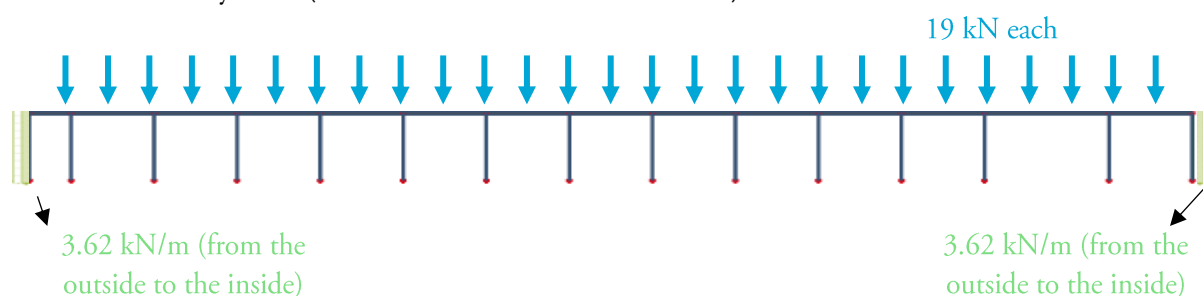


Live loads 5: Internal wind (vertical and horizontal)

- Wind F (overpressure) as distributed load on the columns
- Wind F (overpressure) as point load of 29 kN upwards on every beam, due to the secondary beam (derivation is found above Table B-5)



- Wind G (under pressure) as distributed load on the columns
- Wind G (underpressure) as point load of 19 kN downwards on every beam, due to the secondary beam (derivation is found above Table B-5)



B.2.2.1 Load combinations

The load combinations as written down in B.2.1.1 “Load combinations” are applied in the x-direction as well.

B.3 Connection design

In the base design, not much attention is given to the design of the connections. In this appendix, mezzanine floor beam connections, column base connection, and beam-column connections are further designed. For the beam-column connections, the initial design by Royal HaskoningDHV is first determined. It was found that these designs lead to insufficient stiffness, leading to a change in the base design. These final designs are used as input for the main load bearing structure.

B.3.1 Mezzanine floor beam connections

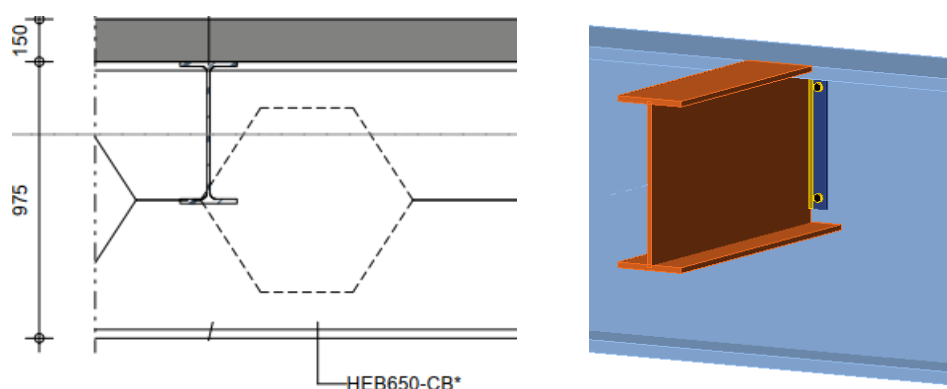


Figure B-3: Connection between the floor beam (IPE 450) and the secondary beam (HEB 650-CB) Left: design made by Royal HaskoningDHV, right: design made for this research, to be able to compare this design to the alternatives. This connection is not verified whether the end plate, bolts, and welds are strong enough. This drawing is only meant to provide insight in what the connection could look like in a regular design.

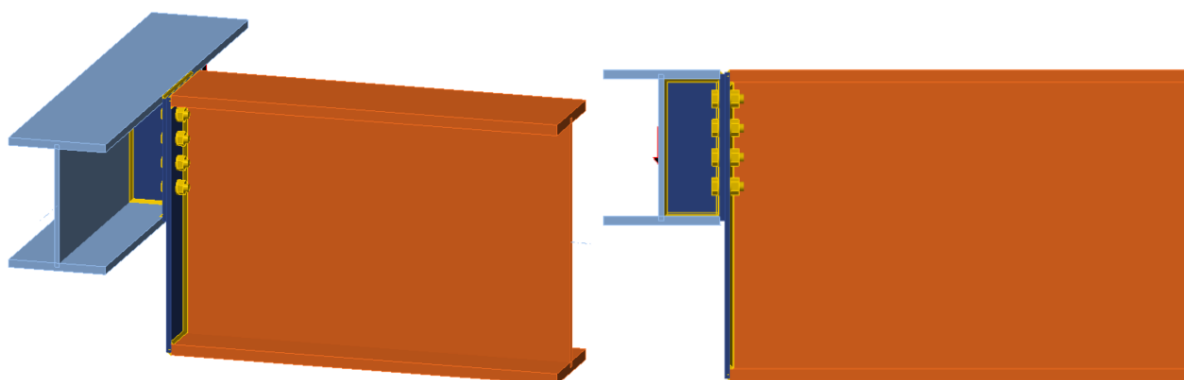


Figure B-4: Connection between the primary mezzanine beam (HEB 450, shown in blue) and the secondary mezzanine beam (HEB 650-CB, shown in orange) (own illustration, made with IDEA StatiCa) This connection is not verified whether the end plate, bolts, and welds are strong enough. This drawing is only meant to provide insight in what the connection could look like in a regular design.

B.3.2 Column base connection

For the column base connection, the stiffness of the footing and the stiffness of the column and the footing needs to be determined. This calculation is based upon Royal HaskoningDHV Internal Document (2020b).

A footing of 4 by 4 meter is schematised with a soil stiffness of 20 MN/m^3 . With a bending moment of 1000 kNm, the rotation of this footing is determined (2.182 mrad). This can be seen in Figure B-5.

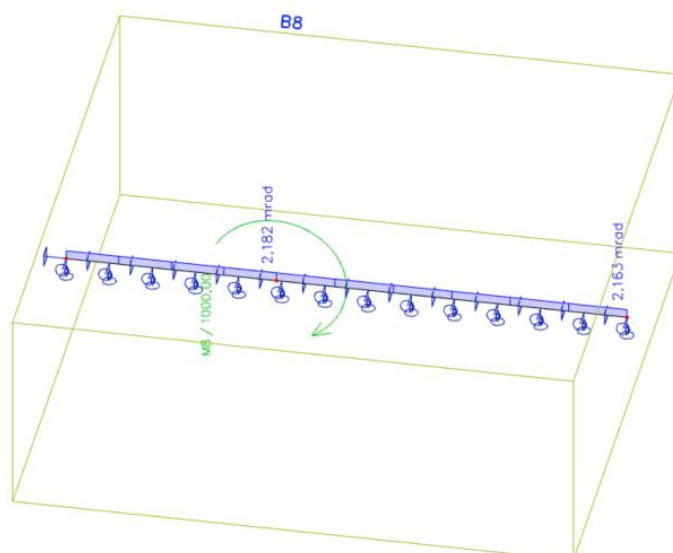


Figure B-5: Resulting deformation of the footing

Here, a bending moment of 1000 kN is placed on top of the footing. The line support is a flexible support based on the soil stiffness of 20 MN/m³. As the footing is 4 meters long, this results in a line support with stiffness 80 MNm/m².

This leads to the following calculation of the footing's spring stiffness:

$$\text{stiffness footing} = \frac{\text{bending moment}}{\text{rotation}} = \frac{1000 * 10^{-3}}{2.182 * 10^{-3}} = 458 \text{ MNm/rad}$$

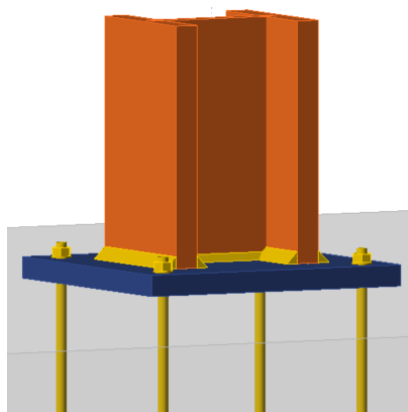


Figure B-6: Connection of the main column and the end plate with anchors on top of the concrete footing (own illustration, made with IDEA StatiCa)

In Figure B-6, the connection between the column and the footing is shown. The stiffness of this connection has been calculated with the software IDEA StatiCa and has led to a stiffness of 73.2 MNm/rad. The total stiffness of the connection is as follows:

$$\frac{1}{S_{\text{column base}}} = \frac{1}{S_{\text{footing}}} + \frac{1}{S_{\text{column and footing}}} = \frac{1}{458} + \frac{1}{72.3} = \frac{1}{0.016}$$

This leads to the stiffness of the column base of 62 MNm/rad. It is decided to apply a lower boundary of 50 MNm/rad for the stiffness. This choice has been made, as the stability of the building should mainly be gained from the stiffness of the beams and the columns (Royal HaskoningDHV Internal Document, 2020b).

B.3.3 Beam-column connections

B.3.3.1 Rule of thumb

The initial joint stiffness is determined based upon the simplification proposed by M. Steenhuis (Jaspart & Weynand, 2016) and is calculated with the following formula:

$$S_{j,appr} = \frac{E * z^2 * t_{fc}}{k_f} \quad \text{eq. B-1}$$

Table B-6: Explanation of parameters of eq. B-1

Parameter	Explanation
E	Elastic modulus, which is 210 MPa for steel
z	Moment arm (distance between the compression and tensile resultants)
t_{fc}	Thickness of the column flange
k_f	Flexibility factor depending upon connection type

Table B-7: Approximation of the moment arm for different types of connections

Type of connection	Moment arm	Source
Welded connection	$z = h_b$	(Staalbouwkundig Genootschap, 1999)
Extended end plate without a haunch	$z = h_b$	(Staalbouwkundig Genootschap, 1999)
Flush end plate without a haunch	$z = 0.8 * h_b$	(Staalbouwkundig Genootschap, 1999)
End plate without a haunch, only extended towards the bottom	$z = 0.9 * h_b$	Based upon the moment arm formula of the fully extended and flush end plate
Welded connection with haunch (height = half the height of the beam)	$z = 1.5 * h_b$	(Staalbouwkundig Genootschap, 1999)
Extended end plate with haunch (height = half the height of the beam)	$z = 1.5 * h_b$	(Staalbouwkundig Genootschap, 1999)
Flush end plate with haunch (height = half the height of the beam)	$z = 1.3 * h_b$	(Staalbouwkundig Genootschap, 1999)
End plate extended to the bottom, with haunch	$z = 1.4 * h_b$	Based upon the two above mentioned moment arm formulas

B.3.3.2 Connection design in x-direction

As can be seen in Figure 6-9, the beams in the x-direction are continuous beams, which are connected on top of the column. Drawings of this connection are shown in Figure B-7.

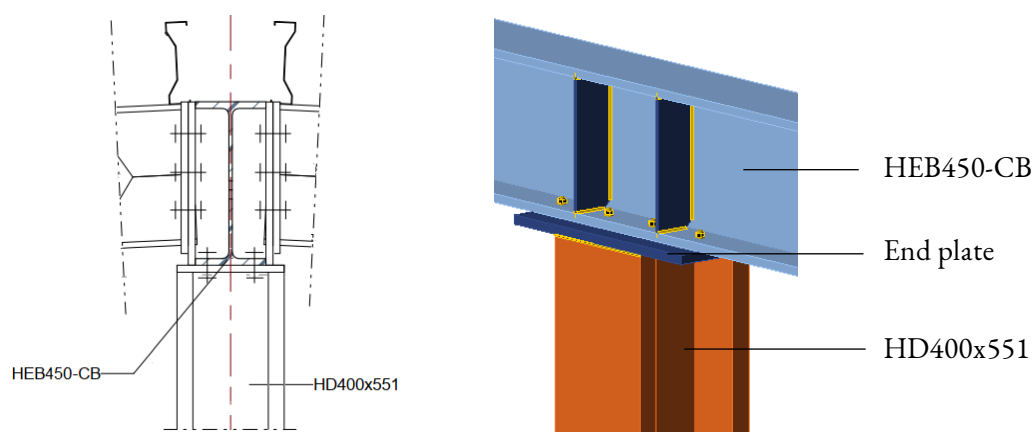


Figure B-7: Connection between the continuous roof beam and the main column
Left: (Royal HaskoningDHV Internal Document, 2020c), right: own illustration made with IDEA StatiCa

In Table B-8, the connection between the continuous beam and the façade column is schematised and calculated according to eq. B-1. The connection shown in Figure B-7 is schematised in Table B-8. As the actual design is a connection between a continuous beam and a column, eq. B-1 is changed into eq. B-2.

$$S_{j,appr} = \frac{E * z^2 * t_{flange\ beam}}{k_f} \quad \text{eq. B-2}$$

Table B-8: Flexibility factor for connections in Figure B-7 (x-direction) (Staalbouwkundig Genootschap, 1999)

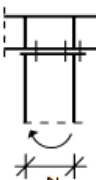
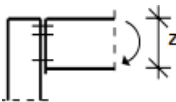
Type	Design	k_f
Continuous beam (x-direction) on top of main column: Extended end plate connection		8.5
Continuous beam (x-direction) connected to façade column: Single sided end plate connection		11.5

Table B-9: Stiffness calculation of the connection between the roof beam and the columns (x-direction)

Interior column		Exterior column	
E	210000	E	210000
Type of column	HD400x551	Type of beam	HEB 450-CB
Height column	455	Height beam	675
$z = h_c$	455	$z = 0.9 * h_b$	607.5
Beam type	HEB 450-CB	Column type	HEB 400
Beam flange thickness	26	Column flange thickness	24
k_f	8.5	k_f	11.5
$S_{j,appr} [MNm/rad]$	133.0	$S_{j,appr} [MNm/rad]$	161.7

The connection stiffness in the x-direction is relatively low. This means that the frame does act as a stiff frame, as it is meant to do. Therefore, it is proposed to add haunches to the connections. This leads to the design shown in Figure B-8 and stiffness shown in Table B-10.

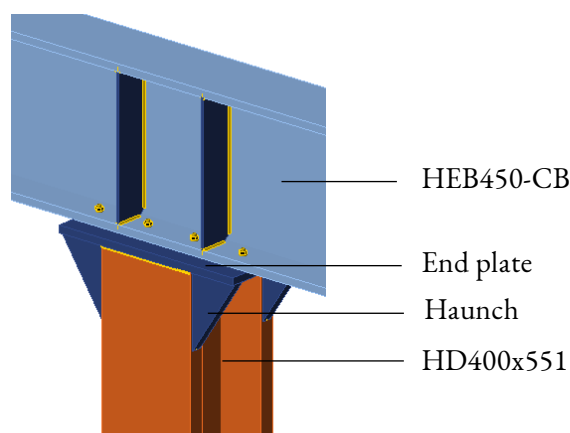


Figure B-8: Connection between the continuous roof beam and the main column including haunches (own illustration made with IDEA StatiCA)

Table B-10: Updated stiffness calculation of the connection between the roof beam and the columns (x-direction)

Interior column		Exterior column	
E	210000	E	210000
Type of column	HD400x551	Type of beam	HEB 450-CB
Height column	455	Height beam	675
$z = 1.5 * h_c$	682.5	$z = 1.4 * h_b$	945
Beam type	HEB 450-CB	Column type	HEB 400
Beam flange thickness	26	Column flange thickness	24
k_f	8.5	k_f	11.5
$S_{j,appr} [MNm/rad]$	299.2	$S_{j,appr} [MNm/rad]$	391.4

B.3.3.3 Connection design in y-direction

Figure 6-8 shows the layout of the roof beams in the y-direction. For this direction, the connection between the roof beam HEB 400-CB and the façade column HEB 400 is shown in Figure B-9 on the left. The connection of the roof beam HEB400-CB and the roof beam HEB500-CB on top of the main column is shown in Figure B-9 on the right.

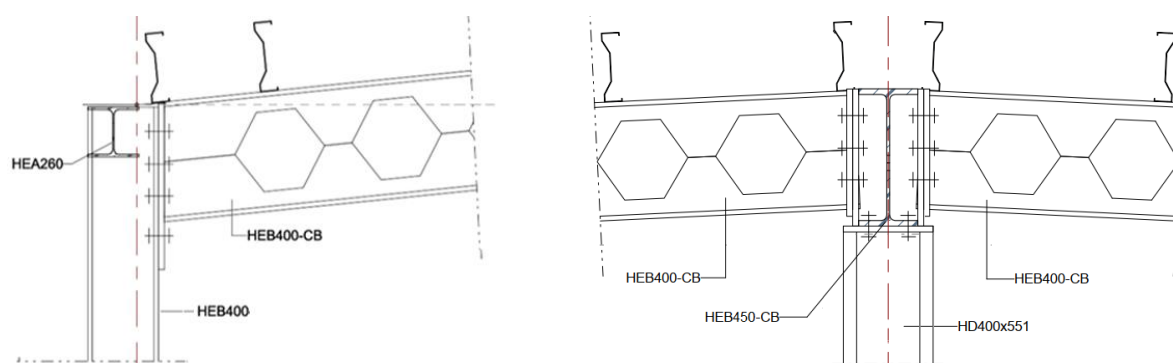


Figure B-9: Drawings of the connections for the y-direction

Left: Drawing of the roof beam in y-direction and the façade column; Right: Drawing of the roof beam in y-direction and the roof beam in x-direction, which is on top of the main column (Royal HaskoningDHV Internal Document, 2020c)

The connections shown in Figure B-9 are schematised in Table B-11. For the connection on the right of Figure B-9, no schematisation exists. Therefore, a combination of the extended end plate connection ($k_f = 8.5$; Table B-9) and a double sided flush end plate connection ($k_f = 6$; Table B-11) is used to schematise this connection. This is further explained after these tables.

Table B-11: Flexibility factor for connections in Figure B-9 (y-direction) (Staalbouwkundig Genootschap, 1999)


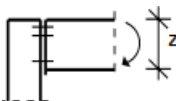
Type	Design	k_f
Roof beam (y-direction) connected to roof beam (x-direction): Double sided flush end plate		6
Roof beam (y-direction) connected to façade column: Single sided end plate connection		11.5

Table B-12: Stiffness calculation of the connection between the roof beam and the columns (y-direction)

Interior column (part 1)		Exterior column	
E	210000	E	210000
Type of column	HEB 400-CB	Type of beam	HEB 400-CB
Height column	600	Height beam	600
$z = 0.9 * h_c$	540	$z = 0.9 * h_b$	540
Beam type	HD 400x551	Column type	HEB 400
Beam flange thickness	68	Column flange thickness	24
k_f	6	k_f	11.5
$S_{j,appr}$ [MNm/rad]	694 → 118.7 (see below)	$S_{j,appr}$ [MNm/rad]	127.8

For the interior column, the final stiffness is calculated as follows:

$$\frac{1}{S_{y-direction}} = \frac{1}{S_{beam-column(y)}} + \frac{1}{S_{beam-column(x)}} = \frac{1}{143.2} + \frac{1}{694} = 0.008$$

$$S_{y-direction} = 118.7 \text{ MNm/rad}$$

The connection stiffness in the y-direction is relatively low. This means that the frame does not act as a stiff frame, as it is meant to do. Therefore, it is proposed to add haunches to the connections. An example of such a design is shown in Figure B-10. This leads to the design shown in Figure B-11 and to the stiffness shown in Table B-10.

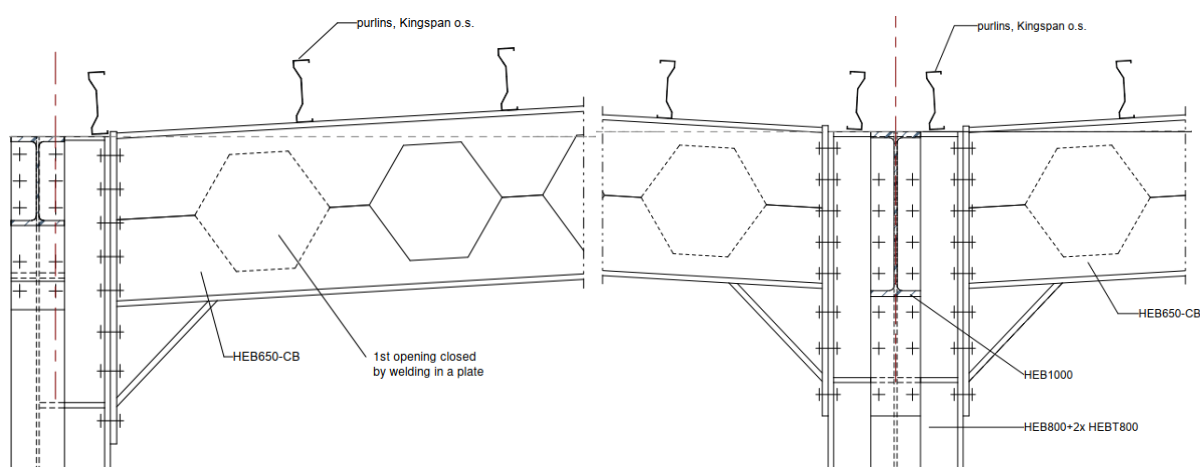


Figure B-10: Details of connections between column and roof beams for another building of the same client. These drawings are made for another building, but they do provide insight in what the design could look like with haunches included. Left: Drawing of the roof beam and the façade column; Right: Drawing of the internal connection between roof beams and column. In this design, the roof beam is not continuous. (Royal HaskoningDHV Internal Document, 2020b)

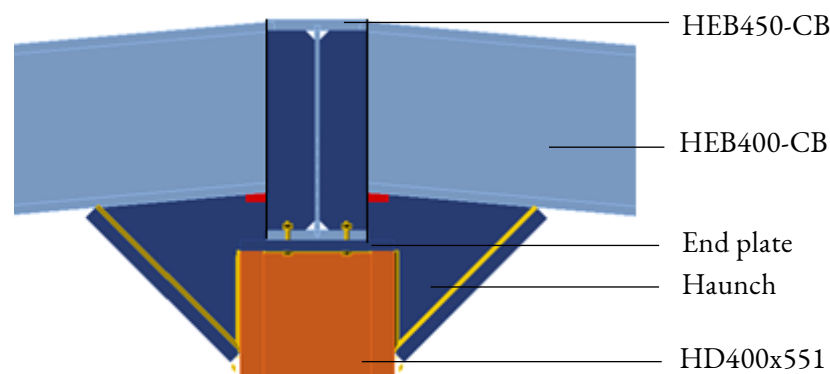


Figure B-11: Final design for the connection between the main column and roof beams
(own illustration made with IDEA StatiCA)

Table B-13: Updated stiffness calculation of the connection between the roof beam and the columns (y-direction)

Interior column		Exterior column	
E	210000	E	210000
Type of column	HEB 400-CB	Type of beam	HEB 400-CB
Height column	600	Height beam	600
$z = 1.4 * h_c$	840	$z = 1.4 * h_c$	840
Beam type	HD 400x551	Column type	HEB 400
Beam flange thickness	68	Column flange thickness	24
k_f	6	k_f	11.5
$S_{j,appr}$ [MNm/rad]	1679 \rightarrow 254 (see below)	$S_{j,appr}$ [MNm/rad]	309.2

For the interior column, the final stiffness is calculated as follows:

$$\frac{1}{S_{y-direction}} = \frac{1}{S_{beam-column(y)}} + \frac{1}{S_{beam-column(x)}} = \frac{1}{299.2} + \frac{1}{1679} = 0.003938$$

$$S_{y-direction} = 254.0 \text{ MNm/rad}$$

B.3.4 Continuous beam design

Due to the larger span in the x-direction, a larger beam is necessary. However, this is modelled as a continuous beam. This can be done, as the connection as shown in the following figures is applied. This shows that it is possible to connect a smaller and larger beam to be a continuous beam. This insight will also be used for the other design alternatives.

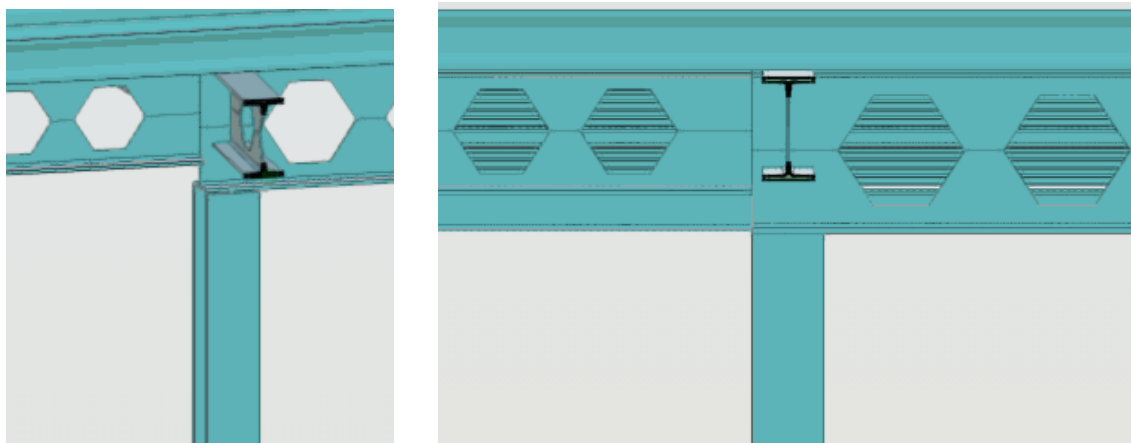


Figure B-12: Continuous beam with two sizes of beams (left: 3D view, right: 2D view)
(Royal HaskoningDHV Internal Document, 2020c)

B.4 Mezzanine floor design

The following pages contain the mezzanine floor design. First, some general remarks are given, which is followed by calculations of the mezzanine floor beams and column.

The secondary beam is a castellated beam (Appendix paragraph B.4.2 “Mezzanine secondary beam check”). However, a regular HEB beam is modelled instead of the castellated beam. This is done in the same manner as explained in Appendix B.1 “Schematisation of stabilisation system (as modelled)” and results in a regular HEB 800 beam, as can be seen in the following table.

Table B-14: Translating a castellated beam to a regular beam with the section modulus in the strong direction
This has been done for the calculation in SCIA (Royal HaskoningDHV Internal Document, 2019)

Castellated beam	$W_{y,elastic}$ [$\times 10^3$ mm ³]	Regular beam	$W_{y,elastic}$ [$\times 10^3$ mm ³]
HEB 650-CB	10094	HEB 800	8977

The chosen column profile leads to some overcapacity (Appendix paragraph B.4.4 “Mezzanine column check”). This is because the mezzanine floor column is based upon the connection design, an example of such a connection is shown in Figure B-13. Here, the width of the primary beam is governing. As the width of the IPE 500 primary beam is 200 mm, the column must at least be made from an HEB 240 profile.

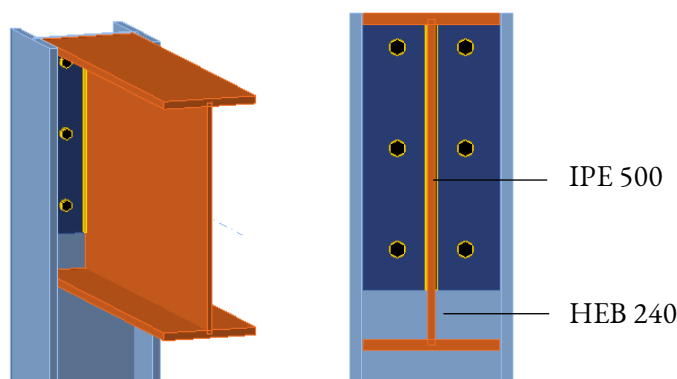


Figure B-13: Example of a connection between the mezzanine primary beam and a mezzanine column
(own illustration, made with IDEA StatiCa)

On the left side, the 3D-view of the connection is shown, on the right a front view is given. This connection is not verified whether the end plate, bolts, and welds are strong enough. This drawing is only meant to provide insight in what the connection could look like in a regular design.

B.4.1 Mezzanine floor beam check

$$L_w := 8.430\text{m}$$

Define cross section

Steel strength

$$f_y := 355\text{MPa}$$

$$E := 210\text{GPa}$$

$$G_v := 81000 \frac{\text{N}}{\text{mm}^2}$$

$$\varepsilon_{yk} := \sqrt{\frac{235\text{MPa}}{f_y}} = 0.814$$

IPE 450

$$h := 450\text{mm}$$

$$b := 190\text{mm}$$

$$t_w := 9.4\text{mm}$$

$$t_f := 14.6\text{mm}$$

$$r := 21\text{mm}$$

$$\text{weight} := 77.6 \frac{\text{kg}}{\text{m}}$$

$$A_{\text{tot}} := 9882\text{mm}^2$$

$$h_w := h - 2t_f - 2r = 0.379\text{m}$$

$$W_{\text{ply}} := 1702 \cdot 10^3 \text{mm}^3$$

$$W_{\text{plz}} := 276.4 \cdot 10^3 \text{mm}^3$$

Plastic section modulus

$$I_y := 482.0 \cdot 10^6 \text{mm}^4$$

$$I_z := 16.76 \cdot 10^6 \text{mm}^4$$

$$I_w := 780970 \cdot 10^6 \cdot \text{mm}^6$$

$$I_t := 660.5 \cdot 10^3 \text{mm}^4$$

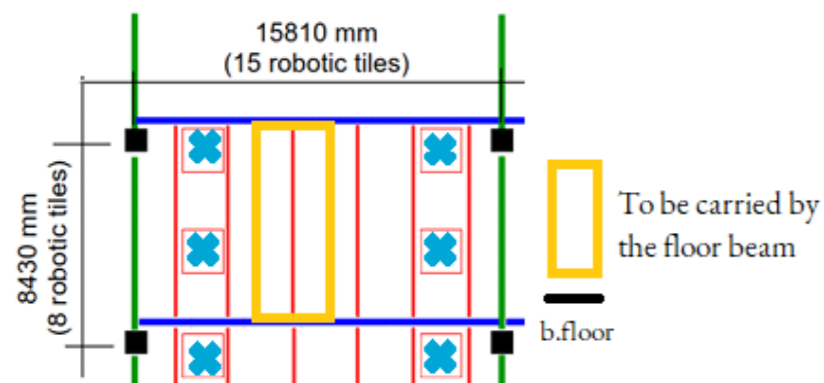
Warping and torsion constant

$$\gamma_{M0} := 1$$

$$\gamma_{M1} := 1$$

Safety factors

Loads



$$b_{\text{floor}} := 2635\text{mm}$$

$$G_{\text{self.floor}} := 3.10 \frac{\text{kN}}{\text{m}}$$

Self-weight ComFlor75 in composite state

$$G_{\text{self.beam}} := \text{weight} \cdot 9.81 \frac{\text{N}}{\text{kg}} = 0.761 \frac{\text{kN}}{\text{m}}$$

$$Q_{\text{load1}} := 3 \frac{\text{kN}}{\text{m}}$$

Robotic live load

$$Q_{\text{load2}} := 0.25 \frac{\text{kN}}{\text{m}}$$

Services on floor

$$q_G := (G_{\text{self.floor}}) \cdot b_{\text{floor}} + G_{\text{self.beam}} = 8.93 \frac{\text{kN}}{\text{m}}$$

$$q_Q := (Q_{\text{load1}} + Q_{\text{load2}}) \cdot b_{\text{floor}} = 8.564 \frac{\text{kN}}{\text{m}}$$

$$q_{\text{SLS}} := q_G + q_Q = 17.494 \frac{\text{kN}}{\text{m}}$$

$$q_{\text{ULS}} := 1.35 \cdot q_G + 1.5 \cdot q_Q = 24.901 \frac{\text{kN}}{\text{m}}$$

$$M_{\text{Ed.SLS}} := \frac{1}{8} \cdot q_{\text{SLS}} \cdot L^2 = 155.397 \cdot \text{kN} \cdot \text{m}$$

$$M_{\text{Ed.ULS}} := \frac{1}{8} \cdot q_{\text{ULS}} \cdot L^2 = 221.197 \cdot \text{kN} \cdot \text{m}$$

$$V_{\text{Ed.SLS}} := \frac{1}{2} \cdot q_{\text{SLS}} \cdot L = 73.735 \cdot \text{kN}$$

$$V_{\text{Ed.ULS}} := \frac{1}{2} \cdot q_{\text{ULS}} \cdot L = 104.957 \cdot \text{kN}$$

Determination of cross section class

Flanges:

$$c_f := \frac{1}{2} \cdot (b - t_w) - r = 69.3 \cdot \text{mm}$$

$$\frac{c_f}{t_f} = 4.747$$

Cross section check:

$$\frac{c_f}{t_f} \leq 9\varepsilon = 1 \quad \frac{c_f}{t_f} \leq 10\varepsilon = 1$$

Conclusion: Flange is class 1

Web:

The beam is subjected to bending

$$c_w := h - 2 \cdot t_f - 2 \cdot r = 378.8 \cdot \text{mm}$$

$$\frac{c_w}{t_w} \leq 72 \cdot \varepsilon = 1$$

Conclusion: Web is class 1

Flange and web:

The cross section is class 1, so plastic global analyses and plastic cross section analysis can be performed.

Plastic moment resistance

$$M_{pl} := \frac{W_{ply} \cdot f_y}{\gamma_{M0}} = 604.21 \cdot \text{kN} \cdot \text{m}$$

Plastic moment capacity

$$UC_{moment} := \frac{M_{Ed,ULS}}{M_{pl}} = 0.366$$

$$UC_{moment} \leq 0.8 = 1$$

Shear resistance

$$A_{v1} := A_{tot} - 2 \cdot b \cdot t_f + (t_w + 2 \cdot r) \cdot t_f = 5.084 \times 10^3 \cdot \text{mm}^2$$

$$A_v := \max(A_{v1}, h_w \cdot t_w) = 5.084 \times 10^3 \cdot \text{mm}^2$$

$$V_{plRd} := \frac{\left[A_v \cdot \left(\frac{f_y}{3} \right) \right]}{\gamma_{M0}} = 1.042 \times 10^3 \cdot \text{kN}$$

$$UC_{shear} := \frac{V_{Ed,ULS}}{V_{plRd}} = 0.101$$

$$UC_{shear} \leq 0.8 = 1$$

V_{Ed} is smaller than $0.5 \cdot V_{plRd}$ so the moment resistance does not have to be calculated based on a reduced yield strength in the web.

Flexural buckling and lateral torsional buckling

Flexural buckling can occur due to normal forces on the beam, but as no normal force is exerted on the beam, flexural buckling can be disregarded.

Lateral torsional buckling can occur due to bending moments on the beam. However, due to the floors, this will be prevented and therefore, it can be disregarded.

Deflection

$$w := \frac{5}{384} \cdot q_{SLS} \cdot \frac{L^4}{E \cdot I_y} = 0.011 \text{ m}$$

$$w_{max} := \frac{L}{360} = 0.023 \text{ m}$$

$$UC_{deflection} := \frac{w}{w_{max}} = 0.485$$

$$UC_{deflection} \leq 0.85 = 1$$

Overview of UC

$$UC_{shear} = 0.101$$

$$UC_{deflection} = 0.485$$

$$UC_{moment} = 0.366$$

$$UC_{deflection,robotic} = 0.429$$

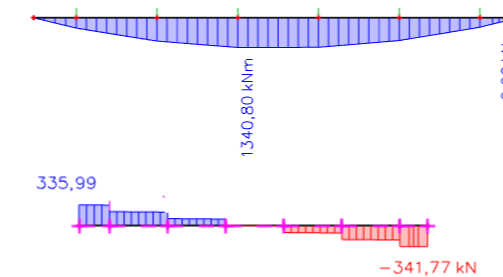
B.4.2 Mezzanine secondary beam check**Input**

From the floor beam calculation:

- Dead loads (ComFlor 75 and floor beam) = 37.64 kN/m²
- Live loads (Services and robotic load on the floor) = 36.10 kN/m²

Define member

$$L_w := 15.810 \text{ m}$$

Loads (ULS; from SCIA)

$$M_{Ed} := 1340.80 \text{ kN} \cdot \text{m}$$

$$V_{Ed} := 341.77 \text{ kN}$$

Define cross section

HEB 650CB = HEB800

$$h := 800 \text{ mm} \quad b := 300 \text{ mm} \quad t_w := 17.5 \text{ mm} \quad t_f := 33 \text{ mm} \quad r := 30 \text{ mm}$$

$$\text{weight} := 229 \frac{\text{kg}}{\text{m}}$$

$$A_{tot} := 33418 \text{ mm}^2$$

$$f_y := 355 \text{ MPa} \quad \xi_w := \sqrt{\frac{235 \text{ MPa}}{f_y}} = 0.814$$

$$h_w := h - 2t_f - 2r = 0.674 \text{ m}$$

$$E := 210 \text{ GPa} \quad G_v := 81000 \frac{\text{N}}{\text{mm}^2}$$

$$W_{ply} := 10230 \cdot 10^3 \text{ mm}^3 \quad W_{plz} := 1553 \cdot 10^3 \text{ mm}^3$$

Plastic section modulus

$$I_y := 3591 \cdot 10^6 \text{ mm}^4 \quad I_z := 149.0 \cdot 10^6 \text{ mm}^4$$

$$I_w := 21617000 \cdot 10^6 \cdot \text{mm}^6 \quad I_t := 9621 \cdot 10^3 \text{ mm}^4$$

Warping and torsion constant

$$\gamma_{M0} := 1 \quad \gamma_{M1} := 1$$

Cross section check**Outstand flanges**

$$c_f := \frac{1}{2} \cdot (b - t_w) - r = 111.25 \text{ mm}$$

$$\frac{c_f}{t_f} = 3.371$$

Cross section check:

$$\frac{c_f}{t_f} \leq 9\epsilon = 1 \quad \frac{c_f}{t_f} \leq 10\epsilon = 1$$

Conclusion: Flange is class 1

Web

Due to the forces on beam 1: bending and compression

Plastic bending resistance (try if ok with class):

Due to symmetry: $\alpha := 0.5$

For α is smaller or equal to 0.5:

$$c_w := h - 2 \cdot t_f - 2 \cdot r = 674 \text{ mm}$$

$$\frac{c_w}{t_w} \leq \frac{36 \cdot \epsilon}{\alpha} = 1$$

Conclusion: Web is class 1

Flange and web

The cross section is class 1, so plastic global analyses and plastic cross section analysis can be performed.

Plastic moment resistance

$$M_{pl} := \frac{W_{ply} \cdot f_y}{\gamma_{M0}} = 3.632 \times 10^3 \cdot \text{kN} \cdot \text{m} \quad \text{Plastic moment capacity}$$

$$UC_{\text{moment}} := \frac{M_{Ed}}{M_{pl} \cdot \gamma_{M0}} = 0.369$$

Shear resistance

$$A_{v1} := A_{\text{tot}} - 2 \cdot b \cdot t_f + (t_w + 2 \cdot r) \cdot t_f = 1.618 \times 10^4 \cdot \text{mm}^2$$

$$A_v := \max(A_{v1}, h_w \cdot t_w) = 0.016 \text{ m}^2$$

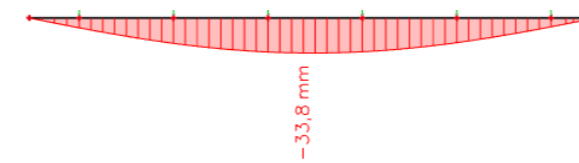
$$V_{plRd} := \frac{\left[A_v \cdot \left(\frac{f_y}{3 \cdot 0.5} \right) \right]}{\gamma_{M0}} = 3.315 \times 10^3 \cdot \text{kN}$$

$$UC_{\text{shear}} := \frac{V_{Ed}}{V_{plRd}} = 0.103 \quad UC_{\text{shear}} \leq 0.85 = 1$$

V_{Ed} is smaller than $0.5 \cdot V_{plRd}$ so the moment resistance does not have to be calculated based on a reduced yield strength in the web.

Deflection

Will be checked with SCIA as multiple point loads are present on the beam, which cannot be represented by a simple forget me not.



$$w := 33.8 \text{ mm}$$

$$w_{\text{max}} := \frac{L}{360} = 0.044 \text{ m}$$

$$UC_{\text{deflection}} := \frac{w}{w_{\text{max}}} = 0.77$$

$$UC_{\text{deflection}} \leq 0.8 = 1$$

Unity checks overview

$$UC_{\text{shear}} = 0.103$$

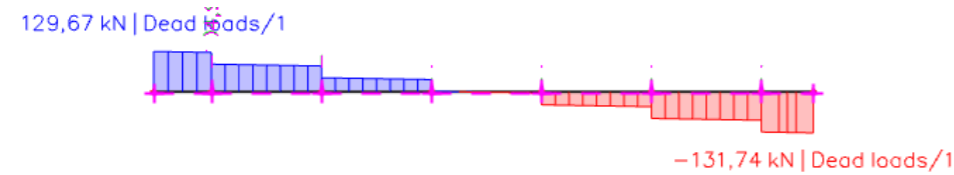
$$UC_{\text{moment}} = 0.369$$

$$UC_{\text{deflection}} = 0.77$$

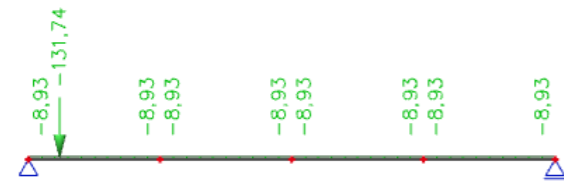
B.4.3 Mezzanine primary beam check

Input from secondary floor beam

Dead loads:



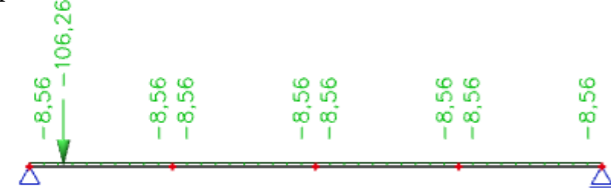
The extreme value on the secondary floor beam is used as input on the primary load beam. Furthermore, the primary floor beam needs to carry a part of the floor directly. The same calculation as performed for the floor beam is applied. Together, this leads to the following dead loads on the primary floor beam:



Live loads:

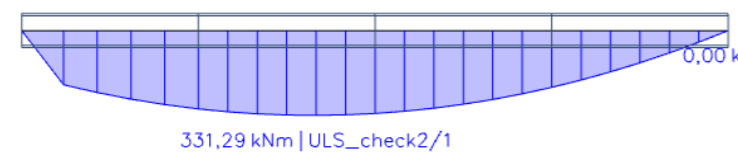


The extreme value on the secondary floor beam is used as input on the primary load beam. Furthermore, the primary floor beam needs to carry a part of the floor directly. The same calculation as performed for the floor beam is applied. Together, this leads to the following live loads on the primary floor beam:



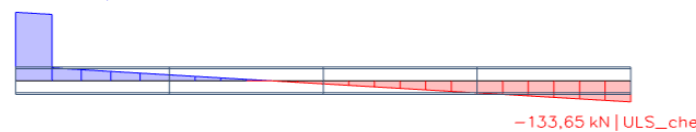
Loads (ULS; from SCIA)

From the input, the maximum moment and shear forces on the beam are calculated.



$$M_{Ed} := 331.29 \text{ kN} \cdot \text{m}$$

430.90 kN | ULS_check2/1



$$V_{Ed} := 430.90 \text{ kN}$$

Define member

$$L_w := 8.430 \text{ m}$$

Define cross section

$$f_y := 355 \text{ MPa}$$

$$\epsilon_s := \sqrt{\frac{235 \text{ MPa}}{f_y}} = 0.814$$

$$\gamma_{M0} := 1$$

HEB400

$$h := 400 \text{ mm}$$

$$b := 300 \text{ mm}$$

$$r := 27 \text{ mm}$$

$$A_{tot} := 19778 \text{ mm}^2$$

$$W_{ply} := 3232 \cdot 10^3 \text{ mm}^3$$

$$I_y := 576.8 \cdot 10^6 \text{ mm}^4$$

$$I_w := 3751100 \cdot 10^6 \text{ mm}^6$$

$$G_v := 81000 \frac{\text{N}}{\text{mm}^2}$$

$$\gamma_{M1} := 1$$

$$t_w := 13.5 \text{ mm} \quad E := 210 \text{ GPa}$$

$$t_f := 24 \text{ mm}$$

$$h_w := h - 2t_f - 2r = 0.298 \text{ m}$$

$$\text{weight} := 155.3 \frac{\text{kg}}{\text{m}}$$

$$W_{plz} := 1104 \cdot 10^3 \text{ mm}^3 \quad \text{Plastic section modulus}$$

$$I_z := 108.2 \cdot 10^6 \text{ mm}^4$$

$$I_t := 3611 \cdot 10^3 \text{ mm}^4 \quad \text{Warping and torsion constant}$$

Cross section check

Outstand flanges

$$c_f := \frac{1}{2} \cdot (b - t_w) - r = 116.25 \text{ mm}$$

$$\frac{c_f}{t_f} = 4.844$$

Cross section check:

$$\frac{c_f}{t_f} \leq 9\epsilon = 1 \quad \frac{c_f}{t_f} \leq 10\epsilon = 1 \quad \text{Conclusion: Flange is class 1}$$

Web

Due to the forces on the beam: bending and compression

Plastic bending resistance (try if ok with class):

Due to symmetry: $\alpha := 0.5$

For α is smaller or equal to 0.5:

$$c_w := h - 2 \cdot t_f - 2 \cdot r = 298 \text{ mm}$$

$$\frac{c_w}{t_w} \leq \frac{36 \cdot \epsilon}{\alpha} = 1 \quad \text{Conclusion: Web is class 1}$$

The cross section is class 1, so plastic global analyses and plastic cross section analysis can be performed.

Plastic moment resistance

$$M_{pl} := \frac{W_{ply} \cdot f_y}{\gamma_{M0}} = 1.147 \times 10^3 \cdot \text{kN} \cdot \text{m}$$

Plastic moment capacity

$$UC_{moment} := \frac{M_{Ed}}{M_{pl} \cdot \gamma_{M0}} = 0.289$$

column

B.4.4 Mezzanine check

Shear resistance

$$A_{v1} := A_{tot} - 2 \cdot b \cdot t_f + (t_w + 2 \cdot r) \cdot t_f = 6.998 \times 10^3 \cdot \text{mm}^2$$

$$A_v := \max(A_{v1}, h_w \cdot t_w) = 6.998 \times 10^3 \cdot \text{m}^2$$

$$V_{plRd} := \frac{\left[A_v \cdot \left(\frac{f_y}{3^{0.5}} \right) \right]}{\gamma_{M0}} = 1.434 \times 10^3 \cdot \text{kN}$$

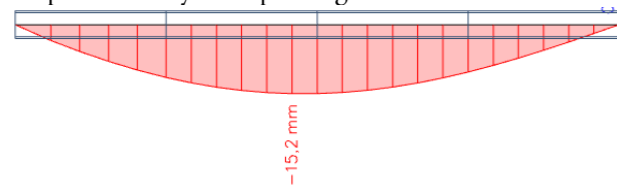
$$UC_{shear} := \frac{V_{Ed}}{V_{plRd}} = 0.3$$

$$UC_{shear} \leq 0.85 = 1$$

V.Ed is smaller than 0.5*V.Pl,Rd so the moment resistance does not have to be calculated based on a reduced yield strength in the web.

Deflection

The deflection will be checked with SCIA as multiple point loads are present on the beam, which cannot be represented by a simple forget me not.



$$w := 15.2 \text{ mm}$$

$$w_{max} := \frac{L}{360} = 0.023 \text{ m}$$

$$UC_{deflection} := \frac{w}{w_{max}} = 0.649$$

$$UC_{deflection} \leq 0.8 = 1$$

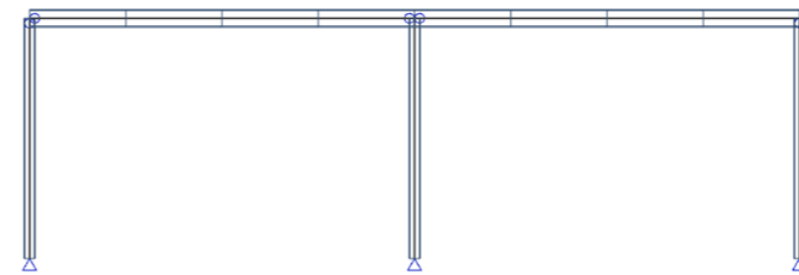
Unity checks overview

$$UC_{shear} = 0.3$$

$$UC_{moment} = 0.289$$

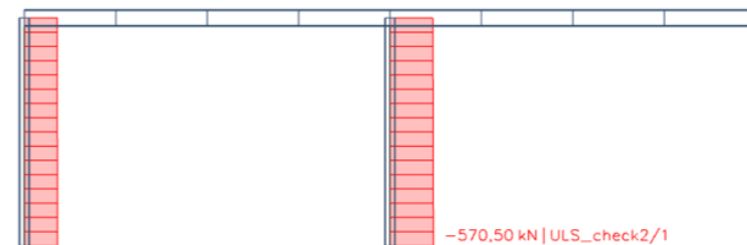
$$UC_{deflection} = 0.649$$

The primary beam and columns are modelled as follows:



Loads (ULS, from SCIA)

The loads on the primary beam are shown in the calculation of this beam. This leads to the following normal forces in the columns:



$$N_{Ed} := 570.50 \text{ kN}$$

Define member

$$L_{xx} := 5.4 \text{ m}$$

$$K_{xx} := 1$$

Pinned connection on both sides

$$L_b := K \cdot L = 5.4 \text{ m}$$

Buckling length

$$\gamma_{M0} := 1$$

$$\gamma_{M1} := 1$$

Define cross section

$$f_y := 355 \text{ MPa}$$

$$\xi_{w} := \sqrt{\frac{235 \text{ MPa}}{f_y}} = 0.814$$

$$E := 210 \text{ GPa}$$

$$G_v := 81000 \frac{\text{N}}{\text{mm}^2}$$

HEB240

$$h := 240 \text{ mm}$$

$$b := 240 \text{ mm}$$

$$t_w := 10 \text{ mm}$$

$$t_f := 18 \text{ mm}$$

$$r := 21 \text{ mm}$$

$$h_w := h - 2t_f - 2r = 0.162 \text{ m}$$

$$A_{tot} := 10599 \text{ mm}^2$$

$$\text{weight} := 83.2 \frac{\text{kg}}{\text{m}}$$

$$W_{ply} := 1053 \cdot 10^3 \text{ mm}^3$$

$$W_{plz} := 498.4 \cdot 10^3 \text{ mm}^3$$

Plastic section modulus

$$I_y := 112.6 \cdot 10^6 \text{ mm}^4$$

$$I_z := 39.23 \cdot 10^6 \text{ mm}^4$$

Cross section check

Outstand flanges

$$c_f := \frac{1}{2} \cdot (b - t_w) - r = 94 \text{ mm}$$

$$\frac{c_f}{t_f} = 5.222$$

Cross section check:

$$\frac{c_f}{t_f} \leq 9\epsilon = 1 \quad \frac{c_f}{t_f} \leq 10\epsilon = 1$$

Conclusion: Flange is class 1

Web

Due to the forces on beam 1: bending and compression

Plastic bending resistance (try if ok with class):

Due to symmetry: $\alpha := 0.5$

For α is smaller or equal to 0.5:

$$c_w := h - 2 \cdot t_f - 2 \cdot r = 162 \text{ mm}$$

$$\frac{c_w}{t_w} \leq \frac{36\epsilon}{\alpha} = 1$$

Conclusion: Web is class 1

Flange and web

The cross section is class 1, so plastic global analyses and plastic cross section analysis can be performed.

Axial resistance

$$N_{plRd} := \frac{(A_{tot} \cdot f_y)}{\gamma_{M0}} = 3.763 \times 10^6 \text{ N}$$

Unity check

$$UC_{axial} := \frac{N_{Ed}}{N_{plRd}} = 0.152$$

Flexural Buckling

Cross section	Limits	Buckling about axis	Buckling curve	
			S 235 S 275 S 355 S 420	S 460
	$h/b > 1.2$	$t_f \leq 40 \text{ mm}$	y-y z-z	a a ₀
		$40 \text{ mm} < t_f \leq 100$	y-y z-z	b a
	$h/b \leq 1.2$	$t_f \leq 100 \text{ mm}$	y-y z-z	b a
		$t_f > 100 \text{ mm}$	y-y z-z	d c

Figure B-14: Determination of buckling curve (NEN, 2016a)

In the strong direction

Elastic critical force

$$N_{cr,y} := \frac{(\pi^2 \cdot E \cdot I_y)}{L_b^2} = 8.003 \times 10^3 \text{ kN}$$

Non dimensional slenderness

$$\lambda_{y} := \sqrt{\frac{(A_{tot} \cdot f_y)}{N_{cr,y}}} = 0.686$$

Imperfection factor: buckling curve (b for y-y)

$$\frac{h}{b} = 1 \quad \alpha_{yimp} := 0.34$$

Value to determine reduction factor χ :

$$\Phi_y := 0.5 \left[1 + \alpha_{yimp} \cdot (\lambda_y - 0.2) + \lambda_y^2 \right] = 0.818$$

Reduction factor for flexural buckling:

$$\chi_y := \frac{1}{\left[\Phi_y + \sqrt{(\Phi_y^2 - \lambda_y^2)} \right]} = 0.792$$

Design buckling resistance compression

$$N_{brd,y} := \frac{(\chi_y \cdot A_{tot} \cdot f_y)}{\gamma_{M1}} = 2.979 \times 10^3 \text{ kN}$$

around strong axes (y-y):

Unity check:

$$UC_{flexural,y} := \left(\frac{|N_{Ed}|}{|N_{brd,y}|} \right) = 0.192$$

In the weak direction

Elastic critical force

$$N_{cr,z} := \frac{(\pi^2 \cdot E \cdot I_z)}{L_b^2} = 2.788 \times 10^3 \text{ kN}$$

Non dimensional slenderness

$$\lambda_z := \sqrt{\frac{(A_{tot} \cdot f_y)}{N_{cr,z}}} = 1.162$$

Imperfection factor: buckling curve (c for z-z)

$$\frac{h}{b} = 1 \quad \alpha_{zimp} := 0.45$$

Value to determine reduction factor χ :

$$\Phi_z := 0.5 \left[1 + \alpha_{zimp} \cdot (\lambda_z - 0.2) + \lambda_z^2 \right] = 1.41$$

Reduction factor for flexural buckling:

$$\chi_z := \frac{1}{\left[\Phi_z + \sqrt{(\Phi_z^2 - \lambda_z^2)} \right]} = 0.452$$

Design buckling resistance compression

$$N_{brd,z} := \frac{(\chi_z \cdot A_{tot} \cdot f_y)}{\gamma_{M1}} = 1.703 \times 10^3 \text{ kN}$$

around weak axis (z-z):

Unity check:

$$UC_{flexural,z} := \left(\frac{|N_{Ed}|}{|N_{brd,z}|} \right) = 0.335$$

UC overview

$$UC_{axial} = 0.152 \quad UC_{flexural,y} = 0.192 \quad UC_{flexural,z} = 0.335$$

B.5 Results of structural calculations

The final design is given in chapter 6.1.2 “Structural system”. Here, the dimensions, supports, and the element types are depicted. For the loads on this system, an overview is given in Appendix B.2.1 “Loads on the 2D model (y-direction)” and Appendix B.2.2 “Loads on the 2D model (x-direction)”. In this appendix, also the load combinations are given. For the SLS and ULS calculations, only the governing load combinations are given.

B.5.1 SLS

The results are found in the following table. This is based upon the deformations shown in the figures below this table. For the horizontal deflection, load combination SLS 16 is governing. For the vertical deflection of the roof beams, load combination SLS 17 is governing. In Table B-3, these load combinations are specified.

Table B-15: SLS results of the structural verifications performed in SCIA

Check	Max. calculated	Max. based on length	UC	Maximal UC
<i>Horizontal deformation</i>		$\frac{h_{column}}{150} = \frac{13500}{150} = 90 \text{ mm}$		
Horizontal deformation (x)	71.5 mm	90 mm	0.80	0.80
Horizontal deformation (y)	66.4 mm	90 mm	0.74	0.80
<i>Vertical deformation</i>		$\frac{L_{beam}}{250}$		
Vertical deformation (x; beam with length 15.81 m)	18.2 mm	63.2 mm	0.29	0.80
Vertical deformation (x; beam with length 23.715 m)	30.1 mm	94.9 mm	0.32	0.80
Vertical deformation (y; beam with length 16.86 m)	33.8 mm	67.4 mm	0.51	0.80



Figure B-15: Horizontal deflection for governing characteristic load situation (SLS 16) for the x-direction



Figure B-16: Horizontal deflection for governing characteristic load situation (SLS 16) for the y-direction



Figure B-17: Vertical deflection for governing characteristic load combination (SLS 17) for the x-direction
In this figure, the maximum deflection for the longer and shorter roof beams are shown separately, as they can both be governing.



Figure B-18: Vertical deflection for governing characteristic load combination (SLS 17) for the y-direction

B.5.2 Buckling lengths and ULS calculation results

In Table B-16, the buckling lengths of the columns are given and in Table B-17, the buckling lengths of the beams are given. The buckling lengths are calculated in SCIA. These buckling lengths are qualitatively checked with Figure B-19 and Figure B-20. Figure B-19 shows the buckling lengths for a sway frame. This holds for the main load-bearing structure. From alterations of each stiffness, it is found that the buckling length reduces with a higher stiffness. This also follows from Figure B-19.

Figure B-20 shows the buckling lengths for a non-sway frame. This holds for the façade columns, as roof bracing transfers the wind loads to the main beams and columns. For pinned connection on both sides of the column, the buckling length is equal to the length of the column, as can be seen in Figure B-20 (c). However, as the column base and the connection with the beam provide some stiffness, a lower buckling length is calculated by SCIA. The roof beams also act non-sway. The buckling length for the main direction is calculated by SCIA, but the buckling length of the perpendicular direction is taken as most unfavourable (as 1).

As two 2D-models are set up, the buckling length of the column in the main direction is applied manually as buckling length for the column in the perpendicular direction, as this cannot be modelled by SCIA correctly. This is included in the buckling factor in the perpendicular direction in Table B-16 and Table B-17.

Table B-16: Buckling lengths of the columns, from SCIA

Member	Type	Length between supports [m]	Stiffness with beam [MNm/rad]	Buckling factor	
				Main	Perp.
Main column (x)	HD 400x551	13.5	299.2	1.82	1.85
Main column (y)	HD 400x551	13.5	254.0	1.85	1.82
Façade column (x)	HEB 400	13.5	391.4	0.60	1
Façade column (y)	HEB 400	13.5	309.2	0.61	1

Table B-17: Buckling lengths of the beams, from SCIA

Member	Type	Length between LTB restraints [m]	Length between supports [m]	Buckling factor	
				Main	Perp.
Beam 1 (x)	HEB 550 (HEB 450-CB)	7.905	15.81	0.64	1
Beam 2 (x)	HEB 1000 (HEB 800-CB)	7.905	23.715	0.64	1
Beam 3 (y)	HEB 500 (HEB 400-CB)	8.43	16.86	0.64	1

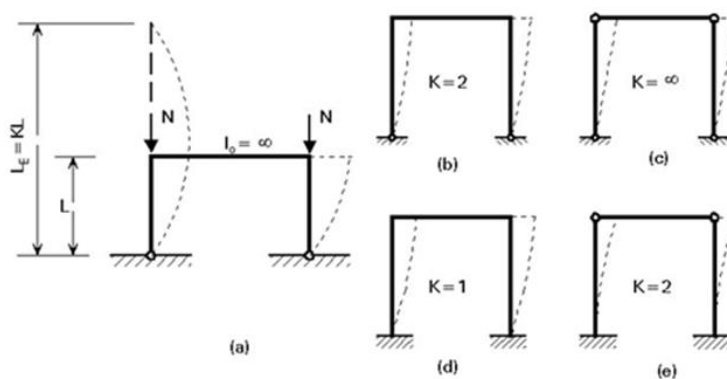


Figure B-19: Buckling lengths for a sway system (Veljkovic, 2019)

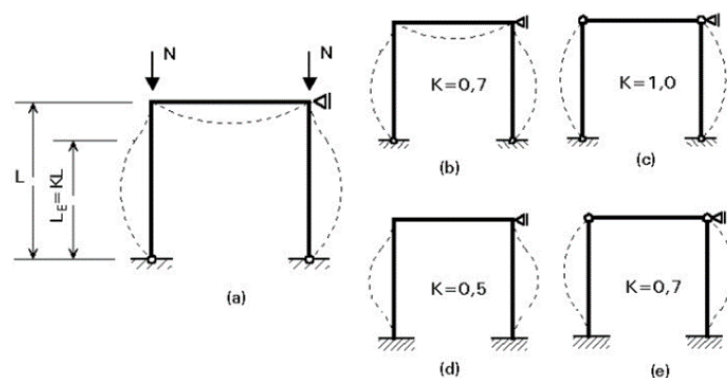


Figure B-20: Buckling lengths for a non-sway system (Veljkovic, 2019)

In Table B-18, the governing unity checks for the different members is given. For this ULS calculation, load combination ULS 6 is governing (see Table B-3 for the specification of this load case). The elements are checked upon the unity check for the section and the unity check for the stability. The internal forces are shown below this table.

Table B-18: Governing unity checks for the members of the base design

Member	Type	UC section	Max. UC section	UC stability	Max. UC stability
Main column (x)	HD 400x551	0.15	0.85	0.70	0.80
Main column (y)	HD 400x551	0.08	0.85	0.53	0.80
Façade column (x)	HEB 400	0.45	0.85	0.63	0.80
Façade column (y)	HEB 400	0.39	0.85	0.65	0.80
Beam 1 (x)	HEB 550 (HEB 450-CB)	0.36	0.85	0.36	0.80
Beam 2 (x)	HEB 1000 (HEB 800-CB)	0.17	0.85	0.75	0.80
Beam 3 (y)	HEB 500 (HEB 400-CB)	0.42	0.85	0.75	0.80

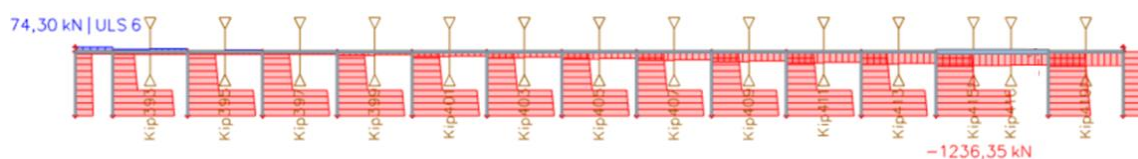


Figure B-21: Normal forces in the frame in the x-direction (for ULS 6)

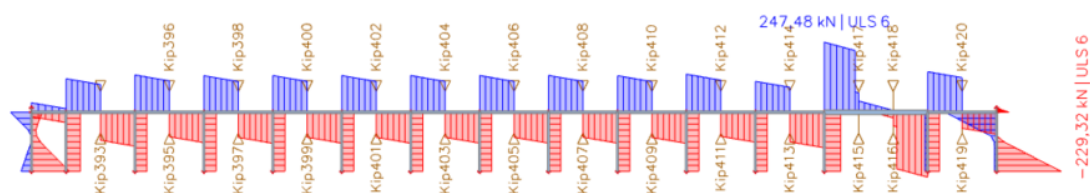


Figure B-22: Shear forces in the frame in the x-direction (for ULS 6)

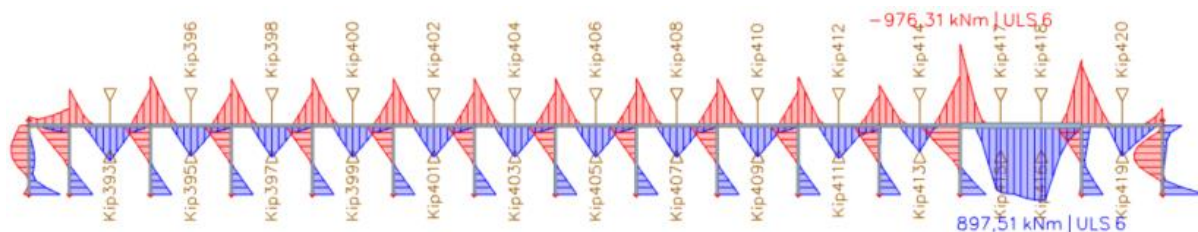


Figure B-23: Bending moments in the frame in the x-direction (for ULS 6)

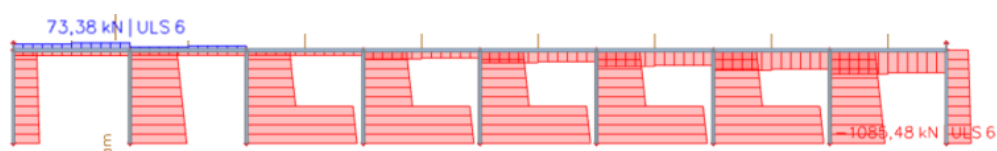


Figure B-24: Normal forces in the frame in the y-direction (for ULS 6)

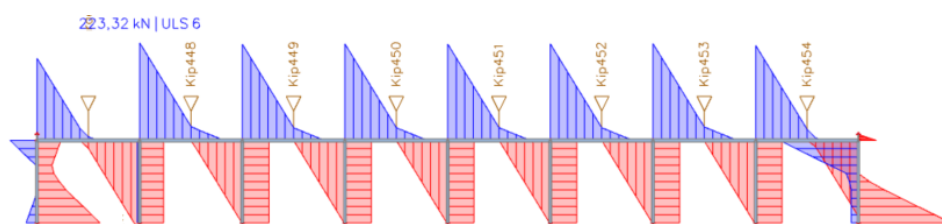


Figure B-25: Shear forces in the frame in the y-direction (for ULS 6)

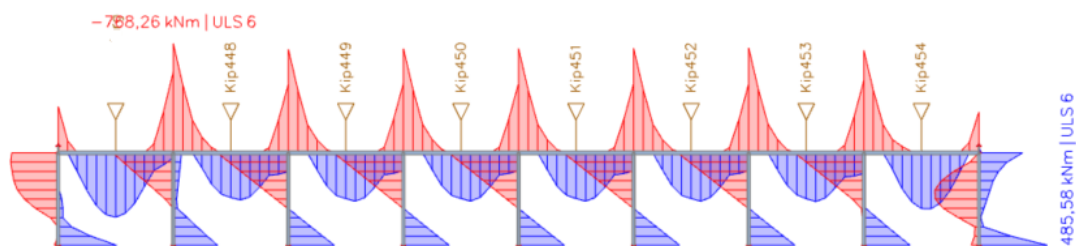


Figure B-26: Bending moments in the frame in the y-direction (for ULS 6)

It is found that the main column and the large beam in the x-direction are governing (shown in Figure B-27). These will be checked with hand calculations in Appendix B.5.2.1 and B.5.2.2. These calculations are also performed for the other beams and columns, but as the calculations follow the same steps, these are not included in this report.



Figure B-27: Location of governing beam (shown in green) and column (shown in blue) in the x-direction

B.5.2.1 ULS calculation of a governing column (shown in blue in Figure B-27), used as an example calculation for all columns

$$L_{xx} := 13.5\text{m}$$

$$K_y := 1.82 \quad \text{Buckling factor in y-y (from SCIA)}$$

$$K_z := 1.85 \quad \text{Buckling factor in z-z (from SCIA)}$$

$$L_g := L = 13.5\text{m} \quad \text{Length between torsional restraints}$$

$$L_{bz} := K_z \cdot L = 24.975\text{m} \quad \text{Length of an equivalent laterally unrestrained beam}$$

$$L_{by} := K_y \cdot L = 24.57\text{m}$$

Loads (ULS, from SCIA)

$$M_{Ed} := 306.8 \text{ kN}\cdot\text{m}$$

$$N_{Ed} := 1236.35 \text{ kN}$$

$$V_{Ed} := 56.56 \text{ kN}$$

Further calculation factors

$$\gamma_{M0} := 1 \quad \gamma_{M1} := 1$$

$$E := 210 \text{ GPa} \quad f_y := 355 \text{ MPa}$$

$$\varepsilon_{sw} := \sqrt{\frac{235 \text{ MPa}}{f_y}} = 0.814 \quad G_v := 81000 \frac{\text{N}}{\text{mm}^2}$$

Define cross section

HD400x551

$$h := 400 \text{ mm} \quad b := 418 \text{ mm}$$

$$t_w := 43 \text{ mm} \quad t_f := 68 \text{ mm}$$

$$A_{tot} := 7.02 \cdot 10^{-2} \text{ m}^2 \quad r := 15 \text{ mm}$$

$$h_w := h - 2t_f - 2r = 0.234 \text{ m}$$

$$W_{ply} := 1.205210^{-3} \text{ m}^3 \quad W_{plz} := 6.046310^{-3} \text{ m}^3$$

$$I_y := 2.260610^{-3} \text{ m}^4 \quad I_z := 8.238110^{-4} \text{ m}^4$$

$$I_w := 3.084410^{-5} \text{ m}^6 \quad I_t := 9.422710^{-5} \text{ m}^4$$

Cross section check

Outstand flanges

$$c_f := \frac{1}{2} \cdot (b - t_w) - r = 172.5 \text{ mm}$$

$$\frac{c_f}{t_f} = 2.537$$

Cross section check:

$$\frac{c_f}{t_f} \leq 9\varepsilon = 1 \quad \frac{c_f}{t_f} \leq 10\varepsilon = 1$$

Conclusion: Flange is class 1

Web

Due to the forces on beam 1: bending and compression

Plastic bending resistance (try if ok with class):

Due to symmetry: $\alpha := 0.5$

For α is smaller or equal to 0.5:

$$c_w := h - 2 \cdot t_f - 2 \cdot r = 234 \text{ mm}$$

$$\frac{c_w}{t_w} \leq \frac{36\varepsilon}{\alpha} = 1$$

Conclusion: Web is class 1

Flange and web

The cross section is class 1, so plastic global analyses and plastic cross section analysis can be performed.

Axial resistance

$$N_{plRd} := \frac{(A_{tot} \cdot f_y)}{\gamma_{M0}} = 2.492 \times 10^7 \text{ N}$$

$$UC_{axial} := \frac{N_{Ed}}{N_{plRd}} = 0.05$$

Plastic moment resistance

The column is turned 90 degrees, so the z-axis will be checked.

$$M_{pl} := \frac{W_{plz} \cdot f_y}{\gamma_{M0}} = 2.146 \times 10^3 \text{ kN}\cdot\text{m}$$

$$UC_{moment} := \frac{M_{Ed}}{M_{pl}} = 0.143$$

Shear resistance

$$A_{v1} := A_{tot} - 2 \cdot b \cdot t_f + (t_w + 2 \cdot r) \cdot t_f = 1.832 \times 10^4 \text{ mm}^2$$

$$A_v := \max(A_{v1}, h_w \cdot t_w) = 0.018 \text{ m}^2$$

$$V_{plRd} := \frac{\left[A_v \cdot \left(\frac{f_y}{3 \cdot 0.5} \right) \right]}{\gamma_{M0}} = 3.754 \times 10^3 \text{ kN}$$

$$UC_{shear} := \frac{V_{Ed}}{V_{plRd}} = 0.015$$

V_{Ed} is smaller than $0.5 \cdot V_{plRd}$ so the moment resistance does not have to be calculated based on a reduced yield strength in the web.

Flexural Buckling

See Figure B-14

In the strong direction

Elastic critical force

$$N_{cr,y} := \frac{(\pi^2 \cdot E \cdot I_y)}{L_{by}^2} = 7.761 \times 10^3 \cdot \text{kN}$$

Non dimensional slenderness

$$\lambda_y := \sqrt{\frac{A_{tot} \cdot f_y}{N_{cr,y}}} = 1.792$$

Imperfection factor: buckling curve (b for y-y)

$$\frac{h}{b} = 0.957 \quad \alpha_{yimp} := 0.34$$

Value to determine reduction factor χ :

$$\Phi_y := 0.5 \left[1 + \alpha_{yimp} \cdot (\lambda_y - 0.2) + \lambda_y^2 \right] = 2.376$$

Reduction factor for flexural buckling:

$$\chi_y := \frac{1}{\left[\Phi_y + \sqrt{\Phi_y^2 - \lambda_y^2} \right]} = 0.254$$

Design buckling resistance compression around strong axes (y-y):

$$N_{brd,y} := \frac{(\chi_y \cdot A_{tot} \cdot f_y)}{\gamma_{M1}} = 6.331 \times 10^3 \cdot \text{kN}$$

Unity check:

$$UC_{flexural,y} := \left(\frac{|N_{Ed}|}{|N_{brd,y}|} \right) = 0.195$$

In the weak direction

Elastic critical force

$$N_{cr,z} := \frac{(\pi^2 \cdot E \cdot I_z)}{L_{bz}^2} = 2.737 \times 10^3 \cdot \text{kN}$$

Non dimensional slenderness

$$\lambda_z := \sqrt{\frac{A_{tot} \cdot f_y}{N_{cr,z}}} = 3.017$$

Imperfection factor: buckling curve (c for z-z)

$$\frac{h}{b} = 0.957 \quad \alpha_{zimp} := 0.45$$

Value to determine reduction factor χ :

$$\Phi_z := 0.5 \left[1 + \alpha_{zimp} \cdot (\lambda_z - 0.2) + \lambda_z^2 \right] = 5.742$$

Reduction factor for flexural buckling:

$$\chi_z := \frac{1}{\left[\Phi_z + \sqrt{\Phi_z^2 - \lambda_z^2} \right]} = 0.094$$

Design buckling resistance compression around weak axis (z-z):

$$N_{brd,z} := \frac{(\chi_z \cdot A_{tot} \cdot f_y)}{\gamma_{M1}} = 2.345 \times 10^3 \cdot \text{kN}$$

Unity check:

$$UC_{flexural,z} := \left(\frac{|N_{Ed}|}{|N_{brd,z}|} \right) = 0.527$$

Lateral torsional buckling

Lateral torsional buckling is not governing for the main column and is therefore not included here.

Bending and axial compression check

For combined bending and axial compression, two methods are given. The national annex provides which method should be applied. However, as the building can be placed at different locations, both methods could apply. From SCIA calculations, it is found that method 2 is governing over method 1. In addition, from a conversation with a structural engineer of Royal HaskoningDHV, it is known that method 2 will be part of the new steel Eurocode. Therefore, it is decided to only check method 2. This is calculated with help of SCIA.

Method 2:

Table B-19: Bending and axial compression check parameters for method 2

Interaction method		alternative method 2	
Cross-section area	A	7,0200e-02	m ²
Plastic section modulus	W _{pl,z}	6,0463e-03	m ³
Design compression force	N _{Ed}	1236,35	kN
Design bending moment (maximum)	M _{y,Ed}	0,00	kNm
Design bending moment (maximum)	M _{z,Ed}	483,72	kNm
Characteristic compression resistance	N _{Rk}	23517,00	kN
Characteristic moment resistance	M _{z,Rk}	2025,50	kNm
Reduction factor	χ _y	0,27	
Reduction factor	χ _z	0,10	
Modified reduction factor	χ _{LT,mod}	1,00	
Interaction factor	k _{yz}	0,42	
Interaction factor	k _{zz}	0,70	

Table B-20: Interaction method 2 parameters

Resulting load type z		linear moment M
Ratio of end moments	ψ _z	-0,63
Equivalent moment factor	C _{mz}	0,40

The calculation can be found in the following steps:

$$C_{mz} = \max(0,6 + 0,4 \times \psi_z, 0,4) = \max(0,6 + 0,4 \times -0,63, 0,4) = \max(0,35, 0,4) = 0,40$$

$$N_{Rk} = A \times f_y = 7,0200 \cdot 10^{-2} [\text{m}^2] \times 335,0 [\text{MPa}] = 23517,00 [\text{kN}]$$

$$M_{z,Rk} = W_{pl,z} \times f_y = 6,0463 \cdot 10^{-3} [\text{m}^3] \times 335,0 [\text{MPa}] = 2025,50 [\text{kNm}]$$

$$k_{yz} = 0,6 \times k_{zz} = 0,6 \times 0,70 = 0,42$$

$$k_{zz} = \min \left\{ C_{mz} \times \left[1 + (2 \times \lambda_{rel,z} - 0,6) \times \frac{N_{Ed}}{N_{Rk}} \right], C_{mz} \times \left(1 + 1,4 \times \frac{N_{Ed}}{N_{Rk}} \right) \right\}$$

$$= \min \left\{ 0,40 \times \left[1 + (2 \times 2,93 - 0,6) \times \frac{1236,35 [\text{kN}]}{23517,00 [\text{kN}]} \right], 0,40 \times \left(1 + 1,4 \times \frac{1236,35 [\text{kN}]}{23517,00 [\text{kN}]} \right) \right\} = \min \{1,52, 0,70\} = 0,70$$

$$\text{Unity check (6.61)} = \frac{|N_{Ed}|}{\chi_y \times \frac{N_{Rk}}{\gamma_{M1}}} + k_{yy} \times \frac{|M_{y,Ed}| + |\Delta M_{y,Ed}|}{\chi_{LT,mod} \times \frac{M_{y,Rk}}{\gamma_{M1}}} + k_{yz} \times \frac{|M_{z,Ed}| + |\Delta M_{z,Ed}|}{\frac{M_{z,Rk}}{\gamma_{M1}}}$$

$$= \frac{1236,35[kN]}{0,27 \times \frac{23517,00[kN]}{1,00}} + 1,04 \times \frac{|0,00[kNm]| + |0,00[kNm]|}{1,00 \times \frac{4037,46[kNm]}{1,00}} + 0,42 \times \frac{|483,72[kNm]| + |0,00[kNm]|}{\frac{2025,50[kNm]}{1,00}} = 0,30 \leq 1,00$$

$$\text{Unity check (6.62)} = \frac{|N_{Ed}|}{\chi_z \times \frac{N_{Rk}}{\gamma_{M1}}} + k_{zy} \times \frac{|M_{y,Ed}| + |\Delta M_{y,Ed}|}{\chi_{LT,mod} \times \frac{M_{y,Rk}}{\gamma_{M1}}} + k_{zz} \times \frac{|M_{z,Ed}| + |\Delta M_{z,Ed}|}{\frac{M_{z,Rk}}{\gamma_{M1}}}$$

$$= \frac{1236,35[kN]}{0,10 \times \frac{23517,00[kN]}{1,00}} + 0,63 \times \frac{|0,00[kNm]| + |0,00[kNm]|}{1,00 \times \frac{4037,46[kNm]}{1,00}} + 0,70 \times \frac{|483,72[kNm]| + |0,00[kNm]|}{\frac{2025,50[kNm]}{1,00}} = 0,70 \leq 1,00$$

Unity check = max(Unity check (6.61), Unity check (6.62)) = max(0,30, 0,70) = **0,70 ≤ 1,00**

UC overview for the governing column (shown in blue in Figure B-27)

Type	Unity check
Axial force	0.05
Bending moment	0.143
Shear force	0.015
Flexural buckling	0.527
Bending and axial compression method 2	0.70

B.5.2.2 ULS calculation of a governing beam (shown in green in Figure B-27), used as an example calculation for all beams

$$G_v := 81000 \frac{N}{mm^2}$$

$$L_{xx} := 23.715m$$

$$K_y := 0.63 \quad \text{Buckling factor in y-y (from SCIA)}$$

$$K_z := 1 \quad \text{Buckling factor in z-z (from SCIA)}$$

$$L_g := L = 23.715m \quad \text{Length between torsional restraints}$$

$$L_b := 7905mm \quad \text{Length between LTB supports}$$

$$L_{cr,y} := K_y \cdot L = 14.94m \quad \text{Buckling length (main direction)}$$

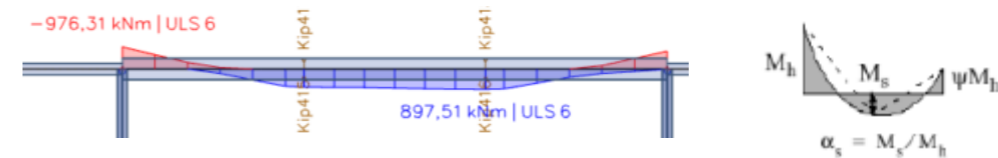
$$L_{cr,z} := K_z \cdot L = 23.715m \quad \text{Buckling length (perpendicular direction)}$$

Loads (ULS, from SCIA)

$$M_{Ed} := 897.15kN \cdot m$$

$$N_{Ed} := 225.73kN$$

$$V_{Ed} := 4.78kN$$



From this figure and the table above, it becomes clear that:

$$M_s := -897.5 \text{ kN}\cdot\text{m}$$

$$M_{h,max} := 976.3 \text{ kN}\cdot\text{m}$$

$$M_{h,min} := 787.09 \text{ kN}\cdot\text{m}$$

$$\psi := \frac{M_{h,min}}{M_{h,max}} = 0.806 \quad \alpha_s := \frac{M_s}{M_{h,max}} = -0.919$$

Further calculation factors

$$\gamma_{M0} := 1 \quad \gamma_{M1} := 1$$

$$E := 210GPa \quad f_y := 355MPa$$

$$\epsilon_{wv} := \sqrt{\frac{235MPa}{f_y}} = 0.814$$

Define cross section

HEB 1000

$$h := 1000\text{mm} \quad b := 300\text{mm}$$

$$t_w := 19\text{mm} \quad t_f := 36\text{mm}$$

$$A_{\text{tot}} := 40005\text{mm}^2 \quad r := 15\text{mm}$$

$$h_w := h - 2t_f - 2r = 0.898\text{m}$$

$$W_{\text{ply}} := 1486010^3\text{mm}^3 \quad W_{\text{plz}} := 171610^3\text{mm}^3$$

$$I_y := 644710^6\text{mm}^4 \quad I_z := 162.810^6\text{mm}^4$$

$$I_w := 3734000010^6\text{mm}^6 \quad I_t := 1272010^3\text{mm}^4$$

Cross section checkOutstand flanges

$$c_f := \frac{1}{2} \cdot (b - t_w) - r = 125.5\text{mm}$$

$$\frac{c_f}{t_f} = 3.486$$

Cross section check:

$$\frac{c_f}{t_f} \leq 9\varepsilon = 1 \quad \frac{c_f}{t_f} \leq 10\varepsilon = 1$$

Conclusion: Flange is class 1

Web

Due to the forces on beam 1: bending and compression

Plastic bending resistance (try if ok with class):

Due to symmetry: $\alpha := 0.5$ For α is smaller or equal to 0.5:

$$c_w := h - 2t_f - 2r = 898\text{mm}$$

$$\frac{c_w}{t_w} \leq \frac{36\varepsilon}{\alpha} = 1$$

Conclusion: Web is class 1

Flange and web

The cross section is class 1, so plastic global analyses and plastic cross section analysis can be performed.

Axial resistance

$$N_{\text{plRd}} := \frac{(A_{\text{tot}} \cdot f_y)}{\gamma_{M0}} = 1.42 \times 10^7 \text{N}$$

$$UC_{\text{axial}} := \frac{N_{\text{Ed}}}{N_{\text{plRd}}} = 0.016$$

Plastic moment resistance

$$M_{\text{pl}} := \frac{W_{\text{ply}} \cdot f_y}{\gamma_{M0}} = 5.275 \times 10^3 \cdot \text{kN} \cdot \text{m}$$

$$UC_{\text{moment}} := \frac{M_{\text{Ed}}}{M_{\text{pl}}} = 0.17$$

Shear resistance

$$A_{v1} := A_{\text{tot}} - 2 \cdot b \cdot t_f + (t_w + 2r) \cdot t_f = 2.017 \times 10^4 \cdot \text{mm}^2$$

$$A_v := \max(A_{v1}, h_w \cdot t_w) = 0.02\text{m}^2$$

$$V_{\text{plRd}} := \frac{\left[A_v \cdot \left(\frac{f_y}{3^{0.5}} \right) \right]}{\gamma_{M0}} = 4.134 \times 10^3 \cdot \text{kN}$$

$$UC_{\text{shear}} := \frac{V_{\text{Ed}}}{V_{\text{plRd}}} = 1.156 \times 10^{-3}$$

V_{Ed} is smaller than $0.5 \cdot V_{\text{plRd}}$ so the moment resistance does not have to be calculated based on a reduced yield strength in the web.

Flexural Buckling

See

In the strong direction

Elastic critical force

$$N_{\text{cr,y}} := \frac{(\pi^2 \cdot E \cdot I_y)}{L_{\text{cr,y}}^2} = 5.986 \times 10^4 \cdot \text{kN}$$

Non dimensional slenderness

$$\lambda_y := \sqrt{\frac{(A_{\text{tot}} \cdot f_y)}{N_{\text{cr,y}}}} = 0.487$$

Imperfection factor: buckling curve (b for y-y)

$$\frac{h}{b} = 3.333 \quad \alpha_{\text{yimp}} := 0.21$$

Value to determine reduction factor χ :

$$\Phi_y := 0.5 \left[1 + \alpha_{\text{yimp}} \cdot (\lambda_y - 0.2) + \lambda_y^2 \right] = 0.649$$

Reduction factor for flexural buckling:

$$\chi_y := \frac{1}{\left[\Phi_y + \sqrt{(\Phi_y^2 - \lambda_y^2)} \right]} = 0.928$$

Design buckling resistance compression

$$N_{\text{brd,y}} := \frac{(\chi_y \cdot A_{\text{tot}} \cdot f_y)}{\gamma_{M1}} = 1.318 \times 10^4 \cdot \text{kN}$$

around strong axes (y-y):

Unity check:

$$UC_{\text{flexural,y}} := \left(\frac{|N_{\text{Ed}}|}{|N_{\text{brd,y}}|} \right) = 0.017$$

In the weak direction

Elastic critical force

$$N_{cr,z} := \frac{(\pi^2 \cdot E \cdot I_z)}{L_{cr,z}^2} = 599.967 \text{ kN}$$

Non dimensional slenderness

$$\lambda_z := \sqrt{\frac{A_{tot} \cdot f_y}{N_{cr,z}}} = 4.865$$

Imperfection factor: buckling curve (c for z-z)

$$\frac{h}{b} = 3.333 \quad \alpha_{zimp} := 0.34$$

Value to determine reduction factor χ :

$$\Phi_z := 0.5 \left[1 + \alpha_{zimp} (\lambda_z - 0.2) + \lambda_z^2 \right] = 13.129$$

Reduction factor for flexural buckling:

$$\chi_z := \frac{1}{\Phi_z + \sqrt{\Phi_z^2 - \lambda_z^2}} = 0.039$$

Design buckling resistance compression

$$N_{brd,z} := \frac{(\chi_z \cdot A_{tot} \cdot f_y)}{\gamma_{M1}} = 560.84 \text{ kN}$$

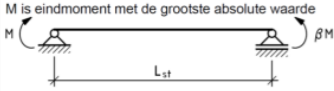
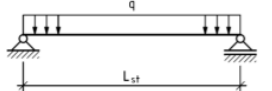

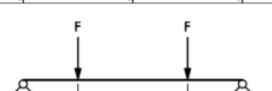
around weak axis (z-z):

Unity check:

$$UC_{flexural,z} := \left(\frac{|N_{Ed}|}{|N_{brd,z}|} \right) = 0.402$$

Lateral torsional buckling

$\frac{h}{t_w} = 52.632$ $k_{red} := 1$ coefficient taking into account deformability of the cross section

Geval	Belasting	C ₁	C ₂
1	M is eindmoment met de grootste absolute waarde 	$1.75 - (1.05 \times \beta) + (0.3 \times \beta^2)$ $-1 \leq \beta \leq 1$ $C_1 \leq 2.3$	0
2		1.13	0.45
3		1.35	0.55
4		1.04	0.42

From this table, coefficients C1 and C2 are calculated:

$$C_1 := \min[1.75 - (1.05 \cdot \psi) + (0.3 \cdot \psi^2), 2.3] = 1.098$$

Coefficient for loading and boundary conditions

$$C_2 := 0$$

Coefficient for position of loading

$$S_{LT} := \sqrt{\frac{E \cdot I_w}{G_v \cdot I_t}} = 2.759 \text{ m}$$

$$C_{LT} := \left[\frac{(\pi \cdot C_1 \cdot L_g)}{I_b} \right] \cdot \left[\sqrt{1 + \left[\frac{(\pi^2 \cdot S_{LT}^2)}{I_b^2} \right] \cdot (C_2^2 + 1)} \right] + \left[\frac{(\pi \cdot C_2 \cdot S_{LT})}{I_b} \right] = 15.363$$

$$M_{crM} := \left(\frac{C_{LT}}{I_g} \right) \cdot \sqrt{E \cdot I_z \cdot G_v \cdot I_t} = 3.845 \times 10^3 \cdot \text{kN} \cdot \text{m}$$

$$M_{cr} := k_{red} \cdot M_{crM} = 3.845 \times 10^3 \cdot \text{kN} \cdot \text{m}$$

$$\lambda_{LT} := \sqrt{\frac{(W_{ply} \cdot f_y)}{M_{cr}}} = 1.171$$

$$\frac{h}{b} = 3.333 \quad \text{so:} \quad \alpha_{LT} := 0.45$$


$$\beta := 0.75$$

$$\lambda_{LT0} := 0.4$$

$$\Phi_{LT} := 0.5 \left[1 + \alpha_{LT} (\lambda_{LT} - \lambda_{LT0}) + \beta \cdot (\lambda_{LT}^2) \right] = 1.203$$

$$\chi_{LT} := \frac{1}{\Phi_{LT} + \sqrt{\Phi_{LT}^2 - \beta \cdot \lambda_{LT}^2}} = 0.54$$

The moment distribution between the lateral restraints of the members, the following needs to be taken into account:

Moment distribution	k _c
	0.90

$$k_c := 0.90$$

$$f := \min \left[1 - 0.5(1 - k_c) \cdot \left[1 - 2 \cdot (\lambda_{LT} - 0.8)^2 \right], 1 \right] = 0.964$$

$$\chi_{LT,mod} := \min \left(\frac{\chi_{LT}}{f}, 1, \frac{1}{\lambda_{LT}^2} \right) = 0.561$$

$$M_{bRd} := \chi_{LT,mod} \cdot W_{ply} \cdot \left(\frac{f_y}{\gamma_{M1}} \right) = 2.957 \times 10^3 \cdot \text{kN} \cdot \text{m}$$

$$UC_{LTB} := \left(\frac{M_{Ed}}{M_{bRd}} \right) = 0.303$$

Bending and axial compression check

For combined bending and axial compression, two methods are given. The national annex provides which method should be applied. However, as the building can be placed at different locations, both methods could apply. From SCIA calculations, it is found that method 2 is governing over method 1. In addition, from a conversation with a structural engineer of Royal HaskoningDHV, it is known that method 2 will be part of the new steel Eurocode. Therefore, it is decided to only check method 2. This is calculated with help of SCIA.

Method 2:

Table B-21: Bending and axial compression check parameters for method 2

Interaction method		alternative method 2	
Cross-section effective area	A _{eff}	3,6486e-02	m ²
Effective section modulus	W _{eff,y}	1,2896e-02	m ³
Design compression force	N _{Ed}	225,73	kN
Design bending moment (maximum)	M _{y,Ed}	-976,31	kNm
Design bending moment (maximum)	M _{z,Ed}	0,00	kNm
Additional moment	ΔM _{y,Ed}	0,00	kNm
Additional moment	ΔM _{z,Ed}	0,00	kNm
Characteristic compression resistance	N _{Rk}	12952,68	kN
Characteristic moment resistance	M _{y,Rk}	4578,24	kNm
Reduction factor	χ _y	0,94	
Reduction factor	χ _z	0,04	
Modified reduction factor	χ _{LT,mod}	0,60	
Interaction factor	k _{yy}	0,80	
Interaction factor	k _{zy}	0,97	

The interaction factors are calculated as follows (the results are shown in Table B-22):

Moment diagram	range	C _{my} and C _{my} and C _{mLT}	
		uniform loading	concentrated load
	-1 ≤ ψ ≤ 1	0,6 + 0,4ψ ≥ 0,4	
	0 ≤ α ≤ 1	-1 ≤ ψ ≤ 1	0,2 + 0,8α ≥ 0,4
	-1 ≤ α < 0	0 ≤ ψ ≤ 1	0,1 - 0,8α ≥ 0,4
	-1 ≤ α < 0	-1 ≤ ψ < 0	0,1(1-ψ) - 0,8α ≥ 0,4
		0,2(-ψ) - 0,8α ≥ 0,4	
	0 ≤ α ≤ 1	-1 ≤ ψ ≤ 1	0,95 + 0,05α _b
		0 ≤ ψ ≤ 1	0,90 + 0,10α _b
	-1 ≤ α < 0	-1 ≤ ψ < 0	0,95 + 0,05α _b (1+2ψ)
		-1 ≤ ψ < 0	0,90 - 0,10α _b (1+2ψ)

For members with sway buckling mode the equivalent uniform moment factor should be taken C_{my} = 0,9 or C_{mLT} = 0,9 respectively.
C_{my}, C_{my} and C_{mLT} should be obtained according to the bending moment diagram between the relevant braced points as follows:

moment factor	bending axis	points braced in direction
C _{my}	y-y	z-z
C _{my}	z-z	y-y
C _{mLT}	y-y	y-y

Figure B-28: Equivalent uniform moment factors (NEN, 2016a)

$$\alpha_{s,y} = \frac{M_{s,y}}{M_{h,y}} = \frac{846,15[\text{kNm}]}{-976,31[\text{kNm}]} = -0,87$$

$$C_{my} = \max(0,1 - 0,8 \times \alpha_{s,y}, 0,4) = \max(0,1 - 0,8 \times -0,87, 0,4) = \max(0,79, 0,4) = 0,79$$

$$C_{my} = \max(0,1 - 0,8 \times \alpha_{s,y}, 0,4) = \max(0,1 - 0,8 \times -0,87, 0,4) = \max(0,79, 0,4) = 0,79$$

$$\alpha_{s,LT} = \frac{M_{s,LT}}{M_{h,LT}} = \frac{846,15[\text{kNm}]}{897,51[\text{kNm}]} = 0,94$$

$$C_{mLT} = \max(0,2 + 0,8 \times \alpha_{s,LT}, 0,4) = \max(0,2 + 0,8 \times 0,94, 0,4) = \max(0,95, 0,4) = 0,95$$

$$N_{Rk} = A_{eff} \times f_y = 3,6486 \cdot 10^{-2}[\text{m}^2] \times 355,0[\text{MPa}] = 12952,68[\text{kN}]$$

$$M_{y,Rk} = W_{eff,y} \times f_y = 1,2896 \cdot 10^{-2}[\text{m}^3] \times 355,0[\text{MPa}] = 4578,24[\text{kNm}]$$

Table B-22: Interaction method 2 parameters

Method for interaction factors		Table B.2	
Resulting load type y		line load q	
End moment	M _{h,y}	-976,31	kNm
Field moment	M _{s,y}	846,15	kNm
Factor	α _{s,y}	-0,87	
Ratio of end moments	ψ _y	0,48	
Equivalent moment factor	C _{my}	0,79	
Resulting load type LT		line load q	
End moment	M _{h,LT}	897,51	kNm
Field moment	M _{s,LT}	846,15	kNm
Factor	α _{s,LT}	0,94	
Ratio of end moments	ψ _{LT}	0,81	
Equivalent moment factor	C _{mLT}	0,95	

$$k_{yy} = \min \left[C_{my} \times \left(1 + 0,6 \times \lambda_{rel,y} \times \frac{N_{Ed}}{\chi_y \times \frac{N_{Rk}}{\gamma_{M1}}} \right), C_{my} \times \left(1 + 0,6 \times \frac{N_{Ed}}{\chi_y \times \frac{N_{Rk}}{\gamma_{M1}}} \right) \right]$$

$$= \min \left[0,79 \times \left(1 + 0,6 \times 0,46 \times \frac{225,73[\text{kN}]}{0,94 \times \frac{12952,68[\text{kN}]}{1,00}} \right), 0,79 \times \left(1 + 0,6 \times \frac{225,73[\text{kN}]}{0,94 \times \frac{12952,68[\text{kN}]}{1,00}} \right) \right] = \min[0,80, 0,80] = 0,80$$

$$k_{zy} = \max \left(1 - \frac{0,05 \times \lambda_{rel,z}}{C_{mLT} - 0,25} \times \frac{N_{Ed}}{\chi_z \times \frac{N_{Rk}}{\gamma_{M1}}}, 1 - \frac{0,05}{C_{mLT} - 0,25} \times \frac{N_{Ed}}{\chi_z \times \frac{N_{Rk}}{\gamma_{M1}}} \right)$$

$$= \max \left(1 - \frac{0,05 \times 4,65}{0,95 - 0,25} \times \frac{225,73[\text{kN}]}{0,04 \times \frac{12952,68[\text{kN}]}{1,00}}, 1 - \frac{0,05}{0,95 - 0,25} \times \frac{225,73[\text{kN}]}{0,04 \times \frac{12952,68[\text{kN}]}{1,00}} \right) = \max(0,87, 0,97) = 0,97$$

$$\text{Unity check (6.61)} = \frac{|N_{Ed}|}{\chi_y \times \frac{N_{Rk}}{\gamma_{M1}}} + k_{yy} \times \frac{|M_{y,Ed}| + |\Delta M_{y,Ed}|}{\chi_{LT,mod} \times \frac{M_{y,Rk}}{\gamma_{M1}}} + k_{yz} \times \frac{|M_{z,Ed}| + |\Delta M_{z,Ed}|}{\frac{M_{z,Rk}}{\gamma_{M1}}}$$

$$= \frac{225,73[\text{kN}]}{0,94 \times \frac{12952,68[\text{kN}]}{1,00}} + 0,80 \times \frac{|-976,31[\text{kNm}]| + |0,00[\text{kNm}]|}{0,60 \times \frac{4578,24[\text{kNm}]}{1,00}} + 1,24 \times \frac{|0,00[\text{kNm}]| + |0,00[\text{kNm}]|}{\frac{385,20[\text{kNm}]}{1,00}} = \mathbf{0,30 \le 1,00}$$

$$\text{Unity check (6.62)} = \frac{|N_{Ed}|}{\chi_z \times \frac{N_{Rk}}{\gamma_{M1}}} + k_{zy} \times \frac{|M_{y,Ed}| + |\Delta M_{y,Ed}|}{\chi_{LT,mod} \times \frac{M_{y,Rk}}{\gamma_{M1}}} + k_{zz} \times \frac{|M_{z,Ed}| + |\Delta M_{z,Ed}|}{\frac{M_{z,Rk}}{\gamma_{M1}}}$$

$$= \frac{225,73[\text{kN}]}{0,04 \times \frac{12952,68[\text{kN}]}{1,00}} + 0,97 \times \frac{|-976,31[\text{kNm}]| + |0,00[\text{kNm}]|}{0,60 \times \frac{4578,24[\text{kNm}]}{1,00}} + 1,24 \times \frac{|0,00[\text{kNm}]| + |0,00[\text{kNm}]|}{\frac{385,20[\text{kNm}]}{1,00}} = \mathbf{0,75 \le 1,00}$$

$$\text{Unity check} = \max(\text{Unity check (6.61)}, \text{Unity check (6.62)}) = \max(0,30, 0,75) = \mathbf{0,75 \le 1,00}$$

UC overview for the governing column (shown in green in Figure B-27)

Type	Unity check
Axial force	0.016
Bending moment	0.17
Shear force	0.001156
Flexural buckling	0.402
Lateral torsional buckling	0.303
Bending and axial compression method 2	0.75

C Alternative A

C.1 Design considerations

C.1.1 Thermal expansion

Thermal expansion can become an issue for longer steel buildings. In a research by Fisher (2005), explanation is given on the maximum building length without expansion joints or between expansion joints. For this design alternative, it is unknown where the building will be located, so therefore the most extreme design temperature change is considered. This means that for a steel building, the allowable building length is maximally 121.92 m (400 feet). According to Fisher (2005), this length can be enlarged or reduced based upon the building characteristics, which is given in Table C-1. This leads to a maximum building length of 140.2 meters. Based upon this length, two design alternatives are set up. These alternatives are given in Table C-2, where for each alternative, advantages and disadvantages are given.

Table C-1: Calculation of maximum length of a building without/between expansion joints (Fisher, 2005)

Explanation	Parameters		
Maximum length of a building (without/between expansion joints)	L_{max}	$L_{max} = L_{allow} + (R_1 - R_2 - R_3 - R_4) * L_{allow}$	
		$L_{max,steel}$	140.2 m
Basic allowable length of a building	L_{allow}	$L_{allow,steel}$	121.92m
Factor if the building is heated and air-conditioned	R_1	$R_1 = 0.15$ if true $R_1 = 0$ if false	0.15
Factor if the building is unheated	R_2	$R_2 = 0.33$ if true $R_2 = 0$ if false	0
Factor if the columns are rigidly connected	R_3	$R_3 = 0.15$ if true $R_3 = 0$ if false	0
Factor if the building has greater stiffness at one side of the building	R_4	$R_4 = 0.15$ if true $R_4 = 0$ if false	0

Table C-2: Design options based upon thermal expansion issues

Design option	Dilatation and non-sway system	Non-sway system
Sketch		
Advantages	The friction area is reduced, so the braces need to carry a lower wind load. The bracing is located at the façade, so the wind is carried to the foundation directly.	No additional columns are needed.
Disadvantages	For a dilatation, two structural systems arise, which means that extra columns and beams (and extra materials) are needed.	Compared to the dilatation system, the bracing needs to carry a higher wind load. The wind is not directly transferred to the foundation, which is a less efficient design than the dilatation design.

Based upon the explanation given in Table C-2, it is investigated how much material is needed for both design options. Therefore, the wind load for both structures is defined to calculate the materials needed for the horizontal bracing in the roof. Based upon this calculation, the dilation system only has limited advantages. Based upon this discovery, it is decided to use a non-sway system solely.

C.1.2 Connection design

For a non-sway frame, usually hinged connections are applied. Hinged connections are usually easier to mount, which can be seen in the following figure. On the left of this figure, an example of a moment resistant connection is shown, showing that welding is necessary to create such a connection. On the right of the figure, a shear connection without welds is shown. The shear connection is cheaper and easier to mount and is therefore chosen for the connections between the beams and for the connections between the beams and columns.

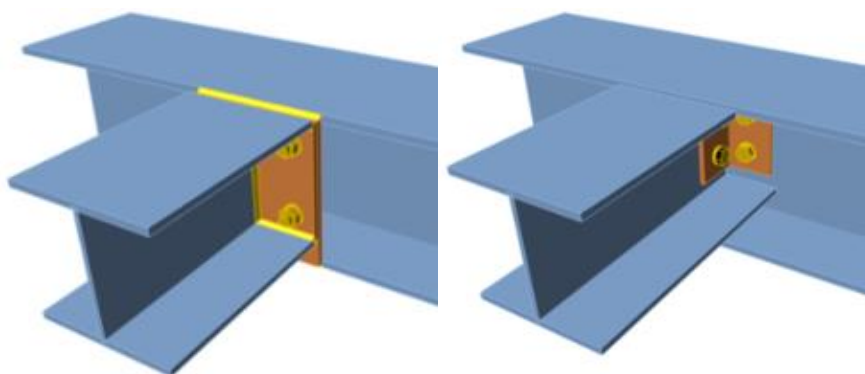


Figure C-1: Example of two beam-beam connections

Left: moment resisting connection and right: shear connection (own illustration, made with IDEA StatiCa)

For the column base, the differences are not significant. Creating a moment resistant connection as shown in Figure C-2 on the left requires the same mounting process as the shear connection shown in Figure C-2 on the right. In that case, a moment resistant connection is favourable, as the maximum bending moment in the column will reduce in case of a moment resistant connection.

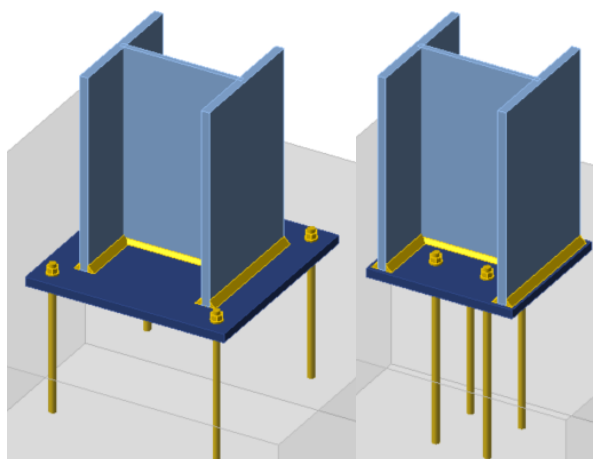


Figure C-2: Example of two steel column base connections

Left: moment resisting connection, right: shear connection (own illustration, made with IDEA StatiCa)

C.2 Loads

The non-sway frame ensures that the wind only needs to be carried by the façade columns, the horizontal roof bracing, and the vertical bracing. The other beams and columns only need to carry the vertical loads.

The façade columns are modelled as shown in Figure C-3. On this system, the loads as explained in Appendix B paragraphs B.2.1 “Loads on the 2D model (y-direction)” and B.2.2 “Loads on the 2D model (x-direction)” are applied. The only difference is the fact that for the non-sway system, the centre-to-centre distance of the façade columns is governing, meaning that beams in between the main beams also carry the wind load. This design difference is made because of the deflection of the diagonal element. In case the regular centre-to-centre distance is applied for this design (15.81 m by 16.86 m), the diagonal must span 23.11 meters, which is too long for the deflection requirements. For a smaller centre-to-centre distance (7.905 m by 8.43 m), the diagonal only must span 11.56 meters, which means that the diagonals do not deflect too much. This means that the loads from Table B-2 and Table B-5 are applied, but the centre-to-centre distance is reduced for ‘Live loads 4’. This is given in the following tables.

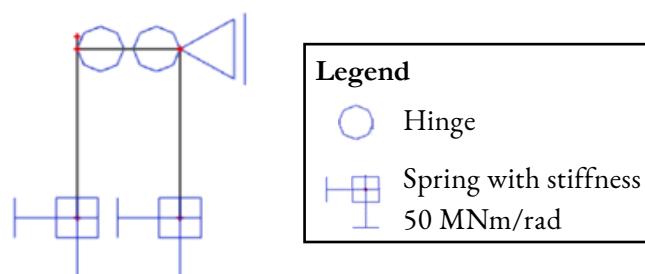


Figure C-3: Schematisation of local façade column check

Table C-3: Loads on non-sway frame (Y-direction)

Loads	Load	CTC	Line load
<i>Dead loads</i>			
From Table B-2			
<i>Live loads 1 (vertical)</i>			
From Table B-2			
<i>Live loads 2 (snow, vertical)</i>			
From Table B-2			
<i>Live loads 3 (external wind, vertical)</i>			
From Table B-2			
<i>Live loads 4 (external wind, horizontal)</i>			
Friction due to wind	3.8 kN		
Wind D	0.98 kN/m ²	7.905	7.75 kN/m
Wind E	0.61 kN/m ²	7.905	4.82 kN/m
Wind D on parapet	1.75 kN/m ²	7.905	13.83 kN/m
<i>Live loads 5 (internal wind vertical+horizontal)</i>			
From Table B-2			

Live loads 4: Wind D+E (y-direction)

- Friction force on beam = 3.8 kN, halfway every beam
- Wind D on column = 8.26 kN/m
- Wind D on parapet = 14.75 kN/m
- Wind E on column = 5.14 kN/m

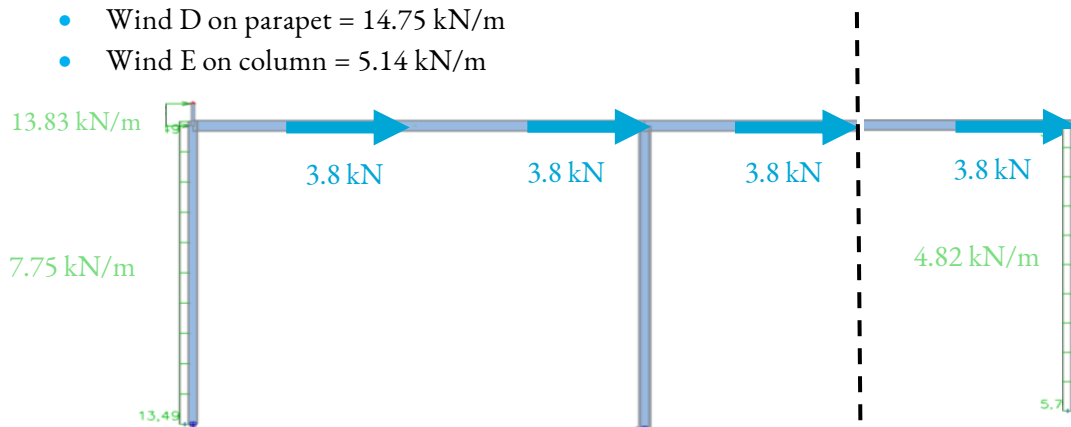
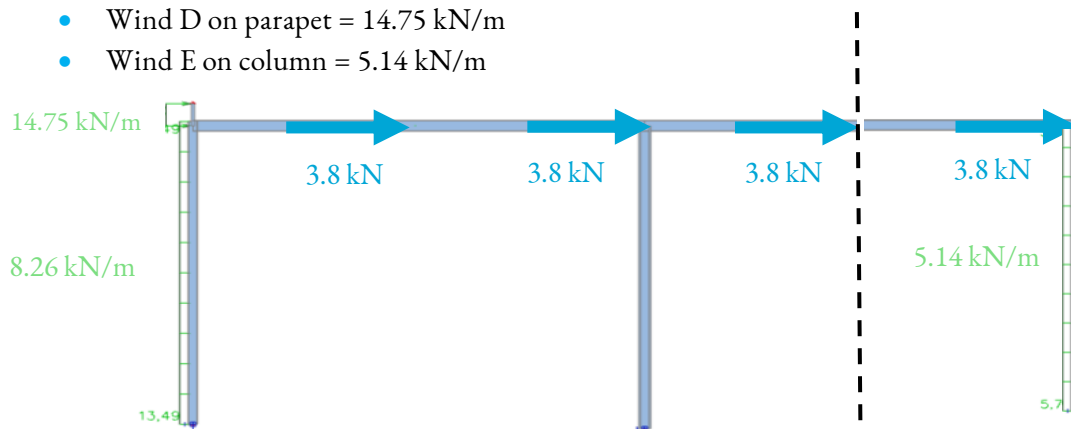


Table C-4: Loads on non-sway frame (X direction)

Loads	Surface load	CTC	Line load
<i>Dead loads (vertical)</i>			
From Table B-5			
<i>Live loads 1 (vertical)</i>			
From Table B-5			
<i>Live loads 2 (snow, vertical)</i>			
From Table B-5			
<i>Live loads 3 (external wind, vertical)</i>			
From Table B-5			
<i>Live loads 4 (external wind, horizontal)</i>			
Friction due to wind	3.8 kN		
Wind D	0.98 kN/m ²	8.43	8.26 kN/m
Wind E	0.61 kN/m ²	8.43	5.14 kN/m
Wind on parapet	1.75 kN/m ²	8.43	14.75 kN/m
<i>Live loads 5 (internal wind, vertical)</i>			
From Table B-5			
<i>Live loads 5 (internal wind, horizontal)</i>			
From Table B-5			

Live loads 4: Wind D+E (x-direction)

- Friction force on beam = 3.8 kN, halfway every beam
- Wind D on column = 8.26 kN/m
- Wind D on parapet = 14.75 kN/m
- Wind E on column = 5.14 kN/m



The wind load on the horizontal bracing is calculated with the 2D sections as shown in Figure 6-14 and Figure 6-15, with the total wind load (including friction). This leads to a reaction force in the vertical support and column base support. The reaction force in the vertical support is applied as a point load on the horizontal bracing.

Live loads 4: Wind D+E (y-direction)

- Friction force on beam = 3.8 kN, halfway every beam
- Wind D on column = 8.26 kN/m
- Wind D on parapet = 14.75 kN/m
- Wind E on column = 5.14 kN/m

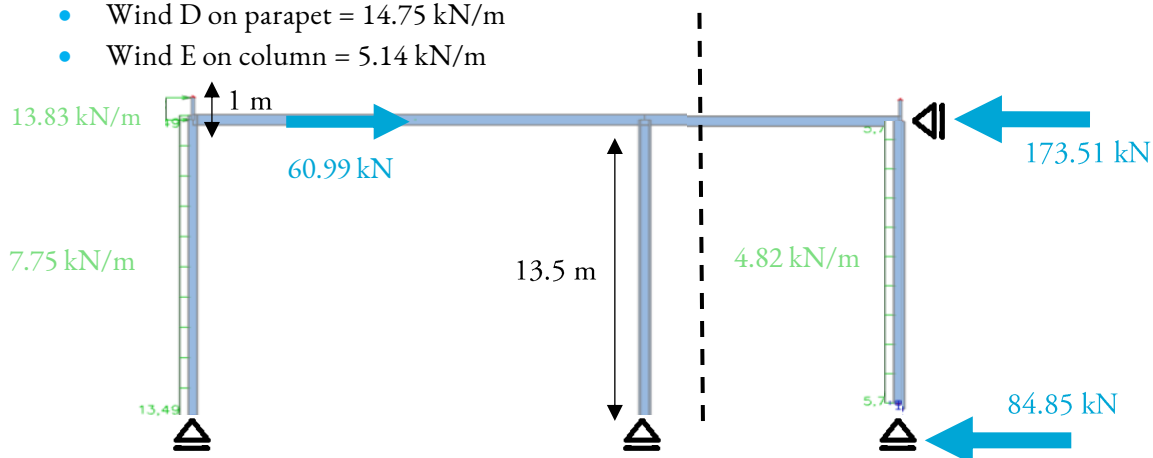


Figure C-4: Overview of the horizontal wind loads in the y-direction
On the right side at the top: the total loads on the roof bracing, on the right side at the bottom: the total loads going to the foundation

Live loads 4: Wind D+E (x-direction)

- Friction force on beam = 3.8 kN, halfway every beam
- Wind D on column = 8.26 kN/m
- Wind D on parapet = 14.75 kN/m
- Wind E on column = 5.14 kN/m

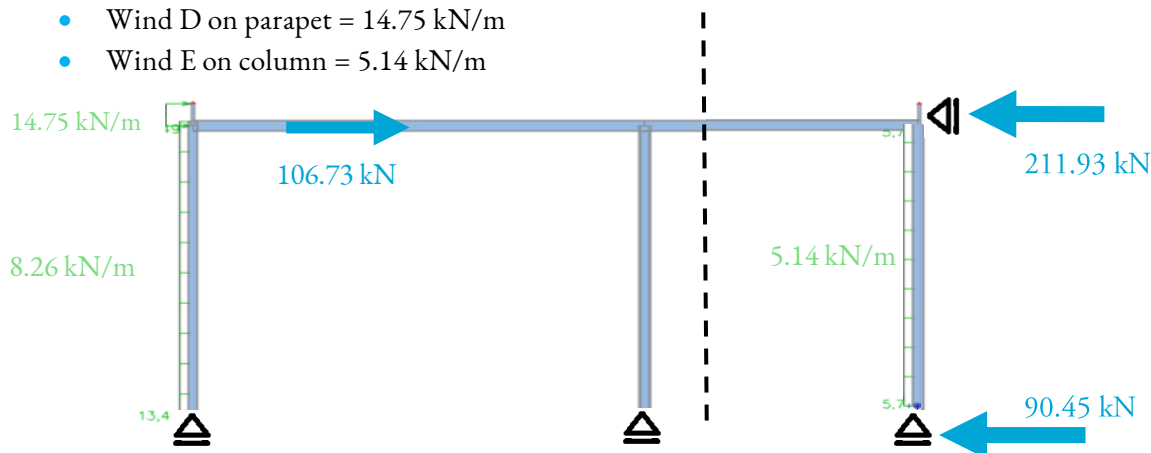


Figure C-5: Overview of the horizontal wind loads in the x-direction

On the right side at the top: the total loads on the roof bracing, on the right side at the bottom: the total loads going to the foundation

C.3 Bracing design

C.3.1 Horizontal bracing

The roof bracing is designed as a frame on two supports, where the diagonals only carry tension forces. A schematic representation of this system is given in Figure C-6, where the principle of the calculation is shown. This is based upon Barendsz et al. (2019).

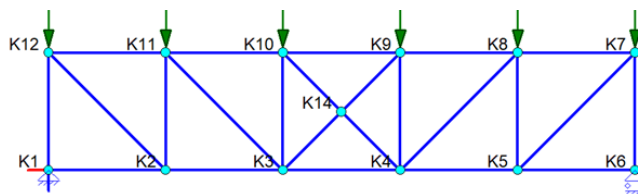


Figure C-6: Principle showing how the roof bracing is calculated (this is an example for a smaller building)

The actual design of the roof bracing for the wind coming from the x-direction can be found in Figure C-7. In this figure, the two bracing areas in the building are placed closer to each other. This will provide insight in the normal forces in the beams between the two bracings and provides insight in the flow of forces throughout the building. This means that this is a simplification of the actual building. In this figure, also the supports are shown in blue. These supports represent the vertical bracing in the façade.

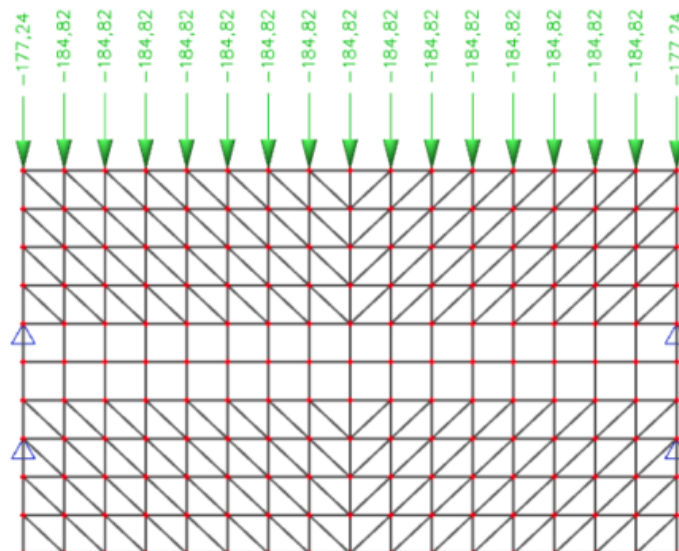


Figure C-7: Screenshot of SCIA model of the bracing carrying the wind coming from the x-direction
The supports are shown in blue. These supports represent the bracing in the façade.

The bracing for the wind coming from the y-direction can be found in Figure C-8. This is only one bracing system, with on both sides supports to be able to carry the wind from both directions. The supports are shown in blue in these figures and represent the bracing in the façade.

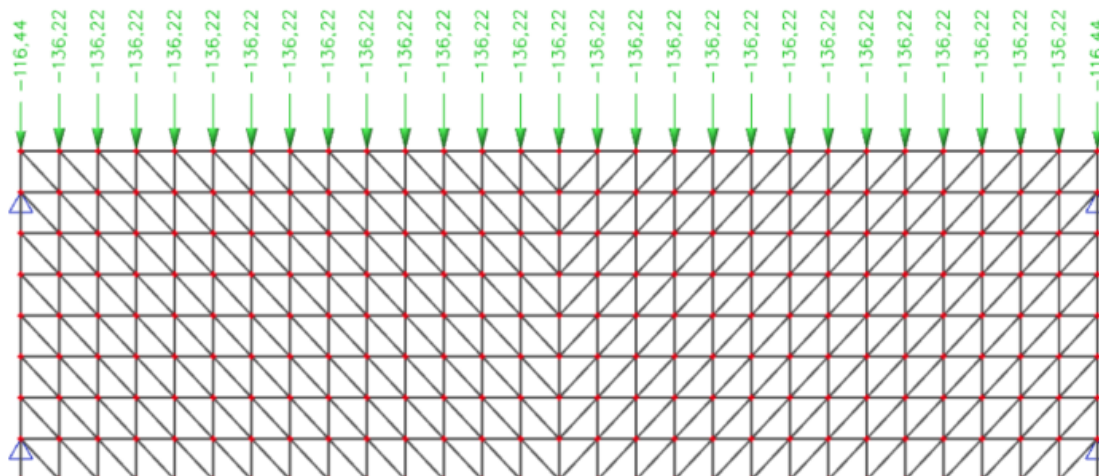


Figure C-8: Screenshot of SCIA model of the bracing carrying the wind coming from the y-direction
The supports are shown in blue. These supports represent the bracing in the façade.

From the roof bracing design shown in Figure C-7 and Figure C-8, the governing normal forces in the beams are found and given in Table C-5. It is decided to take the largest forces in the beams, which makes this design conservative, yet safe. The normal forces are combined with the vertical forces on the system to find the dimensions of the beams in the non-sway frame.

Table C-5: Largest normal forces in the horizontal roof bracing system

This is used as input for the two 2D-sections, where these forces are combined with the other wind loads on the beams

Member	Type	Normal force [kN]
Beam 1 (x)	HEB 450	-922.51
Beam 3 (y)	HEB 600	-560.28

C.3.2 Vertical bracing

The vertical bracing is calculated separately, as shown in the following figure. Here, it is visualised that the bracing element is as wide as two grid lines. This does mean that the normal force in the diagonals becomes too large for an angled profile that only carries tension forces. Therefore, the diagonals are made from circular hollow sections that also take up compression forces.

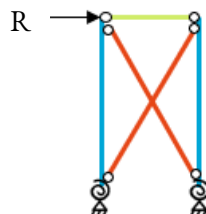


Figure C-9: Schematisation of vertical wind bracing with the wind load on the system

The load on the vertical bracing in the x-direction is equal to the largest reaction force in the supports of Figure C-7 and the load on the vertical bracing in the y-direction is equal to the largest support reaction of Figure C-8. The support reactions are as follows:

- $R_{vertical\ bracing,x} = 971.16\ kN$
- $R_{vertical\ bracing,y} = 1417.06\ kN$

C.4 Results of structural calculations

Structural calculations of the SLS and ULS for this alternative have been made.

C.4.1 SLS

The results of the deflection of the system are found from the SCIA model that has been set up for this design alternative, the results are given in the following table.

The horizontal deformation is defined by the bracing in the roof: the bracing in the roof carries the wind load and should resist the maximum deflection. This is shown in Figure C-10.

The vertical deformation is based upon the schematisation of the two sections in x- and y-direction shown in the figures in paragraph 6.2.2.2 “Schematisation of two sections”. For the beams in the y-direction, the deflection is governing over the ULS checks (which will be explained in the following paragraph).

Table C-6: SLS results of the structural verifications performed in SCIA

Check	Max. calculated	Max. based on length	UC	Maximal UC
<i>Horizontal deformation</i>		$\frac{h_{column}}{150} = \frac{13500}{150} = 90\ mm$		
Horizontal deformation (x)	38.5 mm	90 mm	0.43	0.80
Horizontal deformation (y)	63.5	90 mm	0.70	0.80
<i>Vertical deformation</i>		$\frac{L_{beam}}{250}$		
Beam 1 (x, 15.81 m long)	33.8	63.2 mm	0.53	0.80
Beam 2 (x, 23.715 m long)	72.4	94.9 mm	0.76	0.80
Beam 3 (y, 16.86 m long)	51 mm	67.4 mm	0.76	0.80
Diagonal (11.6 m long)	37 mm	46.4 mm	0.80	0.80

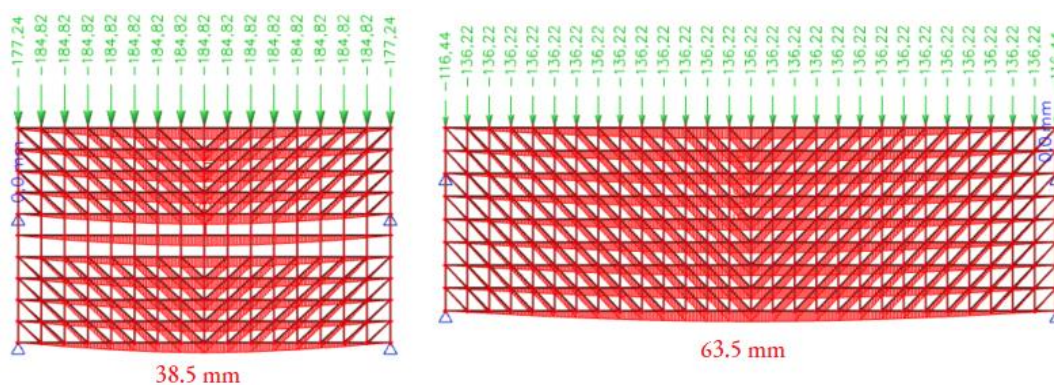


Figure C-10: Horizontal deflection of the bracing systems due to the wind load (from SCIA)
Left: wind from the x-direction, right: wind from the y-direction

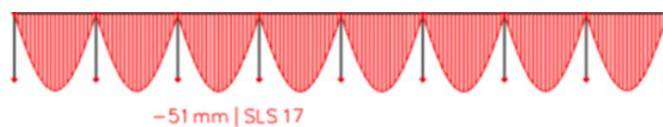


Figure C-11: Deflection of beams in y-direction (from SCIA)

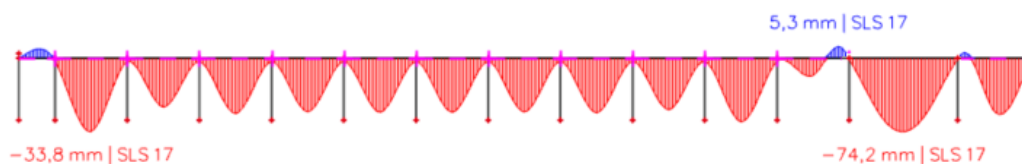


Figure C-12: Deflection of beams in x-direction

C.4.1.1 Deflection of the diagonal

The choice of profile was chosen based upon the deflection of the diagonal. It was found that an angled steel profile was needed to provide for enough stiffness in such a way that the deflection is limited. The calculation of the deflection of the diagonal is as follows:

Define cross section

Angled profile: 160×160×15

$E := 210 \text{ GPa}$

weight := 36.8

$I_y := 1099 \cdot 10^4 \text{ mm}^4$

$$L_{\text{diagonal}} := \sqrt{\left(\frac{15.81}{2}\right)^2 + \left(\frac{16.86}{2}\right)^2} \cdot \text{m} = 11.56 \text{ m}$$

Loads

$$q := \frac{\text{weight}}{100} \frac{\text{kN}}{\text{m}}$$

$$q_{\text{ULS}} := 1.35 \cdot q = 0.5 \cdot \frac{\text{kN}}{\text{m}} \quad q_{\text{SLS}} := q = 0.37 \cdot \frac{\text{kN}}{\text{m}}$$

Deflection

$$w := \frac{5}{384} \cdot q_{\text{SLS}} \cdot \frac{L_{\text{diagonal}}^4}{E \cdot I_y} = 37.03 \cdot \text{mm}$$

$$w_{\text{max}} := \frac{L_{\text{diagonal}}}{250} = 0.05 \text{ m}$$

$$UC_{\text{deflection}} := \frac{w}{w_{\text{max}}} = 0.8$$

$$UC_{\text{deflection}} \leq 1 = 1$$

C.4.2 Buckling lengths and ULS calculation results

In Table C-7, the buckling lengths of the columns are given. The columns are connected with a hinge at the top, but it is decided to give the connection with the foundation some stiffness. This ensures a lower buckling length than 1. The results shown in Table C-7 are checked quantitatively with Figure B-20.

Table C-7: Buckling lengths of the columns, from SCIA

Member	Type	Length between supports [m]	Buckling factor	
			Main	Perp.
Main column (x)	HEB 400	13.5	0.76	0.80
Main column (y)	HEB 400	13.5	0.80	0.76
Façade column (x)	HEB 360	13.5	0.79	0.79
Façade column (y)	HEB 360	13.5	0.79	0.79

Table C-8 gives the buckling lengths of the beams. The beams in the x-direction are continuous, ensuring in a lower buckling length than the beams in the y-direction, which are connected by a hinge on both sides. This also ensures that the beams in the y-direction must be stronger than the beams in the x-direction, to resist for the deflection. To make it possible to connect the secondary beams (in the y-direction) with the primary beams (in the x-direction), the primary beams should at least be as high as the secondary beams. In this design, it is aimed to use traditional castellated beams (with a height 1.5 times higher than the height of the regular beam) (Grünbauer, n.d.). However, a lot more material is needed in that case, so non-standard (modern) castellated beams are used instead. The translation of a regular beam to a non-standard castellated beam is given in Table C-9.

Table C-8: Buckling lengths of the beams, from SCIA

Member	Type	Length between LTB restraints [m]	Length between supports [m]	Buckling factor	
				Main	Perp.
Beam 1 (x)	HEB 450 (HEB 360-CB)	7.905	15.81	0.80	1
Beam 2 (x)	HEB 700 (HEB 550-CB)	7.905	23.715	0.62	1
Beam 3 (y)	HEB 600 (HEB 500-CB)	7.905	16.86	1	1
Horizontal bracing elements					
Beam 1 (x)	HEB 450 (HEB 360-CB)	7.905	15.81 (main) 7.905 (perp.)	0.70	0.73
Beam 2 (x)	HEB 700 (HEB 550-CB)	7.905	23.715 (main) 7.905 (perp.)	0.70	0.73
Beam 3 (y)	HEB 600 (HEB 500-CB)	8.43	16.86 (main) 8.43 (perp.)	1	0.79
Diagonal	Angle (HFLeq) 160x160x15	11.557	11.557	1	1
Façade beam (x)	HEB 450	7.905	7.905	0.75	0.73
Façade beam (y)	HEB 400	8.43	16.86 (main) 8.43 (perp.)	1	0.76
Vertical bracing elements					
Colum	HEB 700		13.5	1	0.86
Diagonal	CHS 406.4/20		15.64 (main) 15.92 (perp.)	1	1

Table C-9: Translation of a non-standard castellated beam to a regular beam (Grünbauer, n.d.)

Castellated	Height [mm]	$W_{y,elastic}$ [$\times 10^3$ mm ³]	Regular beam	$W_{y,elastic}$ [$\times 10^3$ mm ³]
HEB 360-CB	690	4952	HEB 450	3551
HEB 500-CB	665	5987	HEB 600	5701

In Table C-10, the governing unity checks for the different members is given. For the main columns and beams, ULS 7 is governing (see Table B-3 for the specification of this load case). However, these beams are not close the maximum unity check as the deflection given in Table C-6 is governing over the ULS checks. For the façade columns, carrying wind load, ULS 5 is governing.

Table C-10: Governing unity checks for the members of the Alternative A

Member	Type	UC section	Max. UC section	UC stability	Max. UC stability
Main column (x)	HEB 400	0.18	0.85	0.72	0.80
Main column (y)	HEB 400	0.15	0.85	0.59	0.80
Façade column (x)	HEB 360	0.30	0.85	0.79	0.80
Façade column (y)	HEB 360	0.28	0.85	0.67	0.80
Beam 1 (x)	HEB 450 (HEB 360-CB)	0.72	0.85	0.72	0.80
Beam 2 (x)	HEB 700 (HEB 550-CB)	0.35	0.85	0.60	0.80
Beam 3 (y)	HEB 600 (HEB 500-CB)	0.38	0.85	0.50	0.80
Horizontal bracing elements					
Beam 1 (x)	HEB 450 (HEB 360-CB)	0.57	0.85	0.60	0.80
Beam 2 (x)	HEB 700 (HEB 550-CB)	0.35	0.85	0.68	0.80
Beam 3 (y)	HEB 600 (HEB 500-CB)	0.35	0.85	0.70	0.80
Diagonal	Angle (HFLeq) 160x160x15	0.41	0.85	0.00	0.80
Façade beam (x)	HEB 450	0.13	0.85	0.75	0.80
Façade beam (y)	HEB 400	0.08	0.85	0.76	0.80
Vertical bracing elements					
Column	HEB 700	0.16	0.85	0.78	0.80
Diagonal	CHS 406.4/20	0.24	0.85	0.70	0.80

The governing forces in the elements are also shown in the following figures. For the beams in the x-direction, the shear forces and bending moments of the vertical load combination (ULS 7) is governing.

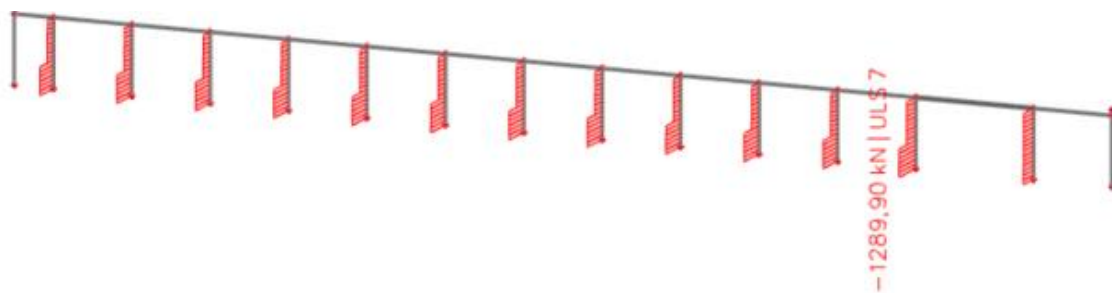


Figure C-13: Normal forces in the frame in the x-direction (for ULS 7)

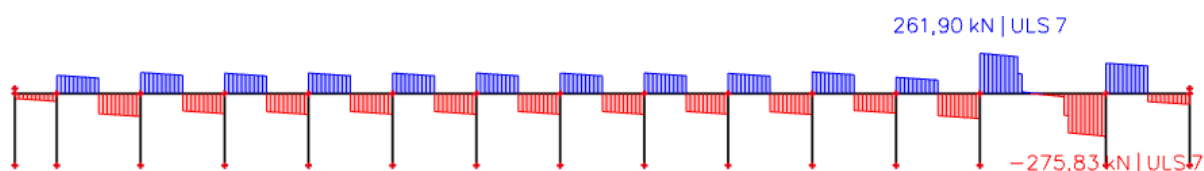


Figure C-14: Shear forces in the frame in the x-direction (for ULS 7)

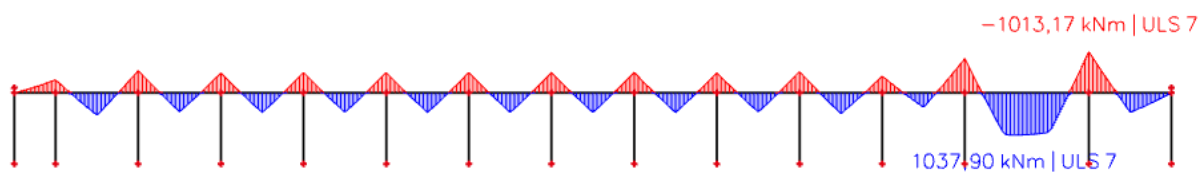


Figure C-15: Bending moments in the frame in the x-direction (for ULS 7)

For the beams in the y-direction, the wind load combination ULS 6 is governing. The forces in the beams and columns are shown in the following figures.

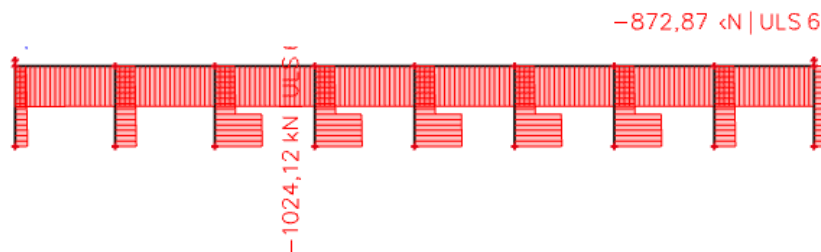


Figure C-16: Normal forces in the frame in the y-direction (for ULS 6)

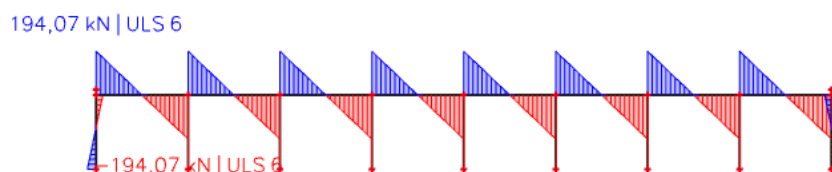


Figure C-17: Shear forces in the frame in the y-direction (for ULS 6)

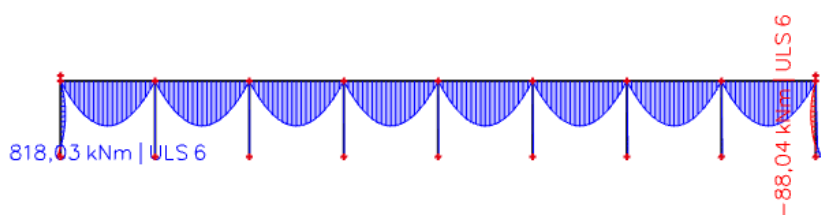


Figure C-18: Bending moments in the frame in the y-direction (for ULS 6)

C.5 Element overview

MAIN LOAD-BEARING STRUCTURE

Element	Type	Wt. [kg/m]	Length [m]	Number (y)	Number (x)	Total nr	Total [kg]
Column (main)	HEB 400	158	13,5	4	13	52	110916
Column (main)	HEB 400	158	12,71	3	13	39	78319
Column (façade)	HEB 360	145	13,5	26	46	72	153576
Roof beam (y)	HEB 500-CB	191	16,86	8	27	216	695576
Roof beam (x, small)	HEA 360-CB	145	15,81	11	12	132	302603
Roof beam (x, small)	HEA 360-CB	145	7,905	11	1	11	12608
Roof beam (x, large)	HEB 550-CB	203	23,715	7	1	7	33699
Façade beam (y)	HEA 260	69,5	8,43	8	2	16	9374
Façade beam (x)	HEA 260	69,5	7,905	2	20	40	21976
Lateral support (x)	SHS 120/120/10	31,8	7,905	4	20	80	20110
							<i>1426122</i>
Horizontal bracing elements							
Diagonal	160/160/15	36,8	11,557	8	8	64	27218
Diagonal	160/160/15	36,8	11,557	8	28	224	95263
Façade beam (y)	HEB 400	158	8,43	8	2	16	21311
Façade beam (x)	HEB 450	174	7,905	2	8	16	22008
							<i>165800</i>
Vertical bracing elements							
Column	HEB 700	245	13,5	8	8	16	52920
Diagonal	CHS 406.4/20	191	20,79	8	8	16	48639
							<i>101559</i>
							<i>Total: 1693481</i>

MAIN LOAD-BEARING STRUCTURE: Same as for the Base design, given in Appendix B.6 “Element overview”

D Alternative B

D.1 Material and product properties

D.1.1 Material properties

The material characteristics of timber elements can differ. In this research, the material characteristics of EN 14080 for GL 24h are applied and EN 338 for C24, given in the following table.

Table D-1: Properties of GL24h (NEN, 2013) and C24 (NEN, 2016b)

Property	Symbol	GL24h	C24
Strength properties [N/mm²]			
Bending strength	$f_{m,k}$	24	24
Tensile strength //	$f_{t,0,k}$	19.2	14.5
Tensile strength \perp	$f_{t,90,k}$	0.5	0.4
Compression strength //	$f_{c,0,k}$	24	21
Compression strength \perp	$f_{c,90,k}$	2.5	2.5
Shear strength	$f_{v,k}$	3.5	4.0
Stiffness properties [N/mm²]			
Modulus of elasticity (mean) //	$E_{0,mean}$	11 500	11 000
Modulus of elasticity (5%) //	$E_{0,0.05}$	9600	7400
Modulus of elasticity (mean) \perp	$E_{90,mean}$	300	370
Shear modulus (mean)	G_{mean}	650	690
Shear modulus (5%)	$G_{0.05}$	540	
Density [kg/m³]			
Density (5%)	ρ_k	385	350
Density (mean)	ρ_{mean}	420	420

D.1.2 Product properties

For specific products, certain calculation steps are performed. In this paragraph, this will be explained.

The load-bearing structure is located inside. This means that service class 1 applies. According to EN 1995-1-1, service class 1 is characterised by a moisture content that corresponds to a temperature of 20°C and a relative humidity of the air only exceeding 65% a few weeks per year. This means that the average moisture content of most softwoods will not exceed 12%.

For a rectangular glued laminated timber element, $f_{m,k}$ and $f_{t,0,k}$ may be increased by the factor k_h if the reference depth in bending or the width in tension is less than 600 mm:

$$k_h = \min\left(\left(\frac{600\text{mm}}{\text{height}}\right)^{0.1}, 1.1\right) \quad \text{eq. D-1}$$

The design value of a strength property needs to be calculated as follows according to EN 1995-1-1 (from which the parameters are explained in the following tables):

$$X_d = k_{mod} * \frac{X_k}{\gamma_M} \quad \text{eq. D-2}$$

Table D-2: Parameters in eq. D-2 (NEN, 2005b)

Parameter	Definition
X_d	Design value of a strength property
k_{mod}	Modification factor (includes the effect of the load duration and the moisture content)
X_k	Characteristic (5%) value of a strength property
γ_M	Partial factor for a material property, given in Table D-3

Table D-3: Values for k_{mod} for service class 1 (NEN, 2005b), the load duration class is given in Table D-4

Material type	Permanent action	Long term action	Medium term action	Short term action	Instantaneous action
Solid timber	0.6	0.7	0.8	0.9	1.1
Glulam	0.6	0.7	0.8	0.9	1.1

Table D-4: Examples of load-duration assignment

Load-duration class	Examples of loading (NEN, 2005b)	Applied to in this thesis
Permanent	Self-weight	Self-weight
Long-term	Storage	–
Medium-term	Imposed floor load, snow	Live loads on mezzanine floor
Short-term	Snow, wind	Snow, wind
Instantaneous	Accidental load, wind	–

Table D-5: Recommended partial factor γ_M for different material types (NEN, 2005b)

Material type	Recommended partial factor γ_M
Solid timber	1.3
Glued laminated timber	1.25
Connections	1.3

Timber is sensitive for creep behaviour over time. Therefore, one should calculate with the deformation factor k_{def} from the following table.

Table D-6: Values for k_{def} for different material types for service class 1 (NEN, 2005b)

Material type	k_{def}
Solid timber	0.6
Glued laminated timber	0.6

D.1.3 Fire safety

During fire, the accidental load combination given in Table A-1 is applied. The loads accompanying this load combination are calculated in SCIA.

The next step for the determination of the strength during fire, is calculating the reduced cross section. This is calculated with help of the Calculatis tool of Stora Enso. Here, the duration of the fire, location of the fire, and load combination factor are input factors. An example of the reduced cross section is given in Figure D-1.

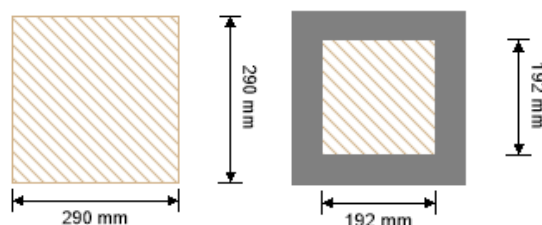


Figure D-1: Reduced cross section for a fire duration of 60 minutes (from Stora Enso Calculatis tool)

During fire, the design resistance needs to be calculated as follows (according to EN 1995-1-2):

$$X_{d,fi} = k_{mod,fi} * \frac{f_{20}}{\gamma_{M,fi}} \quad \text{eq. D-3}$$

Table D-7: Parameters in eq. D-3

Parameter	Definition
$X_{d,fi}$	Design value of the strength property during fire
k_{mod}	Modification factor during fire
f_{20}	20% fractile value of the resistance at room temperature, which is calculated as follows: $f_{20} = k_{fi} * X_k$, where $k_{fi} = 1.15$ for glulam
$\gamma_{M,fi}$	Partial factor for timber in fire, $\gamma_{M,fi} = 1$ is recommended

D.2 Loads

The non-sway frame ensures that the wind only needs to be carried by the façade columns, the horizontal roof bracing, and the vertical bracing. The other beams and columns only need to carry the vertical loads.

D.2.1 Wind loads

The façade columns are modelled as shown in Figure D-2. On this system, the loads as explained in Appendix C.2 “Loads” are applied. The only difference compared to the steel non-sway system is the support at the column base, which is seen if Figure D-2 is compared to Figure C-3.

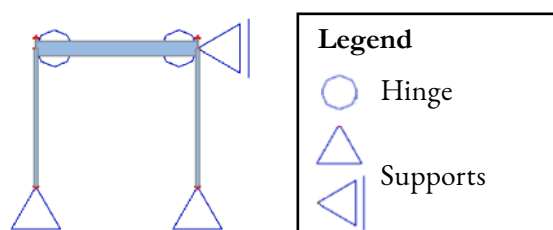


Figure D-2: Schematisation of local façade column check

Based upon the horizontal loads given in Appendix C.2 “Loads”, the loads on the roof bracing can be calculated. As the system is supported by hinges instead of a stiff column base connection, the loads are higher than for Alternative A given in Appendix C.2 “Loads”. The following results are found for the loads on the timber roof bracing:

- The total friction forces are calculated the same way as shown in A.2.2.3 “Friction forces”:

- $F_{fr} = c_{fr} * q_{p10} * A_{fr}$

- For the x-direction: $A_{fr,x} = L_{building} * b = 221.34 * 16.81 = 1866 \text{ m}^2$

- For the y-direction: $A_{fr,y} = 134.88 * 15.81 = 1066 \text{ m}^2$

- The total friction force for the x-direction: $F_{fr,x} = 0.04 * 1.43 * 1866 = 106.73 \text{ kN}$

- The total friction force for the y-direction: $F_{fr,y} = 0.04 * 1.43 * 1066 = 60.99 \text{ kN}$

- From this calculation, the wind load from the columns on the internal beams can be calculated for the x-direction at the top of the column:

$$F_{wind,int,x} := q_{wind,D,x} \cdot 0.5 \cdot h_{column} + q_{wind,parapet,x} \cdot h_{parapet} + F_{fr,x} = 211.399 \cdot \text{kN}$$

- The other part of the wind due to D and E on the columns is transferred to the foundation:

$$F_{wind,int,x,foundation} := q_{wind,D,x} \cdot 0.5 \cdot h_{column} = 89.914 \cdot \text{kN}$$

- And for the y-direction, the same applies:

$$F_{wind,int,y} := q_{wind,D,y} \cdot 0.5 \cdot h_{column} + q_{wind,parapet,y} \cdot h_{parapet} + F_{fr,y} = 159.138 \cdot \text{kN}$$

$$F_{wind,int,y,foundation} := q_{wind,D,y} \cdot 0.5 \cdot h_{column} = 84.315 \cdot \text{kN}$$

- The outside columns need to carry the wind friction that is governing on the side of the building as well, this means the following for the friction on the roof for the external beams:

- $F_{fr,facade} = c_{fr} * q_{p10} * L_{building} \rightarrow$ for the x-direction: $L_{building} = 221.34 \text{ m}$ and for the y-direction: $L_{building} = 134.88 \text{ m}$

- Roof friction force (x-direction): $F_{fr,facade,x} = 0.04 * 1.43 * 221.34 = 12.66 \text{ kN}$

- Roof friction force (y-direction): $F_{fr,facade,y} = 0.04 * 1.43 * 134.88 = 7.72 \text{ kN}$

- The load that is transferred from the outside columns to the outside beams and foundation in the x-direction are as follows:

$$F_{wind,ext,x} := 0.5 \cdot (q_{wind,D,x} \cdot 0.5 \cdot h_{column} + q_{wind,parapet,x} \cdot h_{parapet} + F_{fr,x}) + q_{fr,facade,x} \cdot (0.5 \cdot h_{column} + h_{parapet}) = 203.819 \cdot \text{kN}$$

$$F_{wind,ext,x,foundation} := 0.5 \cdot (q_{wind,D,x} \cdot 0.5 \cdot h_{column}) + q_{fr,facade,x} \cdot 0.5 \cdot h_{column} = 130.417 \cdot \text{kN}$$

- The load that is transferred from the outside columns to the outside beams and foundation in the y-direction are as follows:

$$F_{wind,ext,y} := 0.5 \cdot (q_{wind,D,y} \cdot 0.5 \cdot h_{column} + q_{wind,parapet,y} \cdot h_{parapet} + F_{fr,y}) + q_{fr,facade,y} \cdot (0.5 \cdot h_{column} + h_{parapet}) = 139.361 \cdot \text{kN}$$

$$F_{wind,ext,y,foundation} := 0.5 \cdot (q_{wind,D,y} \cdot 0.5 \cdot h_{column}) + q_{fr,facade,y} \cdot 0.5 \cdot h_{column} = 94.235 \cdot \text{kN}$$

These results are combined in the figures on the following page.

Live loads 4: Wind D+E (y-direction)

- Friction force on beam = 3.8 kN, halfway every beam
- Wind D on column = 8.26 kN/m
- Wind D on parapet = 14.75 kN/m
- Wind E on column = 5.14 kN/m

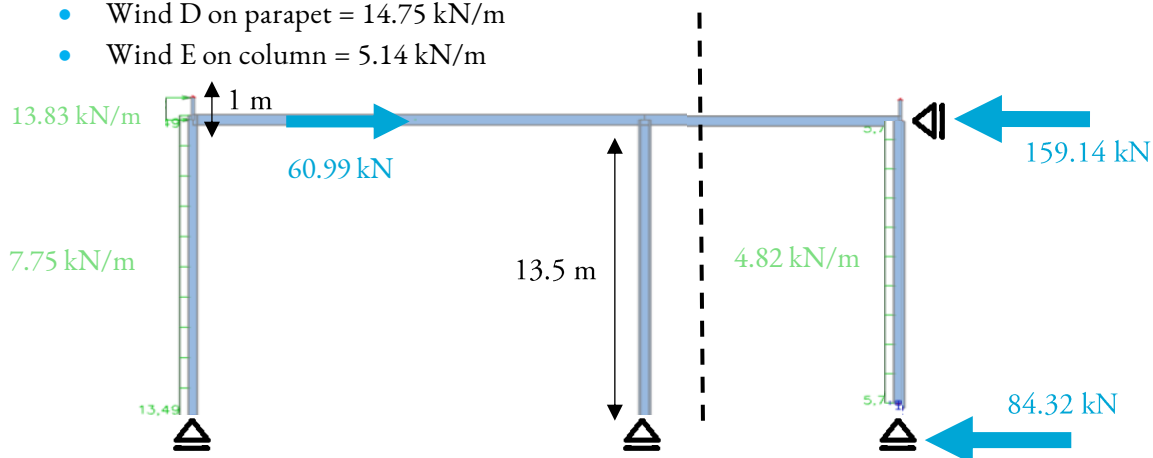


Figure D-3: Overview of the horizontal wind loads in the y-direction

On the right side at the top: the total loads on the roof bracing, on the right side at the bottom: the total loads going to the foundation

Live loads 4: Wind D+E (x-direction)

- Friction force on beam = 3.8 kN, halfway every beam
- Wind D on column = 8.26 kN/m
- Wind D on parapet = 14.75 kN/m
- Wind E on column = 5.14 kN/m

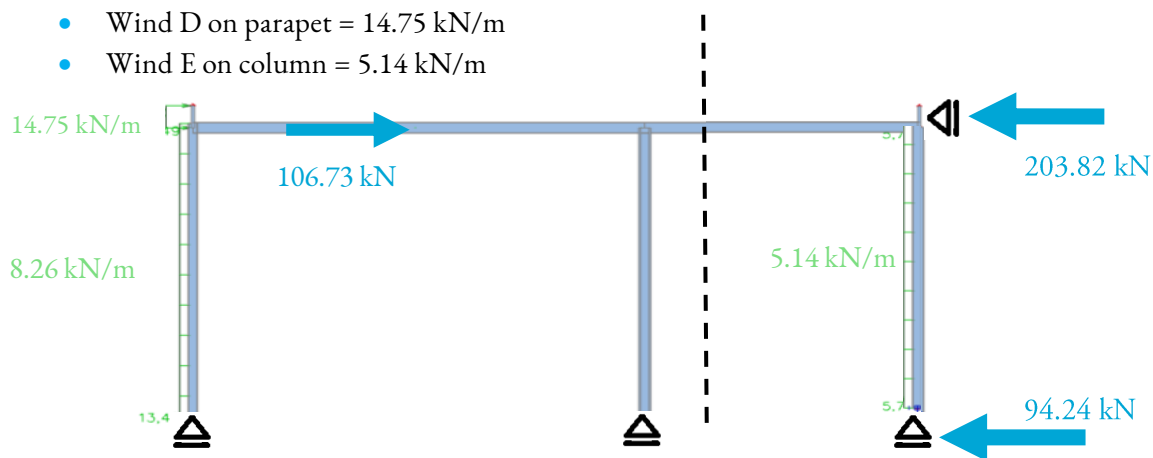


Figure D-4: Overview of the horizontal wind loads in the x-direction

On the right side at the top: the total loads on the roof bracing, on the right side at the bottom: the total loads going to the foundation

D.3 Roof bracing design

D.3.1 Horizontal bracing

The loads are then placed on top of the bracing elements in the roof. This is visualised in the following figures. Compared to the steel bracing design (Alternative A), an important difference is found. The steel bracing only carried tensile forces. This is not possible for a timber design. Therefore, the diagonals carry compressive and tensile forces.

The design of the roof bracing for the wind coming from the x-direction can be found in Figure D-5. In this figure, the two bracing areas in the building are placed closer to each other. This will provide insight in the normal forces in the beams between the two bracings and provides insight in the flow of forces throughout the building. This means that this is a simplification of the actual building. In this figure, also the supports are shown in blue. These supports represent the vertical bracing in the façade.

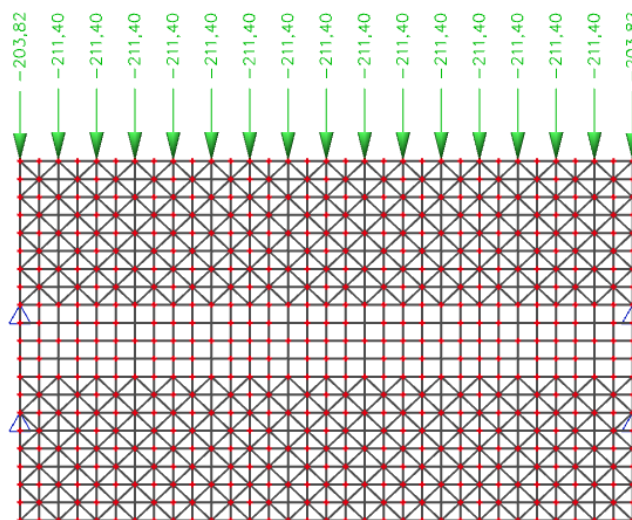


Figure D-5: Screenshot of SCIA model of the timber bracing carrying the wind coming from the x-direction. The supports are shown in blue. These supports represent the bracing in the façade.

The bracing for the wind coming from the y-direction can be found in Figure D-6. This is only one bracing system, with on both sides supports to be able to carry the wind from both directions. The supports are shown in blue in these figures and represent the bracing in the façade.

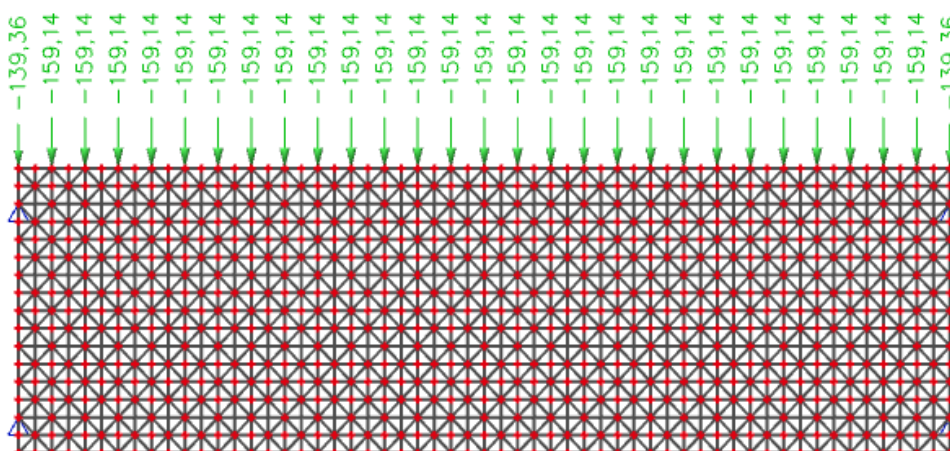


Figure D-6: Screenshot of SCIA model of the timber bracing carrying the wind coming from the y-direction. The supports are shown in blue. These supports represent the bracing in the façade.

From the roof bracing design shown in Figure D-5 and Figure D-6, the governing normal forces in the beams are found and given in Table D-8. It is decided to take the largest forces in the beams, which makes this design conservative, yet safe. The normal forces are combined with the vertical forces on the system to find the dimensions of the beams in the non-sway frame.

Table D-8: Largest normal forces in the horizontal roof bracing system

This is used as input for the two 2D-sections, where these forces are combined with the other wind loads on the beams

Member	Type	Normal force [kN]
Beam 1 (x)	GL24h 1150x192	-821.34
Beam 3 (y)	GL24h tapered (average h=1361, b=195)	-686.00

D.3.2 Vertical bracing

The vertical bracing is calculated as a separate system, as shown in Figure 6-22. Due to the large normal force in the diagonals, a steel circular hollow section is applied in this design. In this figure, a horizontal load is shown. This load is equal to the reaction forces in the supports. For the vertical bracing in the x-direction, this load is equal to the largest reaction force in the supports of Figure D-5 and the load on the vertical bracing in the y-direction is equal to the largest support reaction of Figure D-6.

The support reactions from the horizontal bracings are as follows:

- $R_{vertical\ bracing,x} = 1193.70\ kN$
- $R_{vertical\ bracing,y} = 1238.69\ kN$

D.4 Roof plan of the structure

In the following figure, a 3D-view of the roof is shown. This is a 3D-view of the top view shown on the next page.

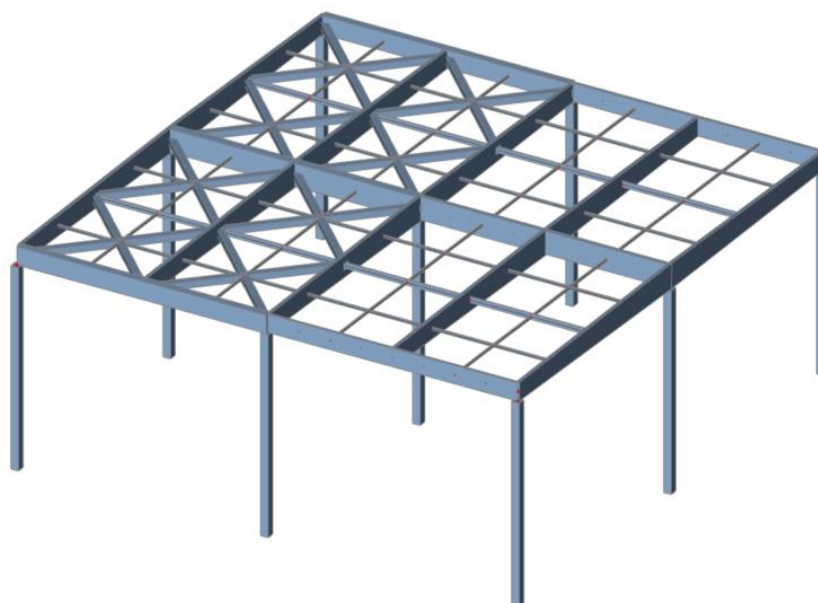


Figure D-7: 3D-view of a part of the roof beams, bracings, lateral supports, and columns (own illustration, made with SCIA Engineer)

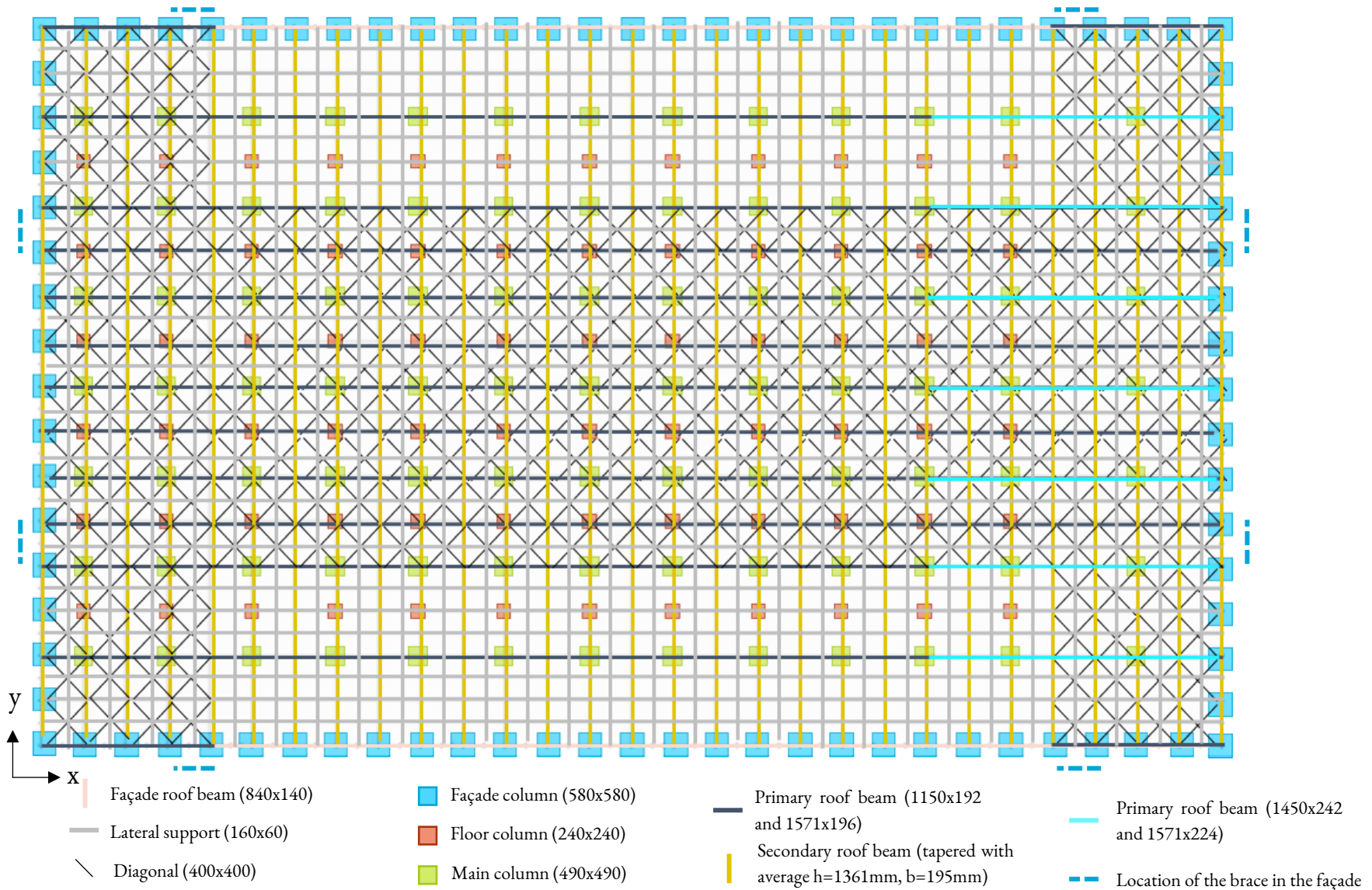


Figure D-8: Top view of the structure at the dotted green line shown in Figure 6-4, including the lateral supported beams that were excluded in Figure 6-18

D.5 Results of structural calculations

The final design is given in chapter 6.3 “Alternative B: Non-sway structure”. In these chapters, the load combinations are also given. For this design, the elements that are not part of the bracing system are checked for the governing load combination ULS 7 and SLS 17. The elements that are part of the bracing system are checked for ULS 6 and SLS 16.

D.5.1 SLS

The results are found in the following table, this is based upon the deflection calculation by SCIA. Here, the initial deflection is calculated. In the table, the final deflection including the deformation factor (as explained in D.1.2 “Product properties”) is given. Also, the deflection of the diagonals is given in the table. The diagonals only need to carry horizontal forces (wind) and their own weight. It is therefore checked if the deflection of the diagonals due to their own weight is limited.

For the horizontal deformation of the building, the initial deflection of the braces due to the wind load (as shown in Figure C-10) is calculated with help of SCIA. This is given in the table as well (no deformation factor is needed for a short-term wind load). It can be noticed that the unity check is relatively low. This choice has been made to limit the loads on the beams in the bracing area, as these beams will have to be much heavier with a higher normal force due to the wind.

Table D-9: Final deflection results of the structural verifications performed

Check	Max. calculated	Max. based on length	UC	Maximal UC
<i>Vertical deformation</i>		$\frac{L_{beam}}{250}$		
Beam (x, length 23.715 m)	54.16 mm	94.9 mm	0.57	0.80
Beam (y, length 16.86 m)	46.84 mm	67.4 mm	0.70	0.80
Diagonal (length 11.6 m)	31.52 mm	46.2 mm	0.68	0.80
<i>Horizontal deformation</i>		$\frac{h_{column}}{150} = \frac{13500}{150} = 90 \text{ mm}$		
Wind from x-direction	16.6 mm	90 mm	0.19	0.80
Wind from y-direction	32.4 mm	90 mm	0.36	0.80

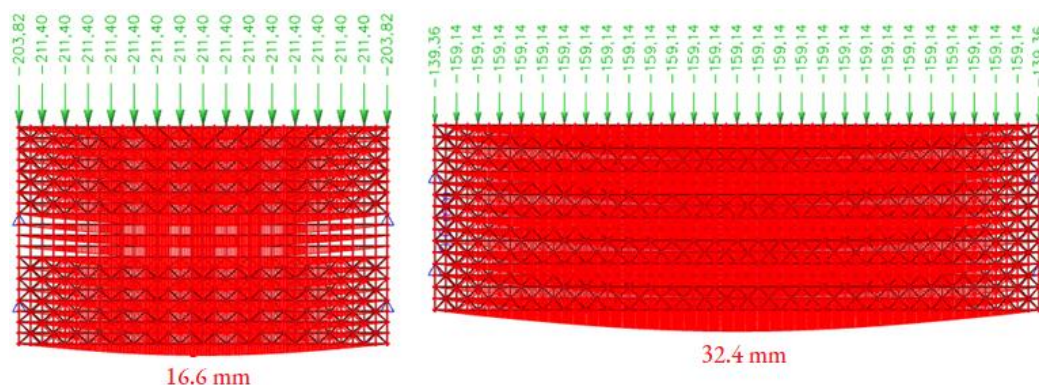


Figure D-9: Horizontal deflection of the bracing systems due to the wind load (from SCIA)
Left: wind from the x-direction, right: wind from the y-direction

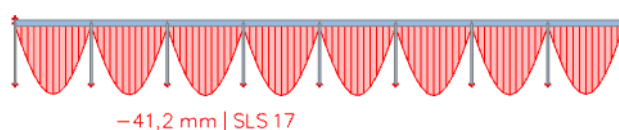


Figure D-10: Initial deflection of beams in y-direction (from SCIA)

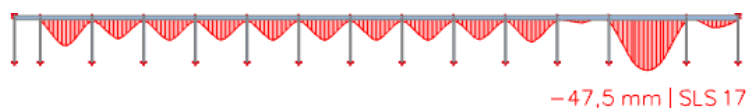


Figure D-11: Initial deflection of the smaller beams in x-direction

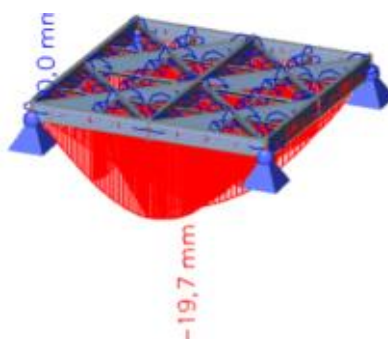


Figure D-12: Initial deflection of a part of the bracing system due to their self-weight (from SCIA)

D.5.2 Buckling lengths and ULS calculation results

The buckling lengths are also calculated. The building is non-sway due to the bracing system. Furthermore, the beams and columns are connected by hinges and the column bases are also connected with a hinge to the foundation. This means that the buckling factors for the beams and columns are equal to 1 (see Figure B-20). The beams are laterally restrained in the other direction, which results in the buckling lengths shown in the following table.

Table D-10: Buckling lengths of the beams

Member	Length between LTB restraints [m]	Length between supports [m]	Buckling factor	
			Main	Perp.
Beam (x)	3.953	23.715	1	1
Beam (y)	4.215	16.86	1	1

In Table B-18, the governing unity checks for the different members is given. For these calculations, SCIA is used to calculate the forces in the elements. Then, this is checked with hand calculations. These calculations are very similar, so therefore only the calculations of the façade column and two beams outside the bracing (in x- and y-direction) are provided in the next sub-chapters.

Table D-11: Governing unity checks for the members of Alternative B

Member	Type	UC section	Max. UC section	UC stability	Max. UC stability
Main column	GL24h 490x490	0.31	0.85	0.76	0.80
Façade column	GL24h 580x580	0.80	0.85	0.80	0.80
Beam, lower (x) ¹	GL24h 1150x192	0.75	0.85	0.75	0.80
Beam, lower (x) ¹	GL24h 1450x242	0.72	0.85	0.72	0.80
Beam (y)	GL24h tapered (av h=1361, b=195)	0.56	0.85	0.76	0.80
Façade beam	GL24h 840x140	0.73	0.85	0.53	0.80
<i>Horizontal bracing elements</i>					
Beam, lower (x)	GL24h 1150x460	0.48	0.85	0.75	0.80
Beam, lower (x)	GL24h 1450x500	0.29	0.85	0.80	0.80
Beam (y)	GL24h tapered (av h=1361, b=390)	0.26	0.85	0.69	0.80
Diagonal	GL24h 400x400	0.27	0.85	0.00	0.80
<i>Vertical bracing elements</i>					
Diagonal	CHS 406.4x16	0.27	0.85	0.79	0.80

The governing forces in the elements outside the bracing are due to the vertical load combination (ULS 7). This is shown in the following figures for the x- and y-direction.

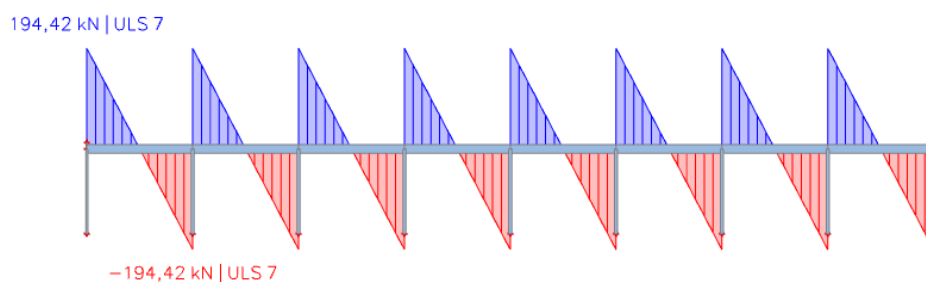


Figure D-13: Shear forces in the frame in the y-direction (for ULS 7)

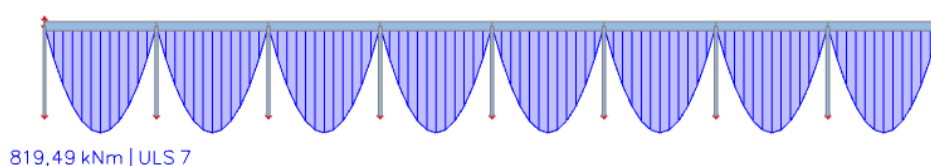


Figure D-14: Bending moments in the frame in the y-direction (for ULS 7)

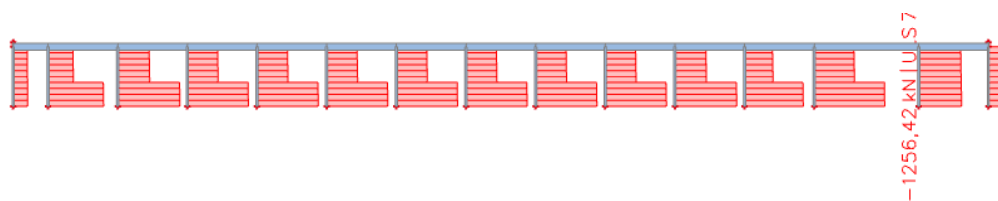


Figure D-15: Normal forces in the frame in the x-direction, for the higher beams (for ULS 7)

¹ The higher beams (located at the highest point of the tapered beams) will be strong enough if the lower beams are strong enough. Therefore, they are not checked separately.

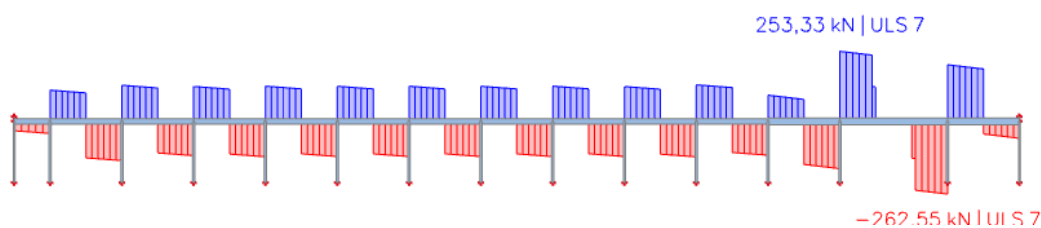


Figure D-16: Shear forces in the frame in the x-direction, for the lower beams (for ULS 7)

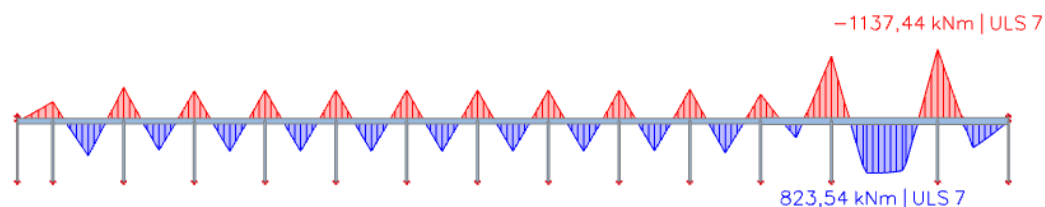


Figure D-17: Bending moments in the frame in the x-direction, for the lower beams (for ULS 7)

For the elements in the bracing, wind load combination ULS 6 is governing. The results are shown in the following figures.



Figure D-18: Normal forces in the beams in the y-direction (for ULS 6)

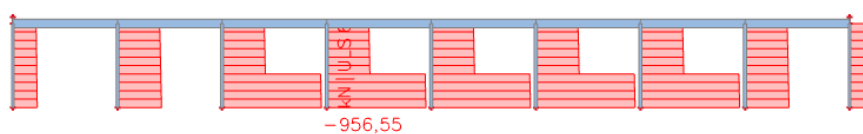


Figure D-19: Normal forces in the columns in the y-direction (for ULS 6)

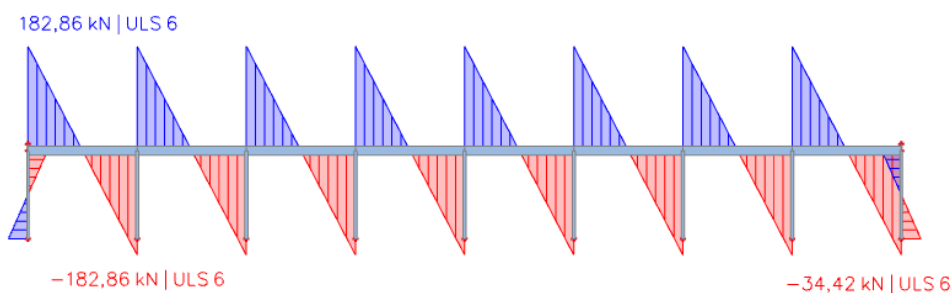


Figure D-20: Shear forces in the frame in the y-direction (for ULS 6)

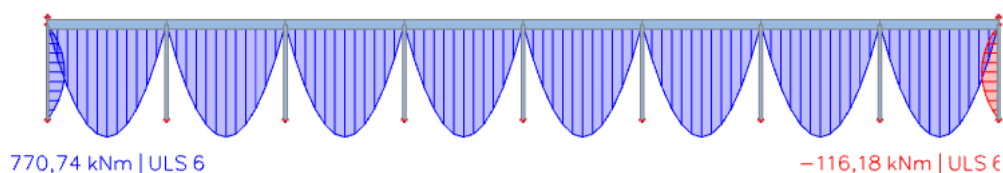


Figure D-21: Bending moments in the frame in the y-direction (for ULS 6)

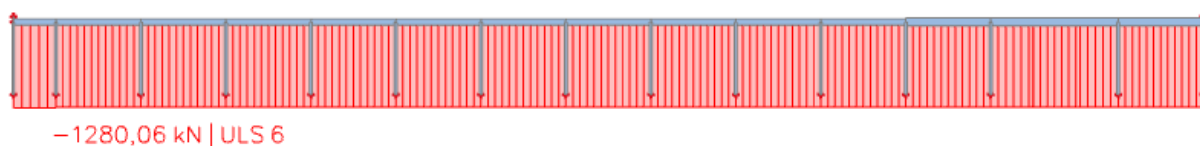


Figure D-22: Normal forces in the beams in the x-direction (for ULS 6)

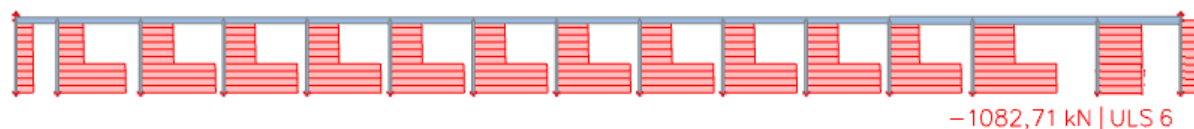


Figure D-23: Normal forces in the columns in the x-direction (for ULS 6)

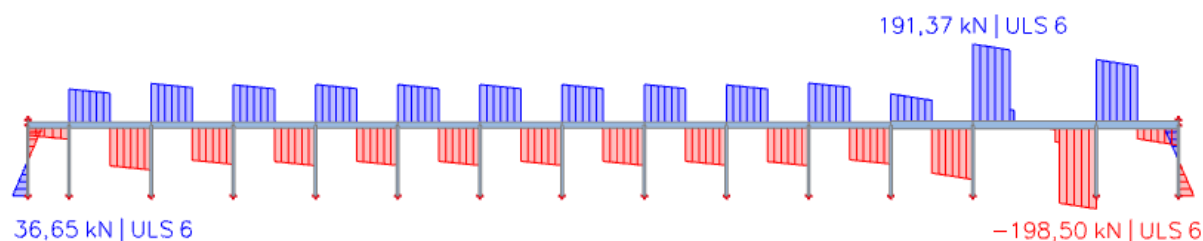


Figure D-24: Shear forces in the frame in the x-direction (for ULS 6)

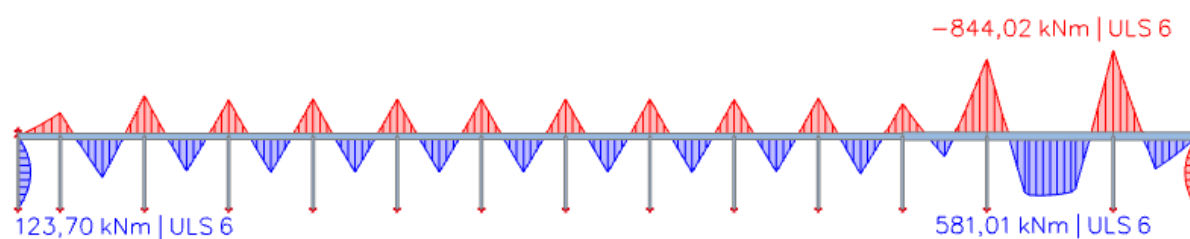


Figure D-25: Bending moments in the frame in the x-direction (for ULS 6)

D.5.3 Calculation of specific elements

In the following sections, the calculation of two beams outside the bracing (in x- and y-direction) and a façade column is provided. The other elements inside the bracing area are calculated in the same way and therefore not included in this appendix. For the main columns, the influence of bending and axial compression is not necessary, making this calculation simpler than the façade column.

D.5.3.1 Calculation of beam (y)

$$L := 16.860\text{m} \quad \text{Length of beam}$$

$$L_{ef} := \frac{L}{4} = 4.215\text{m} \quad \text{Distance between torsional restraints by means of beams in the other direction}$$

Cross section properties

$$h_s := 1150\text{mm} \quad \text{Height of beam at the support}$$

$$\alpha := 0.05 \quad \text{5 \% angle of the roof}$$

$$h_a := h_s + \alpha \cdot \frac{1}{2} \cdot L = 1.571 \times 10^3 \cdot \text{mm} \quad \text{Height of beam at the apex (rule of thumb (De Groot, 2018))}$$

The beam is modelled as a straight beam, so the average height and average width need to be calculated:

$$h_{\text{average}} := \frac{(h_a + h_s)}{2} = 1.361 \times 10^3 \cdot \text{mm} \quad \text{Average height of the beam}$$

$$b := h_{\text{average}} \cdot \frac{1}{7} = 194.393 \cdot \text{mm} \quad \text{Width of beam (as 1/6 to 1/8 is considered economical)}$$

$$A := h_{\text{average}} \cdot b = 0.265 \text{ m}^2 \quad \text{Average area of the beam}$$

$$\text{weight} := \rho_{\text{mean}} \cdot A = 111.098 \frac{\text{kg}}{\text{m}} \quad \text{Average weight of the beam}$$

$$I_y := \frac{1}{12} \cdot b \cdot h_{\text{average}}^3 = 4.082 \times 10^{10} \cdot \text{mm}^4 \quad \text{Average moment of inertia in y-direction}$$

$$I_z := \frac{1}{12} \cdot h_{\text{average}} \cdot b^3 = 8.33 \times 10^8 \cdot \text{mm}^4 \quad \text{Average moment of inertia in z-direction}$$

$$I_t := \frac{1}{3} \cdot b^3 \cdot h_{\text{average}} \cdot \left[1 - 0.63 \cdot \frac{b}{h_{\text{average}}} + 0.525 \cdot \left(\frac{b}{h_{\text{average}}} \right)^5 \right] = 3.032 \times 10^{-3} \text{ m}^4 \quad \text{Average torsional moment of inertia}$$

$$W_y := \frac{1}{6} \cdot b \cdot h_{\text{average}}^2 = 5.999 \times 10^7 \cdot \text{mm}^3 \quad \text{Average section modulus in y-direction}$$

The average width is taken all over the beam, leading to the following areas at the support and at the apex:

$$A_s := h_s \cdot b = 0.224 \text{ m}^2 \quad \text{Area of the beam at the support}$$

$$A_a := h_a \cdot b = 0.305 \text{ m}^2 \quad \text{Area of the beam at the apex}$$

Loads (ULS 7, from SCIA)

$$N_{t,0,d} := 0\text{N} \quad \text{Tension force parallel to the grain}$$

$$N_{c,0,d} := 0\text{kN} \quad \text{Compression force parallel to the grain}$$

$$N_{c,90,d} := 0\text{N} \quad \text{Compression force perpendicular to the grain}$$

$$V_{\text{Ed,ULS}} := 194.42\text{kN} \quad \text{Shear force at the support}$$

$$M_{\text{Ed,ULS,max}} := 820\text{kN} \cdot \text{m} \quad \text{Bending moment at the centre of the beam (maximum)}$$

$$M_{\text{Ed,ULS,a}} := 0\text{kN} \cdot \text{m} \quad \text{Bending moment at the apex}$$

Calculating the bending moment at the critical cross section:

$$x := \frac{\frac{1}{2}L}{1 + \frac{h_a}{h_s}} = 3.562\text{m} \quad \text{Location of the critical cross section}$$

For a parabola, the following applies: $y = a \cdot (x-p)^2 + q$, where (p,q) is the top of the parabola

$$a := \frac{-M_{\text{Ed,ULS,max}}}{(0.5 \cdot L)^2} = -11.539 \cdot \frac{\text{kN}}{\text{m}}$$

Bending moment at the critical cross section:

$$M_{\text{Ed,ULS,c}} := a \cdot (x - 0.5 \cdot L)^2 + M_{\text{Ed,ULS,max}} = 546.583 \cdot \text{kN} \cdot \text{m}$$

Ultimate Limit State calculation

Tension parallel to the grain

$$\sigma_{t,0,d} := \frac{N_{t,0,d}}{A_a} = 0 \cdot \text{MPa}$$

$$UC_{\text{tension}} := \frac{\sigma_{t,0,d}}{f_{t,0,d}} = 0$$

Compression parallel to the grain

$$\sigma_{c,0,d} := \frac{N_{c,0,d}}{A_a} = 0$$

$$UC_{\text{compression}} := \frac{\sigma_{c,0,d}}{f_{c,0,d}} = 0$$

Shear capacity (at the supports)

$$\tau := \frac{3}{2} \cdot \frac{V_{\text{Ed,ULS}}}{A_s} = 1.305 \cdot \text{MPa}$$

$$UC_{\text{shear}} := \frac{\tau}{f_{v,d}} = 0.518$$

Compression perpendicular to the grain (at the supports)

$$\sigma_{c,90,d} := \frac{N_{c,90,d}}{A_s} = 0$$

$k_{c,90} := 1.75$ for glulam with a discrete support

$$UC_{\text{compr.pp}} := \frac{\sigma_{c,90,d}}{f_{c,90,d} \cdot k_{c,90}} = 0$$

Bending moment capacity (at the critical cross section)

D4.1 Single-tapered beams (Blaß & Sandhaas, 2017)

$$x_{\text{crit}} := \frac{\frac{1}{2}L}{1 + \frac{h_a}{h_s}} = 3.562 \text{ m} \quad \text{Location of the critical cross section}$$

$$h_c := \alpha \cdot x + h_s = 1.328 \times 10^3 \cdot \text{mm}$$

$$W_{y,c} := \frac{1}{6} \cdot b \cdot h_c^2 = 5.715 \times 10^7 \cdot \text{mm}^3 \quad \text{Section modulus in y-direction of the critical cross section}$$

$$\sigma_{m,y,d} := \frac{M_{\text{Ed,Uls,c}}}{W_{y,c}} = 9.564 \cdot \text{MPa}$$

$$\beta := 0 \quad \text{Angle of force compared to beam (parallel)}$$

The beams can be subjected to tension forces and compression forces. Therefore, both must be checked.

$$k_{m,\beta,t} := \frac{1}{\sqrt{1 + \left(\frac{f_{m,d}}{f_{t,90,d}}\right)^2 \cdot \tan(\beta)^4 + \frac{f_{m,d}}{0.75 \cdot f_{v,d}} \cdot \tan(\beta)^2}} = 1$$

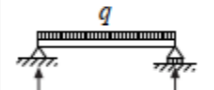

$$k_{m,\beta,c} := \frac{1}{\sqrt{1 + \left(\frac{f_{m,d}}{f_{c,90,d}}\right)^2 \cdot \tan(\beta)^4 + \frac{f_{m,d}}{1.5 \cdot f_{v,d}} \cdot \tan(\beta)^2}} = 1$$

$$UC_{\text{bmt}} := \frac{\sigma_{m,y,d}}{f_{m,d} \cdot k_{m,\beta,t}} = 0.553$$

$$UC_{\text{bmc}} := \frac{\sigma_{m,y,d}}{f_{m,d} \cdot k_{m,\beta,c}} = 0.553$$

Lateral torsional buckling

Load condition according to Table D2-1 in Blaß & Sandhaas (2017):

Load case	Actual moment diagram	m
		0.88

$$m := 0.88$$

$$M_{y,\text{crit}} := \frac{\pi}{L_{\text{ef}} \cdot m} \cdot \sqrt{E_{0.05} \cdot I_z \cdot G_{0.05} \cdot I_t} = 3.065 \times 10^6 \text{ J}$$

$$\sigma_{m,\text{crit}} := \frac{M_{y,\text{crit}}}{W_y} = 51.087 \cdot \text{MPa} \quad k_y := 0.5 \cdot \left[1 + \beta_c \cdot (\lambda_{\text{rel},y} - 0.3) + \lambda_{\text{rel},y}^2 \right] = 0.752$$

$$\lambda_{\text{rel},m} := \sqrt{\frac{f_{m,k}}{\sigma_{m,\text{crit}}}} = 0.685$$

$$k_{\text{crit}} := 1.56 - \lambda_{\text{rel},m} \cdot 0.75 = 1.046 \quad \text{for } 0.75 < \lambda_{\text{rel},m} < 1.4 \quad (6.34 \text{ in EN 1995-1-1})$$

$$\sigma_{m,d} := \frac{M_{\text{Ed,Uls,max}}}{W_y} = 13.669 \cdot \text{MPa}$$

$$UC_{\text{LTB}} := \frac{\sigma_{m,d}}{k_{\text{crit}} \cdot f_{m,d}} = 0.756$$

Combined bending and axial compression force

$$\lambda_y := L \cdot \sqrt{\frac{A}{I_y}} = 42.921 \quad \text{C.11 in EC1995-1-1}$$

$$\lambda_{\text{rel},y} := \frac{\lambda_y}{\pi} \cdot \sqrt{\frac{f_{c,0,k}}{E_{0.05}}} = 0.683$$

$$\lambda_z := L \cdot \sqrt{\frac{A}{I_z}} = 300.447 \quad \text{C.11 in EC1995-1-1}$$

$$\lambda_{\text{rel},z} := \frac{\lambda_z}{\pi} \cdot \sqrt{\frac{f_{c,0,k}}{E_{0.05}}} = 4.782$$

Both are larger than 0.3, so the following equations need to be followed:

$$\beta_c := 0.1 \quad \text{for glulam}$$

$$k_z := 0.5 \cdot \left[1 + \beta_c \cdot (\lambda_{\text{rel.z}} - 0.3) + \lambda_{\text{rel.z}}^2 \right] = 12.157$$

$$k_{c,y} := \frac{1}{k_y + \sqrt{k_y^2 - \lambda_{\text{rel.y}}^2}} = 0.936 \quad k_{c,z} := \frac{1}{k_z + \sqrt{k_z^2 - \lambda_{\text{rel.z}}^2}} = 0.043$$

For the combination of bending and normal force, the following needs to be checked:

$$UC_{\text{bending.normal}} := \left(\frac{\sigma_{\text{m.d}}}{k_{\text{crit}} \cdot f_{\text{m.d}}} \right)^2 + \frac{\sigma_{\text{c.0.d}}}{k_{c,z} \cdot f_{\text{c.0.d}}} = 0.572$$

Service Limit State

Deflection

With help of SCIA, the deflection due to dead loads is calculated and the deflection due to SLS 17 (dead loads, live loads 1, and snow loads) is calculated as follows:

From SCIA: $u_{\text{inst.G}} := 7.6\text{mm}$

$$u_{\text{inst.G.Q}} := 32.4\text{mm}$$

$$u_{\text{inst.Q}} := u_{\text{inst.G.Q}} - u_{\text{inst.G}} = 24.8 \cdot \text{mm}$$

$$u_{\text{fin.G}} := u_{\text{inst.G}} \cdot (1 + k_{\text{def}}) = 12.16 \cdot \text{mm}$$

$$\psi_2 := 0 \quad \text{Factor for the quasi-permanent value of variable action (Category: Snow)}$$

$$u_{\text{fin.Q}} := u_{\text{inst.Q}} \cdot (1 + \psi_2 \cdot k_{\text{def}}) = 24.8 \cdot \text{mm}$$

$$u_{\text{fin}} := u_{\text{fin.G}} + u_{\text{fin.Q}} = 36.96 \cdot \text{mm}$$

$$u_{\text{max}} := \frac{L}{250} = 67.44 \cdot \text{mm}$$

$$UC_{\text{final.deflection}} := \frac{u_{\text{fin}}}{u_{\text{max}}} = 0.548$$

Unity checks overview

$$UC_{\text{tension}} = 0$$

$$UC_{\text{shear}} = 0.518$$

$$UC_{\text{compression}} = 0$$

$$UC_{\text{compr.pp}} = 0$$

$$UC_{\text{bm.t}} = 0.553$$

$$UC_{\text{bending.normal}} = 0.572$$

$$UC_{\text{bm.c}} = 0.553$$

$$UC_{\text{LTB}} = 0.756$$

$$UC_{\text{final.deflection}} = 0.548$$

D.5.3.2 Calculation of beam (x)

Cross section properties

$h := 1450\text{mm}$	Height of beam
$b := \frac{1}{7} \cdot h = 207.143 \cdot \text{mm}$	Width of beam
$L := 23.715\text{m}$	Length of beam
$L_{ef} := \frac{7.905}{2} \text{m}$	Distance between torsional restraints by means of beams in the other direction
$W_y := \frac{1}{6} \cdot b \cdot h^2 = 7.259 \times 10^7 \cdot \text{mm}^3$	Section modulus in y-direction
$I_y := \frac{1}{12} \cdot b \cdot h^3 = 5.263 \times 10^{10} \cdot \text{mm}^4$	Moment of inertia in y-direction
$I_z := \frac{1}{12} \cdot h \cdot b^3 = 1.074 \times 10^9 \cdot \text{mm}^4$	Moment of inertia in z-direction
$I_t := \frac{1}{3} \cdot b^3 \cdot h \cdot \left[1 - 0.63 \cdot \frac{b}{h} + 0.525 \cdot \left(\frac{b}{h} \right)^5 \right] = 3.909 \times 10^{-3} \text{m}^4$	Torsional moment of inertia
$A := h \cdot b = 3.004 \times 10^5 \cdot \text{mm}^2$	Area of the beam

Loads (ULS 7, from SCIA)

$$M_{Ed,ULS} := 898.05\text{kN} \cdot \text{m}$$

$$V_{Ed,ULS} := 210.5\text{kN}$$

$$N_{Ed,ULS} := 0\text{kN}$$

Bending moment capacity

$$\sigma_{m,y,d} := \frac{M_{Ed,ULS}}{W_y} = 12.372 \cdot \text{MPa}$$

$$UC_{\text{bendingmoment}} := \frac{\sigma_{m,y,d}}{f_{m,d}} = 0.716$$

Shear capacity

$$\tau_d := 1.5 \cdot \frac{V_{Ed,ULS}}{A} = 1.051 \cdot \text{MPa}$$

$$UC_{\text{shear}} := \frac{\tau_d}{f_{v,d}} = 0.417$$

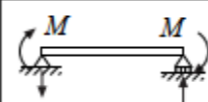
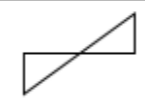
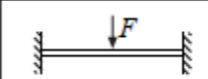

Compression parallel to the grain

$$\sigma_{c,0,d} := \frac{N_{Ed,ULS}}{A} = 0$$

$$UC_{\text{compression}} := \frac{\sigma_{c,0,d}}{f_{c,0,d}} = 0$$

Lateral torsional buckling

Load condition according to Table D2-1 in Blaß & Sandhaas (2017):

Load case	Actual moment diagram	m
		0.43
		0.59

From the moment diagram of the continuous beam, this lies between these two load cases. As least favourable, the following is calculated with:

$$m := 0.59$$

$$M_{y,crit} := \frac{\pi}{L_{ef} \cdot m} \cdot \sqrt{E_{0.05} \cdot I_z \cdot G_{0.05} \cdot I_t} = 6.285 \times 10^6 \text{J}$$

$$\sigma_{m,crit} := \frac{M_{y,crit}}{W_y} = 86.588 \cdot \text{MPa}$$

$$\lambda_{rel,m} := \sqrt{\frac{f_{m,k}}{\sigma_{m,crit}}} = 0.526$$

$$k_{crit} := 1 \quad \text{for} \quad \lambda_{rel,m} < 0.75 \quad (6.34 \text{ in EN 1995-1-1})$$

$$\sigma_{m,d} := \frac{M_{Ed,ULS}}{W_y} = 12.372 \cdot \text{MPa}$$

$$UC_{LTB} := \frac{\sigma_{m,d}}{k_{crit} \cdot f_{m,d}} = 0.716$$

Combined bending and axial compression force

$$\lambda_y := L \cdot \sqrt{\frac{A}{I_y}} = 56.656 \quad \text{C.11 in EC1995-1-1}$$

$$\lambda_{rel,y} := \frac{\lambda_y}{\pi} \cdot \sqrt{\frac{f_{c,0,k}}{E_{0.05}}} = 0.902$$

$$\lambda_z := L \cdot \sqrt{\frac{A}{I_z}} = 396.592 \quad \text{C.11 in EC1995-1-1}$$

$$\lambda_{rel,z} := \frac{\lambda_z}{\pi} \cdot \sqrt{\frac{f_{c,0,k}}{E_{0.05}}} = 6.312$$

Both are larger than 0.3, so the following equations need to be followed:

$$\beta_c := 0.1 \quad \text{for glulam}$$

$$k_y := 0.5 \cdot \left[1 + \beta_c \cdot (\lambda_{\text{rel.y}} - 0.3) + \lambda_{\text{rel.y}}^2 \right] = 0.937$$

$$k_z := 0.5 \cdot \left[1 + \beta_c \cdot (\lambda_{\text{rel.z}} - 0.3) + \lambda_{\text{rel.z}}^2 \right] = 20.721$$

$$k_{c.y} := \frac{1}{k_y + \sqrt{k_y^2 - \lambda_{\text{rel.y}}^2}} = 0.84$$

$$k_{c.z} := \frac{1}{k_z + \sqrt{k_z^2 - \lambda_{\text{rel.z}}^2}} = 0.025$$

For the combination of bending and normal force, the following needs to be checked:

$$UC_{\text{bending.normal}} := \left(\frac{\sigma_{\text{m.d}}}{k_{\text{crit}} \cdot f_{\text{m.d}}} \right)^2 + \frac{\sigma_{\text{c.0.d}}}{k_{c.z} \cdot f_{\text{c.0.d}}} = 0.513$$

Deflection

With help of SCIA, the deflection due to dead loads is calculated and the deflection due to SLS 17 (dead loads, live loads 1, and snow loads) is calculated as follows:

$$\text{From SCIA:} \quad u_{\text{inst.G}} := 15.7 \text{ mm}$$

$$u_{\text{inst.G.Q}} := 57.9 \text{ mm}$$

$$u_{\text{inst.Q}} := u_{\text{inst.G.Q}} - u_{\text{inst.G}} = 42.2 \cdot \text{mm}$$

$$u_{\text{fin.G}} := u_{\text{inst.G}} \cdot (1 + k_{\text{def}}) = 25.12 \cdot \text{mm}$$

$$\psi_2 := 0 \quad \text{Factor for the quasi-permanent value of variable action (Category: Snow)}$$

$$u_{\text{fin.Q}} := u_{\text{inst.Q}} \cdot (1 + \psi_2 \cdot k_{\text{def}}) = 42.2 \cdot \text{mm}$$

$$u_{\text{fin}} := u_{\text{fin.G}} + u_{\text{fin.Q}} = 67.32 \cdot \text{mm}$$

$$u_{\text{max}} := \frac{L}{250} = 94.86 \cdot \text{mm}$$

$$UC_{\text{final.deflection}} := \frac{u_{\text{fin}}}{u_{\text{max}}} = 0.71$$

Overview of unity checks

$$UC_{\text{final.deflection}} = 0.71$$

$$UC_{\text{shear}} = 0.417$$

$$UC_{\text{bendingmoment}} = 0.716$$

$$UC_{\text{LTB}} = 0.716$$

$$UC_{\text{compression}} = 0$$

$$UC_{\text{bending.normal}} = 0.513$$

The longer beam has the same dimensions as the shorter beam. This is different than for Alternative A, because for steel as a material, the deflection was governing. However, for timber, the bending moment capacity and lateral torsional buckling are governing.

D.5.3.3 Calculation of façade column

$$h := 580 \text{ mm}$$

Height of column

$$b := h = 580 \cdot \text{mm}$$

Width of column

$$L := 13.5 \text{ m}$$

Length of column

$$L_{\text{ef}} := L$$

Effective buckling length of the column

$$W_y := \frac{1}{6} \cdot b \cdot h^2 = 3.252 \times 10^7 \cdot \text{mm}^3$$

Section modulus in y-direction

$$I_y := \frac{1}{12} \cdot b \cdot h^3 = 9.43 \times 10^9 \cdot \text{mm}^4$$

Moment of inertia in y-direction

$$I_z := \frac{1}{12} \cdot h \cdot b^3 = 9.43 \times 10^9 \cdot \text{mm}^4$$

Moment of inertia in z-direction

$$I_t := \frac{1}{3} \cdot b^3 \cdot h \cdot \left[1 - 0.63 \cdot \frac{b}{h} + 0.525 \cdot \left(\frac{b}{h} \right)^5 \right] = 0.034 \text{ m}^4$$

Torsional moment of inertia

$$A := h \cdot b = 3.364 \times 10^5 \cdot \text{mm}^2$$

Area of the column

Loads (from SCIA)

$$M_{\text{Ed.ULS}} := 400.43 \text{ kN} \cdot \text{m} \quad \text{ULS 6}$$

$$V_{\text{Ed.ULS}} := 119.47 \text{ kN} \quad \text{ULS 6}$$

Ultimate Limit State calculation Compression parallel to the grain

$$\sigma_{\text{c.0.d}} := \frac{N_{\text{c.d.ULS}}}{A} = 1.262 \times 10^6 \text{ Pa}$$

$$UC_{\text{compression}} := \frac{\sigma_{\text{c.0.d}}}{f_{\text{c.0.d}}} = 0.082$$

Bending moment capacity

$$\sigma_{\text{m.y.d}} := \frac{M_{\text{Ed.ULS}}}{W_y} = 12.314 \cdot \text{MPa}$$

$$UC_{\text{bendingmoment}} := \frac{\sigma_{\text{m.y.d}}}{f_{\text{m.d}}} = 0.799$$

Shear capacity

$$\tau_d := 1.5 \cdot \frac{V_{\text{Ed.ULS}}}{A} = 0.533 \cdot \text{MPa}$$

$$UC_{\text{shear}} := \frac{\tau_d}{f_{\text{v.d}}} = 0.308$$

Flexural buckling

$$\lambda_y := L \cdot \sqrt{\frac{A}{I_y}} = 80.63 \quad \text{C.11 in EC1995-1-1}$$

$$\lambda_{rel,y} := \frac{\lambda_y}{\pi} \cdot \sqrt{\frac{f_{c,0,k}}{E_{0.05}}} = 1.297$$

$$\lambda_z := L \cdot \sqrt{\frac{A}{I_z}} = 80.63 \quad \text{C.11 in EC1995-1-1}$$

$$\lambda_{rel,z} := \frac{\lambda_z}{\pi} \cdot \sqrt{\frac{f_{c,0,k}}{E_{0.05}}} = 1.297$$

Both are larger than 0.3, so the following equations need to be followed:

$$\beta_c := 0.1 \quad \text{for glulam}$$

$$k_y := 0.5 \cdot \left[1 + \beta_c \cdot (\lambda_{rel,y} - 0.3) + \lambda_{rel,y}^2 \right] = 1.391$$

$$k_z := 0.5 \cdot \left[1 + \beta_c \cdot (\lambda_{rel,z} - 0.3) + \lambda_{rel,z}^2 \right] = 1.391$$

$$k_{c,y} := \frac{1}{k_y + \sqrt{k_y^2 - \lambda_{rel,y}^2}} = 0.528$$

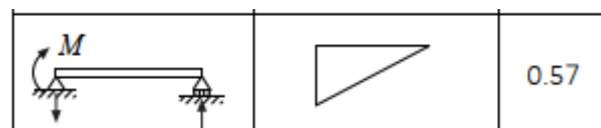
$$k_{c,z} := \frac{1}{k_z + \sqrt{k_z^2 - \lambda_{rel,z}^2}} = 0.528$$

$$UC_{buckling,y} := \frac{\sigma_{c,0,d}}{k_{c,y} \cdot f_{c,0,d}} = 0.155$$

$$UC_{buckling,z} := \frac{\sigma_{c,0,d}}{k_{c,z} \cdot f_{c,0,d}} = 0.155$$

Lateral torsional buckling

Load condition according to Table D2-1 in Blaß & Sandhaas (2017):



From the moment diagram of the continuous beam, this lies between these two load cases. As least favourable, the following is calculated with:

$$m := 0.57$$

$$M_{y,crit} := \frac{\pi}{L_{ef} \cdot m} \cdot \sqrt{E_{0.05} \cdot I_z \cdot G_{0.05} \cdot I_t} = 1.641 \times 10^7 \text{ J}$$

$$\sigma_{m,crit} := \frac{M_{y,crit}}{W_y} = 504.71 \cdot \text{MPa}$$

$$\lambda_{rel,m} := \sqrt{\frac{f_{m,k}}{\sigma_{m,crit}}} = 0.218 \quad UC_{bending,normal} = 0.794$$

$$k_{crit} := 1 \quad \text{for } \lambda_{rel,m} < 0.75 \quad (6.34 \text{ in EN 1995-1-1})$$

$$\sigma_{m,d} := \frac{M_{Ed,ULS}}{W_y} = 12.314 \cdot \text{MPa}$$

$$UC_{LTB} := \frac{\sigma_{m,d}}{k_{crit} \cdot f_{m,d}} = 0.799$$

Combined bending and axial compression force

$$\lambda_y := L \cdot \sqrt{\frac{A}{I_y}} = 80.63 \quad \text{C.11 in EC1995-1-1}$$

$$\lambda_{rel,y} := \frac{\lambda_y}{\pi} \cdot \sqrt{\frac{f_{c,0,k}}{E_{0.05}}} = 1.297$$

$$\lambda_z := L \cdot \sqrt{\frac{A}{I_z}} = 80.63 \quad \text{C.11 in EC1995-1-1}$$

$$\lambda_{rel,z} := \frac{\lambda_z}{\pi} \cdot \sqrt{\frac{f_{c,0,k}}{E_{0.05}}} = 1.297$$

Both are larger than 0.3, so the following equations need to be followed:

$$\beta_c := 0.1 \quad \text{for glulam}$$

$$k_y := 0.5 \cdot \left[1 + \beta_c \cdot (\lambda_{rel,y} - 0.3) + \lambda_{rel,y}^2 \right] = 1.391$$

$$k_z := 0.5 \cdot \left[1 + \beta_c \cdot (\lambda_{rel,z} - 0.3) + \lambda_{rel,z}^2 \right] = 1.391$$

$$k_{c,y} := \frac{1}{k_y + \sqrt{k_y^2 - \lambda_{rel,y}^2}} = 0.528$$

$$k_{c,z} := \frac{1}{k_z + \sqrt{k_z^2 - \lambda_{rel,z}^2}} = 0.528$$

For the combination of bending and normal force, the following needs to be checked:

$$UC_{bending,normal} := \left(\frac{\sigma_{m,d}}{k_{crit} \cdot f_{m,d}} \right)^2 + \frac{\sigma_{c,0,d}}{k_{c,z} \cdot f_{c,0,d}} = 0.794$$

Overview of unity checks

$$UC_{compression} = 0.082 \quad UC_{bendingmoment} = 0.799 \quad UC_{shear} = 0.308$$

$$UC_{buckling,y} = 0.155 \quad UC_{buckling,z} = 0.155$$

D.5.4 Connection in the bracing system

In the following table, the connection between the timber diagonal and the beams in the roof bracing system is checked as this is often governing for such a system. Here, the splitting failure and the block shear failure are calculated as governing failure modes.

Table D-12: Input for the calculation of the splitting failure and block shear failure

Explanation	Parameter		
Force in the diagonal	N,Ed	680	kN
Width of diagonal	b	400	mm
Height of diagonal	h	400	mm
Thickness of the plate	t,pl	25	mm
Number of plates	n,plates	2	
Number of shear planes to be checked (Inside = 2; Outside = 1)	n,planes	3	
Yield strength of steel plate	f,y	355	N/mm ²
	t,1	40	mm
	t,2	122.5	mm
Diameter of the dowel	d,dowel	20	mm
Number of dowels in the row	n,per row	9	
Number of rows	n,rows	3	
	a,1	100	mm
	a,2	80	mm
	a,3	140	mm
	a,4	60	mm
Ultimate strength dowel	f,u,dowel	400	N/mm ²
Load bearing capacity of each shear plane $M_{y,Rk} = 0.3 \cdot f_{u,k} \cdot d^{2.6}$	M,y,Rk	0,29	kNm
Effective number of dowels $n_{ef} = \min \left\{ \begin{array}{l} n \\ n^{0.9} \sqrt[4]{\frac{a_1}{13d}} \end{array} \right.$	n,ef	5,69	

The governing failure modes are calculated in the following formulas. This is followed by a visualisation of the failure modes.

$$\text{Mode 1: } l + f \quad F_{v,p,Rk} = 0.5 \cdot f_{h,2,k} \cdot t_2 \cdot d + f_{h,1,k} \cdot t_1 \cdot d$$

$$\text{Mode 2: } l + g \quad F_{v,p,Rk} = 0.5 \cdot f_{h,2,k} \cdot t_2 \cdot d + f_{h,1,k} \cdot t_1 \cdot d \cdot \left[\sqrt{2 + \frac{4 \cdot M_{y,Rk}}{f_{h,1,k} \cdot d \cdot t_1^2}} - 1 \right]$$

$$\text{Mode 3: } l + h \quad F_{v,p,Rk} = 0.5 \cdot f_{h,2,k} \cdot t_2 \cdot d + 2.3 \cdot \sqrt{M_{y,Rk} \cdot f_{h,1,k} \cdot d}$$

$$\text{(Mode 4: } m + f \quad F_{v,p,Rk} = 2.3 \cdot \sqrt{M_{y,Rk} \cdot f_{h,2,k} \cdot d} + f_{h,1,k} \cdot t_1 \cdot d, \text{ not possible)}$$

$$\text{Mode 5: } m + g \quad F_{v,p,Rk} = 2.3 \cdot \sqrt{M_{y,Rk} \cdot f_{h,2,k} \cdot d} + f_{h,1,k} \cdot t_1 \cdot d \cdot \left[\sqrt{2 + \frac{4 \cdot M_{y,Rk}}{f_{h,1,k} \cdot d \cdot t_1^2}} - 1 \right]$$

$$\text{Mode 6: } m + h \quad F_{v,p,Rk} = 2.3 \cdot \sqrt{M_{y,Rk} \cdot f_{h,2,k} \cdot d} + 2.3 \cdot \sqrt{M_{y,Rk} \cdot f_{h,1,k} \cdot d}$$

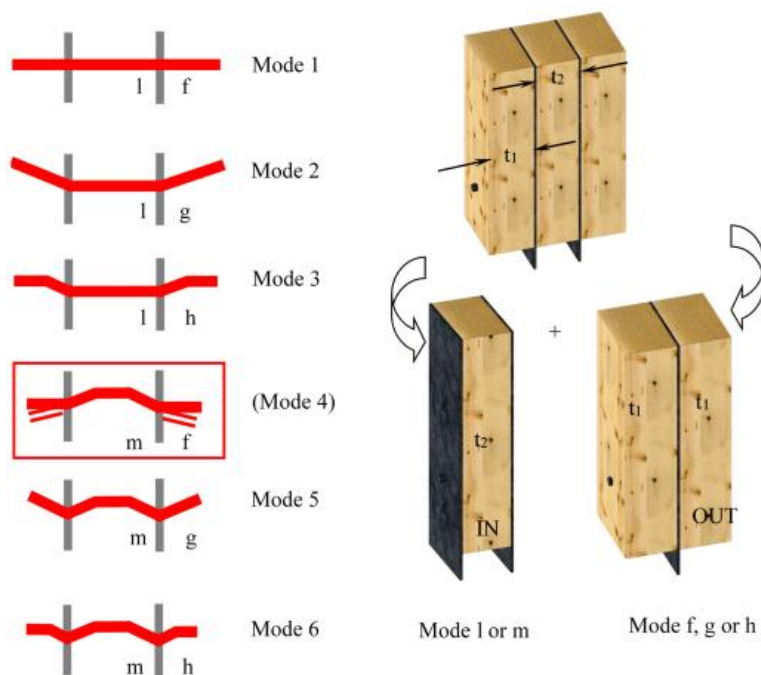


Figure D-26: Failure modes for timber with steel plates (Sandhaas, Munch-Andersen, & Dietsch, 2018)



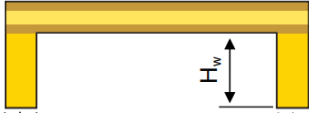

It is found that the smallest failure mode is mode 5, with $F_{v,p,Rk} = 114 \text{ kN}$. This is used to calculate the splitting failure, which is given in the following table. In this table, the governing failure mode is given. This is the largest normal force that can be exerted on the connection. This is a higher force than the force given in Table D-12, so this is a safe connection design.

Table D-13: Calculation of the possible failure modes of the connection

Explanation	Parameter	
<i>Splitting failure</i>	$F_{v,ef,Rk}$	1244 kN
$F_{v,ef,Rk} = n_{rows} * n_{ef} * F_{v,p,Rk}$		
<i>Block shear failure for the inner part</i>	$F_{bs,Rk,in}$	1405 kN
$F_{bs,Rk} = \max \begin{cases} 1.5 \cdot A_{net,t} \cdot f_{t,o,k} \\ 0.7 \cdot A_{net,v} \cdot f_{v,k} \end{cases}$		
In which:		
$A_{net,t} = L_{net,t} \cdot t_2$		
$A_{net,v} = L_{net,v} \cdot t_2 \cdot k_{cr}$		
$L_{net,t} = \sum_i l_{t,i} = a_2 - d_0$		
$L_{net,v} = \sum_i l_{v,i} = 2 \cdot (a_{3,t} + 3 \cdot a_1 - 3.5 \cdot d_0)$		
<i>Block shear failure for the outer part (same formula), in which:</i>	$F_{bs,Rk,out}$	2158 kN
$A_{net,t} = L_{net,t} \cdot t_1$		
$A_{net,v} = L_{net,v} \cdot t_1 \cdot k_{cr}$		
<i>Steel failure</i>	F_{steel}	7100 kN
$F_{steel} = b * t_{pl} * n_{plates} * f_y$		
<i>Governing failure mode</i>		
Splitting failure	$F_{v,Rk}$	1244 kN
	$F_{v,Rd}$	861 kN
	UC	0.79 < 0.80

D.6 Mezzanine floor design

Table D-14: Comparison between timber floor systems

	Lignatur	CLT	CLT rib panel	Kielsteg floor
Visualisation	 (Lignatur AG, 2014)	 (Karacabeyli & Douglas, 2013)	 (Stora Enso, 2018)	 (KIELSTEG Deutschland GmbH, 2015)
Mass	33 – 68 kg/m ²	25.2 – 134.4 kg/m ²	46.5 – 170 kg/m ²	48.4 – 146.5 kg/m ²
Span	Up to 12 – 16 m	Up to 16 m <i>Compared to the rib panel usually used for short spans (Stora Enso, 2018)</i>	Up to 13.5 m <i>Compared to the CLT panel usually used for long spans (Stora Enso, 2018)</i>	Up to 7.5 – 27 m
Width	1000 mm (Flächenelement) n*200 mm (Kastenelement)	225 – 345 mm	540 – 880 mm	120 mm
Thickness	120 – 320 mm	60 – 320 mm	220 – 580 mm	228 – 800 mm
Behaviour in fire	Standard: REI 30 Possible up to REI90	Standard: REI60 Possible up to REI90	REI 0 up to REI60	Standard: REI 30; for thicker profiles (> 280 mm): REI 60
Sustainability of materials	+/- Engineered timber (softwood boards and glue)	+/- Engineered timber (CLT)	+/- Engineered timber (CLT)	- Engineered timber (LVL)
EPD data	Indirectly available	Available	Indirectly available	Available
Sources	(Lignatur AG, 2014)	(Stora Enso, 2017)	(Stora Enso, 2018)	(KIELSTEG Deutschland GmbH, 2015)

D.6.1 Two-way spanning CLT panel

An advantage of a CLT panel is the possibility to span in two directions. Usually, slabs can have a maximum span of 3.5 meter, so to cover an entire floor area, connections in between these slabs are needed (Stora Enso Wood Products GmbH, 2017). These connections are more complicated to design for two-way slabs than for one-way slabs. In the research of Loebus et al. (2017), research was conducted on the internal floor connections for two-way CLT-concrete slabs. The floor must be able to transfer normal forces, shear forces, and bending moments in two ways. As the concrete is poured on site as one piece, no joint issues arise. However, the timber cannot be realised in one piece, so special attention is necessary for the joint in between timber elements. In their research, they found that it is necessary to include a force-fitting element joint in the timber to activate the biaxial load-bearing capacity of the floor. As force-fitting elements, they compared fully threaded screws and glued-in reinforcement bars. They concluded that threaded screws alone are unable to provide enough biaxial stiffness. Therefore, they designed a connection with glued-in reinforcement bars, as shown in the figure below, which does provide enough stiffness.

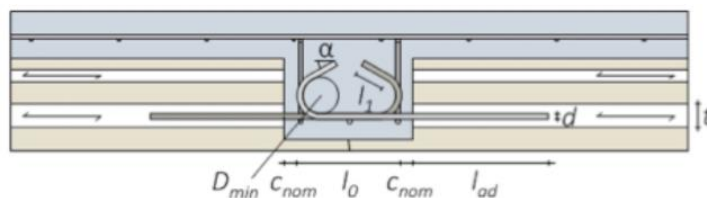


Figure D-27: Force-fitting element joint with glued-in reinforcement bars (Loebus, Dietsch, & Winter, 2017)

For this design, it is aimed to have simple composition of materials and to avoid secondary finishes to the base material. In such a design, the concrete and steel both need to be connected to the timber, which reduces this effect. Therefore, it is decided to design a CLT floor that only spans in one direction.

D.6.2 CLT 5-layer floor panel check

$L_w := 2108\text{mm}$ Length of floor
 $L_{\min} := 2108\text{mm}$ Distance between supports
 $L_{\text{ref}} := L_{\min} = 2.108\text{m}$ Reference length for a simply supported floor (Danielsson, n.d.)

$b_{\text{eff}} := 1000\text{mm}$

$t_{\text{pl}} := 35\text{mm}$

Panel thickness parallel

$t_{\text{pl},3} := 35\text{mm}$

Panel thickness parallel (layer 3)

$t_{\text{pp}} := 35\text{mm}$

Panel thickness perpendicular

$t_1 := t_{\text{pl}} = 35 \cdot \text{mm}$

$t_2 := t_{\text{pp}} = 35 \cdot \text{mm}$

$t_3 := t_{\text{pl},3} = 35 \cdot \text{mm}$

Danielsson (n.d.)

$t_4 := t_{\text{pp}} = 35 \cdot \text{mm}$

$t_5 := t_{\text{pl}} = 35 \cdot \text{mm}$

$h := t_1 + t_2 + t_3 + t_4 + t_5 = 175 \cdot \text{mm}$

$a_1 := t_{\text{pl}} + t_2 = 70 \cdot \text{mm}$

$a_5 := t_{\text{pl}} + t_4 = 70 \cdot \text{mm}$

$A_1 := t_1 \cdot b_{\text{eff}} = 0.035\text{m}^2$

$A_2 := t_2 \cdot b_{\text{eff}} = 0.035\text{m}^2$

Material properties

Strength class = C24

$$G_{\text{self.floor}} := \rho_{\text{mean}} \cdot h \cdot \left(9.81 \frac{\text{m}}{\text{s}^2} \right) = 0.721 \cdot \frac{\text{kN}}{\text{m}}$$

Self-weight of the CLT non-AR floor

Calculation factors

$k_{\text{mod}} := 0.8$

Modification factor

$nr_{\text{laminations}} := 5$

$k_{\text{sys}} := \frac{0.2}{8} \cdot nr_{\text{laminations}} + 1 = 1.125$

System factor for laminations that are glued together (Figure 6.12 EC5)

$k_{\text{def}} := 0.6$

Deformation factor for glulam

$$k_h := \min \left[\left(\frac{600\text{mm}}{t_1 \cdot 2 + t_2 \cdot 3} \right)^{0.1}, 1.1 \right] = 1.1$$

Depth factor for glulam

$\gamma_M := 1.25$

Effective bending stiffness (Gamma method)

(Danielsson, n.d.)

$$E_1 := E_{0,\text{mean}} = 1.1 \times 10^4 \cdot \frac{\text{N}}{\text{mm}^2}$$

$$\gamma_1 := \frac{1}{1 + \frac{\left(\pi^2 \cdot E_1 \cdot t_1 \right)^2}{L_{\text{ref}}^2} \cdot \frac{t_2}{G_R}} = 0.626$$

Connection efficiency factor

$$I_1 := \frac{1}{12} \cdot b_{\text{eff}} \cdot t_1^3 + \gamma_1 \cdot b_{\text{eff}} \cdot t_1 \cdot a_1^2 = 1.109 \times 10^{-4} \text{m}^4$$

$$E_3 := E_{0,\text{mean}} = 1.1 \times 10^4 \cdot \frac{\text{N}}{\text{mm}^2}$$

$$\gamma_3 := 1 \quad a_3 := 0\text{mm}$$

$$I_3 := \frac{1}{12} \cdot b_{\text{eff}} \cdot t_3^3 + \gamma_3 \cdot b_{\text{eff}} \cdot t_3 \cdot a_3^2 = 3.573 \times 10^{-6} \text{m}^4$$

$$E_5 := E_{0,\text{mean}} = 1.1 \times 10^4 \cdot \frac{\text{N}}{\text{mm}^2}$$

$$\gamma_5 := \frac{1}{1 + \frac{\left(\pi^2 \cdot E_5 \cdot t_5 \right)^2}{L_{\text{ref}}^2} \cdot \frac{t_4}{G_R}} = 0.626$$

$$I_5 := \frac{1}{12} \cdot b_{\text{eff}} \cdot t_5^3 + \gamma_5 \cdot b_{\text{eff}} \cdot t_5 \cdot a_5^2 = 1.109 \times 10^{-4} \text{m}^4$$

$$I_{\text{eff}} := I_1 + I_3 + I_5 = 2.253 \times 10^{-4} \text{m}^4$$

Effective second moment of area

$$EI_{\text{eff}} := E_1 \cdot I_1 + E_3 \cdot I_3 + E_5 \cdot I_5 = 2.478 \times 10^{12} \cdot \text{N} \cdot \text{mm}^2$$

Effective bending stiffness

Effective shear stiffness (Karacabeyli & Douglas, 2013)

$$a := a_1 + a_5 = 140 \cdot \text{mm}$$

$$G_1 := \frac{E_{0,\text{mean}}}{16} = 6.875 \times 10^8 \text{Pa}$$

$$G_3 := G_1$$

$$G_5 := G_1$$

$$G_2 := \frac{G_R}{10} = 5 \times 10^6 \text{Pa}$$

$$G_4 := G_2$$

$$GA_{\text{eff}} := \frac{a^2}{\left[\frac{t_1}{2 \cdot G_1 \cdot b_{\text{eff}}} + \frac{t_2}{G_2 \cdot b_{\text{eff}}} + \frac{t_3}{G_3 \cdot b_{\text{eff}}} + \frac{t_4}{G_4 \cdot b_{\text{eff}}} + \frac{t_5}{2 \cdot G_5 \cdot b_{\text{eff}}} \right]} = 1.39 \times 10^6 \text{N}$$

Loads

$$G_{\text{load1}} := 1.2 \frac{\text{kN}}{\text{m}} \quad \text{Demountable top layer}$$

$$G_{\text{load2}} := 0.25 \frac{\text{kN}}{\text{m}} \quad \text{Services}$$

$$G_{\text{self}} := \rho_{\text{mean}} \cdot 9.81 \frac{\text{N}}{\text{kg}} \cdot h = 0.721 \cdot \frac{\text{kN}}{\text{m}} \quad \text{Self-weight CLT floor}$$

$$Q_{\text{load1}} := 3 \frac{\text{kN}}{\text{m}} \quad \text{Robotic live load}$$

$$q_G := (G_{\text{load1}} + G_{\text{load2}} + G_{\text{self}}) \cdot b_{\text{eff}} = 2.171 \cdot \frac{\text{kN}}{\text{m}}$$

$$q_Q := Q_{\text{load1}} \cdot b_{\text{eff}} = 3 \cdot \frac{\text{kN}}{\text{m}}$$

$$q_{\text{SLS}} := q_G + q_Q = 5.171 \cdot \frac{\text{kN}}{\text{m}}$$

$$q_{\text{ULS}} := 1.35 \cdot q_G + 1.5 \cdot q_Q = 7.431 \cdot \frac{\text{kN}}{\text{m}}$$

$$M_{\text{Ed.SLS}} := \frac{1}{8} \cdot q_{\text{SLS}} \cdot L^2 = 2.872 \cdot \text{kN} \cdot \text{m}$$

$$V_{\text{Ed.SLS}} := \frac{1}{2} \cdot q_{\text{SLS}} \cdot L = 5.45 \cdot \text{kN}$$

$$M_{\text{Ed.ULS}} := \frac{1}{8} \cdot q_{\text{ULS}} \cdot L^2 = 4.128 \cdot \text{kN} \cdot \text{m}$$

$$V_{\text{Ed.ULS}} := \frac{1}{2} \cdot q_{\text{ULS}} \cdot L = 7.832 \cdot \text{kN}$$

Flexural strength

Design bending moment resistance

$$f_{\text{md}} := f_{\text{mk}} \cdot \frac{k_{\text{mod}}}{\gamma_M} \cdot k_{\text{sys}} = 17.28 \cdot \frac{\text{N}}{\text{mm}^2}$$

$$M_{\text{y.Rd}} := f_{\text{md}} \cdot \frac{I_{\text{eff}}}{(\gamma_1 \cdot a_1 + 0.5 \cdot t_1)} = 63.517 \cdot \text{kN} \cdot \text{m}$$

$$UC_{\text{bending,strength}} := \frac{M_{\text{Ed.ULS}}}{M_{\text{y.Rd}}} = 0.065$$

$$UC_{\text{bending,strength}} \leq 1 = 1$$

Maximum design bending moment

$$\sigma_{\text{bending}} := \frac{M_{\text{Ed.ULS}}}{EI_{\text{eff}}} \cdot E_1 \cdot \frac{t_1}{2} = 3.206 \times 10^5 \text{ Pa}$$

$$(D7-6) \text{ in Bla}\beta \text{ \& Sandhaas (2017)}$$

$$\sigma_{\text{normalstress}} := \frac{M_{\text{Ed.ULS}}}{EI_{\text{eff}}} \cdot \gamma_1 \cdot E_1 \cdot a_1 = 8.023 \times 10^5 \text{ Pa}$$

$$\sigma_{\text{y.d.max}} := \sigma_{\text{bending}} + \sigma_{\text{normalstress}} = 1.123 \cdot \text{MPa}$$

$$UC_{\text{flexural,strength}} := \frac{\sigma_{\text{y.d.max}}}{f_{\text{md}}} = 0.065$$

Shear strength

$$f_{\text{vd}} := f_{\text{vk}} \cdot \frac{k_{\text{mod}}}{\gamma_M} \cdot k_{\text{sys}} = 2.88 \cdot \frac{\text{N}}{\text{mm}^2}$$

First moment of area (According to Annex 5 of Blaβ & Sandhaas (2017)):

$$S_{1,\text{short}} := \gamma_1 \cdot E_1 \cdot A_1 \cdot a_1 + E_2 \cdot A_2 \cdot \frac{(t_2 + t_3)}{2} + \gamma_3 \cdot E_3 \cdot \frac{A_1}{2} \cdot 0 = 1.731 \times 10^{10} \cdot \text{N} \cdot \text{mm}$$

$$\tau_{\text{d.max}} := V_{\text{Ed.ULS}} \cdot \frac{S_{1,\text{short}}}{EI_{\text{eff}} \cdot b_{\text{eff}}} = 0.055 \cdot \frac{\text{N}}{\text{mm}^2} \quad (D7-8) \text{ in Bla}\beta \text{ \& Sandhaas (2017)}$$

$$V_{\text{rL}} := \frac{(f_{\text{vd}} \cdot EI_{\text{eff}} \cdot b_{\text{eff}})}{S_{1,\text{short}}} = 412.258 \cdot \text{kN}$$

$$UC_{\text{shear}} := \frac{V_{\text{Ed.ULS}}}{V_{\text{rL}}} = 0.019$$

Deflections

Breneman (2014)

$$u_{\text{inst.G}} := \frac{(5 \cdot q_G \cdot L_{\text{min}}^4)}{384 \cdot EI_{\text{eff}}} + \frac{(q_G \cdot L_{\text{min}}^2)}{8 \cdot \left(\frac{5}{6} \cdot GA_{\text{eff}}\right)} = 1.266 \cdot \text{mm} \quad \text{due to permanent loading}$$

$$u_{\text{inst.Q}} := \frac{(5 \cdot q_Q \cdot L_{\text{min}}^4)}{384 \cdot EI_{\text{eff}}} + \frac{(q_Q \cdot L_{\text{min}}^2)}{8 \cdot \left(\frac{5}{6} \cdot GA_{\text{eff}}\right)} = 1.75 \cdot \text{mm} \quad \text{due to variable loading}$$

$$u_{\text{fin.G}} := u_{\text{inst.G}} \cdot (1 + k_{\text{def}}) = 2.026 \cdot \text{mm}$$

$$\psi_2 := 0.8 \quad \text{Factor for the quasi-permanent value of variable action (Category E: Storage areas)}$$

$$u_{\text{fin.Q}} := u_{\text{inst.Q}} \cdot (1 + \psi_2 \cdot k_{\text{def}}) = 2.59 \cdot \text{mm}$$

$$u_{\text{max.inst}} := \frac{L_{\text{ref}}}{360} = 5.856 \cdot \text{mm}$$

$$u_{\text{max.fin}} := \frac{L_{\text{ref}}}{360} = 5.856 \cdot \text{mm}$$

$$UC_{\text{inst.deflection}} := \frac{(u_{\text{inst.G}} + u_{\text{inst.Q}})}{u_{\text{max.inst}}} = 0.515$$

$$UC_{\text{inst.deflection}} \leq 1 = 1$$

$$UC_{\text{fin.deflection}} := \frac{(u_{\text{fin.G}} + u_{\text{fin.Q}})}{u_{\text{max.fin}}} = 0.788$$

$$UC_{\text{fin.deflection}} \leq 1 = 1$$

Unity checks overview

$$UC_{\text{flexural.strength}} = 0.065$$

$$UC_{\text{inst.deflection}} = 0.515$$

$$UC_{\text{shear}} = 0.019$$

$$UC_{\text{fin.deflection}} = 0.788$$

All unity checks are below 0.8, so the floor is strong enough.

Vibrations

Furthermore, the floor is checked upon vibrations with the Calculatis Tool of Stora Enso, from which it is found that vibration issues will not arise.

D.6.3 CLT 3-layer floor panel check

CLT panel properties

$$L_{\text{CLT}} := 8430 \text{ mm}$$

Length of CLT panel

$$L_{\text{min}} := 2108 \text{ mm}$$

Distance between supports

$$L_{\text{ref}} := 0.8 \cdot L_{\text{min}} = 1.686 \text{ m}$$

Reference length for a continuous floor (Danielsson, n.d.)

$$b_{\text{eff}} := 1000 \text{ mm}$$

Effective width of CLT panel

$$t_{\text{p1}} := 55 \text{ mm}$$

Panel thickness parallel

$$t_{\text{pp}} := 65 \text{ mm}$$

Panel thickness perpendicular

$$t_6 := t_{\text{p1}} = 55 \text{ mm}$$

Panel thickness of layer 6

$$t_7 := t_{\text{pp}} = 65 \text{ mm}$$

Panel thickness of layer 7

$$t_8 := t_{\text{p1}} = 55 \text{ mm}$$

Panel thickness of layer 8

$$h := t_6 + t_7 + t_8 = 175 \text{ mm}$$

Total height of the CLT panel

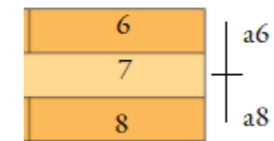
$$a_6 := \frac{(t_6 + t_7)}{2} = 60 \text{ mm}$$

$$a_8 := \frac{(t_7 + t_8)}{2} = 60 \text{ mm}$$

$$A_6 := t_6 \cdot b_{\text{eff}} = 0.055 \text{ m}^2$$

$$A_8 := t_8 \cdot b_{\text{eff}} = 0.055 \text{ m}^2$$

$$A_7 := t_7 \cdot b_{\text{eff}} = 0.065 \text{ m}^2$$



Danielsson (n.d), numbers are added for clarification for this research

Material properties

Strength class = C24

$$G_{\text{self.floor}} := \rho_{\text{mean}} \cdot h \cdot \left(9.81 \frac{\text{m}}{\text{s}^2} \right) = 0.721 \cdot \frac{\text{kN}}{\text{m}^2}$$

Self-weight of the CLT floor

Calculation factors

$$k_{\text{mod}} := 0.8$$

Modification factor dependent upon service class, material and load duration class. In this case, the service class is 1, the material is CLT, but this is not an option in EC 1995-1-1, so glulam is applied. The load duration class depends upon the type of load. For the ULS, k.mod for variable action Q is applied, which is a medium-term load case. (Blaß & Sandhaas, 2017)

$$n_{\text{laminations}} := 3$$

$$k_{\text{sys}} := \frac{0.2}{8} \cdot n_{\text{laminations}} + 1 = 1.075$$

System factor for laminations that are glued together

(Figure 6.12 EC1995-1-1)

$$k_{\text{def}} := 0.8$$

Deformation factor for CLT, according to Danielsson (n.d.)

$$k_{\text{h}} := \min \left[\left(\frac{600 \text{ mm}}{t_6 \cdot 2 + t_7 \cdot 1} \right)^{0.1}, 1.1 \right] = 1.1$$

Depth factor for glulam

$$\gamma_M := 1.25$$

Material factor

Effective bending stiffness (Gamma method)

(Danielsson, n.d.)

$$E_6 := E_{0,\text{mean}} = 1.1 \times 10^4 \cdot \frac{\text{N}}{\text{mm}^2}$$

$$\gamma_6 := \frac{1}{1 + \frac{\left(\pi^2 \cdot E_6 \cdot t_6\right) \cdot t_7}{L_{\text{ref}}^2 \cdot G_R}} = 0.268 \quad \text{Connection efficiency factor}$$

$$I_6 := \frac{1}{12} \cdot b_{\text{eff}} \cdot t_6^3 + \gamma_6 \cdot b_{\text{eff}} \cdot t_6 \cdot a_6^2 = 6.696 \times 10^{-5} \text{ m}^4$$

$$E_7 := E_{90,\text{mean}} = 370 \cdot \frac{\text{N}}{\text{mm}^2} \quad E_8 := E_{0,\text{mean}} = 1.1 \times 10^4 \cdot \frac{\text{N}}{\text{mm}^2}$$

$$\gamma_8 := \frac{1}{1 + \frac{\left(\pi^2 \cdot E_8 \cdot t_8\right) \cdot t_7}{L_{\text{ref}}^2 \cdot G_R}} = 0.268$$

$$I_8 := \frac{1}{12} \cdot b_{\text{eff}} \cdot t_8^3 + \gamma_8 \cdot b_{\text{eff}} \cdot t_8 \cdot a_8^2 = 6.696 \times 10^{-5} \text{ m}^4$$

$$I_{\text{eff}} := I_6 + I_8 = 1.339 \times 10^8 \cdot \text{mm}^4 \quad \text{Effective second moment of area}$$

$$EI_{\text{eff}} := E_6 \cdot I_6 + E_8 \cdot I_8 = 1.473 \times 10^{12} \cdot \text{N} \cdot \text{mm}^2 \quad \text{Effective bending stiffness}$$

Effective shear stiffness

Karacabeyli & Douglas (2013)

$$a := a_6 + a_8 = 120 \cdot \text{mm}$$

$$G_6 := \frac{E_{0,\text{mean}}}{16} = 6.875 \times 10^8 \text{ Pa} \quad G_8 := G_6$$

$$G_7 := \frac{G_R}{10} = 5 \times 10^6 \text{ Pa}$$

$$GA_{\text{eff}} := \frac{a^2}{\left[\frac{t_6}{2 \cdot G_6 \cdot b_{\text{eff}}}\right] + \left[\frac{t_7}{G_7 \cdot b_{\text{eff}}}\right] + \left[\frac{t_8}{2 \cdot G_8 \cdot b_{\text{eff}}}\right]} = 1.101 \times 10^6 \text{ N}$$

Loads (from SCIA)

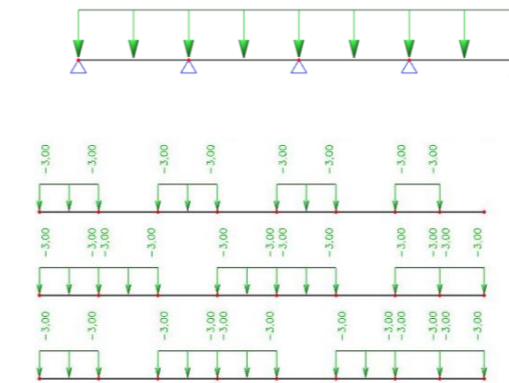


Figure: SCIA model of the loads on the floor (set up for this research), where also continuous floor loads are applied to find the highest possible internal forces.

$$M_{\text{Ed,SLS}} := 2.38 \text{ kN} \cdot \text{m}$$

$$V_{\text{Ed,SLS}} := 6.56 \text{ kN}$$

$$M_{\text{Ed,ULS}} := 3.08 \text{ kN} \cdot \text{m}$$

$$V_{\text{Ed,ULS}} := 8.47 \text{ kN}$$

Flexural strength

Design bending moment resistance

$$f_{\text{md}} := f_{\text{mk}} \cdot \frac{k_{\text{mod}}}{\gamma_M} \cdot k_{\text{sys}} = 16.512 \cdot \frac{\text{N}}{\text{mm}^2}$$

$$M_{y,\text{Rd}} := f_{\text{md}} \cdot \frac{I_{\text{eff}}}{\left(\gamma_6 \cdot a_6 + 0.5 \cdot t_6\right)} = 50.728 \cdot \text{kN} \cdot \text{m}$$

$$UC_{\text{bending,strength}} := \frac{M_{\text{Ed,ULS}}}{M_{y,\text{Rd}}} = 0.061$$

$$UC_{\text{bending,strength}} \leq 1 = 1$$

Maximum design bending moment

$$\sigma_{\text{bending}} := \frac{M_{\text{Ed,ULS}}}{EI_{\text{eff}}} \cdot E_6 \cdot \frac{t_6}{2} = 6.325 \times 10^5 \text{ Pa} \quad \text{(D7-6) in Blaß & Sandhaas (2017)}$$

$$\sigma_{\text{normalstress}} := \frac{M_{\text{Ed,ULS}}}{EI_{\text{eff}}} \cdot \gamma_6 \cdot E_6 \cdot a_6 = 3.7 \times 10^5 \text{ Pa} \quad \text{(D7-7) in Blaß & Sandhaas (2017)}$$

$$\sigma_{y,\text{d,max}} := \sigma_{\text{bending}} + \sigma_{\text{normalstress}} = 1.003 \cdot \text{MPa}$$

$$UC_{\text{flexural,strength}} := \frac{\sigma_{y,\text{d,max}}}{f_{\text{md}}} = 0.061$$

$$UC_{\text{flexural,strength}} \leq 1 = 1$$

Shear strength

$$f_{vd} := f_{vk} \cdot \frac{k_{mod}}{\gamma_M} = 2.56 \cdot \frac{N}{mm^2}$$

First moment of area (According to Annex 5 of Blaß & Sandhaas (2017)):

$$S_{1,short} := \gamma_6 \cdot E_6 \cdot A_6 \cdot a_6 + E_7 \cdot \frac{A_7}{2} \cdot 0 = 9.733 \times 10^9 \cdot N \cdot mm$$

$$\tau_{d,max} := V_{Ed,ULS} \cdot \frac{S_{1,short}}{EI_{eff} \cdot b_{eff}} = 0.056 \cdot \frac{N}{mm^2} \quad (D7-8) \text{ in Blaß \& Sandhaas (2017)}$$

$$V_{rL} := \frac{(f_{vd} \cdot EI_{eff} \cdot b_{eff})}{S_{1,short}} = 387.425 \cdot kN$$

$$UC_{shear} := \frac{V_{Ed,ULS}}{V_{rL}} = 0.022$$

Deflections

Breneman (2014)

The proposed calculation check is based upon a simply supported beam. By using the reference length, the effect of the continuous floor is included and it is possible to gain insight on the deflection of the continuous floor.

$$u_{inst,G} := \frac{(5 \cdot q_G \cdot L_{ref}^4)}{384 \cdot EI_{eff}} + \frac{(q_G \cdot L_{ref}^2)}{8 \cdot \left(\frac{5}{6} \cdot GA_{eff}\right)} = 0.996 \cdot mm \quad \text{due to permanent loading}$$

$$u_{inst,Q} := \frac{(5 \cdot q_Q \cdot L_{ref}^4)}{384 \cdot EI_{eff}} + \frac{(q_Q \cdot L_{ref}^2)}{8 \cdot \left(\frac{5}{6} \cdot GA_{eff}\right)} = 1.051 \cdot mm \quad \text{due to variable loading}$$

$$u_{fin,G} := u_{inst,G} \cdot (1 + k_{def}) = 1.794 \cdot mm$$

$$\psi_2 := 0.8 \quad \text{Factor for the quasi-permanent value of variable action (Category E: Storage areas)}$$

$$u_{fin,Q} := u_{inst,Q} \cdot (1 + \psi_2 \cdot k_{def}) = 1.724 \cdot mm$$

$$u_{max,inst} := \frac{L_{ref}}{360} = 4.684 \cdot mm$$

$$u_{max,fin} := \frac{L_{ref}}{360} = 4.684 \cdot mm$$

$$UC_{inst,deflection} := \frac{(u_{inst,G} + u_{inst,Q})}{u_{max,inst}} = 0.437$$

$$UC_{fin,deflection} := \frac{(u_{fin,G} + u_{fin,Q})}{u_{max,fin}} = 0.751$$

D.6.4 Timber secondary mezzanine floor beam checks

Cross section properties

$h := 900mm$	Height of beam
$b := \frac{4 \cdot 1}{6} \cdot h = 600 \cdot mm$	Width of beam
$L_w := 15.81m$	Length of beam
$W_y := \frac{1}{6} \cdot b \cdot h^2 = 8.1 \times 10^7 \cdot mm^3$	Section modulus in y-direction
$I_y := \frac{1}{12} \cdot b \cdot h^3 = 3.65 \times 10^{10} \cdot mm^4$	Moment of inertia in y-direction
$A := h \cdot b = 0.54 \cdot m^2$	Area of the beam

Loads

As simplification, the beams next to the openings, are designed with the same load as the beams which are not next to the openings. This can be seen in the following figure.

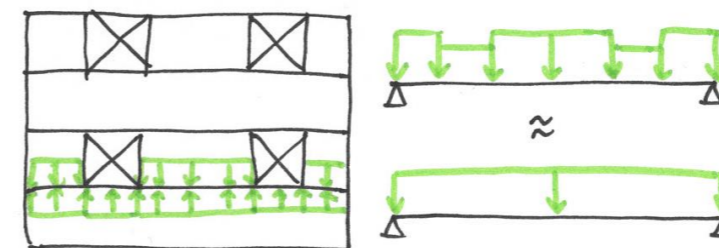


Figure: Load distribution from the floors to the secondary beams

$$b_{floor} := 2108mm \quad \text{Width of the CLT floor that must be carried by the beam.}$$

$$G_{load1} := 1.2 \frac{kN}{m^2} \quad \text{Demountable concrete top floor}$$

$$G_{load2} := 0.25 \frac{kN}{m^2} \quad \text{Services on floor}$$

$$G_{self,floor} := 0.721 \frac{kN}{m^2} \quad \text{Self-weight CLT floor}$$

$$G_{self,beam} := \rho_{mean} \cdot 9.81 \frac{m}{s} \cdot h \cdot b = 1.96 \cdot \frac{kN}{m} \quad \text{Self-weight of the beam}$$

$$Q_{load1} := 2.29 \frac{kN}{m^2} \quad \text{Robotic live load}$$

$$q_G := (G_{load1} + G_{load2} + G_{self,floor}) \cdot b_{floor} + G_{self,beam} = 6.53 \cdot \frac{kN}{m} \quad \text{Permanent loads}$$

$$q_Q := Q_{load1} \cdot b_{floor} = 4.83 \cdot \frac{kN}{m} \quad \text{Variable load}$$

$$q_{SLS} := q_G + q_Q = 11.36 \cdot \frac{\text{kN}}{\text{m}}$$

$$M_{Ed,SLS} := \frac{1}{8} \cdot q_{SLS} \cdot L^2 = 355.01 \cdot \text{kN} \cdot \text{m}$$

$$V_{Ed,SLS} := \frac{1}{2} \cdot q_{SLS} \cdot L = 89.82 \cdot \text{kN}$$

Bending moment capacity

$$\sigma_{m,y,d} := \frac{M_{Ed,ULS}}{W_y} = 6.33 \cdot \text{MPa}$$

$$UC_{\text{bendingmoment}} := \frac{\sigma_{m,y,d}}{f_{m,d}} = 0.41$$

Shear capacity

$$\tau_d := 1.5 \cdot \frac{V_{Ed,ULS}}{A} = 0.36 \cdot \text{MPa}$$

$$UC_{\text{shear}} := \frac{\tau_d}{f_{v,d}} = 0.16$$

Deflection

$$u_{\text{inst},G} := \frac{\left(5 \cdot q_G \cdot L^4\right)}{384 \cdot E_{0,\text{mean}} \cdot I_y} = 13.2 \cdot \text{mm}$$

due to permanent loading

$$u_{\text{inst},Q} := \frac{\left(5 \cdot q_Q \cdot L^4\right)}{384 \cdot E_{0,\text{mean}} \cdot I_y} = 9.37 \cdot \text{mm}$$

due to variable loading

$$u_{\text{fin},G} := u_{\text{inst},G} \cdot (1 + k_{\text{def}}) = 21.12 \cdot \text{mm}$$

$$\psi_2 := 0.8 \quad \text{Factor for the quasi-permanent value of variable action (Category E: Storage areas)}$$

$$u_{\text{fin},Q} := u_{\text{inst},Q} \cdot (1 + \psi_2 \cdot k_{\text{def}}) = 13.87 \cdot \text{mm}$$

$$u_{\text{max}} := \frac{L}{360} = 43.92 \cdot \text{mm}$$

$$UC_{\text{final,deflection}} := \frac{(u_{\text{fin},G} + u_{\text{fin},Q})}{u_{\text{max}}} = 0.8$$

Overview of unity checks

$$UC_{\text{final,deflection}} = 0.8$$

$$UC_{\text{shear}} = 0.16$$

$$UC_{\text{bendingmoment}} = 0.41$$

$$q_{ULS} := 1.35 \cdot q_G + 1.5 \cdot q_Q = 16.06 \cdot \frac{\text{kN}}{\text{m}}$$

$$M_{Ed,ULS} := \frac{1}{8} \cdot q_{ULS} \cdot L^2 = 501.88 \cdot \text{kN} \cdot \text{m}$$

$$V_{Ed,ULS} := \frac{1}{2} \cdot q_{ULS} \cdot L = 126.98 \cdot \text{kN}$$

D.6.5 Timber primary mezzanine floor beam

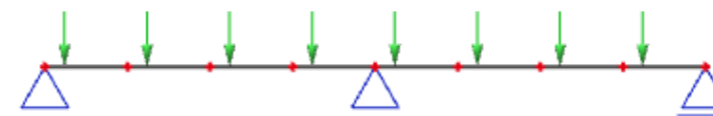
Load transfer of the secondary beam to the primary beam

The secondary beam transfers the following loads to the primary beam:

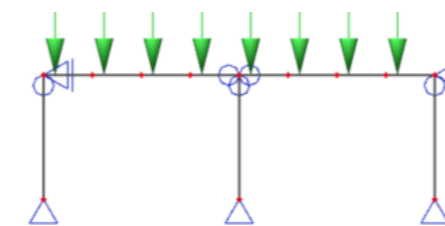
$$V_{Ed,G} := \frac{1}{2} \cdot q_G \cdot L = 51.66 \cdot \text{kN} \quad \text{Dead loads on the primary beam coming from the secondary beam}$$

$$V_{Ed,Q} := \frac{1}{2} \cdot q_Q \cdot L = 38.16 \cdot \text{kN} \quad \text{Live loads on the primary beam coming from the secondary beam}$$

The following system has been checked:

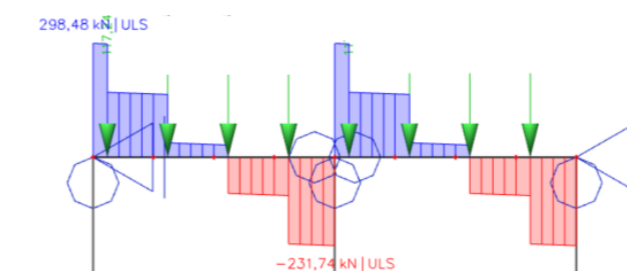


As a total system (beams on top of columns), this looks like the following system:



Resulting forces

$$M_{Ed,ULS} := 569.43 \text{ kN} \cdot \text{m} \quad V_{Ed,ULS} := 228.96 \text{ kN}$$



Cross section (strength class = GL24h)

$$h := 900 \text{ mm} \quad \text{Height of beam}$$

$$b := \frac{4 \cdot 1}{7} \cdot h = 514.286 \cdot \text{mm} \quad \text{Width of beam}$$

$$L := 8.430 \text{ m} \quad \text{Length of beam}$$

$$W_y := \frac{1}{6} \cdot b \cdot h^2 = 6.943 \times 10^7 \cdot \text{mm}^3 \quad \text{Section modulus in y-direction}$$

$$I_y := \frac{1}{12} \cdot b \cdot h^3 = 3.124 \times 10^{10} \cdot \text{mm}^4 \quad \text{Moment of inertia in y-direction}$$

$$A := h \cdot b = 0.463 \cdot \text{m}^2 \quad \text{Area of the beam}$$

Ultimate Limit State calculation

Bending moment capacity

$$\sigma_{m,y,d} := \frac{M_{Ed,ULS}}{W_y} = 8.202 \cdot \text{MPa}$$

$$\frac{f_{m,k}}{\gamma_M} \cdot k_{mod} \cdot k_h = 15.36 \cdot \text{MPa}$$

$$UC_{\text{bendingmoment}} := \frac{\sigma_{m,y,d}}{f_{m,d}} = 0.534$$

Shear capacity

$$\sigma_{v,d} := \frac{3}{2} \cdot \frac{V_{Ed,ULS}}{A} = 7.42 \times 10^5 \text{ Pa}$$

$$UC_{\text{shear}} := \frac{\sigma_{v,d}}{f_{v,d}} = 0.429$$

Service Limit State

Must be checked with SCIA Engineer, as this is not a simple forget me not anymore.

From SCIA: $u_{inst,G} := 6.7 \text{ mm}$

$$u_{inst,Q} := 4.6 \text{ mm}$$

$$u_{fin,G} := u_{inst,G} \cdot (1 + k_{def}) = 10.72 \cdot \text{mm}$$

$$\psi_2 := 0.8 \quad \text{Factor for the quasi-permanent value of variable action (Category E: Storage areas)}$$

$$u_{fin,Q} := u_{inst,Q} \cdot (1 + \psi_2 \cdot k_{def}) = 6.808 \cdot \text{mm}$$

$$u_{fin} := u_{fin,G} + u_{fin,Q} = 17.528 \cdot \text{mm}$$

$$u_{max} := \frac{L}{360} = 23.417 \cdot \text{mm}$$

$$UC_{\text{final.deflection}} := \frac{u_{fin}}{u_{max}} = 0.749$$

Overview of unity checks

$$UC_{\text{final.deflection}} = 0.749$$

$$UC_{\text{bendingmoment}} = 0.534$$

$$UC_{\text{shear}} = 0.429$$

D.6.6 Mezzanine floor column check

Cross section

$$h_{\text{col}} := 240 \text{ mm}$$

Height of column

$$b := h = 240 \cdot \text{mm}$$

Width of column

$$t_{\text{floor}} := 50 \text{ mm} + 175 \text{ mm}$$

Thickness of the top layer and the CLT floor

$$h_{\text{beam}} := 1250 \text{ mm}$$

The height of the primary beam

$$L_{\text{max}} := 5.8 \text{ m}$$

Maximum length of the column

$$L_{\text{col}} := L_{\text{max}} - t_{\text{floor}} - h_{\text{beam}} = 4.325 \text{ m}$$

Length of column

$$W_y := \frac{1}{6} \cdot b \cdot h^2 = 2.304 \times 10^6 \cdot \text{mm}^3$$

Section modulus in y-direction

$$I_y := \frac{1}{12} \cdot b \cdot h^3 = 2.765 \times 10^8 \cdot \text{mm}^4$$

Moment of inertia in y-direction

$$I_z := \frac{1}{12} \cdot h \cdot b^3 = 2.765 \times 10^8 \cdot \text{mm}^4$$

Moment of inertia in z-direction

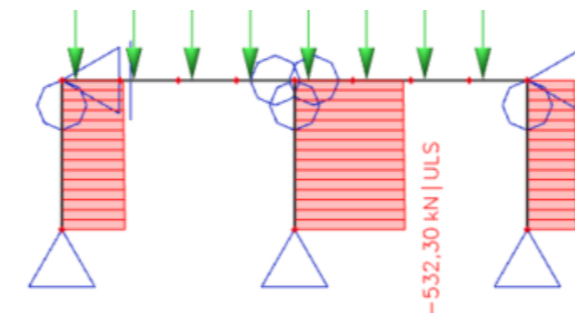
$$A_{\text{col}} := h \cdot b = 5.76 \times 10^4 \cdot \text{mm}^2$$

Area of the column

Material values

Strength class = GL24b

Loads (from SCIA)



$$N_{t,d} := 0 \text{ N}$$

Tension force

$$N_{c,d,ULS} := 532.30 \text{ kN}$$

Compression force (ULS)

For further calculation steps, it is convenient to divide this normal force into a normal force due to dead loads and a normal force due to live loads:

$$N_{\text{dead}} := 224.70 \text{ kN}$$

$$N_{\text{live}} := 152.64 \text{ kN}$$

Tension parallel to the grain

$$\sigma_{t,0,d} := \frac{N_{t,d}}{A} = 0$$

$$UC_{\text{tension}} := \frac{\sigma_{t,0,d}}{f_{t,0,d}} = 0 \quad UC_{\text{tension}} \leq 1 = 1$$

Compression parallel to the grain

$$\sigma_{c,0,d} := \frac{N_{c,d,ULS}}{A} = 9.241 \times 10^6 \text{ Pa}$$

$$UC_{\text{compression}} := \frac{\sigma_{c,0,d}}{f_{c,0,d}} = 0.602 \quad UC_{\text{compression}} \leq 1 = 1$$

Flexural buckling

$$\lambda_y := L \cdot \sqrt{\frac{A}{I_y}} = 62.426 \quad \text{C.11 in EC1995-1-1}$$

$$\lambda_{\text{rel},y} := \frac{\lambda_y}{\pi} \cdot \sqrt{\frac{f_{c,0,k}}{E_{0.05}}} = 1.004$$

$$\lambda_z := L \cdot \sqrt{\frac{A}{I_z}} = 62.426 \quad \text{C.11 in EC1995-1-1}$$

$$\lambda_{\text{rel},z} := \frac{\lambda_z}{\pi} \cdot \sqrt{\frac{f_{c,0,k}}{E_{0.05}}} = 1.004$$

Both are larger than 0.3, so the following equations need to be followed:

$$\beta_c := 0.1 \quad \text{for glulam}$$

$$k_y := 0.5 \cdot \left[1 + \beta_c \cdot (\lambda_{\text{rel},y} - 0.3) + \lambda_{\text{rel},y}^2 \right] = 1.039$$

$$k_z := 0.5 \cdot \left[1 + \beta_c \cdot (\lambda_{\text{rel},z} - 0.3) + \lambda_{\text{rel},z}^2 \right] = 1.039$$

$$k_{c,y} := \frac{1}{k_y + \sqrt{k_y^2 - \lambda_{\text{rel},y}^2}} = 0.765$$

$$k_{c,z} := \frac{1}{k_z + \sqrt{k_z^2 - \lambda_{\text{rel},z}^2}} = 0.765$$

$$UC_{\text{buckling},y} := \frac{\sigma_{c,0,d}}{k_{c,y} \cdot f_{c,0,d}} = 0.787$$

$$UC_{\text{buckling},z} := \frac{\sigma_{c,0,d}}{k_{c,z} \cdot f_{c,0,d}} = 0.787$$

Overview of unity checks

$$UC_{\text{compression}} = 0.602$$

$$UC_{\text{buckling},y} = 0.787$$

$$UC_{\text{buckling},z} = 0.787$$

D.7 Possible improvements of the design

D.7.1 Column base connection

The column base is designed to be a hinged connection. It is possible to reduce member sizes by designing a moment resistant column base connection. In a traditional timber design, this looks like the connection shown on the left of Figure D-28. In this research, the traditional moment resistant connection design is calculated. However, even with a lot of bolts, only a relatively low stiffness can be reached. Thus, this is not considered to be a suitable design. An improvement could be to create a more modern stiff connection by gluing a rod into the timber. This is shown on the right of Figure D-28. This has not been implemented in this design, but could be considered if the design is optimised further.

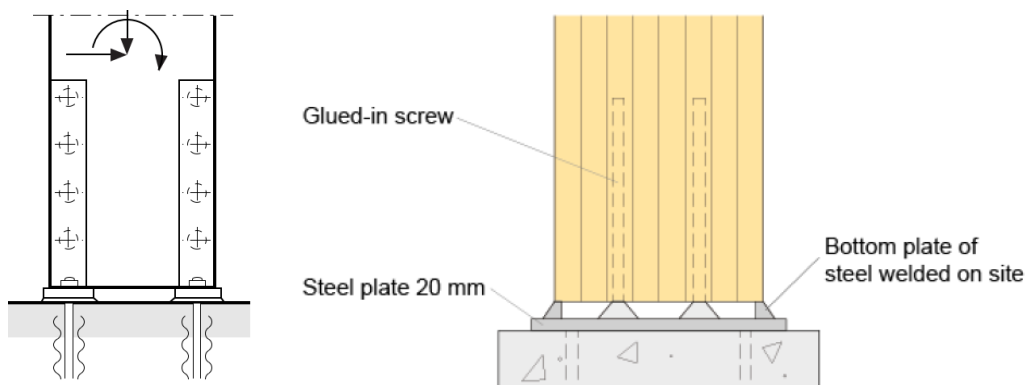


Figure D-28: Column base connection types

Left: Traditional moment resistant connection (Blaß & Sandhaas, 2017).

Right: Connection with a glued-in rod to create extra stiffness (Gross, 2013)

D.7.2 Timber sway frame

It is also possible to design a timber portal frame system in one or two directions. However, this means that the beam-column connection is more difficult to manufacture. Furthermore, more material will be needed compared to a braced frame. It is questioned whether both aspects are wanted in a design.

To provide some insight in what the difference is between a sway and a non-sway system, some remarks can be made. A moment resistant connection in timber can be made in the factory, with a finger joint or made on site with bolts (and a steel plate if necessary). For both types of moment resistant connections, issues arise with the connection of the beams to the columns. For the beams, it is advantageous to have a high and slender cross section, whereas for a column a square cross section is most efficient. This can be solved by incorporating steel elements between the timber beams and columns to create this connection. An advantage of a finger joint is that a way higher stiffness can be reached compared to a bolted connection. However, this does lead to transportation issues, as the column and beam will be already connected in the factory. Therefore, an extra connection halfway the beam or column is necessary. At this location, the bending moment should be close to zero, to prevent the need of another moment resisting connection.

D.7.3 Applying a Lignatur floor

In the design, a CLT floor is considered. However, it is expected that a Lignatur floor can ensure a reduction of floor height and weight. Therefore, the CLT panels are compared to the Lignatur floors. This is done based upon rules of thumb from Lignatur, which are given in the figure below. For a floor length of 2.108 m, the height of the beam is 120 mm. However, in this figure, the maximally allowed deflection is L over 450. This is not allowed for this design (it should be maximally L over 360). Therefore, an overestimation of 1.25 is included. This leads to a thickness of 150 mm and shows that the Lignatur floor can reduce the amount of material needed. Nevertheless, this is only an initial investigation and is therefore not included in the final calculation of mass.

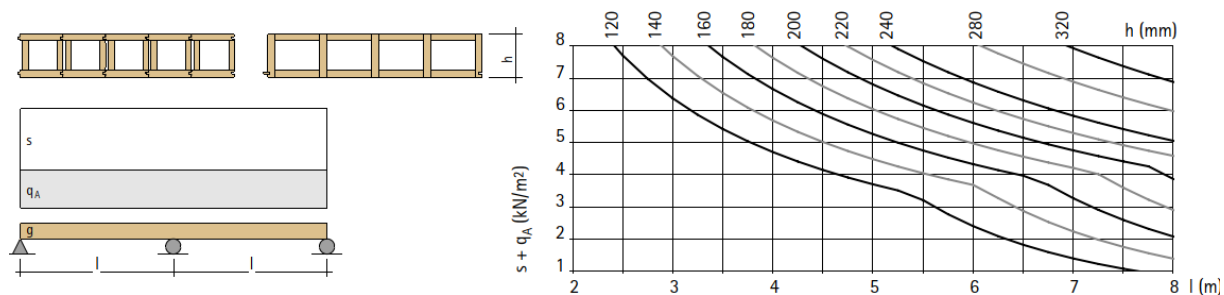


Figure D-29: Explanation on how to determine the height of the Lignatur floor element (Lignatur AG, 2014)

D.8 Element overview

MAIN LOAD-BEARING STRUCTURE

Element	Type	Wt. [kg/m]	Length [m]	Number (y)	Number (x)	Total nr	Total [kg]
Column (main)	GL24h 490x490	115,2	12,71	7	13	91	133297
Column (façade)	GL24h 580x580	161,5	12,71	34	54	88	180603
Roof beam (y)	GL24h tapered beam (average h=1361,b=195)	127,4	16,86	4	19	76	163232
Roof beam, lower 1 (x)	GL24h 1150x192	106,0	15,81	0	0	0	0
Roof beam, lower 2 (x)	GL24h 1450x242	168,4	23,715	0	0	0	0
Roof beam, higher 1 (x)	GL24h 1571x196	147,8	15,81	2	8,5	17	39724
Roof beam, higher 2 (x)	GL24h 1571x242	182,5	23,715	2	1,5	3	12983
Façade beam (x)	GL24h 840x140	56,4	7,905	2	20	40	17849
Lateral support (y)	GL24h 160x60	4,6	8,43	16	28	448	17403
Lateral support (x)	GL24h 160x60	4,6	7,905	16	28	448	16319
							<i>581410</i>
Horizontal bracing elements							
Roof beam (y, wind from x)	GL24h tapered beam (average h=1361,b=390)	254,8	16,86	8	10	80	343646
Roof beam (y, wind from y)	GL24h tapered beam (average h=1361,b=390)	254,8	16,86	4	19	76	326464
Roof beam, lower 1 (x, wind y)	GL24h 1150x460	253,9	15,81	7	8,5	59,5	238861
Roof beam, lower 2 (x, wind y)	GL24h 1450x500	348,0	23,715	3	1,5	4,5	37138
Roof beam, high 1 (x, wind y)	GL24h 1571x460	346,9	15,81	2	8,5	17	93230
Roof beam, high 2 (x, wind y)	GL24h 1571x500	377,0	23,715	2	1,5	3	26825
Roof beam, lower 1 (x, wind x)	GL24h 1150x460	253,9	15,81	15	2	30	120434
Roof beam, lower 2 (x, wind x)	GL24h 1450x500	348,0	23,715	3	2	6	49517
Roof beam, high 1 (x, wind x)	GL24h 1571x460	346,9	15,81	4	2	8	43873

Roof beam, high 2 (x, wind x)	GL24h 1571x500	377,0	23,715	4	2	8	71532
Diagonal (wind from x)	GL24h 400x400	76,8	11,557	32	8	256	227211
Diagonal (wind from y)	GL24h 400x400	76,8	11,557	16	20	320	284014
							1862745

Vertical bracing elements

Diagonal	CHS 406.4/16	154	15,916	2	2	4	9804
							<i>Total glulam: 1862745</i>
							<i>Total steel: 9804</i>

MEZZANINE FLOOR

Element	Type	Wt [kg/m ²]	Area [m ²]	Weight [kg]	Number (y)	Number (x)	Total [kg]
Floor (concrete)	CLT (C24), thickness 175 mm	84	115,5	9702	10	11	1067254
Floor (top floor)	Concrete layer 50 mm thick	120	115,5	13860	10	11	1524648

MEZZANINE FLOOR BEAMS AND COLUMNS

Element	Type	Wt [kg/m]	Length [m]	Number (y)	Number (x)	Total nr	Total [kg]
Secondary beam	GL24h 900x600	259,2	15,81	40	11	440	1803099
Secondary beam	GL24h 900x600	259,2	7,905	40	1	40	81959
Primary beam	GL24h 900x515	222,5	8,43	10	13	130	243816
Column (floor)	GL24h 240x240	27,6	4,5	6	12	72	8958
							<i>Total glulam: 2137832</i>

E Alternative C

E.1 Loads on the 2D model

The loads on the 2D model are almost the same as given in Appendix B.2.1 “Loads on the 2D model (y-direction)” and B.2.2 “Loads on the 2D model (x-direction)” of the base design. One difference is the load on the mezzanine floor, which is given in Appendix E.3 “Results of structural calculations”. Another difference is the weight of the secondary roof beam on the main roof beam, as the secondary roof beam is larger than in the base design. This is calculated as follows:

Self-weight from secondary roof beam (HEB 500-CB):

$$q_{\text{own.secondarybeam}} := \frac{191 \text{ kN}}{100 \text{ m}} = 1.91 \cdot \frac{\text{kN}}{\text{m}}$$

$$q_{\text{purlins}} := 2.37 \frac{\text{kN}}{\text{m}}$$

$$q_{\text{dead}} := q_{\text{own.secondarybeam}} + q_{\text{purlins}} = 4.28 \cdot \frac{\text{kN}}{\text{m}}$$

$$V_{\text{Ed.dead}} := \frac{1}{2} \cdot q_{\text{dead}} \cdot L = 36.08 \cdot \text{kN}$$

E.2 Beam-column connections

The beam-column connection in the y-direction is shown in Figure 6-25. In the design, the main roof beam (HEB 650-CB) is connected to the column with a non-extending end plate. The secondary roof beams are connected to the main roof beam with a cleat angled profile. To provide enough stiffness, bracing is added. Due to the use of bolts, the bracing can be removed from the main load-bearing elements.

For the beam-column connections, the rule of thumb as given in B.3.3 “Beam-column connections” are used. The results are found in the following tables. The stiffnesses that are calculated in these tables are relatively low, so demountable bracings ensure enough stiffness.

Table E-1: Flexibility factor for connections in Figure B-9 (y-direction) (Staalbouwkundig Genootschap, 1999)

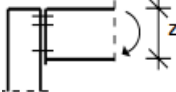
Type	Design	k_f
Roof beam (y-direction) connected to façade column: Single sided end plate connection		11.5

Table E-2: Stiffness calculation of the connection between the roof beam and the columns (y-direction)

Interior column	Exterior column	
	E	210000
	Type of beam	HEB 500-CB
	Height beam	750
	$z = 0.8 * h_b$	600
	Column type	HEB 400
	Column flange thickness	24
	k_f	11.5
$S_{j.appr}$ [MNm/rad]	0 (pinned connection) + brace	$S_{j.appr}$ [MNm/rad] 157.8

Table E-3: Flexibility factor for connections in Figure B-7 (x-direction) (Staalbouwkundig Genootschap, 1999)


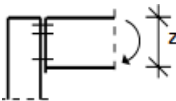
Type	Design	k_f
Continuous beam (x-direction) on top of main column: Extended end plate connection		8.5
Continuous beam (x-direction) connected to façade column: Single sided end plate connection		11.5

Table E-4: Stiffness calculation of the connection between the roof beam and the columns (x-direction)

Interior columns			Exterior column	
E	210000	210000	E	210000
Type of column	HD400x551	HD400x621	Type of beam	HEB 600-CB
Height column	455	471	Height beam	900
$z = 0.8 * h_c$	364	367.8	$z = 0.8 * h_b$	720
Beam type	HEB 600-CB	HEB 600-CB	Column type	HEB 400
Beam flange thickness	30	30	Column flange thickness	22.5
k_f	8.5	8.5	k_f	11.5
$S_{j,appr} [MNm/rad]$	$98.2 + brace$	$105.2 + brace$	$S_{j,appr} [MNm/rad]$	227.2

E.3 Results of structural calculations

The final design is given in chapter 6.4.2 “Schematisation of”. Here, the dimensions, supports, and the element types are depicted. For the loads on this system, Appendix E.1 “Loads on the 2D model” is followed, from which the load combinations given in Appendix B.2.1.1 and 0 are applied. In this chapter, the SLS and ULS calculations are based upon the governing load combinations.

E.3.1 SLS

The results are found in the following table, which is based upon the figures shown below this table. For the horizontal deflection, load combination SLS 16 is governing. For the vertical deflection of the roof beams, load combination SLS 17 is governing. In Table B-3, these load combinations are specified.

Table E-5: SLS results of the structural verifications performed in SCIA

Check	Max. calculated	Max. based on length	UC	Maximal UC
<i>Horizontal deformation</i>		$\frac{h_{column}}{150} = \frac{13500}{150}$		
Horizontal deformation (x)	69.9 mm	90 mm	0.78	0.80
Horizontal deformation (y)	57.7 mm	90 mm	0.65	0.80
<i>Vertical deformation</i>		$\frac{L_{beam}}{250}$		
Vertical deformation (x; beam with length 15.81 m)	10.7	63.2 mm	0.17	0.80
Vertical deformation (x; beam with length 23.715 m)	27.1 mm	94.9 mm	0.29	0.80
Vertical deformation (y; beam with length 16.86 m)	18.9 mm	67.4 mm	0.29	0.80

E.3.2 Buckling lengths and ULS calculation results

The main load-bearing structure acts as a sway frame. The façade columns act as non-sway, as roof bracing transfers the wind loads to the main beams and columns. The roof beams also act non-sway.

In Table E-6, the buckling lengths of the columns are given and in Table E-7, the buckling lengths of the beams are given. The buckling lengths are calculated in SCIA. Due to the lower stiffness compared to the base design, higher buckling factors are found.

As two 2D-models are set up, the buckling length of the column in the main direction is applied manually as buckling length for the column in the perpendicular direction. This is included in the buckling factor in the perpendicular direction in Table E-6 and Table E-7.

Table E-6: Buckling lengths of the columns, from SCIA

Member	Type	Length between supports [m]	Stiffness with beam [MNm/rad]	Buckling factor	
				Main	Perp.
Main column 1 (x)	HD 400x531	13.5	98.2 + Bracing (x)	1.98	1.83
Main column 2 (x)	HD 400x621	13.5	105.2 + Bracing (x)	2.08	1.91
Main column 1 (y)	HD 400x531	13.5	Pinned + Bracing 1 (y)	1.83	1.98
Main column 2 (y)	HD 400x621	13.5	Pinned + Bracing 1 (y)	1.91	2.08
Façade column (x)	HEB 400	13.5	227.2	0.60	1
Façade column (y)	HEB 400	13.5	157.8	0.60	1

Table E-7: Buckling lengths of the beams, from SCIA

Member	Type	Length between LTB restraints [m]	Length between supports [m]	Buckling factor	
				Main	Perp.
Beam 1 (x)	HEB 700 (HEB 600-CB)	7.905	15.81	0.62	1
Beam 2 (x)	HEB 1000 (HEB 800-CB)	7.905	23.715	0.62	1
Beam 3 (y)	HEB 650 (HEB 500-CB)	7.905	16.86	1	1

Table E-8: Buckling lengths of the bracing, from SCIA

Member	Type	Length between supports [m]	Stiffness with beam [MNm/rad]	Buckling factor	
				Main	Perp.
Bracing (x)	SHS120/120/5	0.424	Pinned	1	1
Bracing 1 (y)	RHS200/100/16	1.044	Pinned	1	1

In Table E-9, the governing unity checks for the different members is given. This is based upon load combination ULS 6, which is specified in Table B-3. The elements are checked upon the unity check for the section and the unity check for the stability. The same steps as performed in Appendices B.5.2.1 “ULS calculation of a governing column (shown in blue in Figure B-27)” and B.5.2.2 “ULS calculation of a governing beam (shown in green in Figure B-27)” are performed for these members as well. This is however not included in this report.

Table E-9: Governing unity checks for the members of alternative C

Member	Type	UC section	Max. UC section	UC stability	Max. UC stability
Main column 1 (x)	HD 400x531	0.13	0.85	0.75	0.80
Main column 2 (x)	HD 400x621	0.13	0.85	0.80	0.80
Main column 1 (y)	HD 400x531	0.08	0.85	0.78	0.80
Main column 2 (y)	HD 400x621	0.06	0.85	0.66	0.80
Façade column (x)	HEB 400	0.45	0.85	0.64	0.80
Façade column (y)	HEB 400	0.39	0.85	0.68	0.80
Beam 1 (x)	HEB 700 (HEB 600-CB)	0.27	0.85	0.51	0.80
Beam 2 (x)	HEB 1000 (HEB 800-CB)	0.15	0.85	0.73	0.80
Beam 3 (y)	HEB 650 (HEB 500-CB)	0.30	0.85	0.79	0.80
Bracing (x)	SHS120/120/5	0.55	0.85	0.56	0.80
Bracing (y)	RHS200/100/16	0.66	0.85	0.00	0.80

To give some insight in the forces in the beams and columns, the following figures are made. Here, the normal, shear, and bending forces are depicted for a section in the x-direction and one in the y-direction.

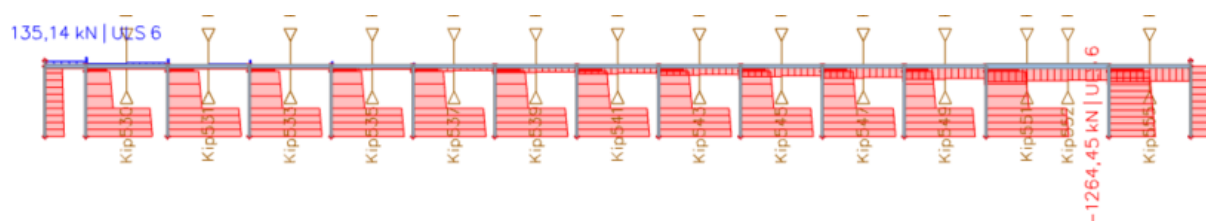


Figure E-1: Normal forces in the frame in the x-direction (for ULS 6)

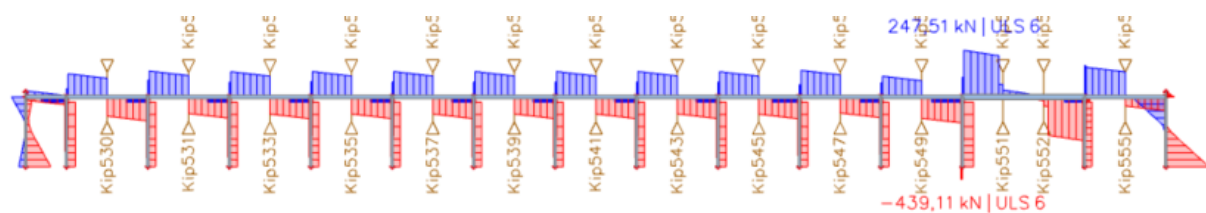


Figure E-2: Shear forces in the frame in the x-direction (for ULS 6)

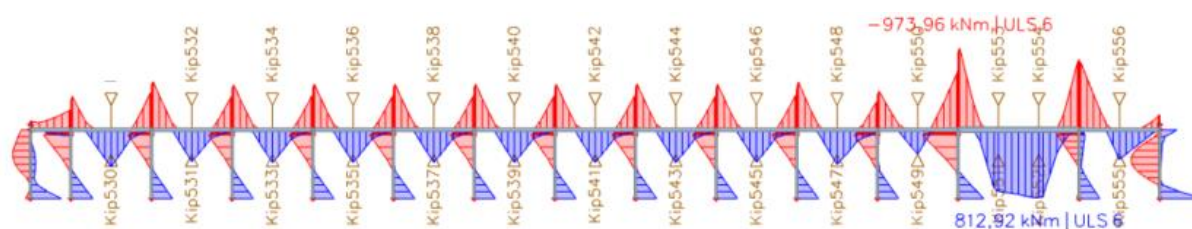


Figure E-3: Bending moments in the frame in the x-direction (for ULS 6)

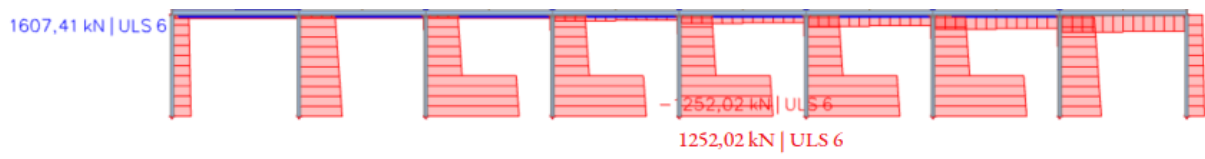


Figure E-4: Normal forces in the frame in the y-direction (for ULS 6)

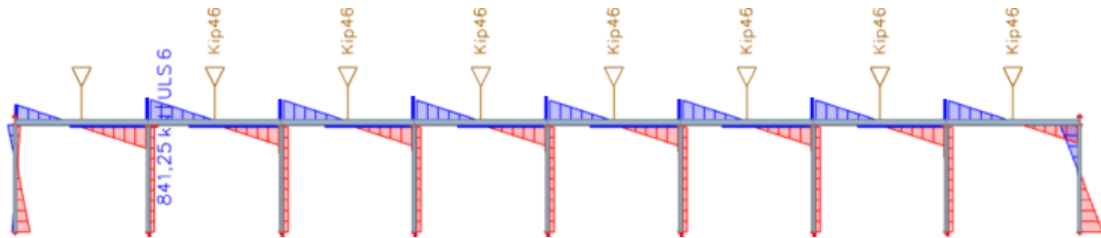


Figure E-5: Shear forces in the frame in the y-direction (for ULS 6)

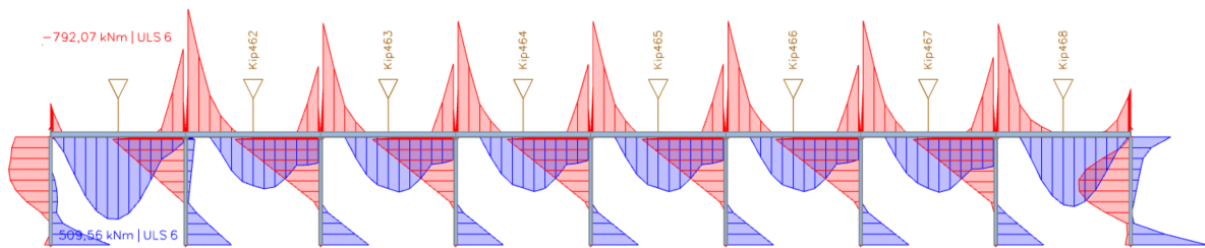
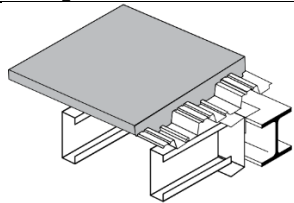
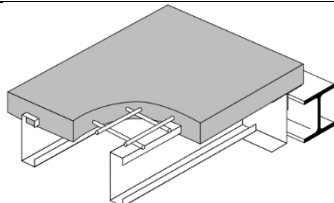
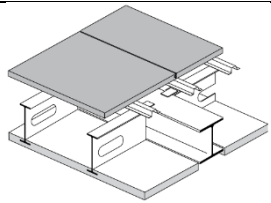



Figure E-6: Bending moments in the frame in the y-direction (for ULS 6)

E.4 Mezzanine floor design

Table E-10: Comparison between concrete (and steel) floor systems

	Composite floor ComFlor75	Quantum deck floor	Slimline floor	Hollow core slab
Visualisation				
Span	(Bouwen met Staal, 2013) 3–4 m without propping, with propping up to 5.5 m	(Bouwen met Staal, 2013) 5–11 m	(Bouwen met Staal, 2013) ≤ 16.2 m	(BIMObject, n.d.) ≤ 16 m, no propping needed
Height	150 mm <i>Excluding the beams</i>	6–7 meter is optimal 250 mm with C220 sections <i>Including the topping</i>	300-500 mm <i>Including the topping and ceiling, excluding the steel section</i>	150-400 mm <i>Excluding topping and beams; Integrated beams can reduce total height</i>
Freedom of shape	Yes	Limited (prefab), irregular shapes can be custom made	Limited (prefab), irregular shapes can be custom made	Limited (prefab), irregular shapes can be custom made
Mass	267 kg/m ²	± 180 kg/m ²	225-275 kg/m ²	±270-490 kg/m ² excl. topping
Concrete topping	Not necessary	Not necessary	Not necessary	Necessary
Diaphragm action	Yes	Yes	Yes	Yes
Construction speed	Steel decking is easy to handle	Prefab, so quick assembling	Prefab, so quick assembling	Prefab, so quick assembling
Heavy equipment	No crane necessary	Crane is necessary	Crane is necessary	Crane is necessary
Transportation	Small volume of sheets	Prefab, so large elements to be transported	Prefab, so large elements to be transported	Prefab, so large elements to be transported
Sustainability of materials	+/- In situ concrete	- Prefab	- Prefab	- Prefab
Sources	(Dutch Engineering BV, 2020)	(Star-Frame Solutions, 2011)	(Bouwen met Staal, 2013; Slimline Buildings, 2020)	(VBI, n.d.)

E.4.1 Floor calculations (robotic function)

For the robotic function, two floor slabs are needed: one with a length of 2108 mm and one with a length of 4215 mm.

In the following figures, the SLS and ULS calculations of the hollow core slabs are shown. For the SLS calculations (Figure F-1), the following loads are applied:

- Top floor: 1.2 kN/m², for a slab of 1200 mm thick, this leads to a line load of 1.44 kN/m;
- Dead loads: 0.25 kN/m², for a slab of 1200 mm thick, this leads to a line load of 0.3 kN/m;
- Imposed floor load: 3 kN/m², for a slab of 1200 mm thick, this leads to a line load of 4.8 kN/m;
- Self-weight of the slab is calculated by the hollow core slab calculator.

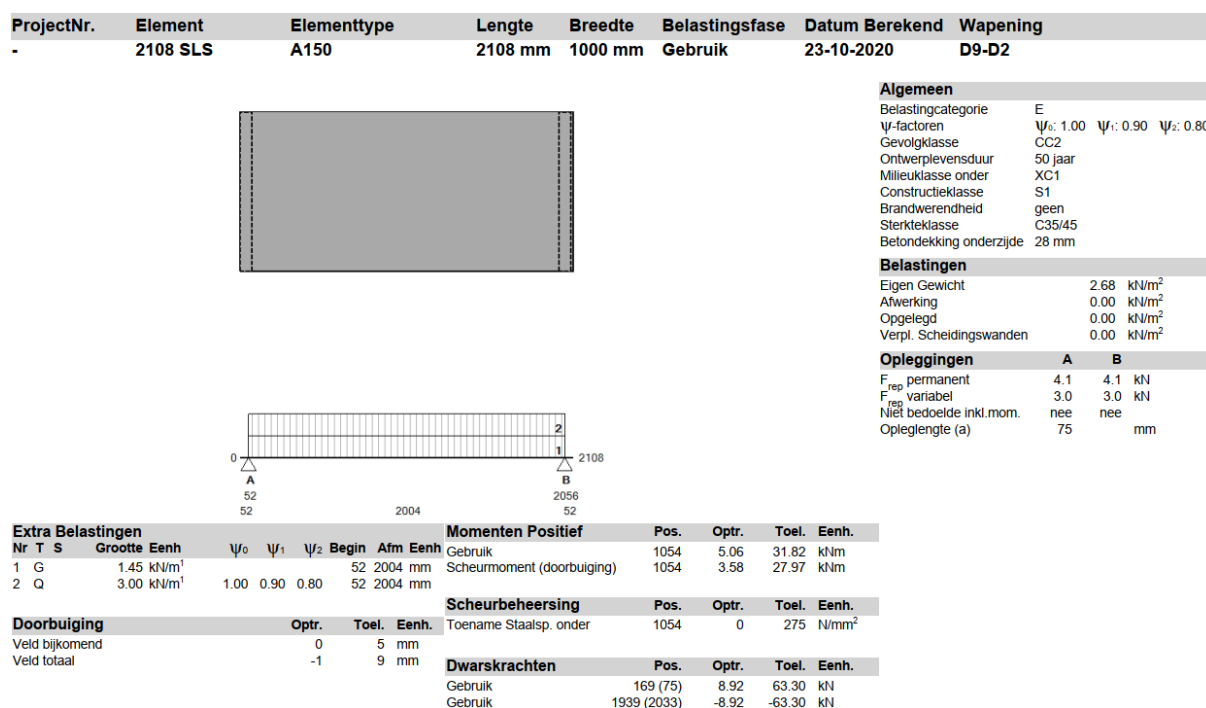

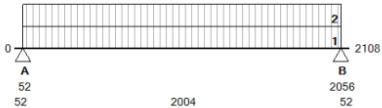


Figure E-7: VBI hollow core slab calculation (2108 mm long) for a robotic load for Alternative C in the SLS state

For the ULS calculation (Figure F-2), the top floor, dead loads, and self-weight are factored with 1.35 and the imposed floor load is factored with 1.5.

ProjectNr.	Element	Elementtype	Lengte	Breedte	Belastingsfase	Datum Berekend	Wapening
-	2108 ULS	A150	2108 mm	1000 mm	Gebruik	23-10-2020	D9-D2





Algemeen

Belastingcategorie E
 Ψ_f -factoren Ψ_f : 1.00 Ψ_f : 0.90 Ψ_f : 0.80
 Gevolgklasse CC2
 Ontwerplevensduur 50 jaar
 Milieuklasse onder XC1
 Constructieklasse S1
 Brandwerendheid geen
 Sterkteklasse C35/45
 Betondekking onderzijde 28 mm

Belastingen

Eigen Gewicht 2.68 kN/m²
 Afwerking 0.00 kN/m²
 Opgelegd 0.00 kN/m²
 Verpl. Scheidingswanden 0.00 kN/m²

Opleggingsen

	A	B
F _{rep} permanent	4.6	4.6
F _{rep} variabel	4.5	4.5
Niët bedoelde inkl.mom.	nee	nee
Oplegglengte (a)	75	mm

Extra Belastingen				Momenten Positief			
Nr	T	S	Grootte Eenh.	Pos.	Optr.	Toel.	Eenh.
1	G		1.96 kN/m ²	1054	6.53	31.82	kNm
2	Q		4.50 kN/m ²	1054	4.59	27.99	kNm

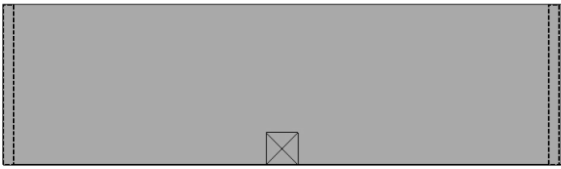
Doorbuiging				Scheurbeheersing			
	Optr.	Toel.	Eenh.	Pos.	Optr.	Toel.	Eenh.
Veld bijkomend	0	5	mm	1054	0	275	N/mm ²
Veld totaal	-1	9	mm				

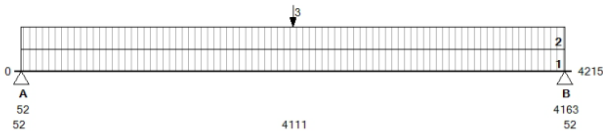
Dwarskrachten				
	Pos.	Optr.	Toel.	Eenh.
Gebruik	166 (75)	11.56	63.31	kN
Gebruik	1942 (2033)	-11.56	-63.31	kN

Figure E-8: VBI hollow core slab calculation (2108 mm long) for a robotic load for Alternative C in the ULS state

The longer floors need to carry the trimmers that carry the shorter floors. This has been modelled as a point load on the longer floors. This point load comes from the shear forces ('dwarskrachten') shown in the figures above.

ProjectNr.	Element	Elementtype	Lengte	Breedte	Belastingsfase	Datum Berekend	Wapening
-	4215 SLS	A150	4215 mm	1200 mm	Gebruik	23-10-2020	S2D10-D4





Algemeen

Belastingcategorie E
 Ψ_f -factoren Ψ_f : 1.00 Ψ_f : 0.90 Ψ_f : 0.80
 Gevolgklasse CC2
 Ontwerplevensduur 50 jaar
 Milieuklasse onder XC1
 Constructieklasse S1
 Brandwerendheid geen
 Sterkteklasse C40/50
 Betondekking onderzijde 28 mm

Belastingen

Eigen Gewicht 2.68 kN/m²
 Afwerking 0.00 kN/m²
 Opgelegd 0.00 kN/m²
 Verpl. Scheidingswanden 0.00 kN/m²

Opleggingsen

	A	B
F _{rep} permanent	17.2	17.2
F _{rep} variabel	7.4	7.4
Niët bedoelde inkl.mom.	nee	nee
Oplegglengte (a)	75	mm

Extra Belastingen				Momenten Positief			
Nr	T	S	Grootte Eenh.	Pos.	Optr.	Toel.	Eenh.
1	G		1.74 kN/m ²	2108	45.11	52.41	kNm
2	Q		3.60 kN/m ²	2108	32.57	41.67	kNm
3	G		14.10 kN	2108			mm

Doorbuiging				Scheurbeheersing			
	Optr.	Toel.	Eenh.	Pos.	Optr.	Toel.	Eenh.
Veld bijkomend	6	9	mm	2108	0.000	0.365	mm
Veld totaal	7	17	mm				

Dwarskrachten				
	Pos.	Optr.	Toel.	Eenh.
Gebruik	166 (75)	32.99	84.52	kN
Gebruik	4049 (4140)	-32.99	-84.52	kN

Figure E-9: VBI hollow core slab calculation (4215 mm long) for a robotic load for Alternative C in the SLS state

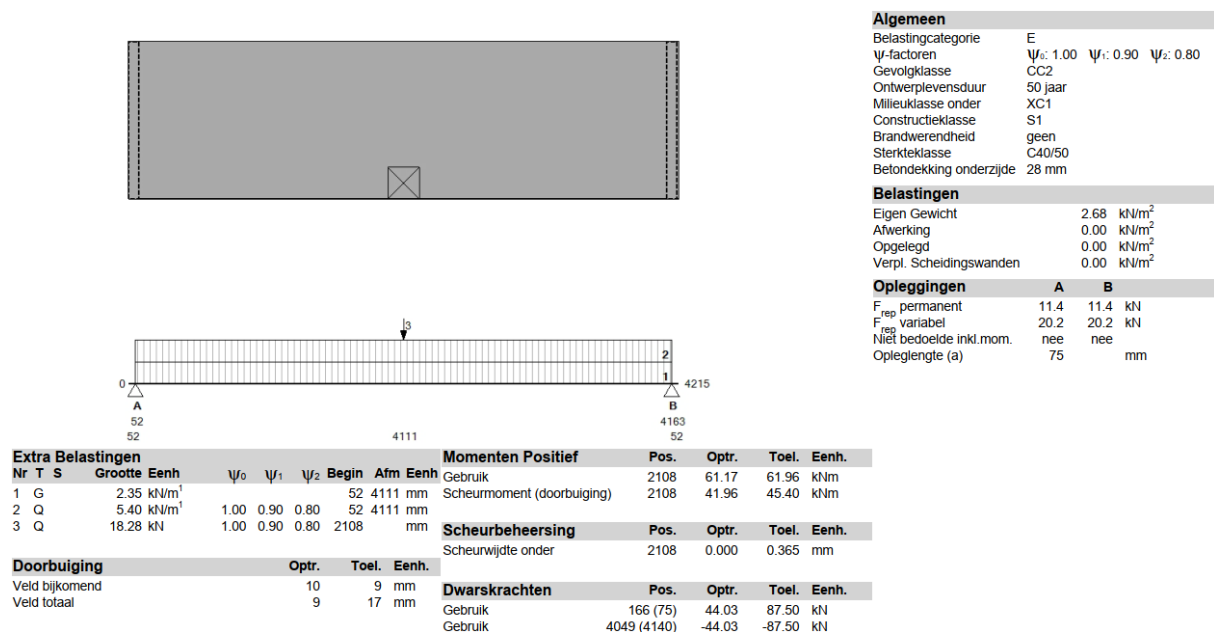


Figure E-10: VBI hollow core slab calculation (4215 mm long) for a robotic load for Alternative C in the ULS state

For the functionality of the building, the specific floor grid remains the same. However, hollow core slabs are usually made from standardised widths. It is aimed to use a standardised width of 900 mm for most floor elements. The remaining elements must be made specifically for this building. This is shown in the following table.

Table E-11: Derivation of the width of the hollow core slab members

Width of floor area [m]	Width of standard slabs [m]	Width of non-standard slabs [m]
1.581 (2x)	1 x 0.900 = 0.9	1.581 - 0.9 = 0.681
2.108 (2x)	2 x 0.900 = 1.8	2.108 - 1.8 = 0.308
8.432	9 x 0.900 = 8.1	8.432 - 8.1 = 0.332

E.4.2 Steel secondary mezzanine floor beam checks for the floor with robotic function

$$L_w := 15.81\text{m}$$

Define cross section

$$f_y := 355\text{MPa}$$

$$E := 210\text{GPa}$$

$$\varepsilon_{\text{w}} := \sqrt{\frac{235\text{MPa}}{f_y}} = 0.814$$

$$G_v := 81000 \frac{\text{N}}{\text{mm}^2}$$

$$\gamma_{M0} := 1$$

$$\gamma_{M1} := 1$$

$$\text{HEB } 650\text{CB} = \text{HEB}800$$

$$h := 800\text{mm}$$

$$b := 300\text{mm}$$

$$t_w := 17.5\text{mm}$$

$$t_f := 33\text{mm}$$

$$r := 30\text{mm}$$

$$h_w := h - 2t_f - 2r = 0.674\text{m}$$

$$A_{\text{tot}} := 33418\text{mm}^2$$

$$\text{weight} := 224.8 \frac{\text{kg}}{\text{m}}$$

$$W_{\text{ply}} := 10230 \cdot 10^3 \text{mm}^3$$

$$W_{\text{plz}} := 1553 \cdot 10^3 \text{mm}^3$$

$$I_y := 3591 \cdot 10^6 \text{mm}^4$$

$$I_z := 149.0 \cdot 10^6 \text{mm}^4$$

$$I_w := 21617000 \cdot 10^6 \cdot \text{mm}^6$$

$$I_t := 9621 \cdot 10^3 \text{mm}^4$$

Loads (from VBI calculator)

$$q_{\text{SLS.VBI}} := \frac{32.99\text{kN}}{1.2\text{m}} = 27.492 \cdot \frac{\text{kN}}{\text{m}}$$

$$q_{\text{ULS.VBI}} := \frac{44.03\text{kN}}{1.2\text{m}} = 36.692 \cdot \frac{\text{kN}}{\text{m}}$$

$$G_{\text{self.beam}} := \text{weight} \cdot 9.81 \frac{\text{N}}{\text{kg}} = 2.205 \cdot \frac{\text{kN}}{\text{m}}$$

$$q_{\text{SLS0}} := q_{\text{SLS.VBI}} + G_{\text{self.beam}} = 29.697 \cdot \frac{\text{kN}}{\text{m}}$$

$$q_{\text{ULS0}} := q_{\text{ULS.VBI}} + 1.35 \cdot G_{\text{self.beam}} = 39.669 \cdot \frac{\text{kN}}{\text{m}}$$

$$M_{\text{Ed.SLS0}} := \frac{1}{8} \cdot q_{\text{SLS0}} \cdot L^2 = 927.867 \cdot \text{kN} \cdot \text{m}$$

$$M_{\text{Ed.ULS0}} := \frac{1}{8} \cdot q_{\text{ULS0}} \cdot L^2 = 1.239 \times 10^3 \cdot \text{kN} \cdot \text{m}$$

$$V_{\text{Ed.SLS0}} := \frac{1}{2} \cdot q_{\text{SLS0}} \cdot L = 234.754 \cdot \text{kN}$$

$$V_{\text{Ed.ULS0}} := \frac{1}{2} \cdot q_{\text{ULS0}} \cdot L = 313.582 \cdot \text{kN}$$

$$N_{\text{Ed.ULS}} := 0\text{kN}$$

Loads (own calculation)

To be sure the calculation from the VBI calculator can be used, also a hand calculation is performed.

$$b_{\text{floor}} := 4215\text{mm}$$

$$G_{\text{load1}} := 1.2 \frac{\text{kN}}{\text{m}^2} \quad \text{Demountable concrete top floor}$$

$$G_{\text{load2}} := 0.25 \frac{\text{kN}}{\text{m}^2} \quad \text{Services on floor}$$

$$G_{\text{self.floor}} := 2.68 \frac{\text{kN}}{\text{m}^2} \quad \text{Self-weight hollow core floor (2108 mm span)}$$

$$G_{\text{self.beam}} := \text{weight} \cdot 9.81 \frac{\text{N}}{\text{kg}} = 2.205 \cdot \frac{\text{kN}}{\text{m}}$$

$$Q_{\text{load1}} := 3 \frac{\text{kN}}{\text{m}^2} \quad \text{Robotic live load}$$

$$q_G := (G_{\text{load1}} + G_{\text{load2}} + G_{\text{self.floor}}) \cdot b_{\text{floor}} = 17.408 \cdot \frac{\text{kN}}{\text{m}}$$

$$q_Q := Q_{\text{load1}} \cdot b_{\text{floor}} = 12.645 \cdot \frac{\text{kN}}{\text{m}}$$

$$L_{\text{trimmer}} := 2108\text{mm}$$

$$q_{\text{t.G}} := (G_{\text{load1}} + G_{\text{load2}} + G_{\text{self.floor}}) \cdot \frac{1}{2} \cdot b_{\text{floor}} = 8.704 \cdot \frac{\text{kN}}{\text{m}}$$

$$F_{\text{t.G}} := \frac{1}{2} \cdot q_{\text{t.G}} \cdot L_{\text{trimmer}} = 9.174 \cdot \text{kN}$$

$$q_{\text{t.Q}} := Q_{\text{load1}} \cdot \frac{1}{2} \cdot b_{\text{floor}} = 6.322 \cdot \frac{\text{kN}}{\text{m}}$$

$$F_{\text{t.Q}} := \frac{1}{2} \cdot q_{\text{t.Q}} \cdot L_{\text{trimmer}} = 6.664 \cdot \text{kN}$$

$$F_{\text{t.SLS}} := F_{\text{t.G}} + F_{\text{t.Q}} = 15.838 \cdot \frac{\text{kN}}{\text{m}}$$

$$F_{\text{t.ULS}} := 1.35 \cdot F_{\text{t.G}} + 1.5 \cdot F_{\text{t.Q}} = 22.381 \cdot \frac{\text{kN}}{\text{m}}$$

$$q_{\text{SLS}} := q_G + q_Q = 30.053 \cdot \frac{\text{kN}}{\text{m}}$$

$$q_{\text{ULS}} := 1.35 \cdot q_G + 1.5 \cdot q_Q = 42.468 \cdot \frac{\text{kN}}{\text{m}}$$

$$M_{\text{Ed.SLS}} := \frac{1}{8} \cdot q_{\text{SLS}} \cdot L^2 + \frac{1}{4} \cdot F_{\text{t.SLS}} \cdot L_{\text{trimmer}} = 947.336 \cdot \text{kN} \cdot \text{m}$$

$$M_{\text{Ed.ULS}} := \frac{1}{8} \cdot q_{\text{ULS}} \cdot L^2 + \frac{1}{4} \cdot F_{\text{t.ULS}} \cdot L_{\text{trimmer}} = 1.339 \times 10^3 \cdot \text{kN} \cdot \text{m}$$

$$V_{\text{Ed.SLS}} := \frac{1}{2} \cdot q_{\text{SLS}} \cdot L + \frac{1}{2} \cdot F_{\text{t.SLS}} = 245.488 \cdot \text{kN}$$

$$V_{\text{Ed.ULS}} := \frac{1}{2} \cdot q_{\text{ULS}} \cdot L + \frac{1}{2} \cdot F_{\text{t.ULS}} = 346.902 \cdot \text{kN}$$

This shows that the hand calculation leads to a bit higher load compared to the VBI calculator, therefore, the hand calculation is taken as governing and used for the further calculations.

As input for the primary beam calculation, the following loads are calculated:

$$V_{Ed,G} := \frac{1}{2} \cdot q_G \cdot L + \frac{1}{2} \cdot F_{t,G} = 142.197 \cdot \text{kN}$$

$$V_{Ed,Q} := \frac{1}{2} \cdot q_Q \cdot L + \frac{1}{2} \cdot F_{t,Q} = 103.291 \cdot \text{kN}$$

Determination of cross section class

Flanges:

$$c_f := \frac{1}{2} \cdot (b - t_w) - r = 111.25 \cdot \text{mm}$$

$$\frac{c_f}{t_f} = 3.371$$

Cross section check:

$$\frac{c_f}{t_f} \leq 9\epsilon = 1 \quad \frac{c_f}{t_f} \leq 10\epsilon = 1$$

Conclusion: Flange is class 1

Web:

The beam is subjected to bending

$$c_w := h - 2 \cdot t_f - 2 \cdot r = 674 \cdot \text{mm}$$

$$\frac{c_w}{t_w} \leq 72 \cdot \epsilon = 1$$

Conclusion: Web is class 1

Flange and web:

The cross section is class 1, so plastic global analyses and plastic cross section analysis can be performed.

Plastic moment resistance

$$M_{pl} := \frac{W_{ply} \cdot f_y}{\gamma_{M0}} = 3.632 \times 10^3 \cdot \text{kN} \cdot \text{m}$$

$$UC_{\text{moment}} := \frac{M_{Ed,ULS}}{M_{pl}} = 0.369$$

Shear resistance

$$A_{v1} := A_{\text{tot}} - 2 \cdot b \cdot t_f + (t_w + 2 \cdot r) \cdot t_f = 1.618 \times 10^4 \cdot \text{mm}^2$$

$$A_v := \max(A_{v1}, h_w \cdot t_w) = 0.016 \text{ m}^2$$

$$V_{plRd} := \frac{\left[A_v \cdot \left(\frac{f_y}{3 \cdot 0.5} \right) \right]}{\gamma_{M0}} = 3.315 \times 10^3 \cdot \text{kN}$$

$$UC_{\text{shear}} := \frac{V_{Ed,ULS}}{V_{plRd}} = 0.105$$

V_{Ed} is smaller than $0.5 \cdot V_{plRd}$ so the moment resistance does not have to be calculated based on a reduced yield strength in the web.

Flexural buckling

Flexural buckling can occur due to normal forces on the beam, but as no normal force is exerted on the beam, flexural buckling can be disregarded.

Lateral Torsional Buckling

Lateral torsional buckling can occur due to bending moments on the beam. Due to the floor lying on top of this beam, torsional buckling is restrained and this can be disregarded.

Deflection

$$w := \frac{5}{384} \cdot q_{SLS} \cdot \frac{L^4}{E \cdot I_y} = 0.032 \text{ m}$$

$$w_{\text{max}} := \frac{L}{360} = 0.044 \text{ m}$$

$$UC_{\text{deflection}} := \frac{w}{w_{\text{max}}} = 0.738$$

Overview of UC

$$UC_{\text{shear}} = 0.105$$

$$UC_{\text{moment}} = 0.369$$

$$UC_{\text{deflection}} = 0.738$$

F Alternative D1

F.1 Mezzanine floor

F.1.1 Floor calculations (office or retail function)

In the following figures, the SLS and ULS calculations of the hollow core slabs are shown. For the SLS calculations (Figure F-1), the following loads are applied:

- Top floor: 1.2 kN/m², for a slab of 1200 mm thick, this leads to a line load of 1.44 kN/m;
- Dead loads: 0.25 kN/m², for a slab of 1200 mm thick, this leads to a line load of 0.3 kN/m;
- Imposed floor load: 4 kN/m², for a slab of 1200 mm thick, this leads to a line load of 4.8 kN/m;
- Self-weight of the slab is calculated by the hollow core slab calculator.

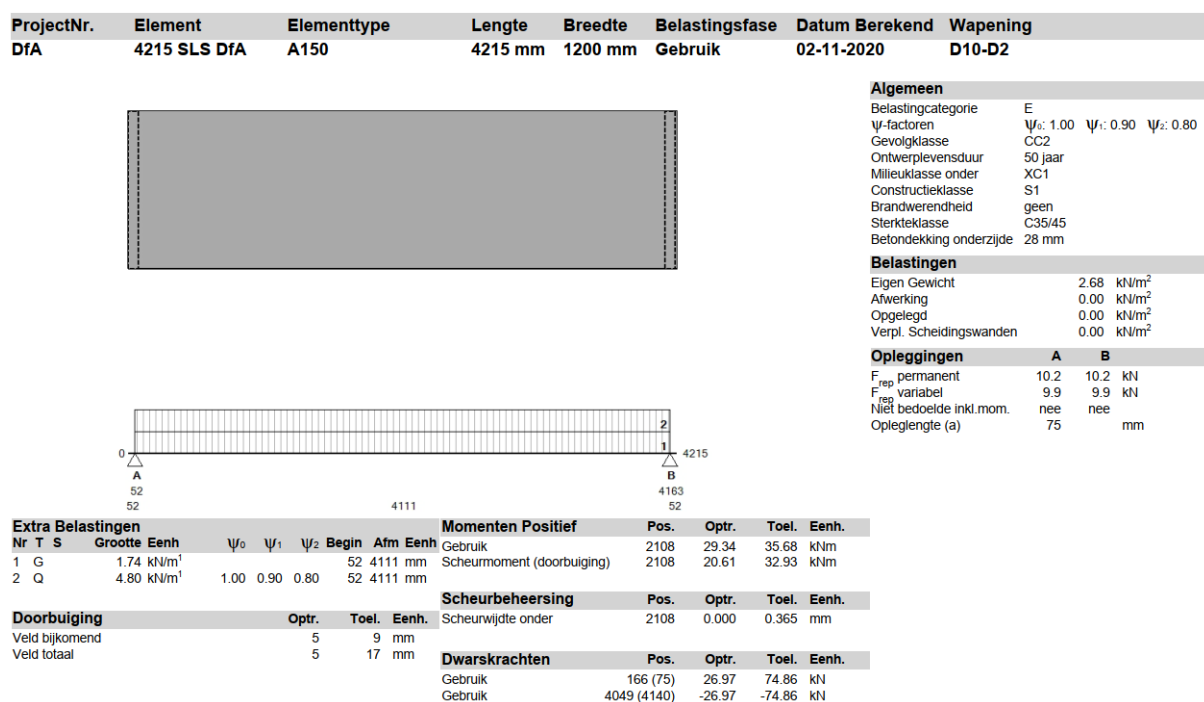


Figure F-1: Hollow core slab calculation for SLS state for Alternative D1, calculated with the VBI calculator

For the ULS calculation (Figure F-2), the top floor and self-weight are factored with 1.35 and the imposed floor load is factored with 1.5.

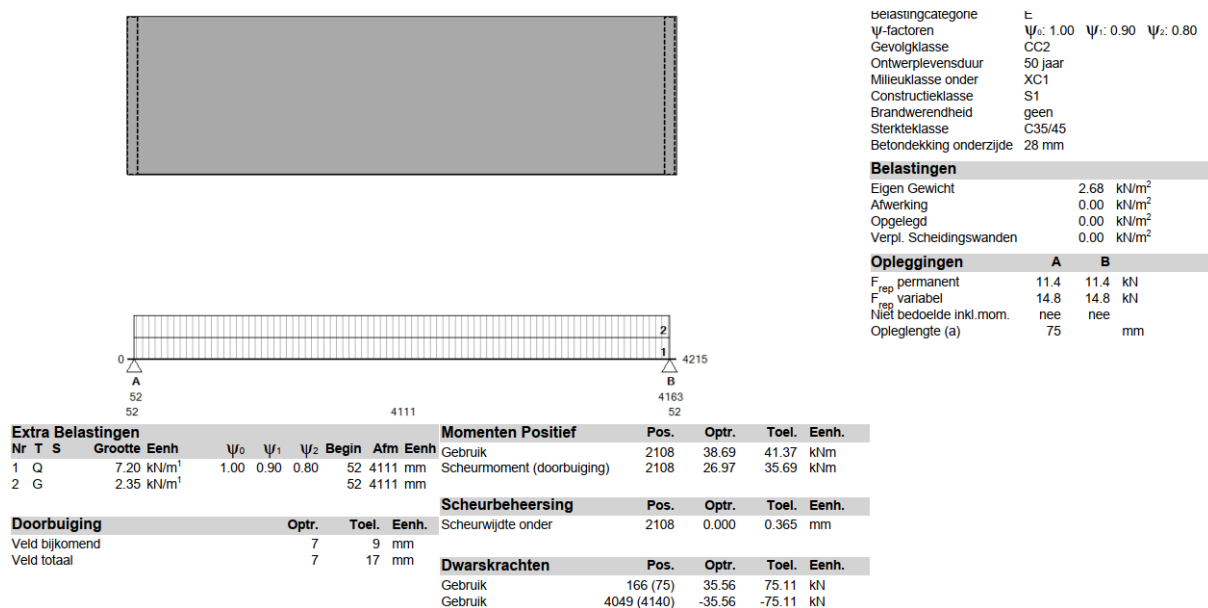


Figure F-2: Hollow core slab calculation for ULS state for Alternative D1, calculated with the VBI calculator

F.2 Results of structural calculations

The loads on the 2D model are the same as given in Appendix B.2.1 “Loads on the 2D model (y-direction)” and B.2.2 “Loads on the 2D model (x-direction)” of the base design. The only difference is the load on the mezzanine floor. For the mezzanine floor, the same calculation steps as given in Appendix B.3 are performed. This leads to the maximum dead load and maximum live load given in the following tables. These are used as input on the columns of the main load-bearing structure.



Figure F-4: Dead loads on the columns, calculated in SCIA

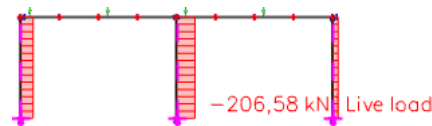


Figure F-3: Live loads on the columns, calculated in SCIA

For this alternative, the same structural system as Alternative A is used. Only the mezzanine floor load changes due to a new mezzanine floor. Therefore, only the main columns need to be checked upon this increased normal force. This normal force is given in Figure F-5 and the corresponding unity checks for the main columns are given in the following table. As the normal force is only slightly increased (see Figure C-13), the same cross section can be used as used for Alternative A.

Table F-1: Governing unity checks for the members of Alternative D1

Member	Type	UC section	Max. UC section	UC stability	Max. UC stability
Main column (x)	HEB 400	0.19	0.85	0.75	0.80

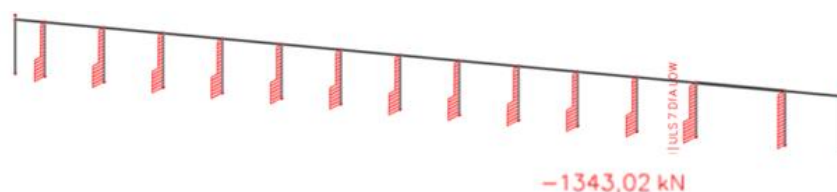


Figure F-5: Normal forces in the frame in the x-direction (for ULS 7)

F.3 Element overview

MAIN LOAD-BEARING STRUCTURE ²

Element	Type	Wt. [kg/m]	Length [m]	Number (y)	Number (x)	Total nr	Total [kg]
Column (main)	HEB 600	216	13,5	4	13	52	151 632
Column (main)	HEB 600	216	12,71	3	13	39	107 069
Column (façade)	HEB 360	145	13,5	26	46	72	140 940
Roof beam (x, small)	HEA 360-CB	145	15,81	11	12	132	302603
Roof beam (x, small)	HEA 360-CB	145	7,905	11	1	11	12608
Roof beam (x, large)	HEB 550-CB	203	23,715	7	1	7	33699
Façade beam (y)	HEA 260	69,5	8,43	8	2	16	9374
Façade beam (x)	HEA 260	69,5	7,905	2	20	40	21976
Lateral support (x)	SHS 120/120/10	31,8	7,905	4	20	80	20110
							<i>1 426 122</i>
Horizontal bracing elements							
Diagonal	160/160/15	36,8	11,557	16	16	256	108872
Diagonal	160/160/15	36,8	11,557	16	56	896	381052
Façade beam (y)	HEB 400	158	8,43	8	2	16	21311
Façade beam (x)	HEB 450	174	7,905	2	8	16	22008
							<i>533 242</i>
Vertical bracing elements							
Column	HEB 700	245	13,5	8	8	16	52 920
Diagonal	CHS 406.4/20	191	20,79	8	8	16	48 639
							<i>101 559</i>
							<i>Total: 1 693 481</i>

² The same elements are used as for Alternative A

G Alternative D2

G.1 Floor calculations (industrial function)

In the following figures, the SLS and ULS calculations of the hollow core slabs are shown. For the SLS calculations (Figure F-1), the following loads are applied:

- Top floor: 1.2 kN/m², for a slab of 1200 mm thick, this leads to a line load of 1.44 kN/m;
- Dead loads: 0.25 kN/m², for a slab of 1200 mm thick, this leads to a line load of 0.3 kN/m;
- Imposed floor load: 4 kN/m², for a slab of 1200 mm thick, this leads to a line load of 4.8 kN/m;
- Self-weight of the slab is calculated by the hollow core slab calculator.

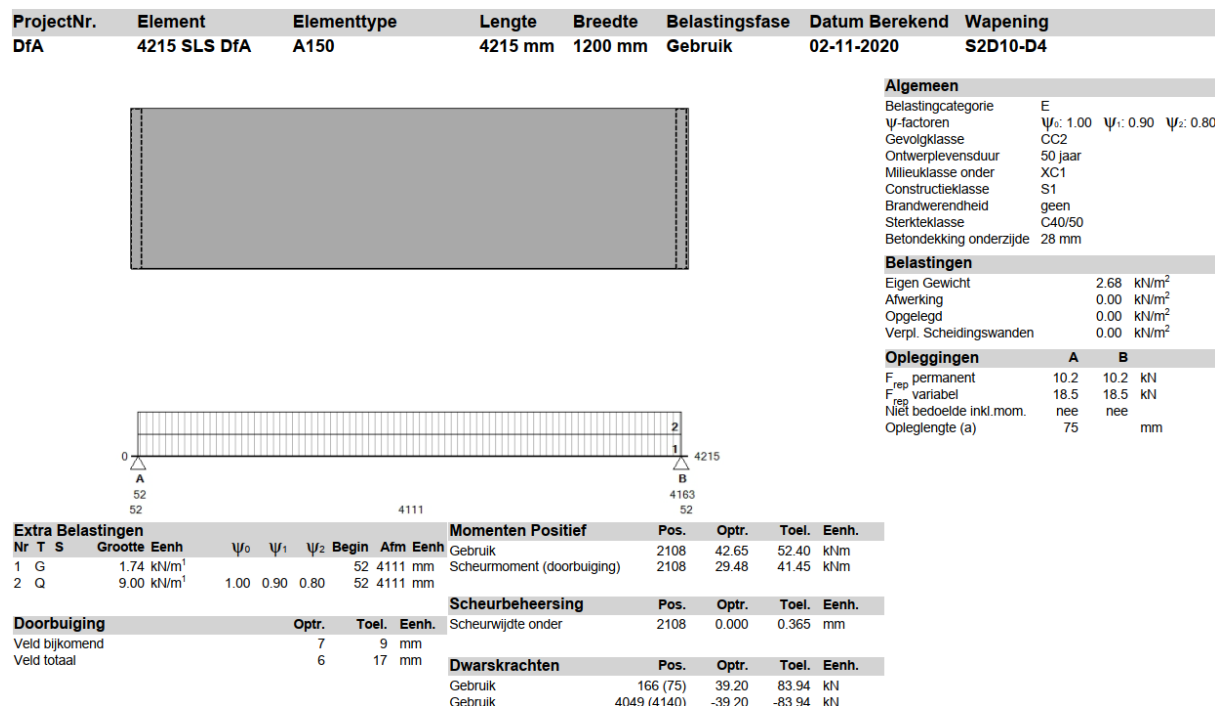


Figure G-1: Hollow core slab calculation for SLS state for Alternative D2, calculated with the VBI calculator

For the ULS calculation (Figure F-2), the top floor and self-weight are factored with 1.35 and the imposed floor load is factored with 1.5.

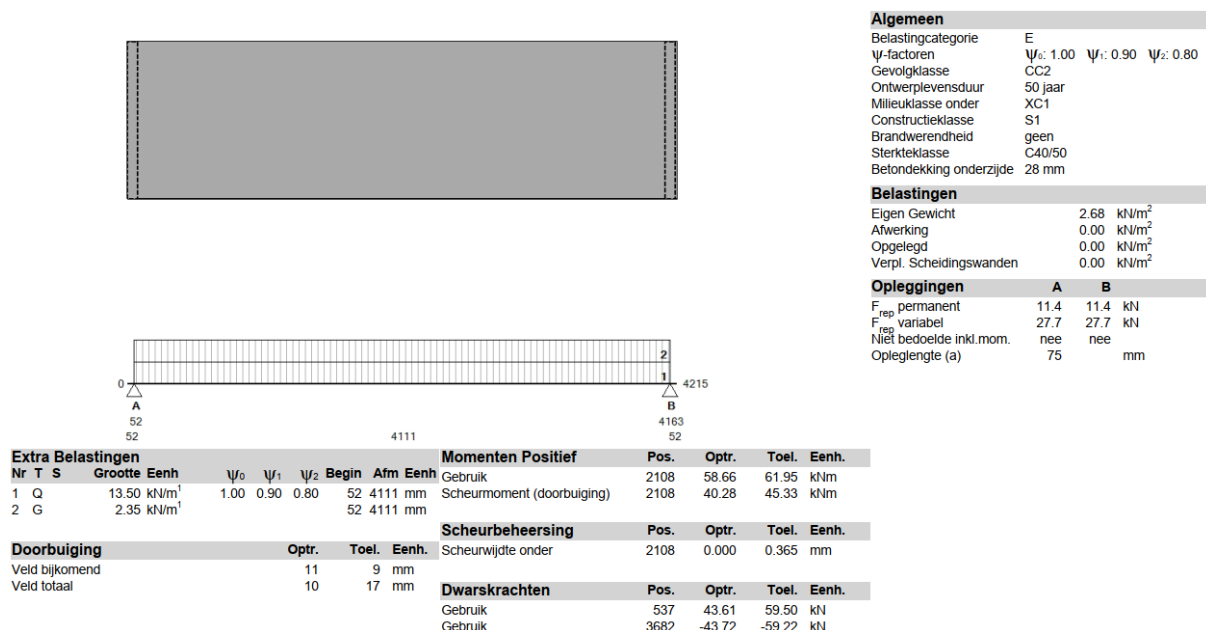


Figure G-2: Hollow core slab calculation for ULS state for Alternative D2, calculated with the VBI calculator

G.2 Results of structural calculations

The loads on the 2D model are the same as given in Appendix B.2.1 “Loads on the 2D model (y-direction)” and B.2.2 “Loads on the 2D model (x-direction)” of the base design. The only difference is the load on the mezzanine floor. For the mezzanine floor, the same calculation steps as given in Appendix B.3 are performed. This leads to the maximum dead load and maximum live load given in the following tables. These are used as input on the columns of the main load-bearing structure.

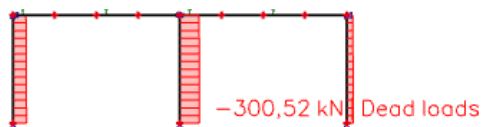


Figure G-4: Dead loads on the columns, calculated in SCIA

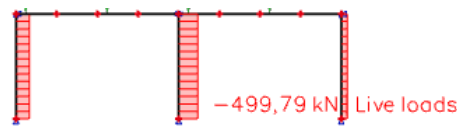


Figure G-3: Live loads on the columns, calculated in SCIA

For this alternative, the same type of structural system as Alternative A is used. The main columns are enlarged, as shown in the following table (HEB 600 instead of HEB 400). These enlarged to be able to carry the increased normal force as given in Figure G-5. The unity checks for the main column is given in the following table.

Table G-1: Governing unity checks for the members of Alternative D2

Member	Type	UC section	Max. UC section	UC stability	Max. UC stability
Main column (x)	HEB 600	0.19	0.85	0.7	0.80

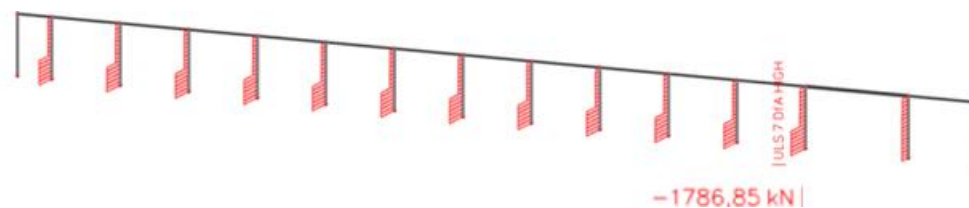


Figure G-5: Normal forces in the frame in the x-direction (for ULS 7)

G.3 Element overview

MAIN LOAD-BEARING STRUCTURE

Element	Type	Wt. [kg/m]	Length [m]	Number (y)	Number (x)	Total nr	Total [kg]
Column (main)	HEB 600	216	13,5	4	13	52	151 632
Column (main)	HEB 600	216	12,71	3	13	39	107 069
Column (façade)	HEB 360	145	13,5	26	46	72	140 940
Roof beam (y)	HEB 500-CB	191	16,86	8	27	216	695 576
Roof beam (x, small)	HEA 360-CB	145	15,81	11	12	132	302 603
Roof beam (x, small)	HEA 360-CB	145	7,905	11	1	11	12 608
Roof beam (x, large)	HEB 550-CB	203	23,715	7	1	7	33 699
Façade beam (y)	HEA 260	69,5	8,43	8	2	16	9 374
Façade beam (x)	HEA 260	69,5	7,905	2	20	40	21 976
Lateral support (x)	SHS 120/120/10	31,8	7,905	4	20	80	20 110
							<i>124 9523</i>
Horizontal bracing elements							
Diagonal	160/160/15	36,8	11,557	16	16	256	108 872
Diagonal	160/160/15	36,8	11,557	16	56	896	381 052
Façade beam (y)	HEB 400	158	8,43	8	2	16	21 311
Façade beam (x)	HEB 450	174	7,905	2	8	16	22 008
							<i>533 242</i>
Vertical bracing elements							
Column	HEB 700	245	13,5	8	8	16	52 920
Diagonal	CHS 406.4/20	191	20,79	8	8	16	48 639
							<i>101 559</i>
							<i>Total: 1 762 947</i>

H Environmental data

In the following tables, the studied EPDs are given. In these tables, the CO₂-equivalent of the One Click LCA tool is used to determine the most and least environmentally friendly option. The environmental profiles are relative to similar materials and is given in the following table. This means that an environmental profile for one material cannot directly be compared to the environmental profile of another material.

Table H-1: Environmental profile of the CO₂-equivalent per kg of material, from the One Click LCA tool






Environmental profile	Icon
Very low	
Low	
Average	
High	
Very high	

Table H-2: Characteristics of the structural steel EPDs



EPD owner	Arcelor Mittal Europe – Long products	SULB Company B.S.C. (c)
Type of material	Structural steel sections, EcoBeams	Structural steels
Recycled material	100%	0%
Production route	Electric Arc Furnace	Direct reduction of iron (DRI), electric arc furnace (EAF), ladle furnace (LF), continuous casting (CCM), and hot rolling
Environmental profile		
End of validity	March 2024	April 2023
Declared unit	1 ton	1 ton
Production site	Differdange, Belval and Rodange (Luxembourg); Hunedoara (Romania); Bergara & Olaberria (Spain)	Al Hidd (Bahrein)

Table H-3: Environmental impact of structural steel EPDs (A1-A3) and shadow price conversion

Steel impact	EPD owner	Declared unit	GWP (fossil) <i>kg CO2-eq</i>	GWP (bio) <i>kg CO2-eq</i>	GWP (total) <i>kg CO2-eq</i>	ODP <i>kg CFC11-eq</i>	AP <i>kg SO2-eq</i>	EP <i>kg PO4-eq</i>	POCP <i>kg C2H4-eq</i>	ADPe <i>kg Sb-eq</i>	APDf <i>kg Sb-eq</i>
Low	Arcelor Mittal	kg	4,84E-01	0,00E+00	4,84E-01	2,25E-12	1,57E-03	1,37E-04	1,19E-04	1,92E-07	2,63E-03
High	SULB	kg	2,67E+00	0,00E+00	2,67E+00	1,10E-07	1,03E-02	9,00E-04	6,08E-04	1,31E-06	1,69E-02
		€/kg	€ 0,05	€ 0,05	€ 0,05	€ 30,00	€ 4,00	€ 9,00	€ 2,00	€ 0,16	€ 0,16
Low	Arcelor Mittal	<u>€ 0,0324</u>	€ 0,0242	€ 0,0000	€ 0,0242	€ 0,0000	€ 0,0063	€ 0,0012	€ 0,0002	€ 0,0000	€ 0,0004
High	SULB	<u>€ 0,1867</u>	€ 0,1335	€ 0,0000	€ 0,1335	€ 0,0000	€ 0,0412	€ 0,0081	€ 0,0012	€ 0,0000	€ 0,0027

Table H-4: Characteristics of the ComFlor steel floor deck EPD


EPD owner	TATA Steel
Type of material	ComFlor 80 0.9mm steel structural floor deck
Recycled material	13%
Production route	Basic Oxygen Furnace
Environmental profile	
End of validity	December 2023
Declared unit	1 m ² of steel structural floor deck
Production site	Port Talbot, Llanwern, Shotton and Dubai

Table H-5: Environmental impact of ComFlor steel deck EPDs (A1-A3) and shadow price conversion

ComFl impact	EPD owner	Declared unit	GWP (fossil)	GWP (bio)	GWP (total)	ODP	AP	EP	POCP	ADPe	APDf
			<i>kg CO2-eq</i>	<i>kg CO2-eq</i>	<i>kg CO2-eq</i>	<i>kg CFC11-eq</i>	<i>kg SO2-eq</i>	<i>kg PO4-eq</i>	<i>kg C2H4-eq</i>	<i>kg Sb-eq</i>	<i>kg Sb-eq</i>
Middle	TATA Steel	m ²	3,11E+01	0,00E+00	3,11E+01	-1,44E-11	7,24E-02	7,60E-03	1,16E-02	2,18E-03	1,56E-01
		€/m ²	€ 0,05	€ 0,05	€ 0,05	€ 30,00	€ 4,00	€ 9,00	€ 2,00	€ 0,16	€ 0,16
Middle	TATA Steel	€ 0,9616	€ 1,5550	€ 0,0000	€ 1,5550	€ 0,0000	€ 0,2896	€ 0,0684	€ 0,0232	€ 0,0003	€ 0,0250

Table H-6: Characteristics of structural concrete (in situ) EPDs



EPD owner	FEDBETON vzw	General Beton Romania
Type of material	Typical Belgian ready-mixed concrete	Ready-mixed concrete
Recycled material	0%	0%
Production route	13% cement, 35% sand, 44% gravel, 7% water, <1% admixture	16-18% cement, 26-33% sand, 41-51% gravel, 7.1-8.6% water, <0.2% additives
Environmental profile		
End of validity	December 2024	November 2022
Declared unit	1 kg of ready-mixed concrete of strength class C30/37	1 kg of ready-mixed concrete of several strength classes, in this research strength class C30/37 is considered
Production site	Several production sites in Belgium	Several production sites in Romania

Table H-7: Environmental impact of structural concrete (in situ) EPDs (A1-A3) and shadow price conversion

In situ impact	EPD owner	Declared unit	GWP (fossil) <i>kg CO2-eq</i>	GWP (bio) <i>kg CO2-eq</i>	GWP (total) <i>kg CO2-eq</i>	ODP <i>kg CFC11-eq</i>	AP <i>kg SO2-eq</i>	EP <i>kg PO4-eq</i>	POCP <i>kg C2H4-eq</i>	ADPe <i>kg Sb-eq</i>	APDf <i>kg Sb-eq</i>
Low	FEDBETON vzw	kg	8,18E-02	0,00E+00	8,18E-02	4,90E-09	2,58E-04	3,81E-05	1,37E-05	9,11E-08	2,92E-04
High	Beton Romania	kg	1,48E-01	0,00E+00	1,48E-01	5,30E-09	3,39E-04	1,04E-04	1,30E-05	1,16E-07	3,51E-04
		€/kg	€ 0,05	€ 0,05	€ 0,05	€ 30,00	€ 4,00	€ 9,00	€ 2,00	€ 0,16	€ 0,16
Low	FEDBETON vzw	€ 0,0055	€ 0,0041	€ 0,0000	€ 0,0041	€ 0,0000	€ 0,0010	€ 0,0003	€ 0,0000	€ 0,0000	€ 0,0000
High	Beton Romania	€ 0,0098	€ 0,0074	€ 0,0000	€ 0,0074	€ 0,0000	€ 0,0014	€ 0,0009	€ 0,0000	€ 0,0000	€ 0,0001

Table H-8: Characteristics of structural concrete (in situ) EPDs



EPD owner	One Click LCA	One Click LCA
Type of material	Generic Dutch ready-mixed concrete	Generic Dutch ready-mixed concrete
Recycled material	0%	40%
Material composition	Portland cement and binders	Portland cement and binders
Environmental profile		
End of validity	2023	2023
Declared unit	1 kg of ready-mixed concrete of strength class C30/37	1 kg of ready-mixed concrete of strength class C30/37

Table H-9: Environmental impact of stages A1-A3 of generic Dutch values for virgin and recycled concrete, used to calculate the bonus for stage D

In situ impact	Explanation	Declared unit	GWP (fossil) <i>kg CO2-eq</i>	GWP (bio) <i>kg CO2-eq</i>	GWP (total) <i>kg CO2-eq</i>	ODP <i>kg CFC11-eq</i>	AP <i>kg SO2-eq</i>	EP <i>kg PO4-eq</i>	POCP <i>kg C2H4-eq</i>	ADP <i>kg Sb-eq</i>
Low	40% recycled content	kg	9,42E-02	0,00E+00	9,42E-02	3,27E-09	2,12E-04	2,78E-05	9,39E-06	2,45E-04
High	0% recycled content	kg	1,23E-01	0,00E+00	1,23E-01	3,37E-09	2,72E-04	3,58E-05	1,12E-05	3,32E-04
		€/kg	€ 0,05	€ 0,05	€ 0,05	€ 30,00	€ 4,00	€ 9,00	€ 2,00	€ 0,16
Low	40% recycled content	€ 0,0059	€ 0,0047	€ 0,0000	€ 0,0047	€ 0,0000	€ 0,0008	€ 0,0003	€ 0,0000	€ 0,0000
High	0% recycled content	€ 0,0076	€ 0,0062	€ 0,0000	€ 0,0062	€ 0,0000	€ 0,0011	€ 0,0003	€ 0,0000	€ 0,0001

Table H-10: Characteristics of concrete hollow core slab EPDs



EPD owner	VBI	Quinn precast
Type of material	Hollow core slab (thickness of 150 mm)	Quinn Hollowcore Slabs
Recycled material	0%	0%
Environmental profile		
End of validity	September 2025	March 2025
Declared unit	1 m ² of hollow core slab (including reinforcement and joint fillers)	1 m length of the 1.2 m wide Hollowcore flooring slabs for several thicknesses, in this research, a thickness of 150 mm is considered
Production site	Huissen (The Netherlands)	Derrylin Fermanagh (Northern Ireland)

Table H-11: Environmental impact of concrete hollow core slab EPDs (A1-A3) and shadow price conversion

Hollow impact	EPD owner	Declared unit	GWP (fossil)	GWP (bio)	GWP (total)	ODP	AP	EP	POCP	ADPe	APDf
			<i>kg CO2-eq</i>	<i>kg CO2-eq</i>	<i>kg CO2-eq</i>	<i>kg CFC11-eq</i>	<i>kg SO2-eq</i>	<i>kg PO4-eq</i>	<i>kg C2H4-eq</i>	<i>kg Sb-eq</i>	<i>kg Sb-eq</i>
Low	VBI	kg	1,40E-01	0,00E+00	1,40E-01	4,57E-09	2,90E-04	5,79E-05	6,10E-05	1,01E-07	4,80E-04
High	Quinn precast	kg	3,01E-01	0,00E+00	3,01E-01	1,96E-08	8,91E-04	1,17E-04	1,06E-04	5,04E-04	9,91E-04
		<i>€/kg</i>	<i>€ 0,05</i>	<i>€ 0,05</i>	<i>€ 0,05</i>	<i>€ 30,00</i>	<i>€ 4,00</i>	<i>€ 9,00</i>	<i>€ 2,00</i>	<i>€ 0,16</i>	<i>€ 0,16</i>
Low	VBI	<u>€ 0,0089</u>	€ 0,0070	€ 0,0000	€ 0,0070	€ 0,0000	€ 0,0012	€ 0,0005	€ 0,0001	€ 0,0000	€ 0,0001
High	Quinn precast	<u>€ 0,0201</u>	€ 0,0150	€ 0,0000	€ 0,0150	€ 0,0000	€ 0,0036	€ 0,0011	€ 0,0002	€ 0,0001	€ 0,0002

Table H-12: Characteristics of structural glulam EPDs

EPD owner	Schilliger Holz	Studiengemeinschaft Holzleimbau e.V.
Type of material	Glued laminated timber	Glued laminated timber
Wood species	Spruce, silver fir	Spruce, pine, larch, fir
Adhesives	0.9% PUR	0.03% PUR, 2.04% MUF, 0.1% PRF
Environmental profile		
End of validity	May 2023	August 2023
Declared unit	1 m ³	1 m ³
Production site	Küssnacht, Switzerland	Germany

Table H-13: Environmental impact of structural glulam EPDs (A1-A3) and shadow price conversion

Glulam impact	EPD owner	Declared unit	GWP (fossil)	GWP (bio)	GWP (total)	ODP	AP	EP	POCP	ADPe	APDf
			<i>kg CO2-eq</i>	<i>kg CO2-eq</i>	<i>kg CO2-eq</i>	<i>kg CFC11-eq</i>	<i>kg SO2-eq</i>	<i>kg PO4-eq</i>	<i>kg C2H4-eq</i>	<i>kg Sb-eq</i>	<i>kg Sb-eq</i>
Low	Schilliger Holz	kg	1,72E-01	-1,62E+00	-1,45E+00	1,24E-08	9,29E-04	2,11E-04	2,90E-04	5,19E-08	1,25E-03
High	Studiengemeinschaft	kg	3,29E-01	-1,61E+00	-1,28E+00	1,85E-09	1,49E-03	3,52E-04	2,58E-04	1,50E-06	2,04E-03
		€/kg	€ 0,05	€ 0,05	€ 0,05	€ 30,00	€ 4,00	€ 9,00	€ 2,00	€ 0,16	€ 0,16
Low	Schilliger Holz	€ 0,0150	€ 0,0086	-€ 0,0811	€ 0,0086	€ 0,0000	€ 0,0037	€ 0,0019	€ 0,0006	€ 0,0000	€ 0,0002
High	Studiengemeinschaft	€ 0,0264	€ 0,0165	-€ 0,0805	€ 0,0165	€ 0,0000	€ 0,0060	€ 0,0032	€ 0,0005	€ 0,0000	€ 0,0003

Table H-14: Bonus of structural glued laminated timber EPDs (stage D) and shadow price conversion

Glulam bonus	EPD owner	Declared unit	GWP (fossil)	GWP (bio)	GWP (total)	ODP	AP	EP	POCP	ADPe	APDf
			<i>kg CO2-eq</i>	<i>kg CO2-eq</i>	<i>kg CO2-eq</i>	<i>kg CFC11-eq</i>	<i>kg SO2-eq</i>	<i>kg PO4-eq</i>	<i>kg C2H4-eq</i>	<i>kg Sb-eq</i>	<i>kg Sb-eq</i>
Largest	Studiengemeinschaft	kg	0,00E+00	0,00E+00	-8,65E-01	-1,93E-12	-8,96E-04	-1,34E-04	-9,13E-05	-2,63E-07	-5,53E-03
Smallest	Schilliger Holz	kg	0,00E+00	0,00E+00	-4,62E-01	-9,36E-08	-4,53E-04	7,38E-06	-3,02E-05	-2,45E-08	-3,57E-03
		€/kg	€ 0,05	€ 0,05	€ 0,05	€ 30,00	€ 4,00	€ 9,00	€ 2,00	€ 0,16	€ 0,16
Largest	Studiengemeinschaft	-€0,0059	€ 0,0000	€ 0,0000	-€ 0,0432	€ 0,0000	-€ 0,0036	-€ 0,0012	-€ 0,0002	€ 0,0000	-€ 0,0009
Smallest	Schilliger Holz	-€0,0024	€ 0,0000	€ 0,0000	-€ 0,0231	€ 0,0000	-€ 0,0018	€ 0,0001	-€ 0,0001	€ 0,0000	-€ 0,0006

Table H-15: Characteristics of structural CLT EPDs



EPD owner	Stora Enso	KLH Massivholz
Type of material	Cross laminated timber	Cross laminated timber
Wood species	Spruce, pine	Spruce, pine, fir, arolla pine
Adhesives	1% Mix of Polyurethane (PUR) and Emulsion polymer isocyanate (EPI)	0.66% Polyurethane (PUR), 0.01% polyvinyl acetate (PVAC)
Environmental profile		
End of validity	May 2022	May 2024
Declared unit	1 m ³	1 m ³
Production site	Ybbs an der Donau and Bad St. Leonhard (Austria)	Teufenbach-Katsch (Austria)

Table H-16: Environmental impact of structural CLT EPDs (A1-A3) and shadow price conversion

CLT impact	EPD owner	Declared unit	GWP (fossil)	GWP (bio)	GWP (total)	ODP	AP	EP	POCP	ADPe	APDf
			<i>kg CO2-eq</i>	<i>kg CO2-eq</i>	<i>kg CO2-eq</i>	<i>kg CFC11-eq</i>	<i>kg SO2-eq</i>	<i>kg PO4-eq</i>	<i>kg C2H4-eq</i>	<i>kg Sb-eq</i>	<i>kg Sb-eq</i>
Low	Stora Enso	kg	1,28E-01	-1,56E+00	-1,43E+00	1,73E-08	5,11E-04	7,38E-04	1,45E-05	7,87E-08	9,81E-04
High	KLH Massivholz	kg	3,94E-01	-1,65E+00	-1,25E+00	4,02E-08	2,04E-03	6,88E-04	3,13E-04	1,29E-06	2,50E-03
		<i>€/kg</i>	<i>€ 0,05</i>	<i>€ 0,05</i>	<i>€ 0,05</i>	<i>€ 30,00</i>	<i>€ 4,00</i>	<i>€ 9,00</i>	<i>€ 2,00</i>	<i>€ 0,16</i>	<i>€ 0,16</i>
Low	Stora Enso	<u>€ 0,0153</u>	€ 0,0064	-€ 0,0778	-€ 0,0714	€ 0,0000	€ 0,0020	€ 0,0066	€ 0,0000	€ 0,0000	€ 0,0002
High	KLH Massivholz	<u>€ 0,0351</u>	€ 0,0197	-€ 0,0823	-€ 0,0626	€ 0,0000	€ 0,0082	€ 0,0062	€ 0,0006	€ 0,0000	€ 0,0004

Table H-17: Bonus of structural cross laminated timber EPDs (stage D) and shadow price conversion

CLT bonus	EPD owner	Declared unit	GWP (fossil)	GWP (bio)	GWP (total)	ODP	AP	EP	POCP	ADPe	APDf
			<i>kg CO2-eq</i>	<i>kg CO2-eq</i>	<i>kg CO2-eq</i>	<i>kg CFC11-eq</i>	<i>kg SO2-eq</i>	<i>kg PO4-eq</i>	<i>kg C2H4-eq</i>	<i>kg Sb-eq</i>	<i>kg Sb-eq</i>
Largest	Stora Enso	kg	0,00E+00	0,00E+00	-1,68E+00	-1,60E-08	-4,83E-04	-7,21E-04	-1,41E-05	-7,81E-08	-8,95E-04
Smallest	KLH Massivholz	kg	0,00E+00	0,00E+00	-4,24E-01	-7,85E-08	-7,92E-04	-4,38E-04	-1,25E-04	-2,92E-07	-3,18E-03
		<i>€/kg</i>	<i>€ 0,05</i>	<i>€ 0,05</i>	<i>€ 0,05</i>	<i>€ 30,00</i>	<i>€ 4,00</i>	<i>€ 9,00</i>	<i>€ 2,00</i>	<i>€ 0,16</i>	<i>€ 0,16</i>
Largest	Stora Enso	<u>-€0,0086</u>	€ 0,0000	€ 0,0000	-€ 0,0838	€ 0,0000	-€ 0,0019	-€ 0,0065	€ 0,0000	€ 0,0000	-€ 0,0001
Smallest	KLH Massivholz	<u>-€0,0079</u>	€ 0,0000	€ 0,0000	-€ 0,0212	€ 0,0000	-€ 0,0032	-€ 0,0039	-€ 0,0003	€ 0,0000	-€ 0,0005

I Environmental impact calculation

I.1 Comparison between end of life methods

Methods have been set up that include the end of life processes more in depth. In the research of Allacker et al. (2014), some of these methods (PAS2050:2011, BPX30-323, ISO/TS 14067, Product Environmental Footprint (PEF), and REAPRo) have been investigated, by comparing them on the following eight criteria:

1. **Comprehensiveness**
A method is comprehensive if it includes all relevant aspects of the life cycle of a product. These aspects are divided in input and output. According to Allacker et al. (2014), the input should include the production of virgin material and the amount of recycled material. The output should include recycling, energy recovery, and disposal.
2. **Accommodating open-loop and closed-loop product system**
Closed-loop recycling means that a product can be recycled back into itself or into a similar product without degradation or waste. Open-loop recycling means that it can be recycled into other types of products and is often described as a downcycling process (Wastiels, 2015). An end of life method should include both recycling options.
3. **Distinguishing % virgin and % recycled content inputs**
The method should give insight in the fraction of virgin and recycled materials in a product.
4. **Considering recyclability and energy recovery rates**
An end of life method should give insight in the fraction of the material in a product that will be recycled or used for energy recovery.
5. **Including material and energy credits**
The method should include substitution effects associated with recycling and/or energy recovery process. This means that credits can be earned in case a material is recycled, because it avoids primary production of virgin materials. The same holds for energy recovery, where credits can be earned from avoided energy production.
6. **Account for changes in inherent properties of materials and/or down-cycling**
Recycled materials are often different compared to the virgin material, for example the conditions of final disposal have changed. These changes need to be considered in the end of life method to provide correct insight in the recycled material.
7. **Physical correctness of flows at product versus overall system**
One can look at products on different levels. On a product level, the life cycle of a specific product is considered. In case a product is recycled at the start and the end of the life cycle, two recycling processes need to be considered. On a system level, multiple products are considered which are related through end of life processes. This means that the product that has been recycled at the start was also considered at the end of life of a previous product. From a system perspective, this means that the recycling has been counted twice, whereas it should only be counted once. A solution to this problem is considering the recycled content at the start only (the 100:0 allocation approach), at the end of life only (the 0:100 allocation approach), or by distributing the recycled content over the previous and following product (the 50:50 allocation approach).
8. **Enabling consistency for a wide range of application**
The method should be consistent and should be applicable to different type of products. The results from the method must be reproducible and comparable.

In the following table, the ten methods to include the end of life processes in depth are weight against the eight criteria. From this table, it is concluded that the PEF methodology is the only approach that includes all eight criteria.

Table I-1: Evaluation of ten equations against eight analysis criteria (Allacker et al., 2014)

Criteria	PAS-2050 recycled content	PAS-2050 and ISO/TS 14067 closed-loop approximation	ISO/TS 14067 open-loop	BPX 30-323-0 closed-loop	BPX 30-323-0 open-loop with market disequilibrium	BPX 30-323-0 open-loop with no market disequilibrium (50/50)	PEF	REAPro recyclability	REAPro energy recoverability	REAPro recycled content
1. Comprehensiveness (includes all blocks)	No	No	No	No	No	Yes	Yes	No	No	No
2a. Accommodates open-loop product system	Yes	No	Yes	No	Yes	Yes	Yes	Yes	NA	NA
2b. Accommodates closed-loop product system	No	Yes	No	Yes	No	Yes (although intended for open-loop)	Yes	Yes	NA	NA
3. Distinguishes % virgin/recycled content inputs	Yes	No	Yes	Yes	No	Yes	Yes	NA	NA	Yes
4a. Considers recyclability rate	No	Yes	Yes	No	Yes	Yes	Yes	Yes	NA	NA
4b. Considers energy recovery	No	No	No	Yes	Yes	Yes	Yes	NA	Yes	NA
5a. Includes material credits	No	Yes	Yes	Yes	Yes	Yes	Yes	Yes	NA	NA
5b. Includes energy credits	No	No	No	Yes	Yes	Yes	Yes	NA	Yes	NA
6. Account for changes in inherent properties of materials and/or down-cycling	No	NA	Yes	NA	No	No	Yes	Yes	NA	NA
7. Avoids double counting at a system level	Yes	Yes	Yes	Yes	Yes	Yes	Yes	Yes	Yes	Yes
8. One formula-fits-all	No	No	No	No	No	No	Yes	No	No	No

Based upon the PEF method, the rules to set up EPDs are updated in 2019 (EN 15804:2012+A2:2019). These updated rules include specific end of life formulas for stages C and D. This method is also checked for the eight criteria of Allacker et al. (2014). The results are found in the following table. From this table, it becomes clear that the EN 15804:2012+A2:2019 is just as complete as the PEF methodology.

Table I-2: Evaluation of the end of life equations of EN 15804:2012+A2:2019 against eight analysis criteria

Criteria	EN 15804 (2019)
1. Comprehensiveness	Yes, but in module A
2a. Accommodates open-loop product system	Yes
2b. Accommodates closed-loop product system	Yes
3. Distinguishes % virgin/recycled content inputs	No, but in module A
4a. Considers recyclability rate	Yes
4b. Considers energy recovery	Yes
5a. Includes material credits	Yes
5b. Includes energy credits	Yes
6. Account for changes in inherent properties of materials and/or downcycling	Yes
7. Avoids double counting at a system level	Yes (cut-off approach)
8. One formula-fits-all	Yes

The main difference between the PEF method and the method of EN 15804:2012+A2:2019 is the allocation of the environmental impact between different product stages. The PEF uses a 50/50 allocation method and the method of EN 15804:2012+A2:2019 uses a cut-off allocation method (Nicholson, Olivetti, Gregory, Field, & Kirchain, 2009). The advantage of these allocation methods is that they can be applied for all type of materials. In the 50/50 allocation method, virgin and waste material are assigned equally to the first and final product. In the PEF formula, this is implemented by dividing the amount of recycled material by 2, meaning that only the previous and current, or current and next lifecycle are considered. In the cut-off method, burdens that are caused by a product are assigned to that product directly. If a product is produced with virgin material only, the burdens are for this production process are for the first uses. If the product is recycled at the end of life, the burdens of the recycling process are allocated to the second user in the chain. To encourage users towards a sustainable market, EN 15804 includes the calculation of stage D, where the potential of the end of life stage is calculated (Seyed Shahabaldin, 2020).

I.1.1 Product Environmental Footprint (PEF) methodology

The PEF has been established by the Institute for Environment and Sustainability of the Directorate General 'Joint Research Centre' of the European Commission. The PEF has been developed as a common approach to quantitatively assess the environmental impact of products throughout their lifecycle (Allacker, Mathieux, Pennington, & Pant, 2017). The PEF evaluates the environmental performance of a good or a service throughout its life by considering the extraction of raw material, production, use, and waste management. It models end of life processes such as reuse, recycling, energy recovery, and disposal. (Manfredi, Allacker, Chomkhamstri, Pelletier, & de Souza, 2012) The PEF equation is as follows:

$$\underbrace{\left(1 - \frac{R_1}{2}\right) E_v}_{A} + \underbrace{\frac{R_1}{2} \cdot E_{recycled}}_B + \underbrace{\frac{R_2}{2} (E_{recycling, EoL} - E_v^* \cdot K)}_C + \underbrace{R_3 \left(E_{ER} - LHV \left(\frac{X_{ER,heat} \cdot E_{SR,heat} +}{X_{ER,elec} \cdot E_{JE,elec}} \right) \right)}_D + \underbrace{\left(1 - \frac{R_2}{2}\right) E_D - \frac{R_1}{2} \cdot E_D^*}_E$$

Figure I-1: PEF equation, where A and B are input and C, D, and E are output (Backx, 2020)

The PEF equation is divided into five thematic blocks (Allacker et al., 2014):

- Block A – Input: Production of virgin material

$$\left(1 - \frac{R_1}{2}\right) * E_v \quad \text{eq. I-1}$$

The division by 2 means that a 50/50 allocation approach is assumed. This distributes the recycled content over the previous and following product. This allocation approach is explained under criteria 7 of Allacker et al. (2014).

Table I-3: Parameters in PEF equation block A

Parameter	Unit	Definition
R_1	-	Recycled content of material, the fraction of material input that has been recycled in a previous system $0 \leq R_1 \leq 1$
E_v	EIC or shadow price	Environmental impact of the acquisition and pre-processing of virgin material

- Block B – Input: Recycled content

$$\frac{R_1}{2} * E_{recycled} \quad \text{eq. I-2}$$

The division by 2 means that a 50/50 allocation approach is assumed.

Table I-4: Parameters in PEF equation block B

Parameter	Unit	Definition
R_1	-	Recycled content of material, the fraction of material input that has been recycled in a previous system $0 \leq R_1 \leq 1$
$E_{recycled}$	EIC or shadow price	Environmental impact for the production process of the recycled material (including collection, sorting, and transportation)

- Block C – Output: Recycling at EoL minus credits from avoided primary production

$$\frac{R_2}{2} * (E_{recycling,EoL} - E_v^* * K) \quad \text{eq. I-3}$$

Table I-5: Parameters in PEF equation block C

Parameter	Unit	Definition
R_2	-	Recyclability rate, the fraction of material that will be recycled in a following system $0 \leq R_2 \leq 1$
$E_{recycling,EoL}$	EIC or shadow price	Environmental impact due to the recycling process at the end of life (including collection, sorting, transportation, and recycled material production processes)
E_v^*	EIC or shadow price	Environmental impact for the acquisition and pre-processing of virgin material assumed to be substituted by recyclable materials If only closed-loop recycling takes place: $E_v^* = E_v$ If only open-loop recycling takes place: $E_v^* = E'_v$
E_v	EIC or shadow price	Environmental impact of the acquisition and pre-processing of virgin material
E'_v	EIC or shadow price	Environmental impact of the acquisition and pre-processing of virgin material substituted through open-loop recycling
K	-	Ratio for differences in quality between the primary and secondary material after recycling $K = \frac{\text{quality secondary material}}{\text{quality primary material}}$

- Block D – Output: Energy recovery

$$R_3 * (E_{ER} - LHV(X_{ER,heat} * E_{SE,heat} + X_{ER,elec} * E_{SE,elec})) \quad \text{eq. I-4}$$

Table I-6: Parameters in PEF equation block D

Parameter	Unit	Definition
R_3	-	Fraction of the material that is used for energy recovery (e.g. incineration with energy recovery) $0 \leq R_3 \leq 1$
E_{ER}	EIC or shadow price	Environmental impact due to the energy recovery process
LHV	e.g. J/kg	Lower Heating Value of the material that is used for energy recovery
$X_{ER,heat}$	-	Efficiency of the energy recovery process for heat as substituted energy source $0 \leq X_{ER,heat} \leq 1$
$E_{SE,heat}$	EIC or shadow price	Avoided environmental impact for heat as substituted energy source
$X_{ER,elec}$	-	Efficiency of the energy recovery process for electricity as substituted energy source $0 \leq X_{ER,elec} \leq 1$
$E_{SE,elec}$	EIC or shadow price	Avoided environmental impact for electricity as substituted energy source

- Block E – Output: Disposal

$$\left(1 - \frac{R_2}{2}\right) * E_D - \frac{R_1}{2} * E_D^* \quad \text{eq. I-5}$$

The division by 2 means that a 50/50 allocation approach is assumed.

Table I-7: Parameters in PEF equation block E

Parameter	Unit	Definition
R_2	-	Recyclability rate, the fraction of material that will be recycled in a following system $0 \leq R_2 \leq 1$
E_D	EIC or shadow price	Environmental impact due to the disposal of waste material (e.g. landfilling or incineration)
R_1	-	Recycled content of material, the fraction of material input that has been recycled in a previous system $0 \leq R_1 \leq 1$
E_D^*	EIC or shadow price	Environmental impact for the disposal of waste material at the EoL of the material from which the recycled content is derived

I.1.2 End of life formulas in EN 15804:2012+A2:2019

Based upon the PEF method, the rules to set up EPDs were updated in 2019 (EN 15804:2012+A2:2019). These new rules include specific end of life formulas for stages C and D. This method has also been checked for the eight criteria of Allacker et al. (2014). The results are given in Table I-2 in Appendix I.1. It can be concluded that this method also includes the criteria and is therefore seen an applicable method.

From July 2022 on, the EPDs must be based upon the updated rules of EN 15804:2012+A2:2019 (Bionova Ltd., 2019). However, at this moment, most EPDs are based upon EN 15804:2012. This ensures that the values for module D cannot be copied from the EPDs directly. Therefore, it is necessary to use the end of life formulas with own data. The formula to calculate module D is as follows:

$$e_{\text{module D}} = e_{\text{module D1}} + e_{\text{module D2}} + e_{\text{module D3}} + e_{\text{module D4}} \quad \text{eq. I-6}$$

- Module D1 – Loads and benefits related to the export of secondary materials

$$e_{\text{module D1}} = \sum_i (M_{MR \text{ out } |i} - M_{MR \text{ in } |i}) * \left(E_{MR \text{ after EoW out } |i} - E_{VMSub \text{ out } |i} \cdot \frac{Q_{R \text{ out } |i}}{Q_{Sub \text{ in } |i}} \right) \quad \text{eq. I-7}$$

Module D1 is based upon Block C of the PEF formula. Some changes are incorporated. As can be seen, no division by 2 is performed, as opposed to the PEF. This shows that a cut-off allocation method has been applied. Furthermore, instead of only considering R_2 (in PEF)/ $M_{MR \text{ out}}$ (in EN 15804:2012+A2:2019), the EN 15804:2012+A2:2019 calculation subtracts the fraction of input material that has been recovered from a previous system. To do this correctly, the factor “ $M_{MR \text{ out } |i} - M_{MR \text{ in } |i}$ ” cannot be less than zero.

Table I-8: Parameters in module D1 in the end of life formula in EN 15804:2012+A2:2019

Parameter	Unit	Definition
i	kg	Any output flow leaving the system boundary
$M_{MR\ out}$	-	Fraction of material exiting the system that will be recovered (recycled) in a subsequent system. $0 \leq M_{MR\ out} \leq 1$
$M_{MR\ in}$	-	Fraction of input material to the product system that has been recovered (recycled) from a previous system. $0 \leq M_{MR\ in} \leq 1$
$E_{MR\ after\ EoW\ out}$	EIC or shadow price	Environmental impact of the recycling process of the recycled material
$E_{VMSub\ out}$	EIC or shadow price	Environmental impact of the acquisition and pre-processing of virgin material (assumed to be substituted by recyclable materials)
$\frac{Q_{R\ out}}{Q_{Sub}}$		Quality ratio between outgoing recovered material (recycled) and the substituted material.
$Q_{R\ out}$		Quality of the outgoing recovered material (recycled), i.e. quality of the recycled material at the point of substitution.
Q_{Sub}		Quality of the substituted material, i.e. quality of primary material or quality of the average input material if primary material is not used.

- Module D2 – Loads and benefits related to the export of secondary fuels

$$e_{\text{module D2}} = \sum_i (M_{ER\ out\ |i} - M_{ER\ in\ |i}) \cdot (E_{ER\ after\ EoW\ out\ |i} - E_{ER\ average}) \quad \text{eq. I-8}$$

This considers the amount of material that is used for energy recovery. Energy recovery is only related to timber elements. From the timber elements, EPDs are available that contain this specific data. It is therefore decided not to consider this part of the formula.

- Module D3 – Loads and benefits related to the export of energy as a result of waste incineration

$$e_{\text{module D3}} = -M_{INC\ out} \cdot (LHV \cdot X_{INC\ heat} \cdot E_{SE\ heat} + LHV \cdot X_{INC\ elec} \cdot E_{SE\ elec}) \quad \text{eq. I-9}$$

This part of the formula considers the amount of material that is used for incineration. This is only related to timber elements. From the timber elements, EPDs are available that contain this specific data. It is therefore decided not to consider this part of the formula.

- Module D4 – Load and benefits related to the export of energy as a result of landfilling with energy recovery

$$e_{\text{module D4}} = -M_{LF} \cdot (LHV \cdot X_{LF\ heat} \cdot E_{SE\ heat} + LHV \cdot X_{LF\ elec} \cdot E_{SE\ elec}) \quad \text{eq. I-10}$$

This part of the formula considers the amount of material that is used for landfilling with energy recovery. As can be seen from the formula, a negative value will be calculated, because the calculation considers that the energy recovery substitutes another energy source. This can be done with biodegradable waste such as timber. From the timber elements, EPDs are available that contain this specific data. It is therefore decided not to consider this part of the formula.

I.1.3 General end of life scenarios

General end of life scenarios provide insight in what percentage of the materials will be reused, recycled, incinerated, or landfilled at the end of a materials service life. These percentages are given in Table I-9.

Table I-9: General end of life scenarios for different materials

Here, the percentage is the chance that a specific end of life scenario occurs.

EoL scenario	Steel	ComFlor steel	Concrete	Glulam and CLT
Reuse	11%	0%	0%	0%
Recycling	88%	85%	71%	0%
Incineration	0%	0%	0%	95%
Landfilling	1%	15%	29%	5%
Source	(Van Herwijnen, 2013) and from various EPDs	From specific EPD	(Van Herwijnen, 2013)	NIBE App WNL 0017 – wood, contaminated (i.e. painted, preserved)

After a material is reused, recycling, incineration, and landfilling is still a possible scenario. Therefore, also the end of life scenarios after reuse has taken place are considered. This is shown in the following table for the general situation.

Table I-10: End of life scenarios for different materials after reuse has taken place

EoL scenario	Steel	ComFlor steel	Concrete	Glulam and CLT
Reuse	0%	0%	0%	0%
Recycling	99%	Same as in Table I-9	Same as in Table I-9	Same as in Table I-9
Incineration	0%	Same as in Table I-9	Same as in Table I-9	Same as in Table I-9
Landfilling	1%	Same as in Table I-9	Same as in Table I-9	Same as in Table I-9

I.1.4 End of life scenarios with higher chance of reuse (with Disassembly Index)

In case it is expected that the building materials will be reused at the end of life, additional measures can be taken to increase the chance of reuse. This is calculated with the Disassembly Index.

In Table I-9, standard distributions for end of life scenarios are given. However, to be able to make a comparison between the base design and a demountable design, the standard values from Table I-9 do not apply anymore. For Alternative C, where Design for Deconstruction is included, it is expected that by following the Design for Deconstruction approach, the chance of reuse increases. For the base design, it is also valuable what the potential chance of reuse is. So, to estimate how much this chance increases, the Disassembly Index (DI) is applied.

The DI shows the ability of an element type to be disassembled from the rest of the structure. This factor is based upon the factors explained in chapter 4.1 “Design for Deconstruction (DfD)” and the technical disassembly factors of Durmisevic (2006). These disassembly factors comply to the different levels in a building, so they are not specifically set up for the load bearing structure. Therefore, it is decided to only use the technical disassembly factors that fit to the load bearing structure. The DI is given in eq. I-11 and the technical disassembly factors used are found in Table I-11.

$$DI = \frac{\text{score } FS_i + \text{score } MoF_i + \text{score } ToC_i + \text{score } AoC_i}{4} \quad \text{eq. I-11}$$

Table I-11: Technical disassembly factors used in the Disassembly Index (Durmisevic, 2006)
 This is used to measure the circularity level of the load bearing structure of a building

Abbr.	General aspect	Specific aspect	Score
FS	Functional separation	Separation of functions (layering of building components, as explained in 4.1 “Design for Deconstruction (DfD)”) 1.0	
		Integration of function with same lifecycle into one element 0.6	
		Integration of function with different lifecycle into one element 0.1	
MoF	Method of fabrication ³	Pre-made geometry (prefabricated elements such as a steel element, hollow core slab with standard width) 1.0	
		Half standardised geometry 0.5	
		Geometry specifically made for the project (elements made on site, hollow core slabs with specific widths) 0.1	
ToC	Type of connections ⁴	Accessory external connection or connection system (dry connection, click connection, magnetic connection) 1.0	
		Direct connection with additional fixing devices (bolt and nut connection, tongue and groove connection, screw connection) 0.8	
		Direct integral connection with inserts (pin or nail connection) 0.6	
		Accessory internal connection ⁵ 0.4	
		Filled soft chemical connection 0.2	
		Filled hard chemical connection (glued, poured, welded, cement-based, or chemically anchored connection) 0.1	
AoC	Accessibility of connections	Accessible 1.0	
		Accessible with additional operation with causes no damage 0.8	
		Accessible with additional operation which is repairable damage 0.6	
		Accessible with additional operation which causes damage 0.4	
		Not accessible – total damage of elements 0.1	

³ In Durmisevic (2006), this is called ‘Standardisation of product edge’

⁴ From (Durmisevic, 2006), the explanations behind the specific aspects are from Van Vliet (2018)

⁵ Accessory connections require additional parts to form a connection. Internal accessories are inserted into the elements, which means that removing this connection from the element can become difficult (Durmisevic, 2006). An example is an extending end plate to a steel beam.

In the following tables, the DI for Alternative C and the base design are given. It can also be stated that the steel elements of the main load-bearing structure of Alternative A have the same score as for Alternative C.

Table I-12: Technical disassembly factor scores for Alternative C, these values are used as the chance of reuse

General aspect	Steel elements	Hollow core (standard size)	Hollow core (non-standard size)	Concrete top floor
Functional separation	1.0	1.0	1.0	1.0
Method of fabrication	1.0	1.0	0.1	0.1
Type of connections	0.8	1.0 ⁶	1.0 ⁶	0.4 ⁷
Accessibility of connections	1.0	1.0 ⁶	1.0 ⁶	0.4 ⁸
Total	0.8		0.87	0.016

Table I-13: Technical disassembly factor scores for the Base design, these values are used as the chance of reuse

General aspect	Steel elements (main)	Steel elements (floor)	ComFlor floor (steel)	ComFlor floor (concrete)
Functional separation	1.0	1.0	1.0	1.0
Method of fabrication	1.0	1.0	1.0	0.1
Type of connections	0.4	0.8	0.85 ⁹	0.1
Accessibility of connections	1.0	1.0	1.0 ⁶	0.1
Total	0.4	0.8	0.85	0.001

To calculate the end of life scenarios after reuse has been taken place, the following table is used.

Table I-14: End of life scenarios for different materials after reuse has taken place

EoL scenario	Steel	ComFlor steel	Concrete
Reuse	0%	Same as in Table I-9	0%
Recycling	99% from 100%–DI%	Same as in Table I-9	71% from 100%–DI%
Incineration	0% from 100%–DI%	Same as in Table I-9	0% from 100%–DI%
Landfilling	1% from 100%–DI%	Same as in Table I-9	29% from 100%–DI%

⁶ The connection between the floor and the steel beams is not designed. To make sure this does not influence the calculation results, a value of 1.0 is therefore chosen.

⁷ This value is chosen as the top floor is raised and fixed at certain locations.

⁸ The top floor is raised, ensuring that it becomes easier to remove the top floor.

⁹ The concrete is connected to the steel. According to the explanation given in Table I-11, a score of 0.1 should be given to this aspect. However, from the ComFlor EPD, a recycling percentage of 85% is found. As this is specific manufacturing data, this higher score is considered.

I.2 Procedure and example calculation of the environmental impact

In the following tables, the environmental impact calculation procedure is given. The title of each table explains which steps are followed. On the left side of each table, the parameters and equations are explained and on the right side of each table, an example calculation is performed. The example calculation is performed for the Base design as explained in chapter 6.1 “Base design: Sway structure (steel and concrete)”.

Table I-15: Input for environmental impact calculation of stages A1-A3

Input (Stages A1-A3)	Example calculation for the Base design
Type of element ‘i’ Mass = Mass per element type (from Table 6-2) <i>shadow price</i> _{A1-A3} = Shadow price per element type based upon EPD data for stages A1-A3 (from Appendix H “Environmental data”)	i = steel main load-bearing structure; steel mezzanine floor; ComFlor steel; ComFlor concrete <ul style="list-style-type: none"> • Steel main load-bearing structure: 1,777,206 kg • Steel mezzanine floor: 1,029,267 kg • ComFlor steel: 12,706 m² • ComFlor in situ concrete: 3,697,272 kg • Steel main load-bearing structure (low environmental impact): € 0,0324/kg material • Steel main load-bearing structure (high environmental impact): € 0,1867/kg material • ComFlor steel (average environmental impact): € 0,9616/m² material¹⁰ • ComFlor in situ concrete (low environmental impact): € 0,0055/kg material • ComFlor in situ concrete (high environmental impact): € 0,0098/kg material
RSL = Reference service life, which is altered from 10 up to 100 years, with steps of 10 years in between. TSL = Technical service life per element type (from Table 7-3):	RSL = 10; 20; 30; 40; 50; 60; 70; 80; 90; 100 <ul style="list-style-type: none"> • Steel main load-bearing structure: 100 years • Steel mezzanine floor: 100 years • ComFlor steel: 100 years • ComFlor in situ concrete: 100 years • Steel main load-bearing structure: 0.11 • Steel mezzanine floor: 0.11 • ComFlor steel: 0.0 • ComFlor in situ concrete: 0.0
<i>M</i> _{reu out} = Fraction of material that will be reused at the end of life (from Table I-9)	

¹⁰ Only one EPD was available for this element type

Table I-16: Processing the data for environmental impact calculation of stages A1-A3

Process (Stages A1-A3)	Example calculation for the Base design				
$total\ EI_{A1-A3} _i = \sum_i mass_i * shadow\ price_{A1-A3} _i$	Main load-bearing structure:				
	<ul style="list-style-type: none"> • Steel main load-bearing structure (low environmental impact): €57,532 • Steel main load-bearing structure (high environmental impact): € 57,532 				
	Total mezzanine floor:				
	<ul style="list-style-type: none"> • Steel mezzanine floor (low environmental impact): € 33,319 • Steel mezzanine floor (high environmental impact): € 192,186 • ComFlor steel (average environmental impact): € 24,922 • ComFlor in situ concrete (low environmental impact): € 20,478 • ComFlor in situ concrete (high environmental impact): € 36,204 				
		Main load-bearing structure		Total mezzanine floor	
	RSL	Low impact	High impact	Low impact	High impact
	10 years	€ 4.939	€ 28.490	€ 7.542	€ 23.429
	20 years	€ 2.500	€ 14.419	€ 3.789	€ 11.820
	30 years	€ 1.687	€ 9.729	€ 2.538	€ 7.950
	40 years	€ 1.280	€ 7.383	€ 1.913	€ 6.016
	50 years	€ 1.036	€ 5.976	€ 1.538	€ 4.855
	60 years	€ 873	€ 5.038	€ 1.288	€ 4.081
	70 years	€ 757	€ 4.368	€ 1.109	€ 3.528
	80 years	€ 670	€ 3.866	€ 975	€ 3.114
	90 years	€ 602	€ 3.475	€ 871	€ 2.791
	100 years	€ 548	€ 3.162	€ 787	€ 2.533

$$\frac{EI_{A1-A3}}{RSL} = \sum_i M_{reu\ out|_i} * \frac{total\ EI_{A1-A3}|_i}{TSL_i} + (1 - M_{reu\ out|_i}) * \frac{total\ EI_{A1-A3}|_i}{RSL}$$

Table I-17: Input for the environmental impact calculation of stage D for concrete and steel elements

Input (Stage D)	Example calculation for the Base design
Mass	Same as for A1-A3
RSL	Same as for A1-A3
<p>$M_{MR\ in}$ = Fraction of recycled material. This is based upon the specific EPD. In Appendix H “Environmental data”, the recycled content of each material is given. From these tables, it is found that only steel from Arcelor Mittal is made from 100% recycled material. The other materials are made from 100% virgin material.</p>	<ul style="list-style-type: none"> • Steel main load-bearing structure (low environmental impact): 1.0 • Steel main load-bearing structure (high environmental impact): 0.0 • Steel mezzanine floor (low environmental impact): 1.0 • Steel mezzanine floor (high environmental impact): 0.0 • ComFlor steel (average environmental impact): 0.0 • ComFlor in situ concrete (low environmental impact): 0.0 • ComFlor in situ concrete (high environmental impact): 0.0
<p>$M_{MR\ out}$ = Fraction of material to be recycled after reuse has taken place (from Table I-10 and Table I-14)</p>	<ul style="list-style-type: none"> • Steel main load-bearing structure: 0.99 • Steel mezzanine floor: 0.99 • ComFlor steel: 0.85 • ComFlor in situ concrete: 0.71
<p>$E_{MR\ after\ EoW\ out}$ = Environmental impact of recycled material. For steel, this is found in EPD data (from Appendix H “Environmental data” under low impact). For concrete, these values are not found in the EPDs. Therefore, generic Dutch values are used instead (in Table H-9).</p>	<ul style="list-style-type: none"> • Steel main load-bearing structure: € 0,0324 • Steel mezzanine floor: € 0,0324 • ComFlor steel: € 0,0324 • ComFlor in situ concrete: € 0,0059 • Steel main load-bearing structure: € 0,1867 • Steel mezzanine floor: € 0,1867 • ComFlor steel: € 0,1867 • ComFlor in situ concrete: € 0,0076
<p>$E_{VM\ Sub\ out}$ = Environmental impact of the acquisition and pre-processing of virgin material. This data must be based upon the same type of data as for the parameter ‘$E_{MR\ after\ EoW\ out}$’. So, for steel EPD data is used (from Appendix H “Environmental data” under high impact). For concrete, generic Dutch values are used (in Table H-9).</p>	<ul style="list-style-type: none"> • Steel main load-bearing structure: 1.0 • Steel mezzanine floor: 1.0 • ComFlor steel: 1.0 • ComFlor in situ concrete: 1.0
<p>$\frac{Q_{R\ out}}{Q_{Sub}}$ = Quality difference between recycled and virgin material. Steel is 100% recyclable without loss of quality (see chapter 3.1 “Steel”). Structural concrete can have a maximum recycled content of 40% due to quality losses. As the recycled content of the product is limited, the quality of the concrete can be guaranteed. This means that in this research, the quality ratio between 40% recycled concrete and 100% virgin concrete is set to 1.</p>	

Table I-18: Processing the data for environmental impact calculation of stage D for concrete and steel elements

Process (Stage D)	Example calculation for the Base design																																																											
$total EI_{stage D} i$ $= mass_i * (M_{MR out} i - M_{MR in} i)$ $* \left(E_{MR after EoW out} i - E_{VMSub out} i \cdot \frac{Q_{R out} i}{Q_{Sub} i} \right)$	<p>Main load-bearing structure:</p> <ul style="list-style-type: none"> Steel main load-bearing structure (low environmental impact): € 0 Steel main load-bearing structure (high environmental impact): -€ 271,227 <p>Total mezzanine floor:</p> <ul style="list-style-type: none"> Steel mezzanine floor (low environmental impact): € 0 Steel mezzanine floor (high environmental impact): -€ 157,081 ComFlor steel (average environmental impact): -€ 1,412 ComFlor in situ concrete (low environmental impact): -€ 4,645 ComFlor in situ concrete (high environmental impact): € 4,645 																																																											
$\frac{EI_{stage D}}{RSL} = \sum_i M_{reu out} i * \frac{total EI_{stage D} i}{TSL_i} + (1 - M_{reu out} i)$ $* \frac{total EI_{stage D} i}{RSL}$	<table border="1"> <thead> <tr> <th rowspan="2">RSL</th> <th colspan="2">Main load-bearing structure</th> <th colspan="2">Total mezzanine floor</th> </tr> <tr> <th>Low impact</th> <th>High impact</th> <th>Low impact</th> <th>High impact</th> </tr> </thead> <tbody> <tr> <td>10 years</td> <td>€ 0</td> <td>-€ 24.438</td> <td>-€ 606</td> <td>-€ 14.759</td> </tr> <tr> <td>20 years</td> <td>€ 0</td> <td>-€ 12.368</td> <td>-€ 303</td> <td>-€ 7.466</td> </tr> <tr> <td>30 years</td> <td>€ 0</td> <td>-€ 8.345</td> <td>-€ 202</td> <td>-€ 5.035</td> </tr> <tr> <td>40 years</td> <td>€ 0</td> <td>-€ 6.333</td> <td>-€ 151</td> <td>-€ 3.819</td> </tr> <tr> <td>50 years</td> <td>€ 0</td> <td>-€ 5.126</td> <td>-€ 121</td> <td>-€ 3.090</td> </tr> <tr> <td>60 years</td> <td>€ 0</td> <td>-€ 4.322</td> <td>-€ 101</td> <td>-€ 2.604</td> </tr> <tr> <td>70 years</td> <td>€ 0</td> <td>-€ 3.747</td> <td>-€ 87</td> <td>-€ 2.256</td> </tr> <tr> <td>80 years</td> <td>€ 0</td> <td>-€ 3.316</td> <td>-€ 76</td> <td>-€ 1.996</td> </tr> <tr> <td>90 years</td> <td>€ 0</td> <td>-€ 2.980</td> <td>-€ 67</td> <td>-€ 1.793</td> </tr> <tr> <td>100 years</td> <td>€ 0</td> <td>-€ 2.712</td> <td>-€ 61</td> <td>-€ 1.631</td> </tr> </tbody> </table>	RSL	Main load-bearing structure		Total mezzanine floor		Low impact	High impact	Low impact	High impact	10 years	€ 0	-€ 24.438	-€ 606	-€ 14.759	20 years	€ 0	-€ 12.368	-€ 303	-€ 7.466	30 years	€ 0	-€ 8.345	-€ 202	-€ 5.035	40 years	€ 0	-€ 6.333	-€ 151	-€ 3.819	50 years	€ 0	-€ 5.126	-€ 121	-€ 3.090	60 years	€ 0	-€ 4.322	-€ 101	-€ 2.604	70 years	€ 0	-€ 3.747	-€ 87	-€ 2.256	80 years	€ 0	-€ 3.316	-€ 76	-€ 1.996	90 years	€ 0	-€ 2.980	-€ 67	-€ 1.793	100 years	€ 0	-€ 2.712	-€ 61	-€ 1.631
RSL	Main load-bearing structure		Total mezzanine floor																																																									
	Low impact	High impact	Low impact	High impact																																																								
10 years	€ 0	-€ 24.438	-€ 606	-€ 14.759																																																								
20 years	€ 0	-€ 12.368	-€ 303	-€ 7.466																																																								
30 years	€ 0	-€ 8.345	-€ 202	-€ 5.035																																																								
40 years	€ 0	-€ 6.333	-€ 151	-€ 3.819																																																								
50 years	€ 0	-€ 5.126	-€ 121	-€ 3.090																																																								
60 years	€ 0	-€ 4.322	-€ 101	-€ 2.604																																																								
70 years	€ 0	-€ 3.747	-€ 87	-€ 2.256																																																								
80 years	€ 0	-€ 3.316	-€ 76	-€ 1.996																																																								
90 years	€ 0	-€ 2.980	-€ 67	-€ 1.793																																																								
100 years	€ 0	-€ 2.712	-€ 61	-€ 1.631																																																								

Table I-19: Result of environmental impact calculation

Result	Example calculation for the Base design				
$\text{Yearly product impact} = \frac{EI_{A1-A3}}{RSL}$	Main load-bearing structure		Total mezzanine floor		
	RSL	Low impact	High impact	Low impact	High impact
<p>This is the same data as given in Table I-16, but for this overview, also shown in this table.</p>	10 years	€ 4.939	€ 28.490	€ 7.542	€ 23.429
	20 years	€ 2.500	€ 14.419	€ 3.789	€ 11.820
	30 years	€ 1.687	€ 9.729	€ 2.538	€ 7.950
	40 years	€ 1.280	€ 7.383	€ 1.913	€ 6.016
	50 years	€ 1.036	€ 5.976	€ 1.538	€ 4.855
	60 years	€ 873	€ 5.038	€ 1.288	€ 4.081
	70 years	€ 757	€ 4.368	€ 1.109	€ 3.528
	80 years	€ 670	€ 3.866	€ 975	€ 3.114
	90 years	€ 602	€ 3.475	€ 871	€ 2.791
	100 years	€ 548	€ 3.162	€ 787	€ 2.533
$\text{Yearly product} + \text{end of life impact} = \frac{EI_{A1-A3}}{RSL} + \frac{EI_D}{RSL}$	Main load-bearing structure		Total mezzanine floor		
	RSL	Low impact	High impact	Low impact	High impact
10 years	€ 5.184	€ 5.461	€ 6.936	€ 8.670	
20 years	€ 2.623	€ 2.764	€ 3.487	€ 4.354	
30 years	€ 1.770	€ 1.865	€ 2.337	€ 2.916	
40 years	€ 1.343	€ 1.415	€ 1.762	€ 2.196	
50 years	€ 1.087	€ 1.146	€ 1.417	€ 1.765	
60 years	€ 917	€ 966	€ 1.187	€ 1.477	
70 years	€ 795	€ 837	€ 1.022	€ 1.272	
80 years	€ 703	€ 741	€ 899	€ 1.118	
90 years	€ 632	€ 666	€ 803	€ 998	
100 years	€ 575	€ 606	€ 727	€ 902	

Table I-20: Input for the environmental impact calculation of stage D for timber elements

Input (Stage D)	Example calculation for Alternative B
Type of element 'i' Mass = Mass per element type (from Table 6-2)	i = glulam main load-bearing structure; glulam mezzanine floor elements; CLT mezzanine floor
$shadow\ price_{stage\ D}$ = Shadow price per element type based upon EPD data for stage D (from Table H-14)	<ul style="list-style-type: none"> • Glulam main load-bearing structure: 1,862,745 kg • Glulam mezzanine floor elements: 2,137,832 kg • CLT mezzanine floor: 1,067,254 kg • Glulam main load-bearing structure (largest bonus → low environmental impact): -€0,0059/kg material • Glulam main load-bearing structure (smallest bonus → high environmental impact): -€0,0024/kg material • Glulam mezzanine floor elements (largest bonus → low environmental impact): -€0,0059/kg material • Glulam mezzanine floor elements (smallest bonus → high environmental impact): -€0,0024/kg material • CLT mezzanine floor (largest bonus → low environmental impact): -€0,0086/kg material • CLT mezzanine floor (smallest bonus → high environmental impact): -€0,0079/kg material

Table I-21: Processing the data for environmental impact calculation of stage D for timber elements

Process (Stage D)	Example calculation for Alternative B						
$Total EI_D = \sum_i mass_i * shadow price_D _i$	<ul style="list-style-type: none"> • Glulam main load-bearing structure (largest bonus → low environmental impact): -€10,906 • Glulam main load-bearing structure (smallest bonus → high environmental impact): -€4,433 • Glulam mezzanine floor elements (largest bonus → low environmental impact): -€12,516 • Glulam mezzanine floor elements (smallest bonus → high environmental impact): -€5,088 • CLT mezzanine floor (largest bonus → low environmental impact): -€9,173 • CLT mezzanine floor (smallest bonus → high environmental impact): -€8,394 						
$\frac{EI_D}{RSL} = \frac{total EI_D}{RSL}$	Glulam load-bearing structure		Glulam mezzanine floor		CLT mezzanine floor		
	RSL	Low impact	High impact	Low impact	High impact	Low impact	High impact
10 years		-€ 1.091	-€ 443	-€ 1.252	-€ 509	-€ 917	-€ 839
20 years		-€ 545	-€ 222	-€ 626	-€ 254	-€ 459	-€ 420
30 years		-€ 364	-€ 148	-€ 417	-€ 170	-€ 306	-€ 280
40 years		-€ 273	-€ 111	-€ 313	-€ 127	-€ 229	-€ 210
50 years		-€ 218	-€ 89	-€ 250	-€ 102	-€ 183	-€ 168
60 years		-€ 182	-€ 74	-€ 209	-€ 85	-€ 153	-€ 140
70 years		-€ 156	-€ 63	-€ 179	-€ 73	-€ 131	-€ 120
80 years		-€ 136	-€ 55	-€ 156	-€ 64	-€ 1.048 ¹¹	-€ 959
90 years		-€ 121	-€ 49	-€ 139	-€ 57	-€ 590	-€ 551
100 years		-€ 109	-€ 44	-€ 125	-€ 51	-€ 437	-€ 411

¹¹ This value is higher, because it is assumed that for the timber floor, the TSL is equal to 75 years. So, if the RSL is longer than 75 years, a new CLT floor is needed.

J Environmental impact calculation results

J.1 Research question 3a: Optimise design for its initial material use

J.1.1 Comparison 1: Determining the effect of the amount of material on the environmental impact

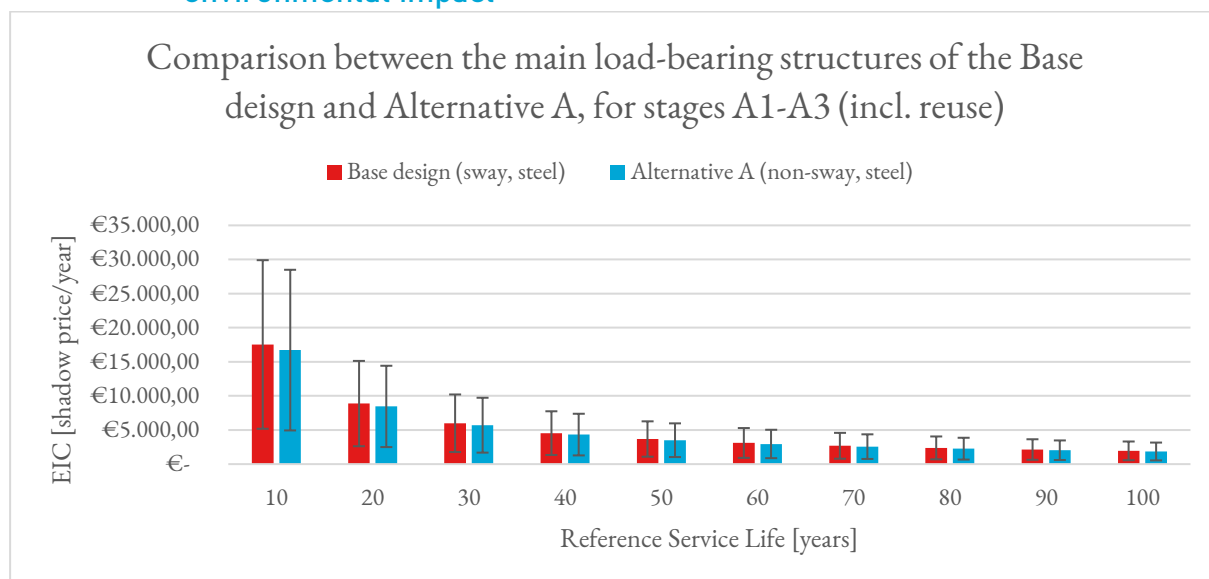


Figure J-1: Comparison between the Base design and Alternative A, for stages A1-A3 (incl. reuse)

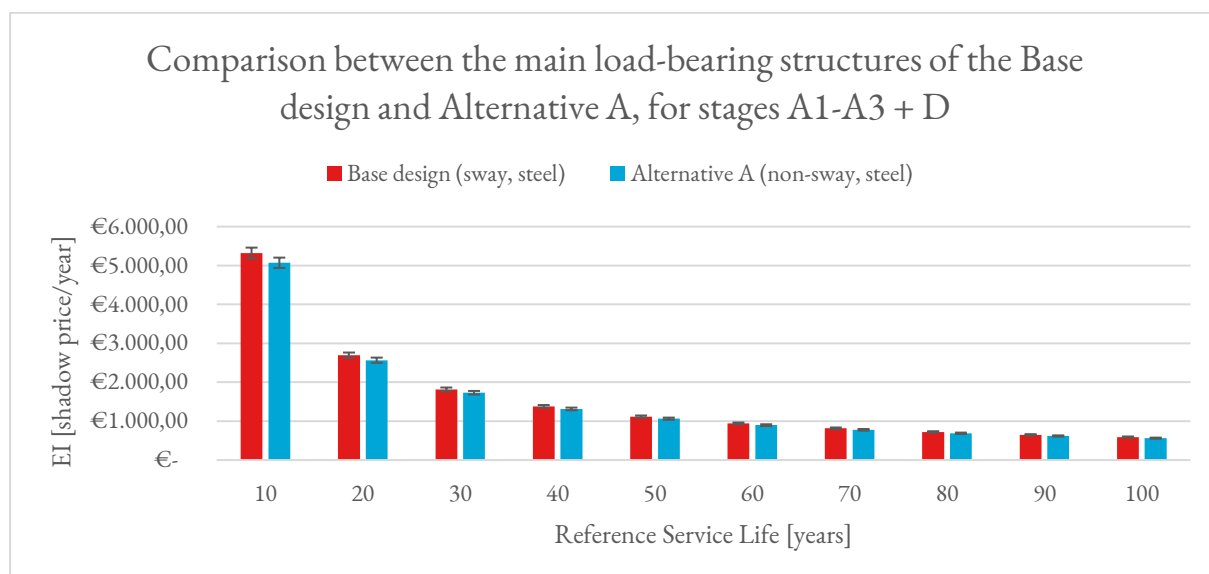


Figure J-2: Comparison between the Base design and Alternative A, for stages A1-A3 and D

J.1.2 Comparison 2: Determining the effect of the type of material on the environmental impact

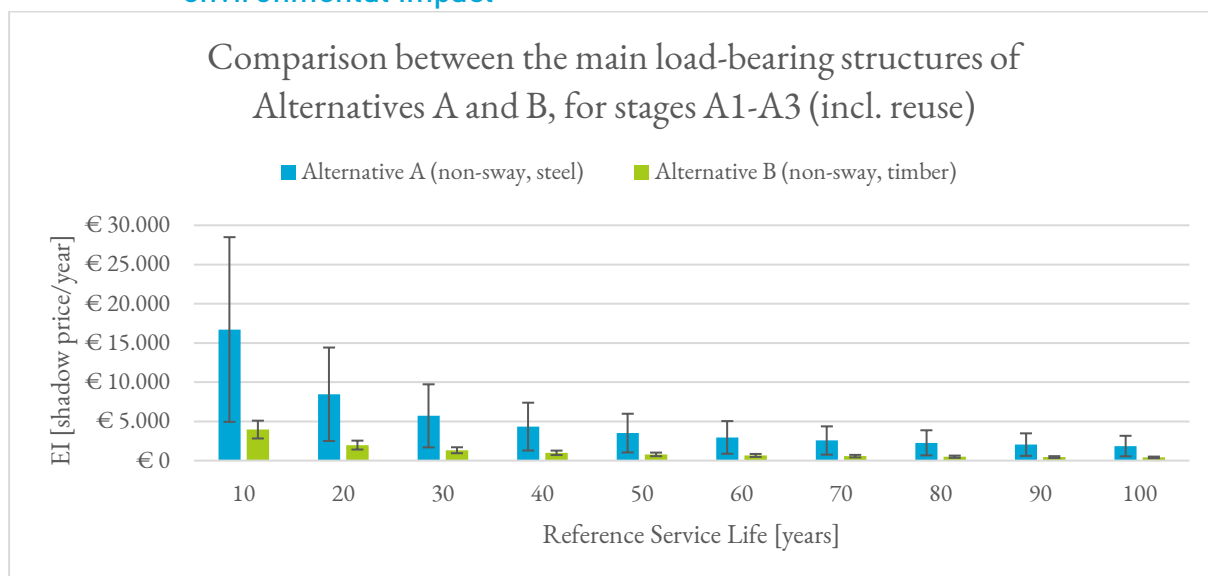


Figure J-3: Comparison between the main load-bearing structure of Alternative A and B (stages A1-A3)

J.1.2.1 Sensitivity of the mezzanine floor

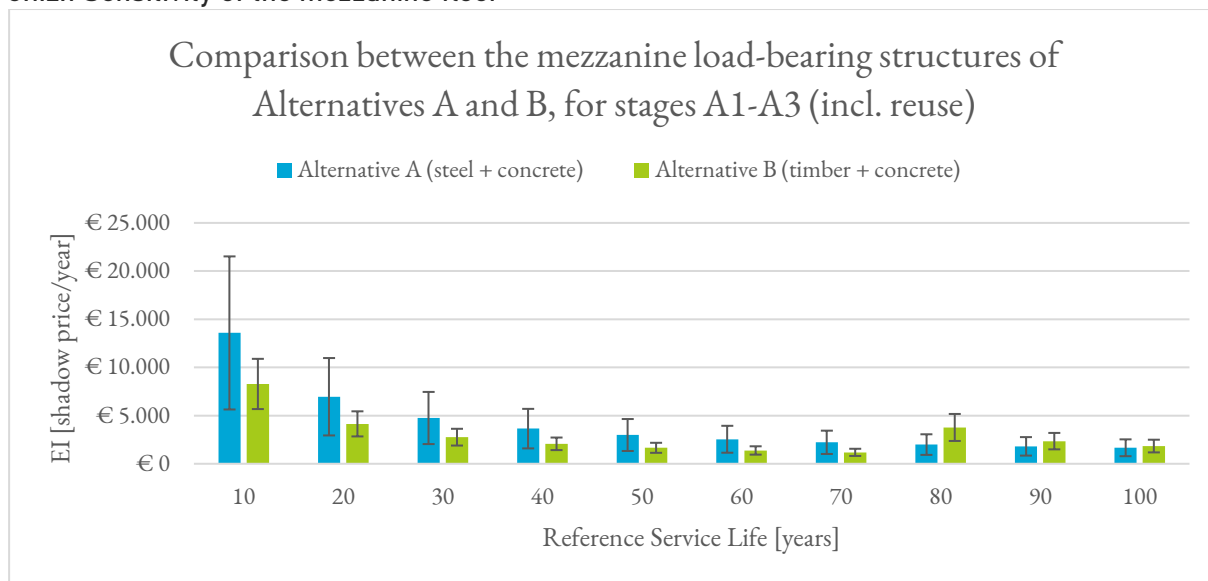


Figure J-4: Comparison between the mezzanine structure of Alternative A and B (stages A1-A3)

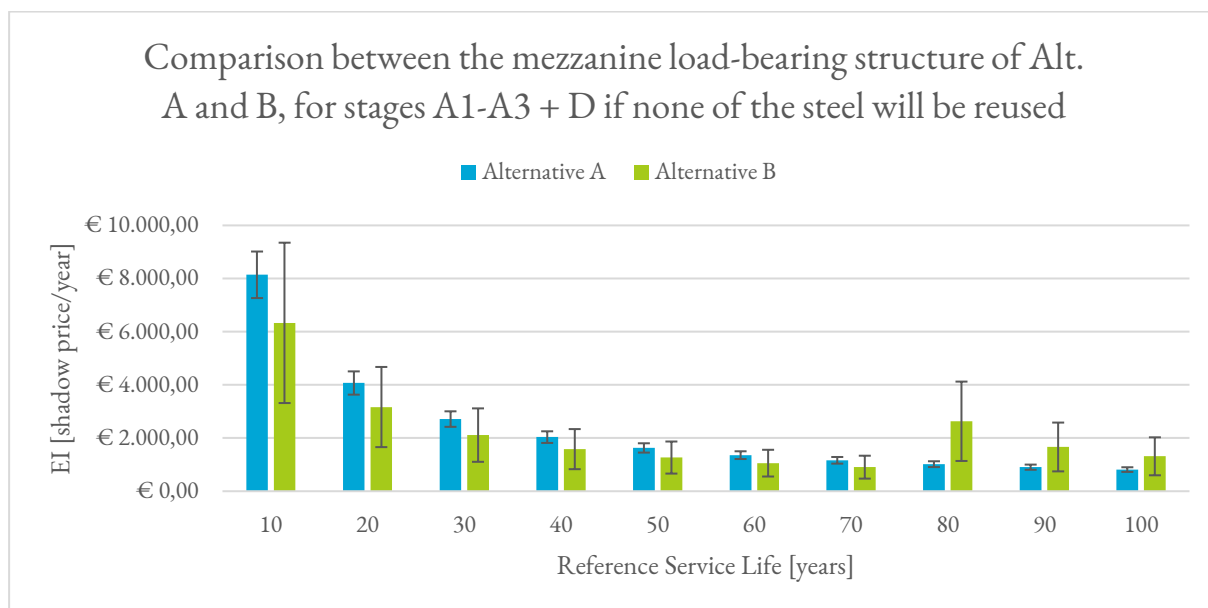


Figure J-5: Comparison between mezzanine structure of Alternative A and B, if none of the steel will be reused

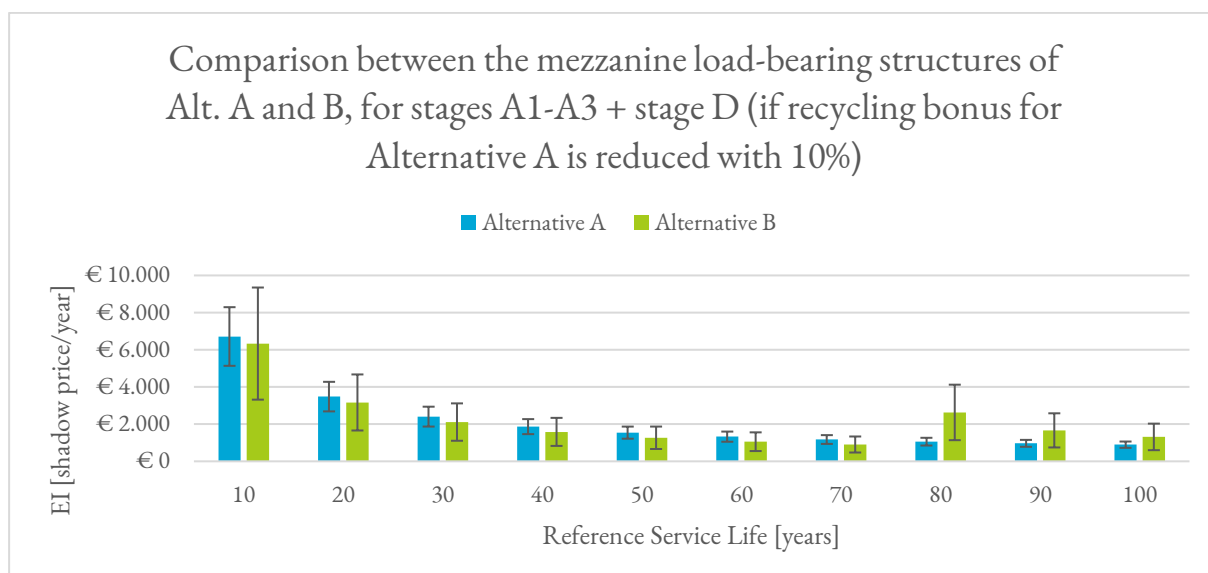


Figure J-6: Comparison between the mezzanine structure of Alternative A and B, if the bonus for recycling of Alternative A is reduced with 10%

J.2 Research question 3b: Optimise design for residual value

J.2.1 Comparison 3: Determining the relationship between the reuse of a traditional design and a demountable design

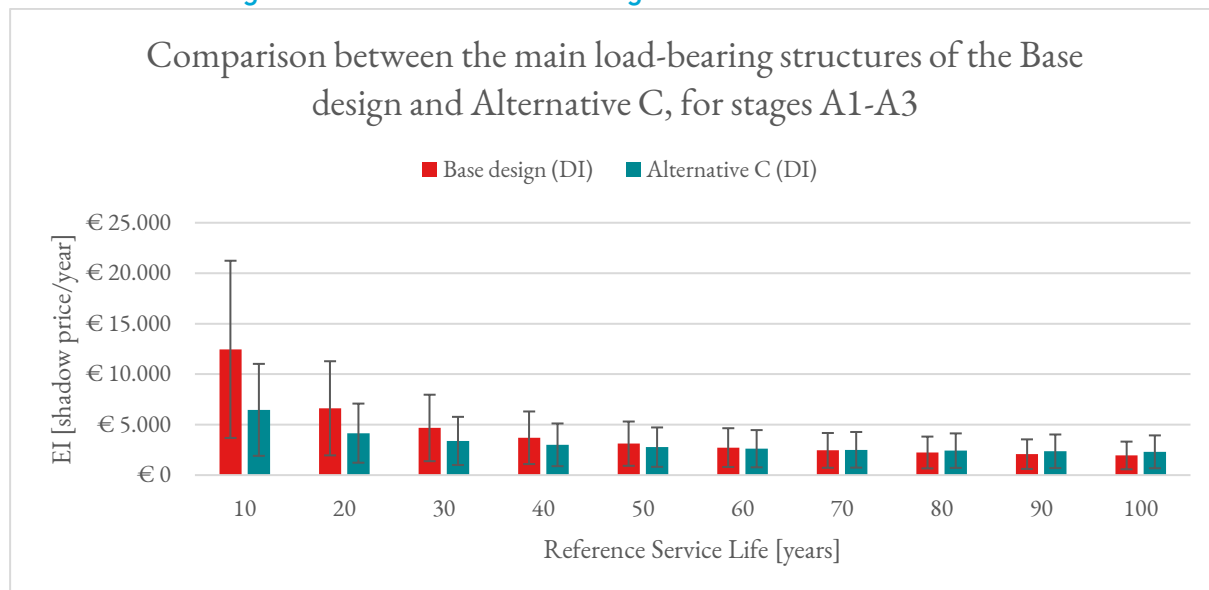


Figure J-7: Comparison between the main load-bearing structure of the Base design and Alternative C for stages A1-A3, where the chance of reuse is based upon the Disassembly Index

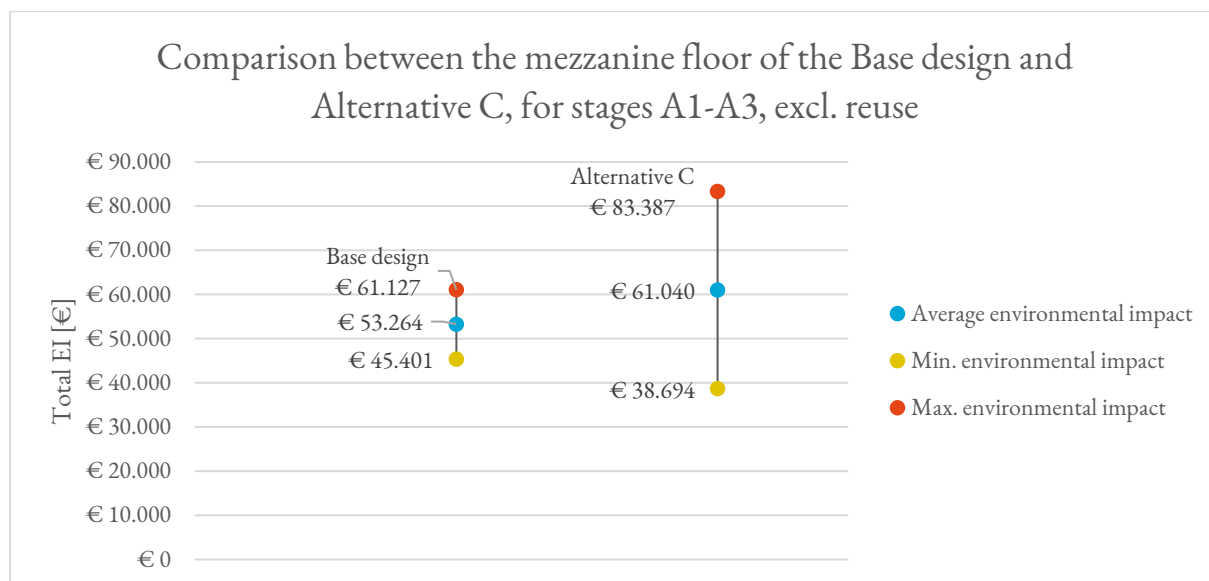


Figure J-8: Comparison between the mezzanine floor of the Base design and Alternative C (stages A1-A3, where the advantage of reusing the elements is not considered)

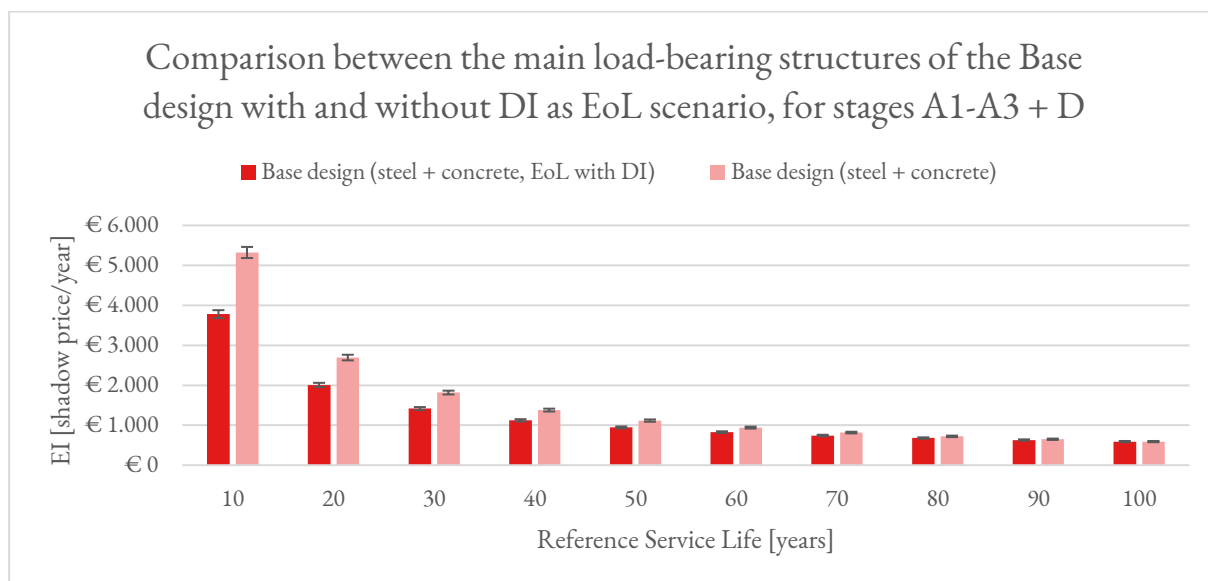


Figure J-9: Comparison between the Base design if the Disassembly Index is used to calculate the chance of reuse (Base design (DI)) and if the general end of life scenarios are used (Base design (no DI))